

Inhibition of Steroidogenic Cytochrome P450 Enzymes as Treatments for the Related Hormone Dependent Diseases

Dissertation

zur Erlangung des Grades des Doktors der Naturwissenschaften
der Naturwissenschaftlich-Technischen Fakultät III
Chemie, Pharmazie, Bio- und Werkstoffwissenschaften
der Universität des Saarlandes

von

MS Sci Qingzhong HU

Saarbrücken, 2010

Die vorliegende Arbeit wurde von September 2005 bis Juni 2010 unter Anleitung von Herrn Prof. Dr. Rolf W. Hartmann an der Naturwissenschaftlich-Technischen Fakultät III der Universität des Saarlandes angefertigt.

Tag des Kolloquiums:	26th, Nov. 2010
Dekan:	Prof. Dr. Stefan Diebels
Berichterstatter:	Prof. Dr. Rolf W. Hartmann
	Prof. Dr. Christian Klein
Vorsitz:	Prof. Dr. Uli Kazmeier
Akad. Mitarbeiter:	Dr. Matthias Engel

陰陽互使 治在權衡相奪

治之與極 無失乎所 用之不惑 治之亦助

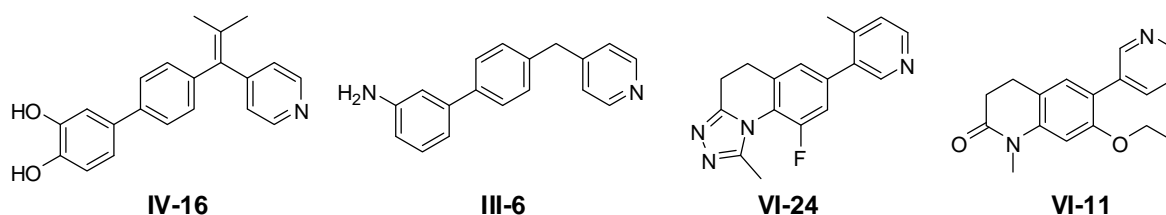
——黃帝內經·素問

ABSTRACT

Steroidogenic CYPs are crucial enzymes in the biosyntheses of steroid hormones, which are responsible for the maintenance of gender characteristics, as well as for the regulation of carbohydrate metabolism, immune system and homeostasis of electrolytes and fluids. It has been established that abnormal concentrations of these hormones are associated with some complicated diseases. Therefore, the control of these hormone levels as promising therapies are imperative. To attain this goal, the inhibition of steroidogenic CYP enzymes catalyzing the production of these hormones is an elegant way.

Since androgen stimulates the proliferation of prostate cancer cells, the inhibition of CYP17, which is the crucial enzyme in androgen biosynthesis, was proposed as a promising therapy. In mimicking the natural steroidal substrates, series of biphenyl methylene heterocycles were designed. After the evolution from imidazoles to pyridines, potent and selective CYP17 inhibitors were identified, for example **IV-16**, which exceed the drug candidate Abiraterone in terms of inhibitory potency and selectivity patterns. Considering the fact that mutated androgen receptor can be activated by cortisol and in some prostate cancer patients high cortisol levels lead to Cushing's syndrome, dual inhibitors of CYP17 and CYP11B1 are designed by combining important structure features of both inhibitors. Compound **III-6** was successfully obtained as a lead for dual inhibition, although the inhibitory potency and selectivity over CYP11B2 requires further improvement.

Moreover, high aldosterone levels are widely acknowledged to show some deleterious effects on heart, vessels, kidney, brain and central nerve system. Due to its pivotal role in aldosterone biosynthesis, CYP11B2 is a superior target for the treatment of diseases related to high aldosterone levels. Based on the previously identified lead compounds, a series of novel heterocycle substituted 4,5-dihydro-[1,2,4]triazolo[4,3-*a*]quinolines were designed, synthesized and biologically evaluated. The resulted compound **VI-24** exhibits an IC_{50} of 4 nM and excellent selectivity over CYP11B1, which shares 93% of homology with CYP11B2. CYP11B2 inhibition is also considered necessary for breast cancer patients under aromatase inhibitor therapy because the estrogen deficiency caused by menopausal and the application of aromatase inhibitor eventually increases aldosterone concentration. Design via hybridization of both CYP19 and CYP11B2 inhibitors leads to compound **V-11** as a promising dual inhibitor.

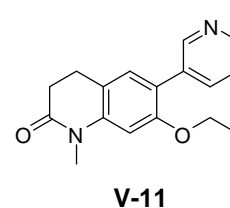
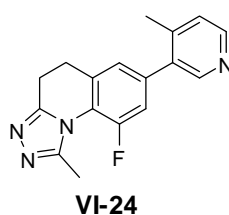
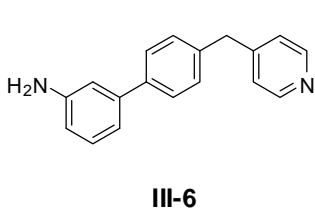
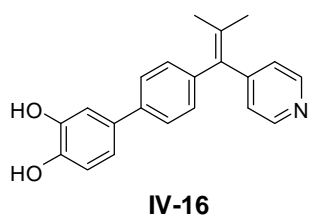


ZUSAMMENFASSUNG

Steroidogene CYP-Enzyme sind für die Biosynthese von Steroidhormonen essentiell. Letztere sind verantwortlich für die Ausbildung von Geschlechtsmerkmalen und deren Aufrechterhaltung sowie für die Regulation des Kohlenhydratstoffwechsels, des Immunsystems und der Homöostase von Elektrolyten und Flüssigkeit. Es ist schon lange bekannt, dass von der Norm abweichende Hormon-Konzentrationen mit schwerwiegenden Krankheiten verbunden sind. Eine Kontrolle der Hormonspiegel stellt daher eine vielversprechende therapeutische Option dar. Zur Erreichung dieses Ziels ist die Hemmung steroidogener CYP-Enzyme, die die entsprechende Hormon- Biosynthese katalysieren, ein eleganter Weg.

Da Androgene die Proliferation von Prostatakarzinomzellen stimulieren, ist die Hemmung von CYP17, dem Schlüssel-Enzym in der Androgen Biosynthese, die Strategie der Wahl. Als Mimetika der natürlichen steroidogenen Substrate, wurde eine Serie an Biphenylmethylen-Heterocyclen konzipiert. Durch Weiterentwicklung von den Imidazolen zu den Pyridinen, konnten potente und selektive CYP17 Hemmstoffe identifiziert werden, z. B. **IV-16**, das bezüglich Hemmpotenz und Selektivität den Arzneistoffkandidaten Abirateron übertrifft. Nach dem bekannt geworden war, dass ein mutierter Androgen-Rezeptor durch Cortisol aktiviert werden kann und dass in einigen Prostatakarzinompatienten hohe Cortisolspiegel zu Cushing-Syndrom führen, wurden duale Hemmstoffe von CYP17 und CYP11B1 konzipiert, in dem entscheidende Strukturmerkmale von beiden Hemmstofftypen strukturell vereint wurden. Verbindung **III-6** wurde dabei als Leitverbindung für einen dualen Hemmstoff erhalten. Dies war zweifelsohne ein Erfolg, wenn gleich Hemmpotenz und Selektivität gegenüber CYP11B2 weiter optimiert werden sollten.

Es ist weiterhin bekannt, dass hohe Aldosteronspiegel einige sehr negative Effekte auf Herz, Blutgefäße, Niere, Gehirn und zentrales Nervensystem aufweisen. CYP11B2 ist ein hervorragendes Target für die Behandlung dieser Krankheiten, da es eine entscheidende Rolle in der Aldosteron-Biosynthese spielt. Basierend auf den kürzlich identifizierten Leitverbindungen, wurde eine Serie von neuen heterocyclisch substituierten 4,5-Dihydro-[1,2,4]triazolo[4,3-*a*]Chinolinen konzipiert, synthetisiert und biochemisch evaluiert. Die resultierende Verbindung **VI-24** zeigt einen IC₅₀ Wert von 4 nM und eine exzellente Selektivität gegenüber CYP11B1, das eine 93%ige Homologie zu CYP11B2 aufweist. Die Hemmung von CYP11B2 wird auch als notwendig für Brustkrebspatientinnen unter Aromatasehemmer-Therapie angesehen, da der Estrogenmangel, hervorgerufen durch Menopause oder Applikation von Aromatasehemmstoffen, zur Ausbildung hoher Aldosteronkonzentrationen führt. Durch Hybridisierung von Aromatase - und CYP11B2 - Inhibitoren wurde letztendlich Verbindung **V-11** als vielversprechender dualer Hemmstoff erhalten.



PAPERS COMPOSING THIS DISSERTATION

This doctoral dissertation comprises six publications, which are referred to in the text by their Roman numerals.

I. Synthesis, Biological Evaluation and Molecular Modelling Studies of Methylene Imidazole Substituted Biaryls as Inhibitors of Human 17 α -Hydroxylase-17,20-lyase (CYP17) – Part II: Core Rigidification and Influence of Substituents at the Methylene Bridge

Qingzhong Hu, Matthias Negri, Kerstin Jahn-Hoffmann, Yan Zhuang, Sureyya Olgen, Marc Bartels, Ursula Müller-Vieira, Thomas Lauterbach, and Rolf W. Hartmann

Bioorganic & Medicinal Chemistry **2008**, *16*, 7715–7727.

II. The Role of Fluorine Substitution in Biphenyl Methylene Imidazole Type CYP17 Inhibitors for the Treatment of Prostate Carcinoma

Qingzhong Hu, Matthias Negri, Sureyya Olgen, and Rolf W. Hartmann

ChemMedChem **2010**, *5*, 899–910.

III. Replacement of Imidazolyl by Pyridyl in Biphenyl Methylenes Results in Selective CYP17 and Dual CYP17 / CYP11B1 Inhibitors for the Treatment of Prostate Cancer

Qingzhong Hu, Carsten Jagusch, Ulrike E. Hille, Jörg Haupenthal, and Rolf W. Hartmann

Journal of Medicinal Chemistry **2010**, *53*, 5749–5758.

IV. Isopropylidene Substitution Increases Activity and Selectivity of Biphenyl Methylene 4-Pyridine Type CYP17 Inhibitors

Qingzhong Hu, Lina Yin, Carsten Jagusch, Ulrike E. Hille, and Rolf W. Hartmann

Journal of Medicinal Chemistry **2010**, *53*, 5049–5053.

V. Selective Dual Inhibitors of CYP19 and CYP11B2: Targeting Cardiovascular Diseases Hiding in the Shadow of Breast Cancer

Qingzhong Hu, Lina Yin, and Rolf W. Hartmann

Journal of Medicinal Chemistry **2010**, Manuscript.

VI. Novel Heterocycle Substituted 4,5-Dihydro-[1,2,4]triazolo[4,3-a]quinolines as Potent and Selective Aldosterone Synthase Inhibitors for the Treatment of Related Cardiovascular Diseases

Qingzhong Hu, Lina Yin, and Rolf W. Hartmann

Journal of Medicinal Chemistry **2010**, Manuscript.

CONTRIBUTION REPORT

The author wishes to clarify his contributions to the papers **I–VI** composing this dissertation.

- I.** Significant contribution to the inhibitor design conception. Syntheses and characterization of most of the new compounds (**1, 2, 4, 7, 8, 10** and **17–21**), with the rest compounds synthesized by Dr. Yan Zhuang (**5, 6, 9** and **23**), Dr. Marc Bartels (**11** and **30–35**), Dr. Kerstin Jahn-Hoffmann (**12–14** and **24–29**), Dr. Carsten Jagusch (**15** and **16**) and Ulrike E. Hille (**22**). Significant contribution to the interpretation of the bio-results to SAR. Significant contribution to the composition of manuscript.
- II.** Significant contribution to the inhibitor design conception. Syntheses and characterization of most of the new compounds (**3, 5, 8, 10** and **12**), with the rest compounds synthesized by Dr. Mariano E. Pinto-Bazurco Mendieta (**1** and **23–26**), Dr. Kerstin Jahn-Hoffmann (**2, 4, 6, 7** and **21**), Dr. Marc Bartels (**19, 20** and **22**) and Dr. Sureyya Olgen (**9, 11** and **13–18**). Significant contribution to the interpretation of the bio-results to SAR. Significant contribution to the composition of manuscript.
- III.** Significant contribution to the inhibitor design conception. Syntheses and characterization of most of the new compounds (**6, 7, 11, 13, 17–20** and **21–23**), with the rest compounds synthesized by Dr. Carsten Jagusch (**1–5, 8–10, 12, 15** and **16**) and Ulrike E. Hille (**24** and **25**). Significant contribution to the interpretation of the bio-results to SAR. Significant contribution to the composition of manuscript.
- IV.** Significant contribution to the inhibitor design conception. Syntheses and characterization of most of the new compounds (**17–22, 27** and **28**), with the rest compounds synthesized by Dr. Carsten Jagusch (**11–16**), Dr. Mariano E. Pinto-Bazurco Mendieta (**1, 5** and **6**), Dr. Kerstin Jahn-Hoffmann (**2–4, 7** and **8**), Lina Yin (**9**) and Ulrike E. Hille (**23**). Significant contribution to the interpretation of the bio-results to SAR. Significant contribution to the composition of manuscript.
- V.** Significant contribution to the inhibitor design conception. Syntheses and characterization of all the new compounds (**1–19**). Significant contribution to the interpretation of the bio-results to SAR. Significant contribution to the composition of manuscript.
- VI.** Significant contribution to the inhibitor design conception. Syntheses and characterization of all the new compounds (**1–27**). Significant contribution to the interpretation of the bio-results to SAR. Significant contribution to the composition of manuscript.

PAPERS EXCLUDED

The author also contributes to the following papers by synthesizing novel compounds and by design conception. However, these works are marginal comparing to the main body of this dissertation and therefore are not included.

VII. Synthesis, biological evaluation and molecular modeling studies of methyleneimidazole substituted biaryls as inhibitors of human 17 α -hydroxylase-17,20-lyase (CYP17) – Part I: heterocyclic modifications of the core structure.

Jagusch, C.; Negri, M.; Hille, U. E.; Hu, Q.; Bartels, M.; Jahn-Hoffmann, K.; Pinto-Bazurco Mendieta, M. A. E.; Rodenwaldt, B.; Müller-Vieira, U.; Schmidt, D.; Lauterbach, T.; Recanatini, M.; Cavalli, A.; Hartmann, R. W.

Bioorg. Med. Chem. **2008**, *16*, 1992–2010.

VIII. CYP17 inhibitors. Annulations of additional rings in methylene imidazole substituted biphenyls: synthesis, biological evaluation and molecular modeling.

Pinto-Bazurco Mendieta, M. A. E.; Negri, M.; Hu, Q.; Hille, U. E.; Jagusch, C.; Jahn-Hoffmann, K.; Müller-Vieira, U.; Schmidt, D.; Lauterbach, T.; Hartmann, R. W.

Arch. Pharm. (Weinheim, Ger.) **2008**, *341*, 597–609.

IX. Novel CYP17 inhibitors: Synthesis, biological evaluation, structure-activity relationships and modeling of methoxy- and hydroxy-substituted methyleneimidazolyl biphenyls.

Hille, U. E.; Hu, Q.; Vock, C.; Negri, M.; Bartels, M.; Müller-Vieira, U.; Lauterbach, T.; Hartmann, R. W.

Eur. J. Med. Chem. **2009**, *44*, 2765–2775.

X. Steroidogenic cytochrome P450 (CYP) enzymes as drug targets: Combining substructures of known CYP inhibitors leads to compounds with different inhibitory profile.

Hille, U. E.; Hu, Q.; Pinto-Bazurco Mendieta, M. A. E.; Bartels, M.; Vock, C. A.; Lauterbach, T.; Hartmann, R. W.

C. R. Chim. **2009**, *12*, 1117–1126.

ACKNOWLEDGEMENTS

I would like to express my sincere gratitude to Prof. Dr. Rolf W. Hartmann for introducing me into the field of steroidogenic CYP enzymes inhibition. His innovative ideas, broad knowledge and enthusiasm for science always guided and encouraged me through my PhD work. The experience of working with him is precious in my academic career.

I would also like to thank my official referee Prof. Dr. Christian Klein for the review of this dissertation.

I appreciate Dr. Carsten Jagusch and Dr. Ralf Heim as fair and guileless group leaders. Thank you for your trust and encouragement.

I am grateful to Dr. Matthias Engel, Dr. Stefan Boettcher, Dr. Martin Frotscher and Ms Barbara Boeffel for their help with my accommodation and in coping with all kinds of bureaucratic procedures when I came to this unacquainted country for the first time.

The help from Dr. Matthias Negri, Dr. Stefan Boettcher and Dr. Josef Zapp in modeling study as well as LC-MS and NMR measurement and resolution, respectively, are highly appreciated.

I thank Dr. Jörg Haupenthal, Christina Zimmer, Sabrina Rau, Gertrud Schmitt, Jeannine Jung, Jannine Ludwig and Martina Jankowski for their hard work in bio-evaluation of synthesized compounds.

I also would like to thank all members of CYP17 and CYP11B2 groups for the cooperation to smooth the research and all the colleagues in AK Hartmann for the friendly atmosphere.

Finally, I would like to express my deep love to my family. Thank you for supporting me to pursue a dream far away. Thank you for sharing my joyance and solacing my fidgetiness. Thank you for being in my life.

ABBREVIATIONS

5 α -R	5 α -reductase
AA	amino acid
ACTH	adrenocortico-tropic hormone
ACE	angiotensin converting enzyme
ADAMTS1	a disintegrin and metalloprotease with thrombospondin motifs
AI	aromatase inhibitor
Ang II	angiotensin II
AR	androgen receptor
AT1R	angiotensin type 1 receptor
ATR	attenuated total reflectance
BC	breast cancer
BM	binding mode
Boc	<i>tert</i> -butoxycarbonyl
BPH	benign prostatic hyperplasia
CAB	combined androgen blockade
CDI	1,1-carbonyl diimidazole
CHIF	corticosteroid hormone-induced factor
CTC	circulating tumor cells
CRH	corticotropin-releasing hormone
CVD	cardiovascular diseases
CYP	cytochrome P450
CYP11A1	P450 _{scc} , cholesterol side-chain cleavage enzyme
CYP11B1	11 β -hydroxylase
CYP11B2	aldosterone synthase
CYP17	17 α -hydroxylase-17,20-lyase
CYP19	aromatase, estrogen synthase
DCM	dichloromethane
DHEA	dehydroepiandrosterone
DHT	dihydrotestosterone
DMA	<i>N, N</i> -dimethylacetamide
DOC	11-deoxycorticosterone
DRE	digital rectal examination
EA	ethyl acetate
ENaC	epithelial sodium channel
ER	estrogen receptor
FSH	follicle-stimulating hormone

GA	genetic algorithm
GnRH	gonadotropin-releasing hormone
HSD	hydroxysteroid dehydrogenase
kDa	kilodalton
LH	luteinizing hormone
LHRH	hypothalamic luteinizing hormone-releasing hormone
MR	mineralocorticoid receptor
NBS	<i>N</i> -bromosuccinimide
NCI	national cancer institute
NMP	<i>N</i> -methylpyrrolidone
Orm1	orosomuroid-1
PAI	plasminogen activator inhibitor
PCa	Prostate cancer
PE	petroleum ether
PgR	progesterone receptor
PSA	prostate specific antigen
RAAS	renin–angiotensin–aldosterone system
RGS2	regulator of G protein signaling-2
ROS	reactive oxygen species
SERM	selective estrogen receptor modulator
SF	selectivity factor
SGK1	serum and glucocorticoid-regulated kinase
TBDMS	<i>tert</i> -butyldimethylsilyl
TBDPS	<i>tert</i> -butyldiphenylsilyl
TNX	tenascin-X
UPAR	urokinase plasminogen activator receptor

CONTENTS

1 Introduction	1
1.1 Cytochrome P450 Enzymes	1
1.1.1 General	1
1.1.2 Structure: Hemoprotein and associated Electron Transfer Partners	1
1.1.3 Catalytic Mechanism	2
1.1.4 Functions of CYP Enzymes	3
1.1.5 Hepatic CYP Enzymes	3
1.1.6 Steroidogenic CYP Enzymes	4
1.2 CYP17 Inhibition as Treatment for Prostate Cancer	6
1.2.1 Prostate Cancer: Incidence and Diagnosis	6
1.2.2 Prostate Cancer Treatment — State of Art	7
1.2.2.I. Watchful Waiting	7
1.2.2.II. Local Therapy: Prostatectomy, Cryotherapy and Radiation Therapy	7
1.2.2.III. Chemotherapy	8
1.2.2.IV. Vaccines and Immunotherapy	9
1.2.2.V. Hormone Therapy	11
1.2.3 CYP17 Inhibition as Treatment for Prostate Cancer	14
1.2.3.I. Mechanism Based Inactivators	15
1.2.3.II. Inhibition via Coordination between sp^2 hybrid N and Heme Iron	15
1.3 CYP11B2 Inhibition for Diseases related to High Aldosterone Levels	18
1.3.1 Aldosterone: Physiology and Pathology	18
1.3.1.I. Mineralocorticoid Regulating Electrolyte and Fluid Homeostasis	18
1.3.1.II. Deleterious Effects of High Aldosterone Levels to Heart, Vessels and Kidney	18
1.3.1.III. Mechanisms of Action — Genomic and Non-genomic	20
1.3.2 CYP11B2, RAAS and Regulation of Aldosterone Biosyntheses	20
1.3.3 Treatment of High Aldosterone Related Diseases — State of Art	21
1.3.3.I. Mineralocorticoid Receptor (MR) Antagonists	21
1.3.3.II. Renin Inhibitors	21
1.3.3.III. Angiotensin Converting Enzyme (ACE) Inhibitors	22
1.3.4 CYP11B2 Inhibition as Treatment for Hypertension, Primary Aldosteronism and Congestive Heart Failure	23
1.3.4.I. Fadrozole, Etomidate, Metyrapone and their Derivatives	23
1.3.4.II. Heterocycle Substituted Methylene Tetrahydronaphthalene or Dihydroindene	24
1.3.4.III. Pyridyl Naphthalenes and Indenes: Semi-unsaturation and Heteratom Inserting	24

1.4	Dual Inhibition	26
1.4.1	Dual CYP17 / CYP11B1 Inhibition For Prostate Cancer Treatment	26
1.4.2	Dual CYP19 / CYP11B2 Inhibition to Cure Cardiovascular Diseases in Breast Cancer Patients	27
2	Work Strategy	29
2.1	Inhibitors Design	29
2.1.1	General	29
2.1.1.I.	Mechanism Inactivator or Reversible Inhibition via N–Fe Coordination	29
2.1.1.II.	Steroidal or Non-steroidal	29
2.1.1.III.	Multi-targeting and Selectivity	29
2.1.2	Combination of Ligand and Structure Approaches	29
2.1.3	Other Considerations: Drug-Like Properties, Solubility and Metabolic Stability	30
2.2	Syntheses	30
2.3	Biological Evaluation	30
3	Results and Discussions	31
3.I.	Synthesis, Biological Evaluation and Molecular Modelling Studies of Methylene Imidazole Substituted Biaryls as Inhibitors of Human 17α-Hydroxylase-17,20-lyase (CYP17) – Part II: Core Rigidification and Influence of Substituents at the Methylene Bridge	32
3.II.	The Role of Fluorine Substitution in Biphenyl Methylene Imidazole Type CYP17 Inhibitors for the Treatment of Prostate Carcinoma	55
3.III.	Replacement of Imidazolyl by Pyridyl in Biphenyl Methylenes Results in Selective CYP17 and Dual CYP17 / CYP11B1 Inhibitors for the Treatment of Prostate Cancer	76
3.IV.	Isopropylidene Substitution Increases Activity and Selectivity of Biphenyl Methylene 4-Pyridine Type CYP17 Inhibitors	93
3.V.	Selective Dual Inhibitors of CYP19 and CYP11B2: Targeting Cardiovascular Diseases Hiding in the Shadow of Breast Cancer	103
3.VI.	Novel Heterocycle Substituted 4,5-Dihydro-[1,2,4]triazolo[4,3-a]quinolines as Potent and Selective Aldosterone Synthase Inhibitors for the Treatment of Related Cardiovascular Diseases	120
4	Summary and Conclusions	134
4.1	CYP17 Inhibitors	134
4.2	Dual Inhibitors of CYP17 / CYP11B1	136

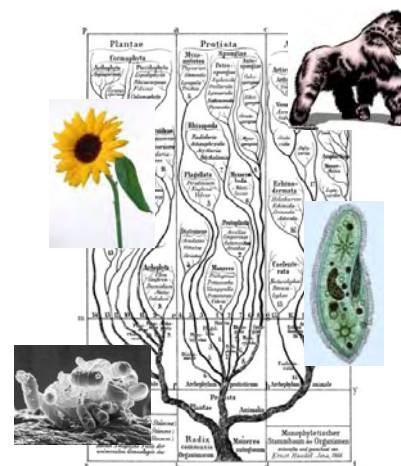
4.3 CYP11B2 Inhibitors	136
4.4 Dual Inhibitors of CYP19 / CYP11B2	137
5 Reference	138

1 Introduction

1.1 Cytochrome P450 Enzymes

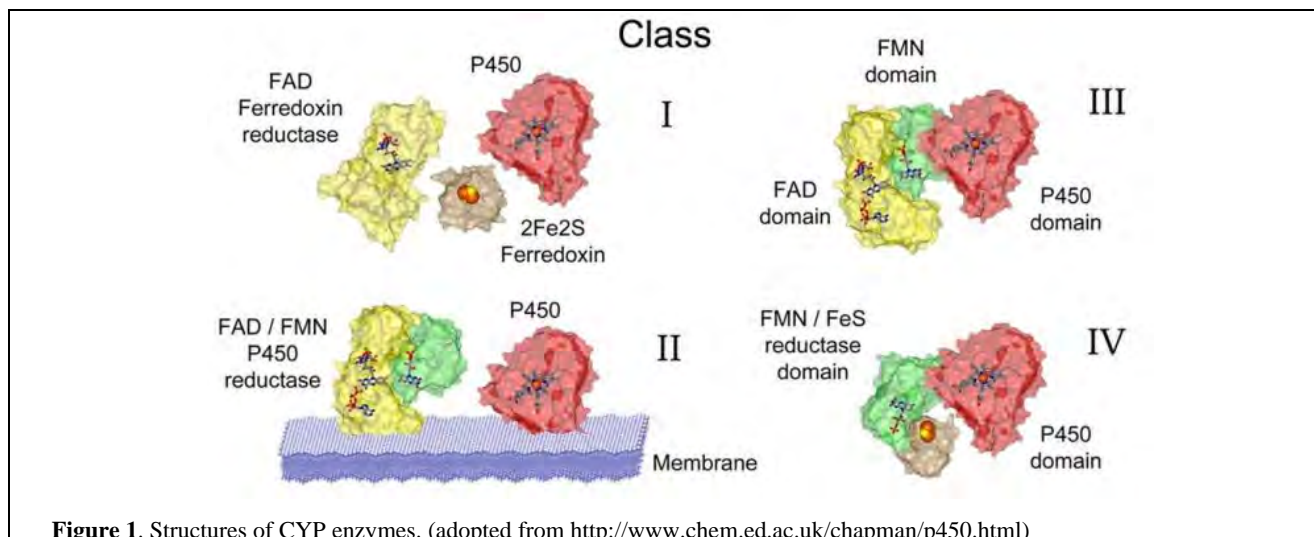
1.1.1 General

It has been postulated that the first cytochrome P450 (CYP) gene emerged about 3.5 billion years ago before the advent of eukaryotes and the existence of an oxygen-rich atmosphere.¹ Accompanying the evolution of life, cytochrome P450 widely spread into every branch of the tree of life, from bacteria to human being. At the same time, the function of cytochrome P450 shifted from nitro-reduction to oxidation. Cytochrome P450 is a huge superfamily, it comprises around 10,000 identified cytochrome P450 genomic and cDNA sequences that have been divided into 781 different families. As the research in genomics and proteomics is intensifying, the members of this superfamily keep increasing. CYPs are categorized into families and subfamilies according to amino acid (AA) sequence identity with CYP as the superfamily name. When CYP enzymes have more than 40% of sequence identity, they are designated as one family, for example CYP1. Sequences that are greater than 55% identical are in the same subfamily labelling with a capital letter after the family number, such as CYP1A. For each member of the subfamily, they are distinguished with an extra number, such as CYP1A2. The corresponding gene for the enzyme shares the same name, but in italics. However, the designation of the number to the family, such as CYP1 and CYP2, does not reflect the phylogenetic relationship. For example, mammalian CYP3 family is more closely related to the insect CYP6 family than to the mammalian CYP4 family.

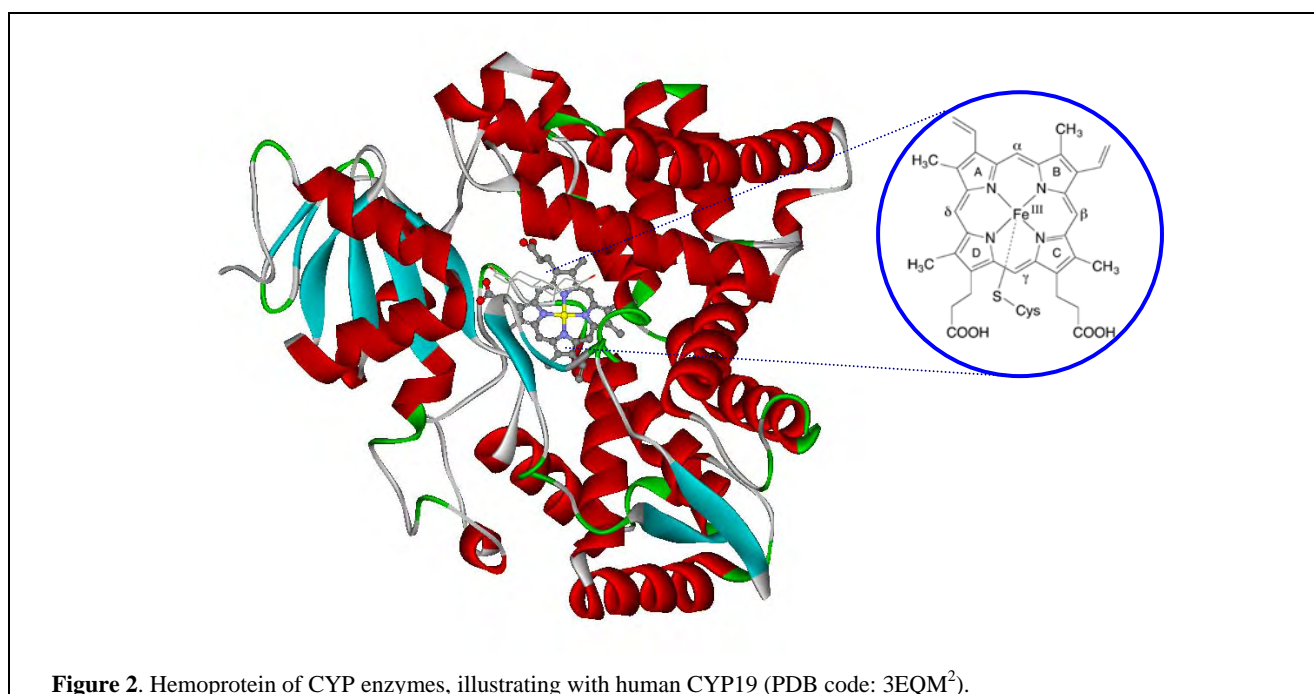


1.1.2 Structure: Hemoprotein and associated Electron Transfer Partners

Most known CYPs are multi-component enzymes consisting of a hemoprotein moiety and associated electron transfer partners (Figure 1). Mitochondrial and most bacterial CYPs, such as CYP11B2, are three component systems (Class I). Besides a hemoprotein, there is a two-component electron shuttle system comprising of ferredoxin and corresponding ferredoxin reductase. The ferredoxin is a kind of iron-sulfur protein, while the ferredoxin reductase is NADPH-dependent and contains FAD (flavin adenine dinucleotide). On the contrary, the microsomal CYPs (Class II) are two component systems containing a heme and a NADPH-dependent cytochrome P450 reductase, which is the combination of FAD and FMN (flavin mononucleotide). Both heme and reductase are membrane bound. The cytochrome P450 reductase catalyzes the transfer of electrons along the pathway $\text{NADPH} \rightarrow \text{FAD} \rightarrow \text{FMN} \rightarrow \text{P450}$. For some cases, cytochrome B5 may also be involved in the electron transfer system, for example CYP17 and CYP3A4. As for Class III CYPs, such as P450 BM3 (CYP102A1), the same cofactors as the class II P450s are observed, but they are soluble and all components are fused into one continuous polypeptide. Moreover, another class of CYPs with all components fused together has been discovered recently. These enzymes are soluble, and comprise the heme domain, ferredoxin, and a NADPH-dependent FMN-containing reductase (Class IV).



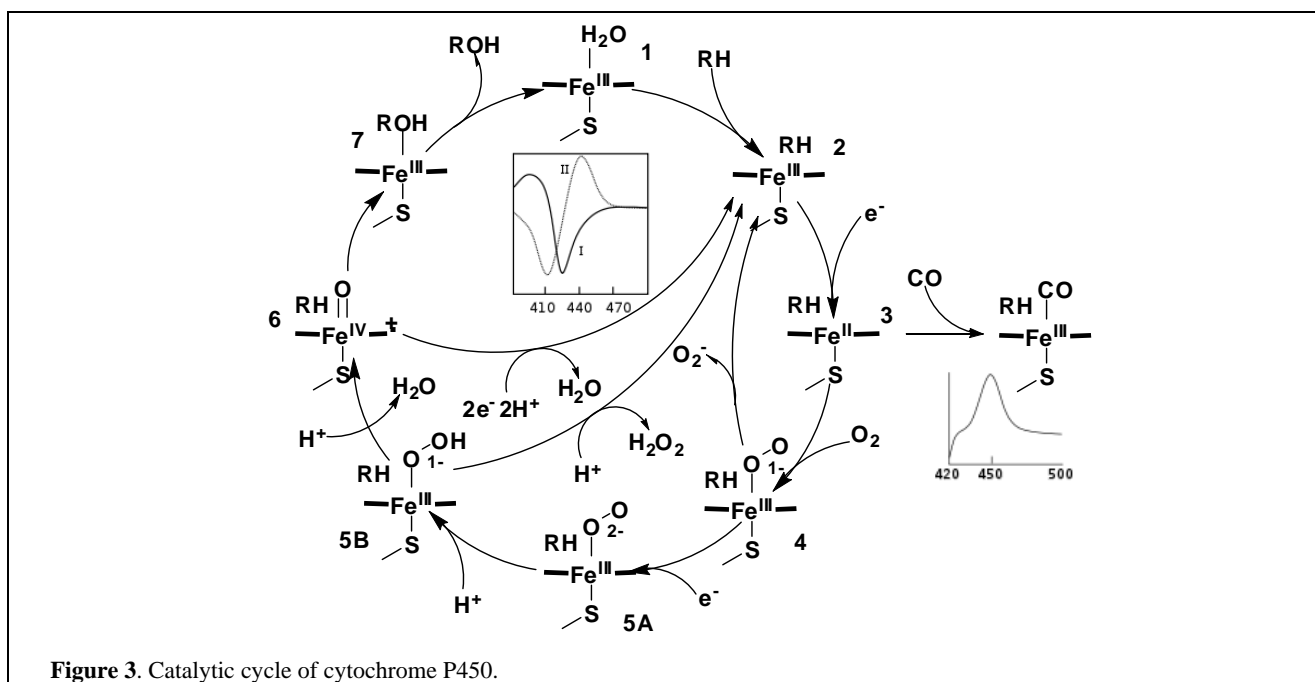
The cytochrome P450s are a series of cysteinato-heme enzymes. In the hemoprotein moiety, iron protoporphyrin as the prosthetic group covalently links to the protein through the sulphur atom of a proximal cysteine ligand (Figure 2). The iron protoporphyrin is the reactive centre to activate oxygen and to oxidize the substrate. Despite poor sequence identity of less than 20% across the superfamily, CYP proteins share similar folding configuration and topology with highly conserved helices A–L. The I and L helices connect with the heme, whereas residues in the B, F and I helices are involved in the recognition, swig, and release of the substrates.³ The most conserved part of the P450 sequence lies in the region containing the Cys, which acts as the thiolate ligand to the heme iron. This conserved sequence is used as the identifying character of CYPs in gene bank.³



1.1.3 Catalytic Mechanism

CYP450s are potent oxidants that are able to catalyze a series of oxidation after the activation of molecule O₂, such as the oxidation of heteroatom, the hydroxylation of saturated carbon-hydrogen bonds, the epoxidation of double bonds and the dealkylation reactions. A common oxidation mechanism has been

proposed involving the sequential two-electron reduction, spin state alternation of the iron, and two protonations⁴ (Figure 3). In the resting state, water is coordinated to the iron as the sixth ligand (1) before the substrate binds in the active site of the enzyme. The binding of substrate often displaces the water molecule, and sometimes changes the state of heme iron from low spin to high spin (2). The change of electronic state favors the transfer of an electron from NAD(P)H via electron transfer system, reducing the ferric ion to ferrous ion (3). This intermediate can be bound by oxygen covalently at the distal axial coordination position of the heme iron leading to an oxy-P450 complex (4). Interestingly, it can also coordinate with CO showing maximum absorption at wave length around 450 nM, which is the origin of the name P450. The oxy-P450 complex as the last relatively stable intermediate is subsequently reduced by a second electron to a peroxo-ferric intermediate (5A), which is then rapidly protonated twice by local transfer from water or from surrounding amino acid side chains, releasing one water molecule, and forming a highly reactive iron(IV)-oxo species (6). After the consequently final oxygenation of the substrate (7) and the release of product, the heme returns to the resting state with a water molecule occupying its distal coordination position.



1.1.4 Functions of CYP Enzymes

Cytochrome P450 enzymes exhibit a wide range of physiological functions. In bacteria and plants, they are mainly involved in detoxification and defense, for example, the biosynthesis of antibiotics. However, for human and animal, CYPs additional function in the biosynthesis of endogenous modulators. It has been established that CYP 1–3 families, which are located predominately in the liver, are responsible for the metabolism of xenobiotics (including drugs). These substances were degraded or furnished with polar groups to facilitate excretion. Yet, CYP 4–51 families are involved in the biosynthesis and deactivation of critical endogenous molecules, which control the development and homeostasis of the body, such as steroid hormones, arachidonic acid, fatty acid, thromboxane, bile acid, prostacyclin and vitamins.

1.1.5 Hepatic CYP Enzymes

As mentioned above, hepatic CYP enzymes are very important in the drug metabolism and excretion. It has been estimated that the metabolism in liver accounts for 73% of the elimination of the 200 top prescribed drugs (Figure 4A).⁵ In this metabolism, 75% of the phase I reactions are achieved by CYP 1–3 families. Among them, 46% of drug oxidations were carried out by the CYP3A family, while 16% by CYP2C9 and 12% for both CYP2C19 and CYP2D6. This ratio is consistent with that of the CYP enzymes expression in liver (Figure 4B), whereby CYP3A4 accounts for 34.4% of the total CYP, whereas 17.3% for CYP2C9, and CYP2E1 and CYP1A2 are 14.6% and 12.5% respectively.^{6,7} This expression ratio may be inherited from ancestors in that they obtained in the long adventure of evolution, and conserved it in the gene. However, it may also be a consequence of induction in the fight with various xenobiotics invading from the outside environment.

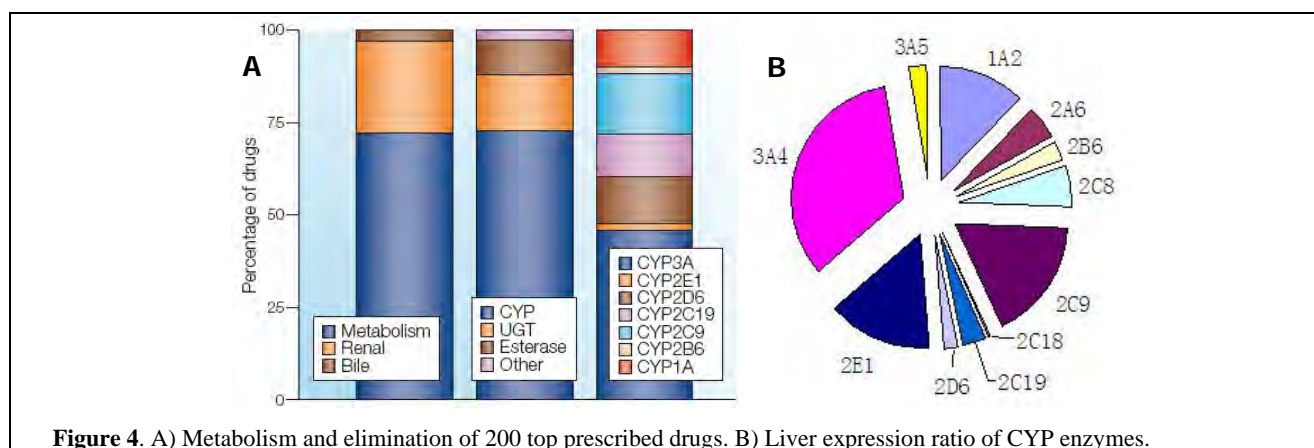


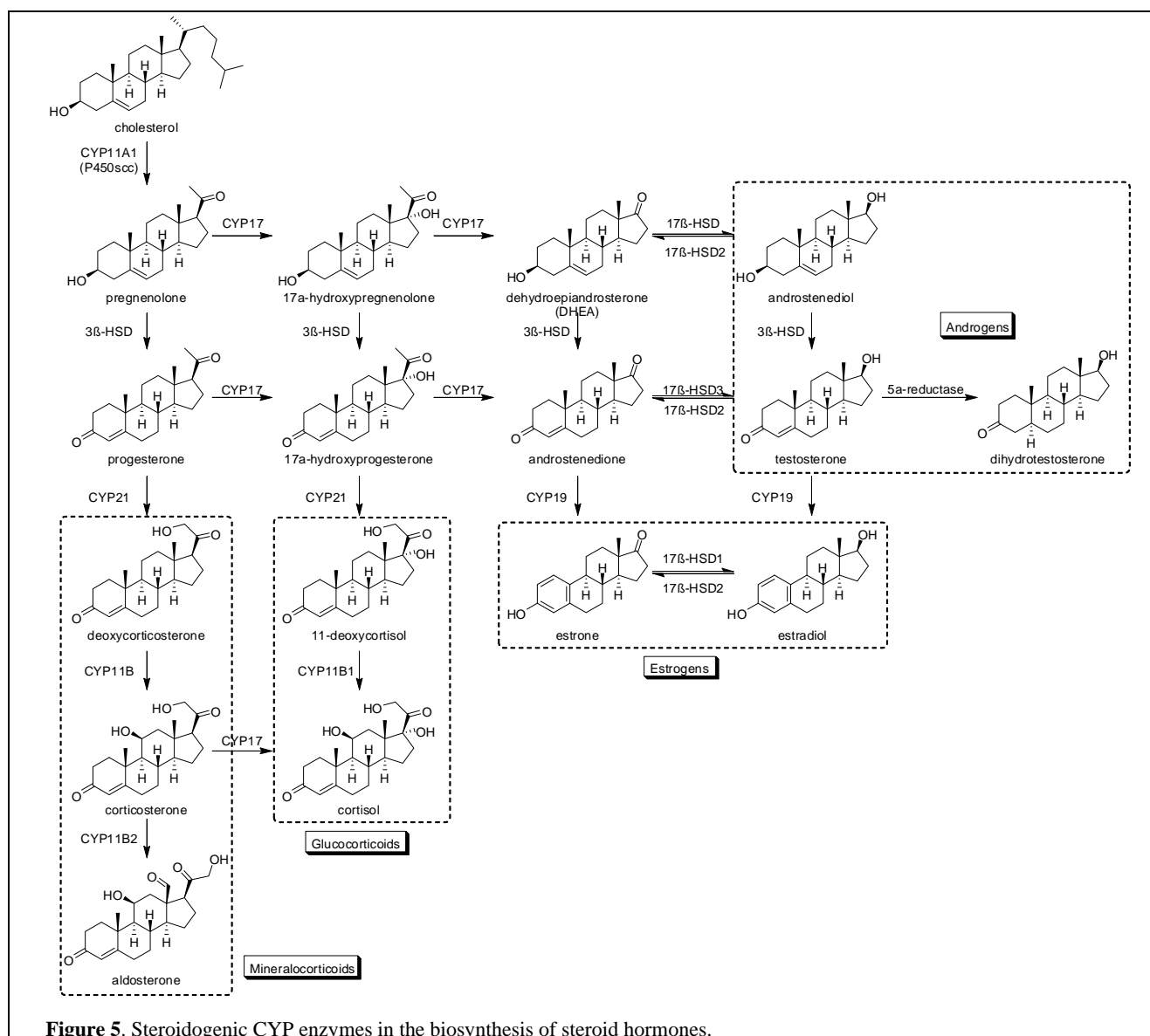
Figure 4. A) Metabolism and elimination of 200 top prescribed drugs. B) Liver expression ratio of CYP enzymes.

The hepatic CYP enzymes are very important in drug discovery and development. For the drugs applied per oral, the first pass effect significantly decreases the plasma drug concentration because the drug is largely metabolized by the hepatic CYPs after gastrointestinal absorption. Therefore, to design drugs hard-to-metabolize but can be excreted aboriginally is a feasible way to improve pharmacokinetic properties. Moreover, compounds inhibiting or inducing hepatic CYP enzymes are at high risk of drug-drug interaction. The inhibition of hepatic CYPs delays the deactivation and excretion of some drugs, whose metabolism are dependent on these enzymes, leading to the accumulation of these drugs inside the body and the consequent toxicity. On the contrary, the induction of hepatic CYP enzymes reducing the plasma drug concentration deteriorates the curative effects. Furthermore, the expression of hepatic CYP enzymes varies among people of different races, genders, ages, and even living environment. It is possible the drug dosage administered is not enough for some people to show response, yet can cause toxicity in other people. Hence, the administration of drugs should according to the situation of patients.

1.1.6 Steroidogenic CYP Enzymes

Steroidogenic CYPs are crucial enzymes in the biosyntheses of steroid hormones, which are responsible for the maintenance of gender characteristics, as well as for the regulation of carbohydrates metabolism, immune system and homeostasis of electrolyte and fluid. The biosyntheses begins with cholesterol, whose side chain is cleaved by CYP11A1 to form pregnenolone (Figure 5). Pregnenolone and progesterone are subsequently converted to dehydroepiandrosterone (DHEA) and androstenedione catalyzed by CYP17,

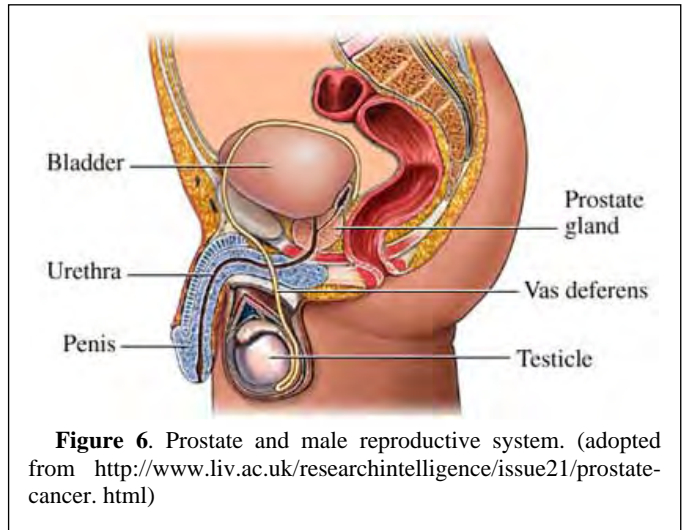
respectively. These two steroids are precursors of androgens (for example: testosterone). Meantime, androstenedione and testosterone can be converted to estrogens (estrone and estradiol), which are catalyzed by aromatase (CYP19). Besides sex hormones, mineralocorticoids (mainly aldosterone) and glucocorticoids (predominantly cortisol) are also synthesized from progesterone and 17 α -hydroxyprogesterone catalyzing by aldosterone synthase (CYP11B2) and 11 β -hydroxylase (CYP11B1), respectively. In these procedures, steroid 21-hydroxylase (CYP21) is involved as the common enzyme. Since some diseases are stimulated by these steroids, the enzymes catalyzing their biosyntheses are possible therapeutic targets. Since CYP11A1 and CYP21 influence the biosyntheses of too many hormones, their inhibition would cause severe toxicity, and they are not suitable targets to be pursued. On the contrary, CYP17 — important for androgen biosyntheses — is a promising target for the treatment of hormone dependent prostate cancer (PCa) and the inhibition of CYP19, which is crucial in estrogen biosyntheses, has already been widely employed in clinic on postmenopausal breast cancer (BC) patients. Moreover, CYP11B1 and CYP11B2, which are responsible for the production of glucocorticoids and mineralocorticoids, respectively, have also been proposed as targets for diseases related to abnormally high concentration of cortisol and aldosterone, for example: Cushing's symptom and congestive heart failure (CHF).



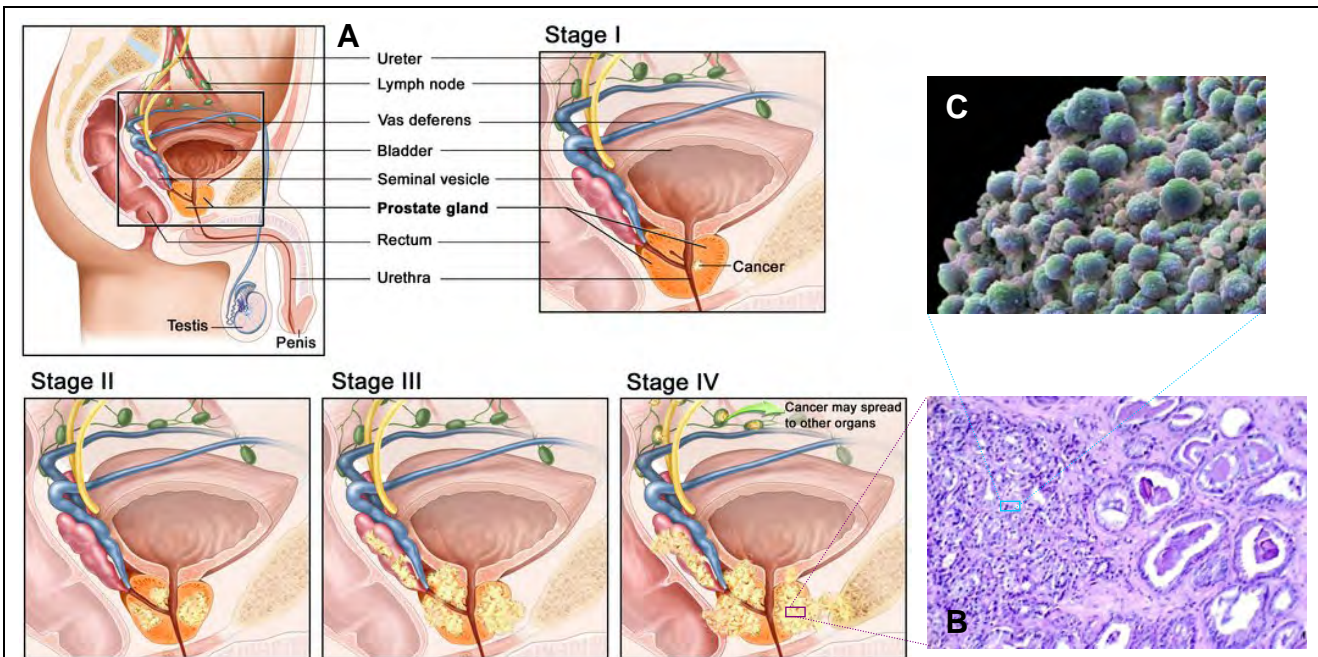
1.2 CYP17 Inhibition as Treatment for Prostate Cancer

1.2.1 Prostate Cancer: Incidence and Diagnosis

Prostate is an important component of the male reproductive system. It lies below the bladder and between the rectum and the public bone (Figure 6 and 7). The urethra originating from the bladder traverses the prostate before exiting to the penis. During ejaculation, sperm is pumped out of the testes and effused into the seminal vesicles via vas deferentia (Figure 7) before being squeezed into the urethra together with the fluids secreted by seminal vesicles and prostate. The fluid secreted by prostate is slightly alkaline to nourish and protect the sperm.



After reaching adulthood, the prostate is vulnerable to some disorders, such as prostatitis, benign prostatic hyperplasia (BPH) and the most severe prostate cancer. It has been estimated that between the years 2003–2007 the incidence rate of prostate cancer was approximately 156.9 per 100,000 men. Moreover, PCa accounted for a quarter of cancer related deaths each year according to NCI report.⁸ Since the symptoms of PCa, like inability and weakness in urination despite a recurring impulse, pains or burning during urination and blood urine, are not specific compared to other prostate disorders, it is necessary to perform early screening if these symptoms are observed. Two screening methods are currently employed in the clinic:



digital rectal examination (DRE) and prostate specific antigen (PSA) blood test. DRE means the examination of the size, shape and texture of the prostate by a figure through the rectum. Although only the back part of the prostate is detectable in this procedure, it is still reliable as most cancers originate there. The observations of stiffness increases, lumps and irregular shapes indicate possible PCa. However, most PCas found by DRE are in the advanced stages with poor prognosis. The other screening method — PSA blood test — determines the plasma level of the protease⁹ produced by the prostate. Patients with a PSA concentration of more than 2.5 or 4 ng/mL are suspected of having of PCa. Although this method is criticized due to its frequent false alarms,¹⁰ which are results of the elevated PSA levels induced by prostatitis, BPH and ejaculation, PSA screening is acknowledged to be successful in reducing prostate cancer mortality.^{11,12} Moreover, the PSA level is also exploited as a biomarker in the treatment of PCa.¹³ The suspected cases identified by DRE or PSA test are ultimately confirmed by ultrasound or magnetic resonance imaging and the most accurate by prostate biopsy.

The tissue obtained through biopsy is subsequently scrutinized under the microscope to check the type, stage and grade of the prostate cancer. Prostatic adenocarcinoma is the predominate type diagnosed, whereas intra- or interepithelial neoplasia and small cell anaplastic prostate carcinoma are rare cases. The most significant discrimination of adenocarcinoma from normal prostate tissue is the shrinkage or even disappearance of stroma and gland lumen (Figure 7B left). The remaining tumorous glands are also irregular in shape. Another hallmark of prostatic adenocarcinoma is the presence of prominent large nucleoli. These histologic appearances are the base of the Gleason grading system, which has been employed as a prognostic factor to predict a patient's time to progression. The cancer can also be staged according to the degree of metastasis. For primary cancer, it can be divided into stage I and II regarding the size and visibility by imaging. Cancer spreading beyond the outer layer of the prostate to nearby tissues, frequently the seminal vesicles, is categorized as stage III; whereas metastasis to local lymph nodes and / or distant organs indicates stage IV. The prostate cancer can metastasize to the bladder, rectum, liver or lungs, yet the most favorable site is bones because the abundant transferrin in bone tissue accelerates the proliferation of cancer cells.¹⁴

1.2.2 Prostate Cancer Treatment — State of Art

1.2.2.I. Watchful Waiting

Watchful waiting implies no treatment other than monitoring the PSA level. It usually applies to patients with less than 10 years life expectancy when the disease progresses very slowly until the life quality is impaired, for example by pain or dysfunction in urination.¹⁵ This is reasonable because it is very probable that these patients would die with PCa other than die of this disease. It is not necessary to have them suffer the possible side effects of the treatment. However, a recent clinical trial showed that the indolent disease would progress aggressively locally or metastasize to distant organs after 15 years. Therefore, early radical therapy is therefore recommended for patients with a life expectancy of 15 years or more.¹⁶

1.2.2.II. Local Therapy: Prostatectomy, Cryotherapy and Radiation Therapy

Local therapy is a set of non-pharmaceutical approaches to treat PCa.

Prostatectomy. The excision of the prostate as well as seminal vesicles is the first line therapy for men

with PCa in stage I or II when they are younger than 70 and otherwise healthy.¹⁵ Prostatectomy is not suitable for advanced disease because it is difficult to remove enough tissue to guarantee negative margins. Although this surgery is relatively safe with an extremely low mortality of 0.4–0.7%, side effects like impotence and incontinence are expected in up to 50% of patients.

Radiation Therapy includes external beam radiation therapy and brachytherapy. The difference between these two kinds of radiation therapy is to cast radiation outside the body or to implant a radiation source (seed) into the tumorous tissue. It is apparent that brachytherapy is more convenient and would usually achieve maximum curative effects with minimum damage to nearby normal tissues. It has been demonstrated that the combination of radiation therapy and hormone therapy is more effective than radiation therapy alone with significantly improved over-all survival and low risk of local recurrency.¹⁷ However, radiation therapy is only suitable for PCa in early stages and the side effects of radiation are inevitable.

Cryotherapy is an alternative to prostatectomy and radiation therapy. It is a minimally invasive surgery effective for recrudescing and radio-resistant PCa in the early stages. Patients under general anesthesia are inserted with needles into the prostate gland through the perineum guided by transrectal ultrasound. Liquid nitrogen is subsequently circulated into the needles to produce a rather low temperature freezing the prostate gland and sometimes seminal vesicles as well. It showed lower risk and discomfort compared to prostatectomy and radiation therapy. It can be repeatedly applied or act as a secondary treatment when other primary treatments fail. However, cryotherapy also causes impotence and the long term efficacy still needs to be proved.

1.2.2.III. Chemotherapy

Cytotoxic agents exert in various ways to destroy cancer cells. Some demolish the membrane integrity of the cancer cells resulting in necrosis, during which the cells swell rapidly, leak cytoplasm and organelle, and ultimately lyse. Some arrest the mitosis and prevent proliferation and differentiation. Others induce apoptosis characterized by cytoplasmic shrinkage, nuclear condensation, and cleavage of DNA into regularly sized fragments. However, cytotoxic agents act on all cells mitosing rapidly. Some normal cells other than cancer cells are therefore simultaneously damaged, especially cells in the bone marrow, digestive tract, and hair follicles, which lead to some common side effects, such as myelosuppression (decreased production of blood cells), mucositis (inflammation of the lining of the digestive tract) and alopecia (hair loss). Despite these side effects, cytotoxic agents are suitable choices for the advanced PCa.

Docetaxel (Figure 8) belonging to the taxane class inhibits the dynamic reorganization of microtubule networks, which is essential to vital interphase and mitotic cellular functions. Due to this mechanism, docetaxel is mainly active in the S phase of the cell cycle. This drug launched in 2004 is the first cytotoxic agents approved to treat PCa. Previously, cytotoxic agents had been regarded for a long time as impotent for PCa. A clinical trial of the combination of docetaxel and prednisone (a glucocorticosteroid, which is believed to be able to augment the efficacy of chemotherapy) demonstrated improved median survival time and reduced hazard ratio compared to mitoxantrone (another cytotoxic agent, described in detail below).¹⁸ Due to the survival achieved, this combination is considered the most effective treatment for metastatic, hormone refractory PCa.

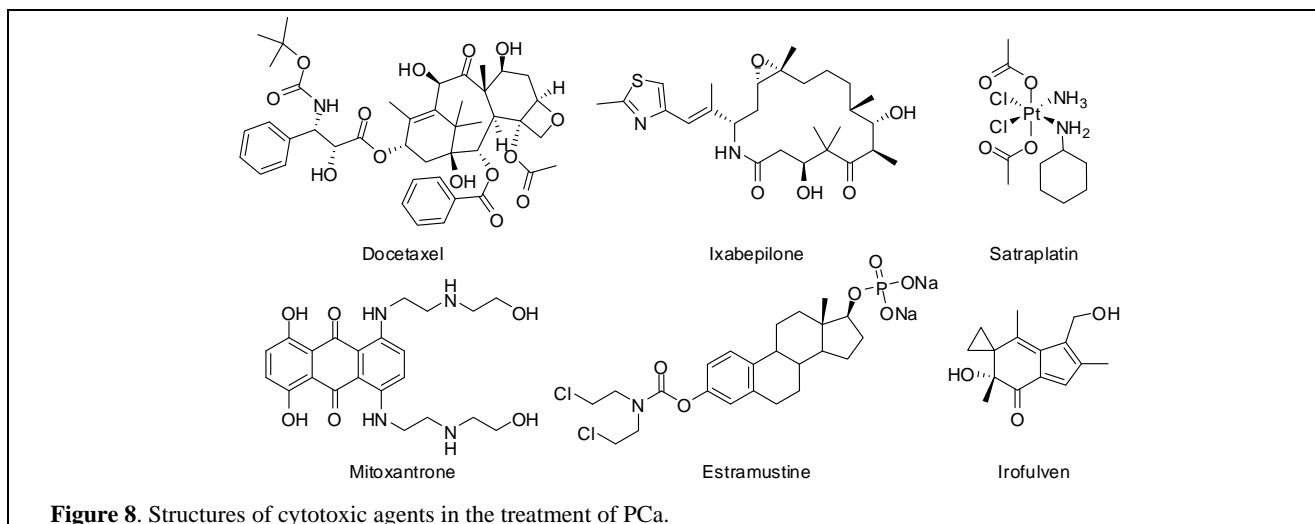


Figure 8. Structures of cytotoxic agents in the treatment of PCa.

Estramustine (Figure 8) is postulated to act in a dual mechanism that the intact molecule stabilizes the microtubule dynamics, whereas some metabolites exhibit antigonadotrophic effects resulting in the suppression of testosterone production.¹⁹ Patients showed good response to estramustine solo²⁰ or the combination of docetaxel / estramustine.²¹ However, severe gastrointestinal and cardiovascular toxicity was observed.

Mitoxantrone (Figure 8) is an anthracenedione antitumor antibiotic. It intercalates DNA leading to intrastrand cross-linking and binds to the phosphate backbone of DNA resulting in DNA strand rupture. Mitoxantrone also interferes with topoisomerase II. These multi actions cause nonspecific arrest of all cell cycle phases, with late S phase as the most sensitive one. Mitoxantrone exhibits no improvement to overall survival, however it is well tolerated and therefore could be a useful palliative treatment.²²

Ixabepilone (Figure 8) is an epothilone tubulin inhibitor in Phase II development for PCa. This drug acts in a similar mechanism as docetaxel by inducing microtubule polymerization, forming multipolar spindles and mitotic arrest. It is expected to overcome the resistance that docetaxel has encountered involving the drug efflux protein P-glycoprotein.

Besides, some more cytotoxic agents are under development; for example: satraplatin (Figure 8), as the third generation of platinum complex, is oral bioavailable; as well as irofulven (Figure 8), which is an illudin analogue, blocks transcription and induces apoptosis after binding to the DNA.

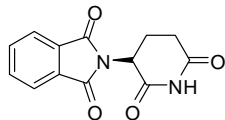
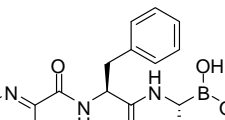
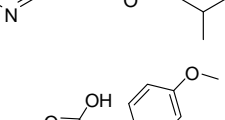
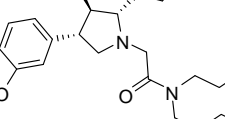
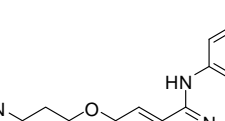
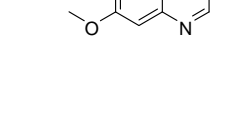
Furthermore, there are some other promising agents in the pipeline acting in various mechanisms (Table 1), such as anti-angiogenesis, proteasome inhibitors and antisense oligonucleotide.

1.2.2.IV. Vaccines and Immunotherapy

Cancer immunotherapy is a set of approaches attempting to awaken the patients' immune system to kill cancer cells after the intervention of vaccines. Although there are still no vaccines launched into the market for PCa, several drug candidates in late clinical trial phases are very promising.

Provenge is composed of modified dendritic cells, which is an important component of immune system and can be isolated from the corresponding patient's blood. These dendritic cells are trained by incubating with a fusion protein comprising prostatic acid phosphatase, which is an enzyme produced by PCa cells, and a dendritic cell-targeting element for 48 hours before being re-administered to the patient. These cells

Table 1. Promising drug candidates in various mechanisms other than cytotoxicity.

Drug	Structure	Mechanism	Phase	Pharmacology	Side effects
Bevacizumab ²³		Monoclonal antibody, targeting vascular endothelial growth factor A	II	PSA level reduction	thrombosis, fatigue
Thalidomide ²⁴		enhances interleukin-2 (IL-2) activity, suppresses TNF-alpha, down-regulates IL-6 and inhibits angiogenesis induced by beta-fibroblast growth factor (β -FGF) and VEGF	II	PSA response	Thromboembolism, constipation, fatigue, neurotoxicities.
Bortezomib ²⁵		Proteasome Inhibitors, stimulates apoptosis	I / II	PSA level reduction, reverse taxane resistance when combined	diarrhea, peripheral neuropathy, hyperglycemia, neutropenia, fatigue
Atrasentan ²⁶		Endothelin-Receptor Antagonists,	III	Delayed time to progression, PSA level reduction	peripheral edema, bone pain, anemia, asthenia
Gefitinib ²⁷		Epidermal Growth Factor Receptor Inhibitors	II	No significant differences in progression rates, time to progression, and overall survival compared to placebo.	rash, diarrhea
Oblimersen ²⁸		Antisense oligonucleotide, blocks the production of Bcl-2	II	PSA level reduction when combining with docetaxel.	fatigue, fever, nausea

consequently lead the immune system to destroy cancer cells producing acid phosphatase. Although this vaccine shows little influence on the PSA level, the overall survival is largely improved.²⁹

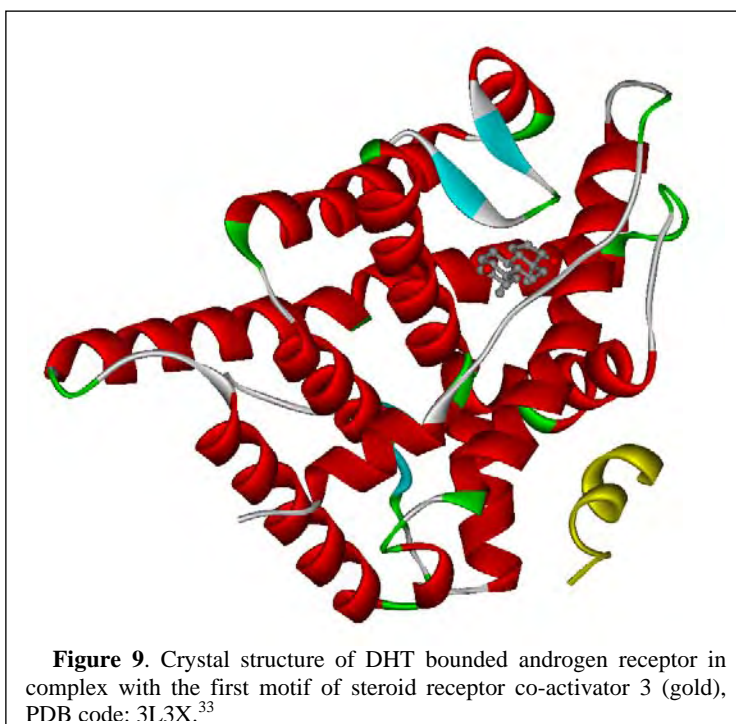
Compared to the personalized approach of provenge, GVAX is more general and therefore less expensive. GVAX is based on PCa tumor cells genetically engineered to secrete granulocyte-macrophage colony-stimulating factor, which is a hormone stimulating immune response. This vaccine showed a dose-dependent prolongation of survival and longer median progression time.³⁰ However, it sometimes fails to invoke immune response in certain patients.

1.2.2.V. Hormone Therapy

Although a lot of PCa therapies have emerged, most of them are only suitable for cancer in early stages. For advanced diseases, especially the ones with metastasis, hormone therapy is the most effective treatment.

Androgens Stimulate Prostate Cancer Proliferation. It has been established that the growth of up to 80% of PCa is androgen dependent.³¹ Therefore, segregation of tumor cells from androgen will effectively prevent cancer cell from proliferation and this is the mechanism base of hormone therapy.

It is believed that androgens promote the cancer growth via binding to androgen receptor (AR), which is highly over-expressed in PCa cells. AR belongs to the steroid and nuclear receptor superfamily,³² and is similar to other members such as estrogen receptor (ER), mineralocorticoid receptor (MR) and progesterone receptor (PgR) in structure (Figure 9) and function manner.³⁴ AR is a soluble protein acting as an intracellular transcription factor. Unbound ARs floating in the cytoplasm are associated with heat shock proteins through interactions with the ligand binding domain.³⁵ Once androgen binds to the AR,



it triggers a series of sequential conformational changes of the receptor which affect receptor protein interactions and receptor DNA interactions. The AR first dissociates from the heat shock proteins, then dimerizes, been phosphorylated and consequently translocates into the nucleus. It is notable that phosphorylation or dephosphorylation of androgen receptor has been deemed as a determinant of androgen agonistic or antagonistic activity.³⁶ The translocated receptor subsequently binds to the androgen response element located in the promoter or enhancer region of gene that AR targeting. Recruitment of other transcription co-regulators³⁷ (for example: steroid receptor co-activator 3 (Figure 9)) and transcriptional machinery³⁸ further initiates the transactivation of AR regulated gene expression, which exhibits various physiological or pathological function; for prostate cancer cells the mitogenic effects. Some evidences³⁹ indicate that the recruitment of different co-regulators (co-activator or co-repressor) is another switch of

agonistic or antagonistic activity. Moreover, besides the genomic effects, the nongenomic pathway of AR has also been observed in prostate,^{40,41} which is the direct interactions between AR and cytosolic proteins from various signaling pathways. These nongenomic actions rapidly activates kinase signaling cascades or modulates intracellular calcium levels, which possibly contribute to the survival and proliferation of PCa cells.⁴²

Central Role of CYP17 in Androgen Biosynthesis. Two major androgens are produced endogenously as substrates of AR: testosterone and 5 α -dihydrotestosterone (5 α -DHT). The biosyntheses of androgen starts from cholesterol, which is produced in the metabolism process of fatty acid. After the side chain of cholesterol is cleaved by CYP11A1, which is the rate limiting step of the whole procedure, pregnenolone and progesterone (after further dehydrogenation catalyzed by 3 β -hydroxysteroid dehydrogenase (3 β -HSD)) are obtained. These two steroids are firstly hydroxylated at the 17 position and then the C17–20 bond is cleaved catalyzing by CYP17 to yield DHEA and androstenedione, which are subsequently converted to testosterone (Figure 5). More than 90% of the circulating testosterone is produced in the Leydig cells in the testes, whereas the rest is synthesized in adrenals. It has also been reported that minor portion of testosterone originates from prostate cancer cell in a paracrine or autocrine manner.^{43–45} Circulating testosterone is predominately sequestered to sex hormone-binding globulin and albumin, with only approximately 2% as free unbound hormone. After testosterone fluxes into the prostate, it is then converted to the most potent androgen DHT catalyzed by 5 α -reductase (5 α -R). These two androgens consequently bind to the AR of prostate cancer cells and stimulate them to proliferate.

Regulation of Androgen Biosynthesis. The androgen biosyntheses is regulated by hypothalamic – pituitary – gonadal / adrenal axes. Hypothalamus is a basic modulator controlling body temperature, immune responses and blood pressure. It secretes many hormones which take effect after being distributed to the pituitary via hypophyseal portal system, for example: gonadotropin-releasing hormone (GnRH, also known as LHRH, hypothalamic luteinizing hormone-releasing hormone) and corticotropin-releasing hormone (CRH) (Figure 10). GnRH and CRH stimulate the release of gonadotropins (Gn, including follicle-stimulating hormone (FSH) and luteinizing hormone (LH)) and adrenocortico-tropic hormone (ACTH) from anterior pituitary, respectively. Consequently, gonadotropins and ACTH trigger the production of androgens in testes and adrenals after binding to the corresponding receptor. When the concentration of testosterone is high enough, it will hold back the release of GnRH and CRH via negative feedback mechanism.

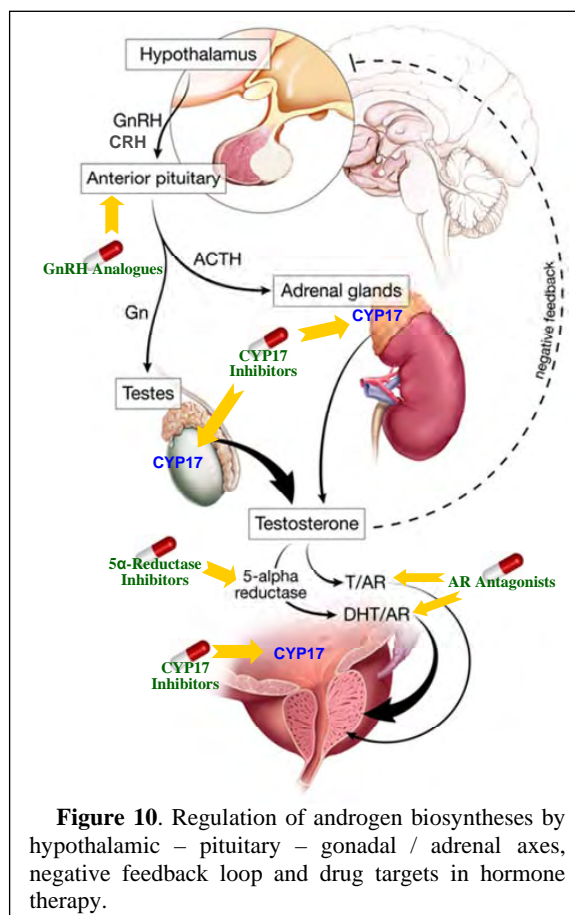


Figure 10. Regulation of androgen biosyntheses by hypothalamic – pituitary – gonadal / adrenal axes, negative feedback loop and drug targets in hormone therapy.

Potential Targets regarding Androgen Stimulation. As mentioned above, the segregation of tumor cells from androgen will be effective treatments for PCa. Two approaches are possible to achieve this goal: blocking AR, by which AR antagonists have been applied in clinic for many years; or interrupting the biosyntheses and release of androgen (Figure 10). For the latter, several nodes in androgen production system are important, yet not all of them are suitable targets. As inhibitors of 5α -R reduce the intracellular prostatic DHT concentration, they are exploited in the treatment of benign prostatic hyperplasia. However, due to testosterone stimulates cancer cell growth as well, 5α -R inhibitors did not show response in PCa patients. Moreover, ACTH controls the biosyntheses of glucocorticoids and mineralocorticoids besides androgen, therefore ACTH and CRH are not feasible targets either. Still there are some methods that have once been employed in clinic but dropped because of obvious drawback or more and more replaced by some other emerging therapies.

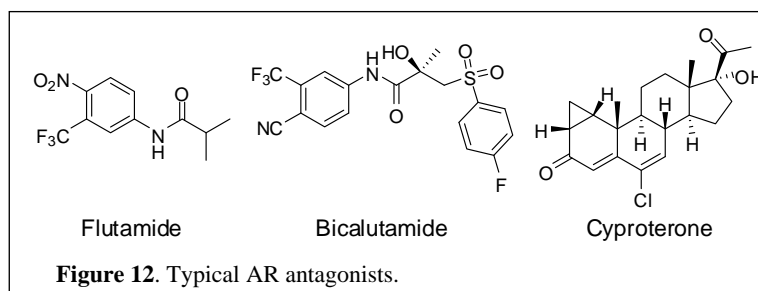
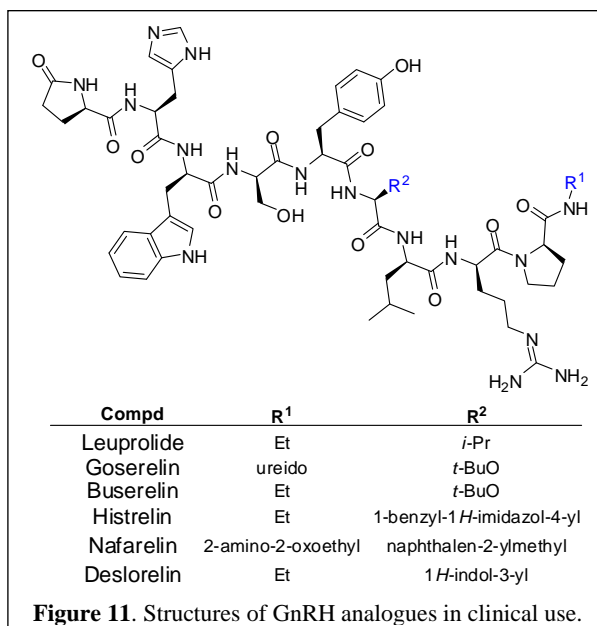
Estrogen and Progesterin. Early attempts to suppress androgens production by estrogen and progesterin application⁴⁶ were soon abandoned because of gynecomastia and elevated cholesterol level resulting in higher risk of cardiovascular diseases.

Orchidectomy. The fact that more than 90% of androgen is produced in testes makes castration an easy and reasonable therapy. It is also inexpensive compared to other long-term therapies. However, not everyone is willing to take permanent impotency as a consequence.

GnRH Analogues (Agonists and Antagonists).

This therapy is also known as “chemical castration”. The initial application of GnRH agonists leads to a surge of FSH and LH secretion after binding to the corresponding receptor in gonadotrope cells in pituitary. This surge causes a large amount of testosterone produced in testes, and tumor growth spurt (termed tumor flare). Nevertheless, after around ten days, these gonadotrope cells are no longer sensitive to endogenous GnRH and GnRH agonists resulting in the decline of testosterone levels comparative to that after castration. This reduction lasts as long as GnRH agonists consecutively administrated.⁴⁷ On the contrary,

GnRH antagonists competitively bind to the GnRH receptor and consequently block the gonadotropins release directly. GnRH analogues, such as leuprolide, goserelin, and buserelin (Figure 11), annihilate androgen produced in testes, however, have no effect on adrenals. Although more than 90% of androgen is no longer produced and the plasma testosterone concentration is reduced to less than 50 ng/dL, the concentrations of androgen



inside prostate are still high enough to enable the growth of cancer cells.^{48,49} Moreover, as side effects GnRH analogues cause testicular atrophy and loss of bone mineral density.

AR antagonists (Antiandrogens). Since GnRH analogues are unable to block the androgen produced in adrenals, which continually stimulate cancer growth, AR antagonists (Figure 12) are exploited in combination. This is the current standard therapy, so-called **combined androgen blockade (CAB**, also known as androgen deprivation). Clinical trials demonstrate the effect of AR antagonists as mono-therapy is not satisfactory, which renders CAB as the best way to apply. Normally, antiandrogen is begun several days before GnRH analogues application in order to prevent the initial tumor flare resulting from the surge of testosterone. Since steroidal AR antagonists are less potent than non-steroidal ones and suppress other steroids produced in adrenals, steroidal AR antagonists are rarely employed. Although CAB achieves delayed disease progression and improved survival,⁵⁰ it is also associated with cardiovascular death.⁵¹ Furthermore, the long term application of antiandrogen induces AR mutations, such as T877A and W741C, which render the receptor's capability to recognize some AR antagonists^{52,53} and glucocorticoids⁵⁴ as agonists, thus resulting in the resistance to CAB.

1.2.3 CYP17 Inhibition as Treatment for Prostate Cancer

All these shortcomings of current therapies invoke CYP17 inhibition as a promising alternative because of its central role in androgen biosyntheses. Inhibition of CYP17 totally blocks the production of androgen not only in testes and adrenals, but also, and importantly, inside prostate cancer cells. This autocrine or paracrine of androgen inside prostate is at least partly responsible for the failure of CAB and the progression of the PC cell from androgen sensitive to “refractory”.

CYP17 comprises 508 amino acids with an approximate molecular weight of 57 kDa and is coded by gene *CYP17* located in chromosome 10 q24.3.⁵⁵ Since this enzyme binds to the endoplasmic reticulum, its crystal structure is not solved yet. Nevertheless, several homology models have been built based on soluble bacterial CYPs⁵⁶ or multi CYP templates (Figure 13).⁵⁷

CYP17 is the hinge in steroid biosyntheses route. In the adrenal zona glomerulosa where no CYP17 expressed, steroidogenesis goes

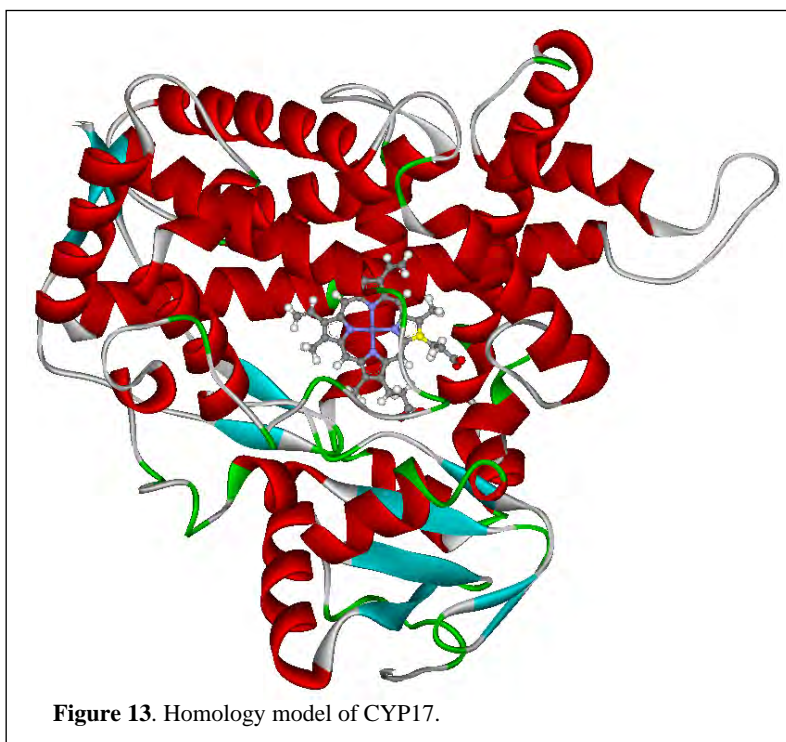


Figure 13. Homology model of CYP17.

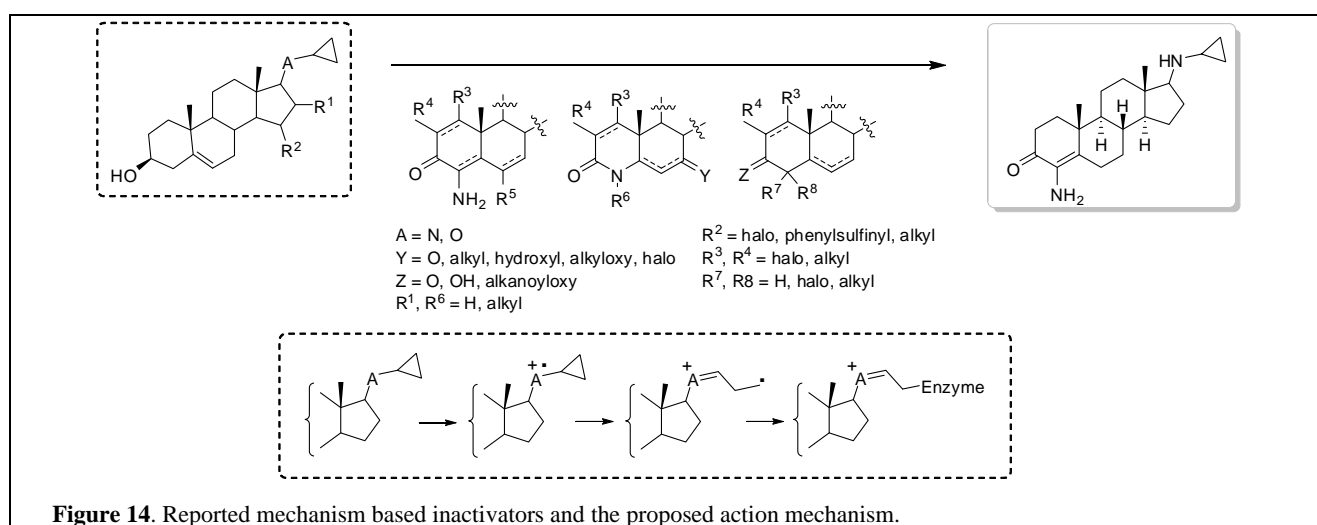
directly to the mineralocorticoid aldosterone. On the contrary, in the zona fasciculata and zona reticularis, the presence of CYP17 ensures the production of other steroids. Nevertheless, this enzyme still acts as a switch to control the syntheses of different steroids in different areas due to its bifunctionality in catalysis, namely

17 α -hydroxylase and 17,20-lyase activities. In the zona fasciculata, 17 α -hydroxylation is predominated leading to the favored glucocorticoids synthesis; whereas in the zona reticularis and gonads, these two activities both present promoting the production of sex hormones (Figure 5).⁵⁸ Although the reason for this interesting phenomenon is still unclear, several regulators of 17,20-lyase activity have been identified, such as the abundance of osidoreductase⁵⁹ and cytochrome b5⁶⁰ as well as the phosphorylation of serine and threonine residues.⁶¹

The inhibition of CYP17 can be achieved via several approaches:

1.2.3.I. Mechanism Based Inactivators

In 1980s, scientists found that cyclopropyl group could irreversibly bind to the P450 enzymes.^{62,63} It is believed that the cyclopropyl compound was activated by enzymatic one-electron oxidation of nitrogen or oxygen atom, which connects directly to the cyclopropyl, thereby resulting in the cleavage of cyclopropyl ring and subsequent reactive radicals. These radicals covalently bind to CYP17 while still binding in the active site, and therefore inactivate the enzyme (Figure 14).^{62,63} This finding was soon applied in the design of CYP17 inhibitors.⁶⁴ Besides cyclopropyl amino or ether, modifications were also created by introducing amino, amide or some other substituents at the steroidal 4-position, thus rearranging the double bonds and inserting methylene to steroidal scaffold.^{65,66} These efforts led to some potent CYP17 inhibitors acting in a time dependent manner. Although these compounds arrested the growth of androgen dependent human prostatic tumor in mice, they were less effective than castration.^{65,66}



1.2.3.II. Inhibition via Coordination between sp^2 hybrid N and Heme Iron

This reversible competitive inhibition mechanism was firstly identified for CYP19 inhibitors,⁶⁷ but soon the application expanded to almost all CYPs inhibitors. Although using O⁶⁹ or S⁶⁸ as the coordination centre was also attempted, N is always the most common and effective one.

Steroidal inhibitors. The early designed CYP17 inhibitors are simple combinations of steroidal scaffolds and various N containing heterocycles. It has been found that pregnenolone analogues are always more potent than the corresponding progesterone ones, which is consistent with the fact that pregnenolone shows higher affinity toward CYP17 compared to progesterone. A lot of heterocycles have been introduced onto the steroidal scaffold, such as pyridine, pyrimidine, imidazole, triazole, oxazole, thiazole, benzoimidazole and so

forth.⁷⁰ Besides inhibition of CYP17, most of the steroidal inhibitors also show 5 α -reductase inhibitors and/or affinity toward the androgen receptor. Nevertheless, good selectivity can still be achieved by some compounds, especially Abiraterone.

Abiraterone (Figure 15) is a potent and selective CYP17 inhibitor showing $K_i < 1$ nM and no interference with CYP19 or 5 α -reductase.⁷¹ The Δ 16–17 double bond is believed to be crucial for the inhibitory potency,⁷² and it is probably also responsible for the irreversible inhibition manner of Abiraterone. Although the short plasma half life (1.6 h) forces a high dose to be applied (500 mg daily), Abiraterone reduces plasma testosterone concentration to less than 0.2 nM in 2 hours after oral administration.⁷³ In the phase II/III clinical trials, patients diagnosed with castration resistant prostate cancer showed good responses to Abiraterone characterized by the reduce of PSA level and circulating tumor cells (CTC) counts.⁷⁴ These successes further prove the conception of CYP17 inhibition as a treatment for PC and elucidate that PCs previously misapprehended as androgen independent are commonly remain hormone driven.⁷⁴

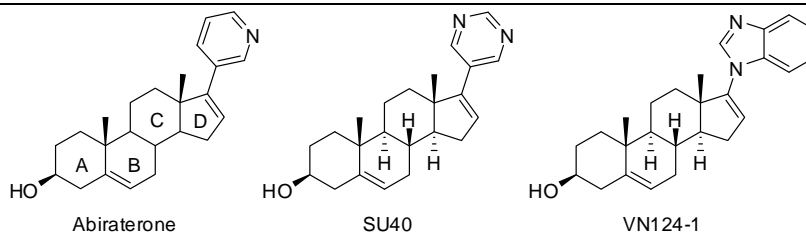


Figure 15. Representative steroidal CYP17 inhibitors.

Su40⁷⁵ (Figure 15) and **VN124-1**⁷⁶ (Figure 15) are CYP17 inhibitors that are even more potent than Abiraterone in vitro and in vivo. Besides inhibiting CYP17, VN124-1 also acts as an AR antagonist, down-regulates AR expression,⁷⁷ and induces endoplasmic reticulum stress response,⁷⁸ which are also thought to contribute its antitumor efficacy.

Although many steroidal inhibitors are very potent, the potential drawbacks of these compounds should not be ignored: the relative short half life or poor bioavailability, the first pass effect when orally administered and the affinity toward steroid receptors which might result in side effects regardless acting as agonists or antagonists.

Non-steroidal inhibitors. Due to the potential shortcomings of steroidal inhibitors described above, it is rational and promising to focus the interest on non-steroidal CYP17 inhibitors. Several classes of non-steroidal compounds have been designed with potent inhibition in vitro or in vivo, and some of them also exhibit good pharmacokinetics properties.

Ketoconazole (Figure 16), as an antimycotic agent showing non-selective inhibition toward CYP enzymes, is the first medication which has been clinically used in treatment of prostate carcinoma as a CYP17 inhibitor. Although withdrawn because of side-effects, Ketoconazole shows good curative effects,⁷⁹ which elucidate the feasibility of prostate carcinoma treatment via CYP17 inhibition.

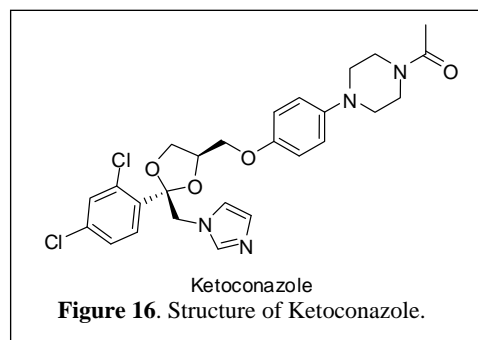
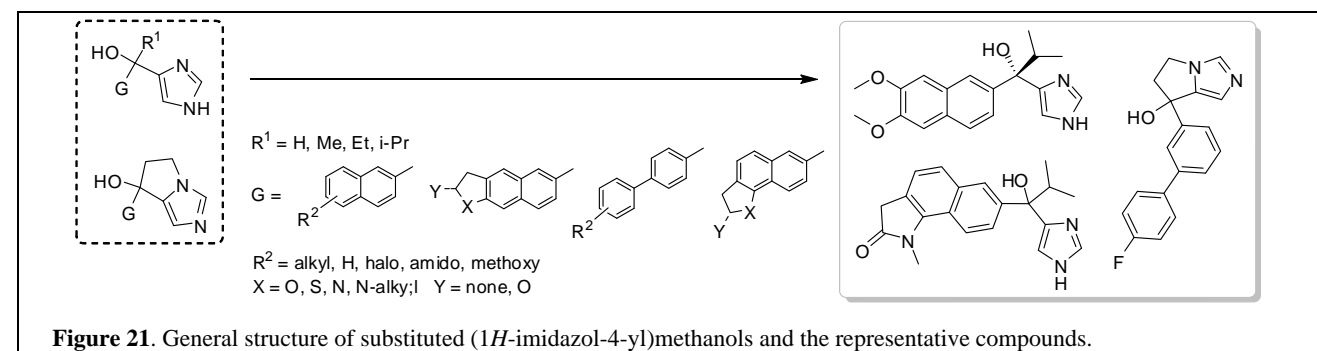
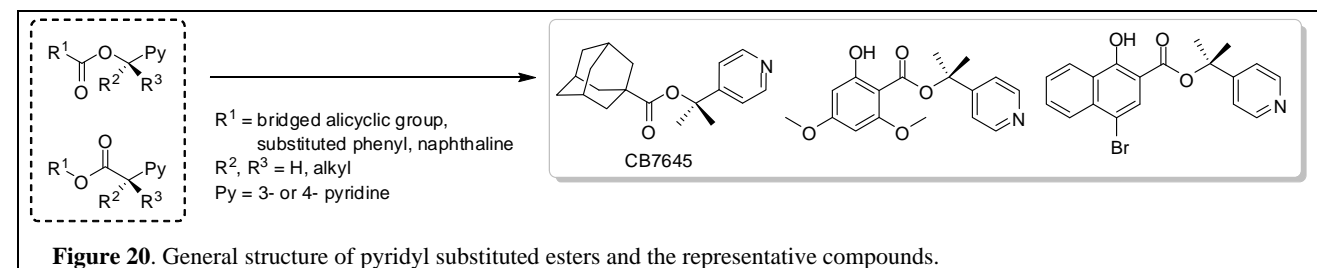
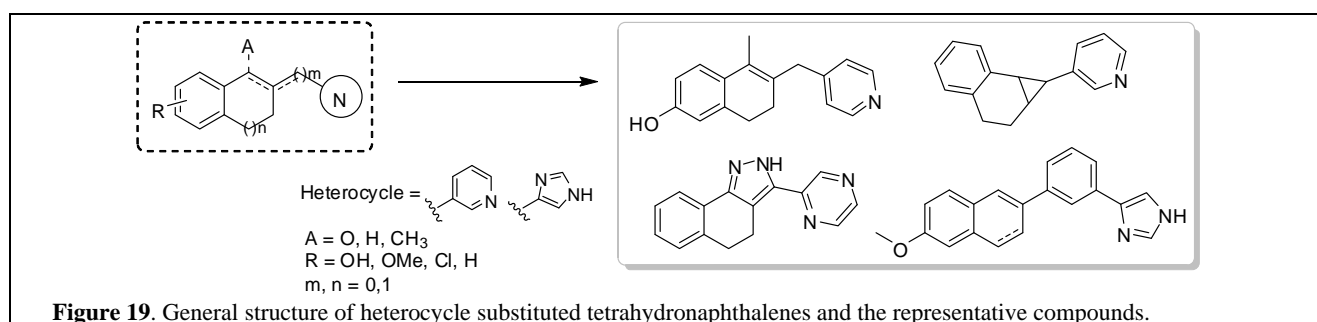
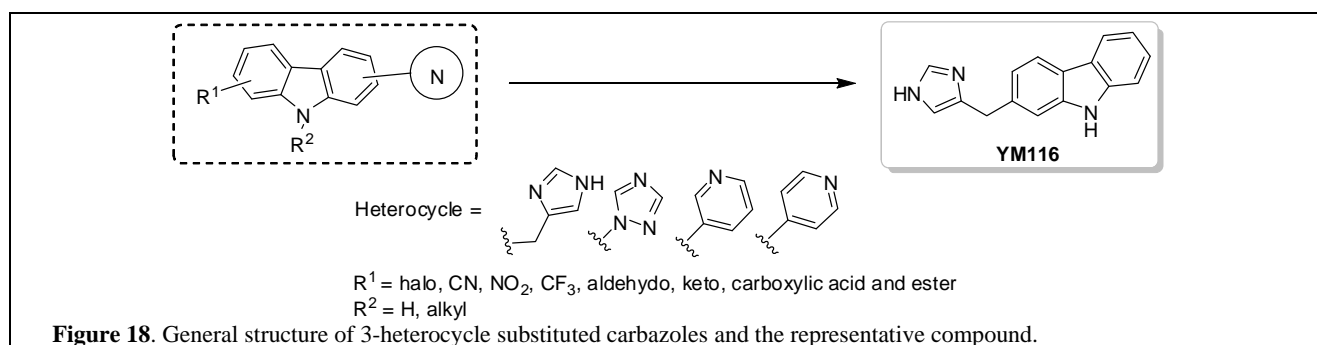
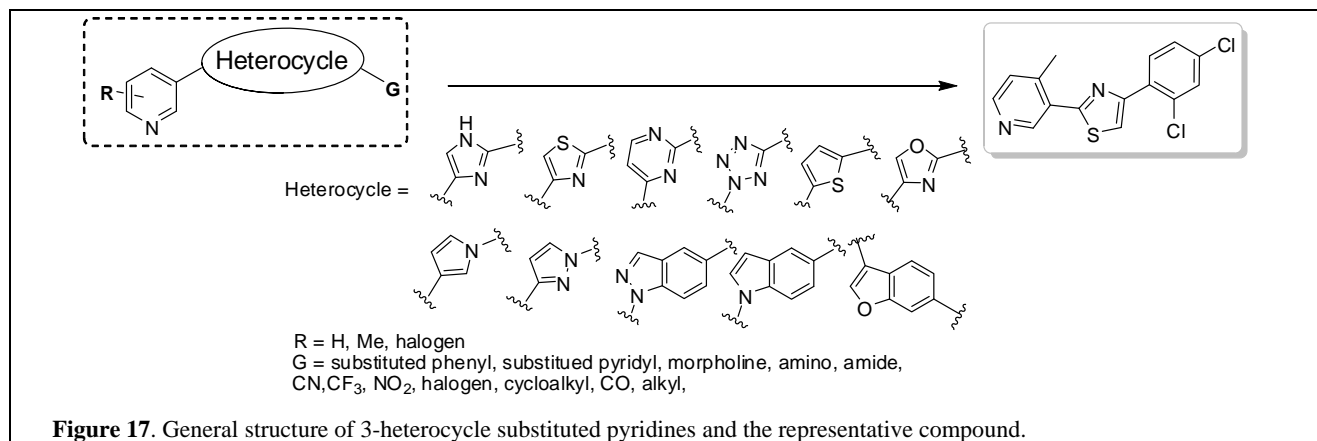
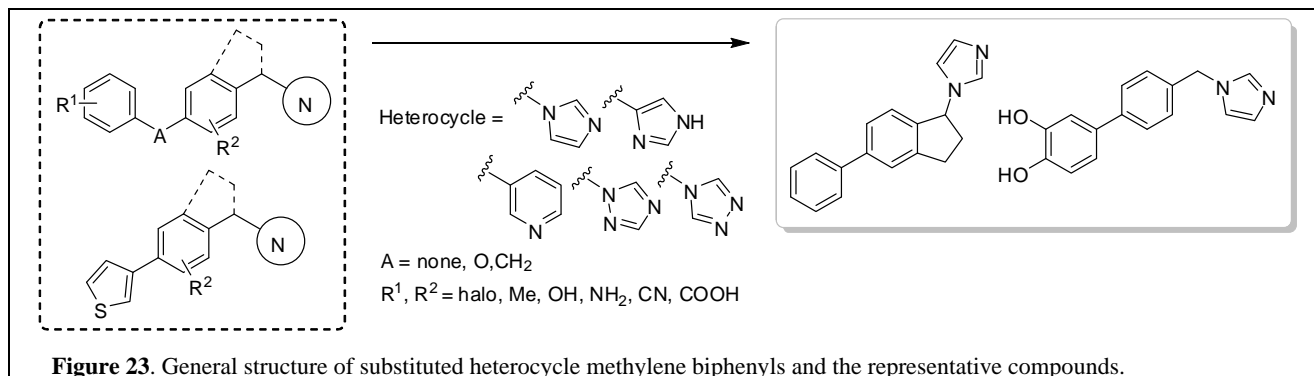
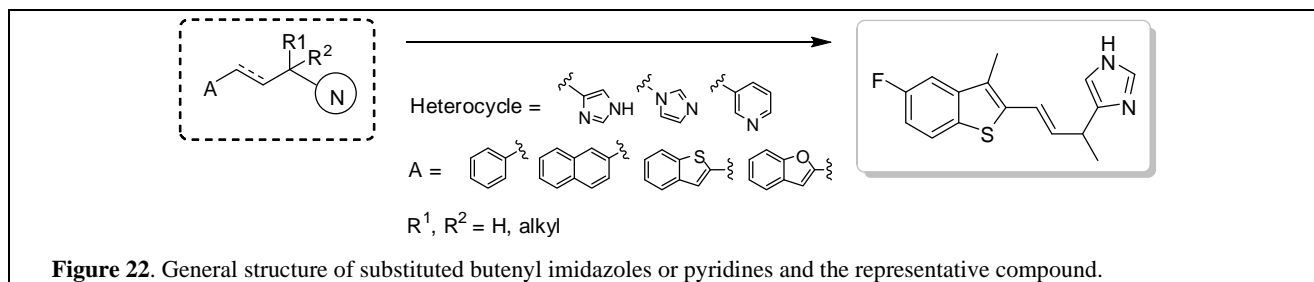


Figure 16. Structure of Ketoconazole.

Furthermore, **3-heterocycle substituted pyridines** (Figure 17),⁸⁰ **heterocycle substituted carbazoles** (Figure 18),^{81,82} **heterocycle substituted tetrahydronaphthalenes** (Figure 19),^{83,84} **pyridyl substituted esters** (Figure





20),⁸⁵⁻⁸⁷ substituted (1H-imidazol-4-yl)methanols (Figure 21),⁸⁸⁻⁹⁰ substituted butenyl imidazoles or pyridines (Figure 22)^{91,92} and substituted heterocycle methylene biphenyls (Figure 23)⁹³⁻⁹⁶ have been designed, synthesized and bio-evaluated. Although some compounds exhibit good pre-clinical results, no compound has been reported to enter into clinical trials. Therefore, more efforts are necessary for non-steroidal CYP17 inhibitors to identify potential drug candidates.

1.3 CYP11B2 Inhibition for Diseases related to High Aldosterone Levels

1.3.1 Aldosterone: Physiology and Pathology

1.3.1.I. Mineralocorticoid Regulating Electrolyte and Fluid Homeostasis

Since its discovery in 1953, aldosterone has long been considered as the mineralocorticoid in circulation only to regulate electrolyte and fluid homeostasis for a long time.⁹⁷ It is widely accepted that after the binding of aldosterone to mineralocorticoid receptor (MR) in epithelial cells of renal collecting ducts, a conformational change of MR is achieved. This renders MR to migrate into the cell nucleus and to ultimately activate gene transcription modulating the activity of amiloride-sensitive epithelial sodium channel (ENaC). As results, sodium and water are retained, thereby leading to the increase of blood volume and consequently elevated blood pressure.

1.3.1.II. Deleterious Effects of High Aldosterone Levels to Heart, Vessels and Kidney

Nevertheless, recent studies have revealed that aldosterone elicits some additional, non-classic effects on vessels, heart, kidney and central nervous system. Accordingly high aldosterone concentration exhibits various deleterious effects on its target organs, the severest being on the heart⁹⁸ (Figure 24). Aldosterone is a potent pro-inflammation factor^{99,100} and is capable of inducing reactive oxygen species (ROS).¹⁰¹ These

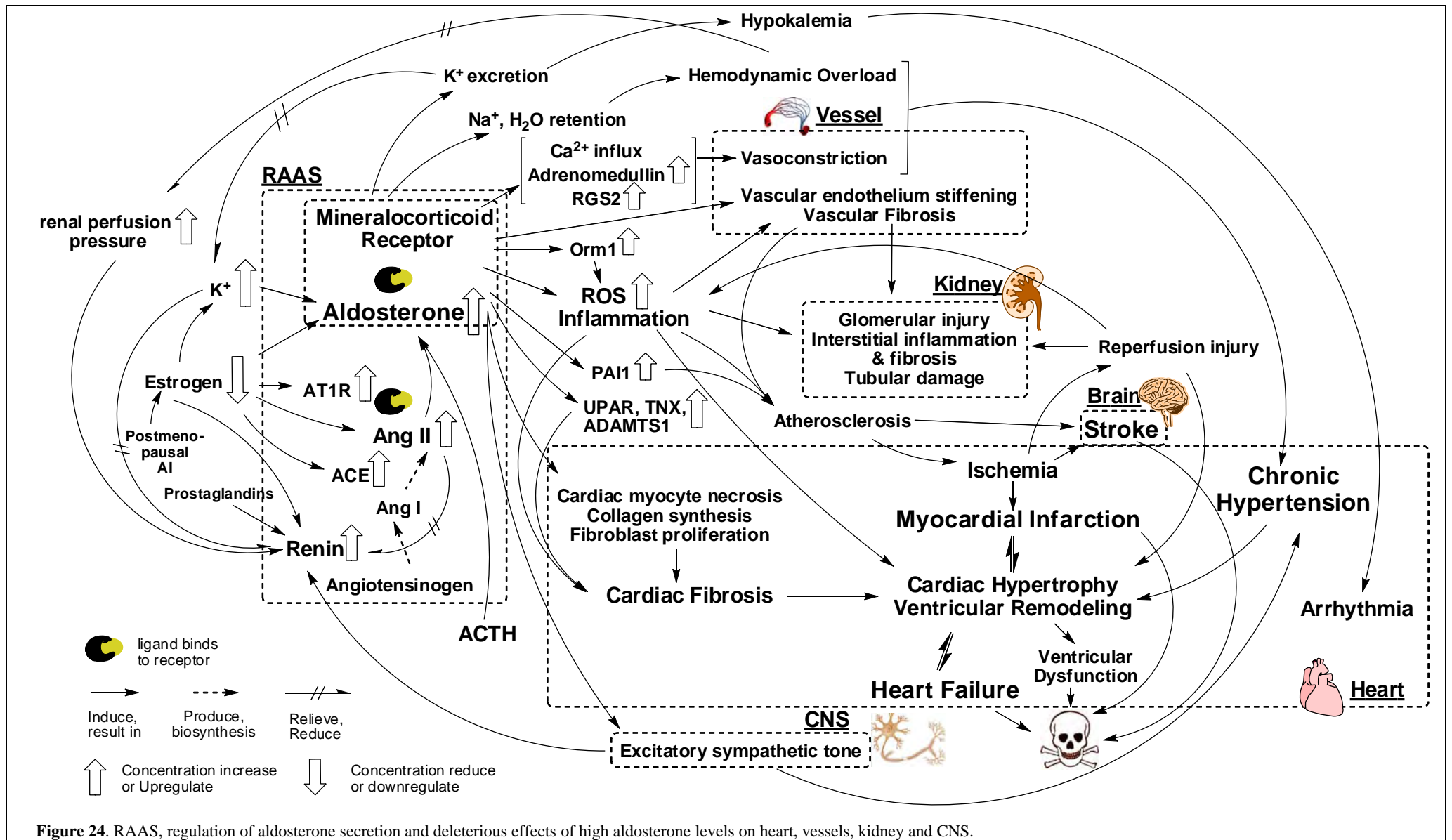


Figure 24. RAAS, regulation of aldosterone secretion and deleterious effects of high aldosterone levels on heart, vessels, kidney and CNS.

effects result in vascular fibrosis and vascular endothelium stiffening¹⁰² and are thought to be closely related to atherosclerosis,^{103,104} which is a high risk factor for stroke and ischemia related myocardial infarction (MI) leading to disability and death. Aldosterone also promotes calcium influx into smooth muscle cells,¹⁰⁴ up-regulates the expression of adrenomedullin and regulator of G protein signaling-2 (RGS2),¹⁰⁵ and engenders excitatory sympathetic tone¹⁰⁶ after acting on CNS. These effects lead to vasoconstriction and, together with the aforementioned blood volume increase, finally result into chronic hypertension. Furthermore, excessive aldosterone causes cardiac myocyte necrosis, collagen synthesis, and fibroblast proliferation, which results in cardiac fibrosis and increase of myocardial stiffness.^{107,108} These damages are mediated in part via the expression of some genes closely related to cardiac fibrosis, for example: tenascin-X (TNX), urokinase plasminogen activator receptor (UPAR) and a disintegrin and metalloprotease with thrombospondin motifs (ADAMTS1).¹⁰⁵ Consequently, cardiac hypertrophy and ventricular remodelling occur as the outcome of severe cardiac fibrosis. Inflammation, chronic hypertension, reperfusion injury, myocardial infarction and some other events stimulated by excessive aldosterone all contribute to this pathological process.^{109,110} The ventricular remodeling causes diastolic dysfunction, diminishes contractile capability, reduces stroke volume and ultimately results in congestive heart failure (CHF), which often leads to sudden death. Besides heart, high aldosterone levels also cause renal vascular fibrosis, glomerular injury, tubular damage and interstitial fibrosis.¹¹¹

1.3.1.III. Mechanisms of Action — Genomic and Non-genomic

It is established that the binding of aldosterone frees MR from its chaperone proteins in the cytoplasm, such as heat shock protein. The aldosterone–MR complex subsequently translocates into the nuclei assisted by actin,¹¹² where various transcriptional coregulators are recruited, such as the histone acetylase CBP/p300, the helicase RHA and the Pol II elongation factor ELL,¹¹³ to initiate the transcription via chromatin remodeling and histone acetylation or methylation.^{114,115} The targeted genes, such as serum and glucocorticoid-regulated kinase (SGK1), epithelial sodium channel (ENaC) and corticosteroid hormone-induced factor (CHIF), are therefore expressed.¹¹⁶ However, there are some aldosterone effects, especially on cardiomyocytes, too rapid to be results of genomic actions.^{117,118} Thus, these effects are considered to be non-genomic, including the activation of ERK1/2,¹¹⁹ as well as PKCε-mediated direct inhibition of Na⁺/K⁺-ATPase activity and Na⁺-K⁺-2Cl⁻ cotransporter activation resulting in [Na⁺] increase.¹¹⁷ It is intriguing that MR, although being a transcript factor, mediates most of the nongenotropic effects of aldosterone, whereas only small portion of the nongenotropic effects appear to be MR-independent.¹²⁰

1.3.2 CYP11B2, RAAS and Regulation of Aldosterone Biosyntheses

The biosyntheses of aldosterone initiates from progesterone and involves CYP21 and CYP11B2. As the first step, the former converts progesterone into 11-deoxycorticosterone (DOC); whereas CYP11B2 as a mitochondrial cytochrome P450 enzyme is crucial due to the subsequently consecutive three steps from DOC to aldosterone depends on its catalysis. Aldosterone is mainly produced in adrenal zona glomerulosa, where the absence of CYP17 guarantees the abundance of progesterone. Nevertheless, recent studies have revealed that the biosyntheses of aldosterone also takes place in heart,¹²¹ vessels and some other target

tissues¹²² as well.

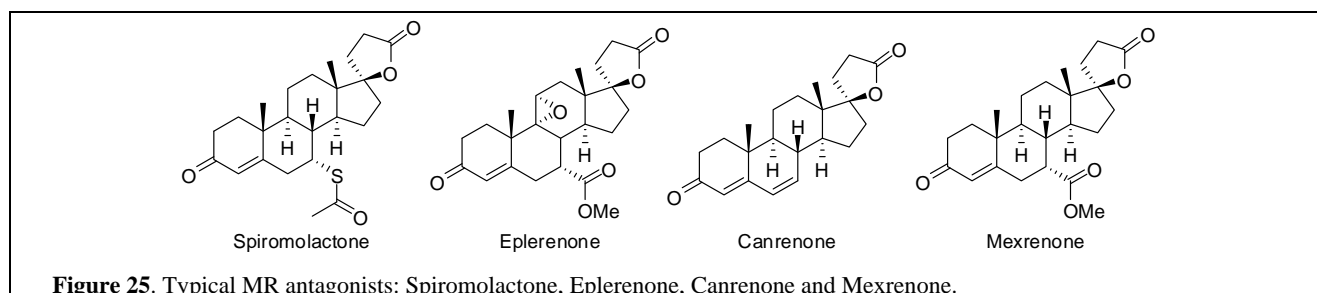
Normally, the secretion of aldosterone is strictly regulated by the negative feedback loop of renin-angiotensin-aldosterone system (RAAS), as well as the concentration of potassium and ACTH. Any disturbances of the balance will result in the abnormality of aldosterone level. Renin is a protease produced by juxtaglomerular cells in kidney. Increased renal perfusion pressure, β -adrenergic stimulation, prostaglandins, and deficiency of estrogen, all promote the secretion of rennin; whereas elevated levels of potassium and angiotensin II (Ang II), as well as α -adrenergic stimulation inhibit it. The circulating rennin tailors angiotensinogen into an inactive peptide angiotensin I, which is subsequently converted into Ang II catalyzed by angiotensin converting enzyme (ACE). A high concentration of Ang II blocks the rennin secretion directly as a small negative feedback loop. After Ang II binds to its receptor AT1R, the syntheses and release of aldosterone from the adrenal cortex are stimulated. Moreover, potassium stimulates aldosterone secretion directly, which is independent of the effects it casts on renin-angiotensin system.¹²³ Aldosterone promotes the excretion of potassium resulting in the decrease of aldosterone as another negative feedback loop. Furthermore, ACTH is the most potent acute aldosterone secretagogue. However, in the long term, continuous stimulation leads to a paradoxical decrease of aldosterone secretion.¹²⁴

1.3.3 Treatment of High Aldosterone Related Diseases — State of Art

Due to the various deleterious effects aldosterone shows on the body, it is necessary and urgent to control the high aldosterone level for the patients with related diseases. Two approaches are feasible to prevent aldosterone from its deleterious effects: antagonism of MR and blocking aldosterone secretion. For the former, MR antagonists have been clinically implemented; while for the latter, targeting RAAS components or other regulators is reasonable. Since ACTH involves in the production and release of many other adrenal steroids, it is not suitable for this purpose. Two therapies targeting RAAS components are currently employed in clinic, namely renin inhibitors and ACE inhibitors; while another promising therapy is still under development — CYP11B2 inhibitors.

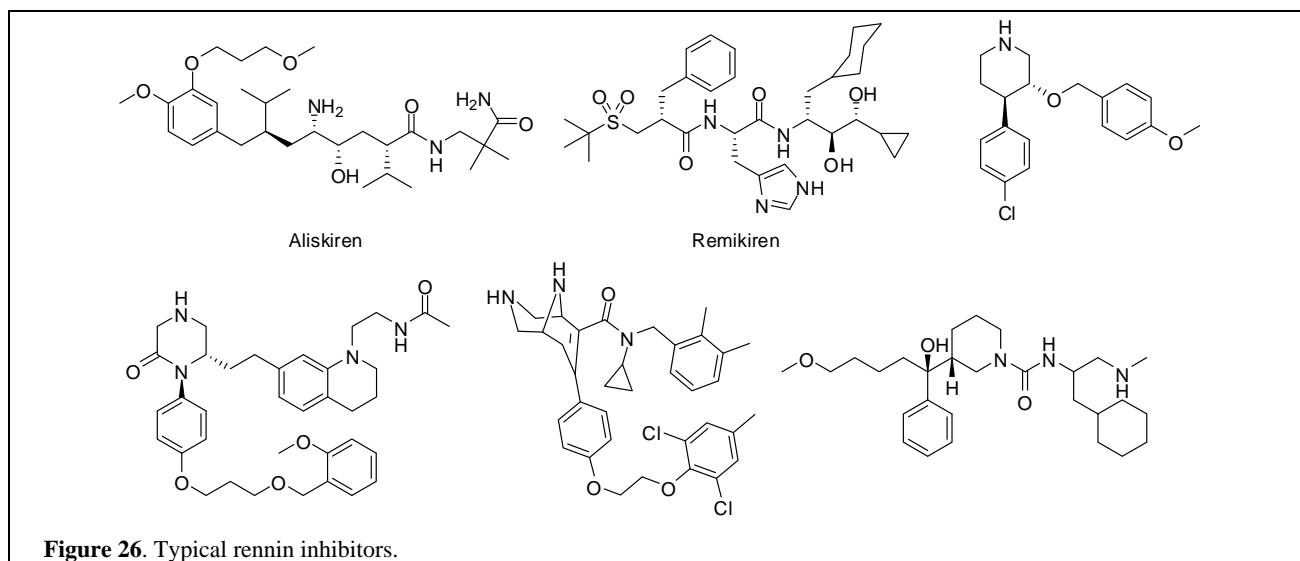
1.3.3.I. Mineralocorticoid Receptor Antagonists

As for MR antagonists, such as Spironolactone, Eplerenone, Canrenone and Mexrenone (Figure 25), although several clinical trails have demonstrated their improvement on morbidity and mortality of heart failure, adverse effects like gynaecomastia and hyperkalemia are common,¹²⁵ and the severest is the possibility of carcinogenesis. Moreover, MR antagonists leave high level of aldosterone unaffected, which can leads to further exacerbation of heart dysfunction in a MR independent non-genomic manner.¹²⁶



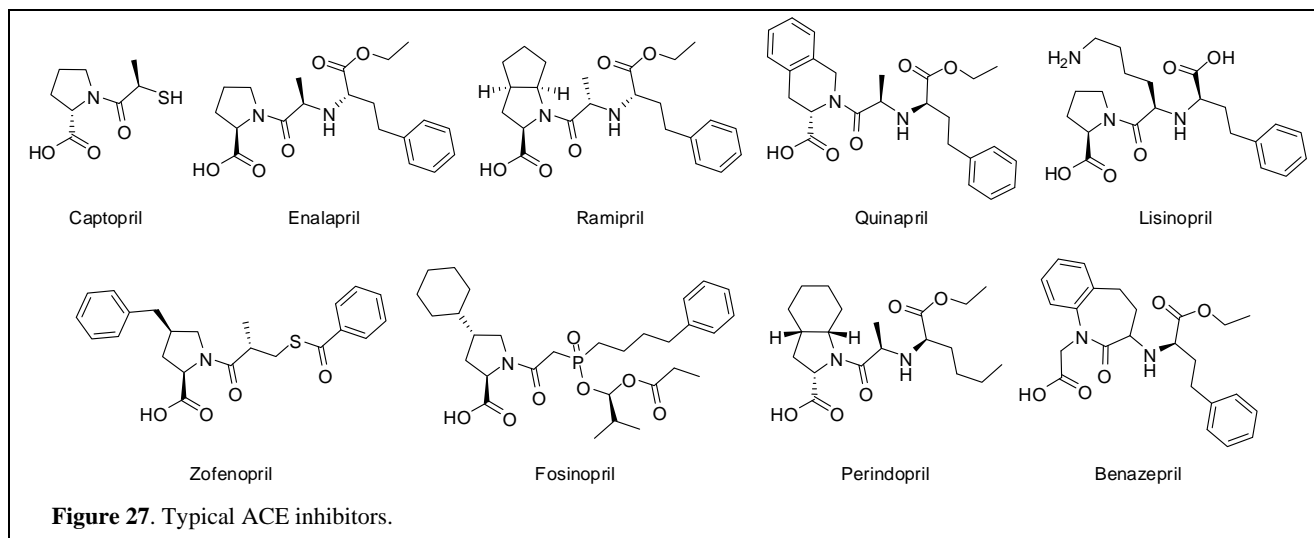
1.3.3.II. Renin Inhibitors

Early attempts to inhibit renin include monoclonal antibodies and peptide analogues; however, they have been discontinued because of immunogenesis and poor oral bioavailability. Aliskiren (Figure 26), as the first orally active renin inhibitor, was approved in 2007 for the treatment of hypertension. It is a potent and specific human renin inhibitor with a plasma half-life around 24 hours, which is due to its resistance to biodegradation by peptidases in intestine and blood.¹²⁷⁻¹²⁹ Later on, some more renin inhibitors were designed with less chiral centers within the cores of piperidine,^{130-132,136} ketopiperazine^{133,134} and 3,9-diazabicyclo[3.3.1] nonene¹³⁵ (Figure 26).



1.3.3.III. Angiotensin Converting Enzyme Inhibitors

Since ACE inhibitors relieve the vasoconstriction irrigated by both Ang II and aldosterone, they are exploited in the treatment of hypertension and CHF. Moreover, ACE inhibitors arrest the progress of diabetic nephropathy independently from the anti-hypertension effects,¹³⁷ and therefore are implemented in the prevention of diabetic renal failure. The first orally active ACE inhibitor Captopril was approved in 1981. Two years later, the first non-mercapto-containing ACE inhibitor enalapril was launched. Despite the huge success of ACE inhibitors in the treatment of hypertension, the long-term plasma aldosterone level is only



slightly influenced, which is known as “aldosterone escape”,¹³⁸ probably due to the complicated regulation mechanism of aldosterone biosyntheses. The remaining abnormally high aldosterone levels continue to impair many organs. Moreover, renal damage is commonly observed for all ACE inhibitors as a significant adverse effect. The reason behind this remains unclear.

1.3.4 CYP11B2 Inhibition as Treatment for Hypertension, Primary Aldosteronism and Congestive Heart Failure

Since primary aldosteronism, hypertension and congestive heart failure are the most severe diseases caused by high aldosterone levels, they are therefore the main indication of CYP11B2 inhibitors. Besides the inhibitory potency toward CYP11B2, another important issue in need of being addressed for CYP11B2 inhibitors is the selectivity against 11 β -hydroxylase (CYP11B1), which is the crucial enzyme in the production of glucocorticoids, especially cortisol. Since the interruption of cortisol biosyntheses leads to severe side effects, the selectivity is therefore considered as an important safety criterion. However, this task is indeed challenging due to more than 93% homology between these two enzymes.

1.3.4.I. Fadrozole, Etomidate, Metyrapone and their Derivatives

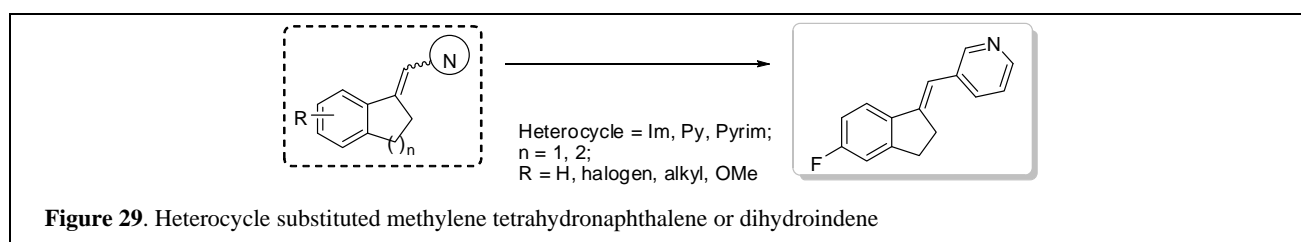
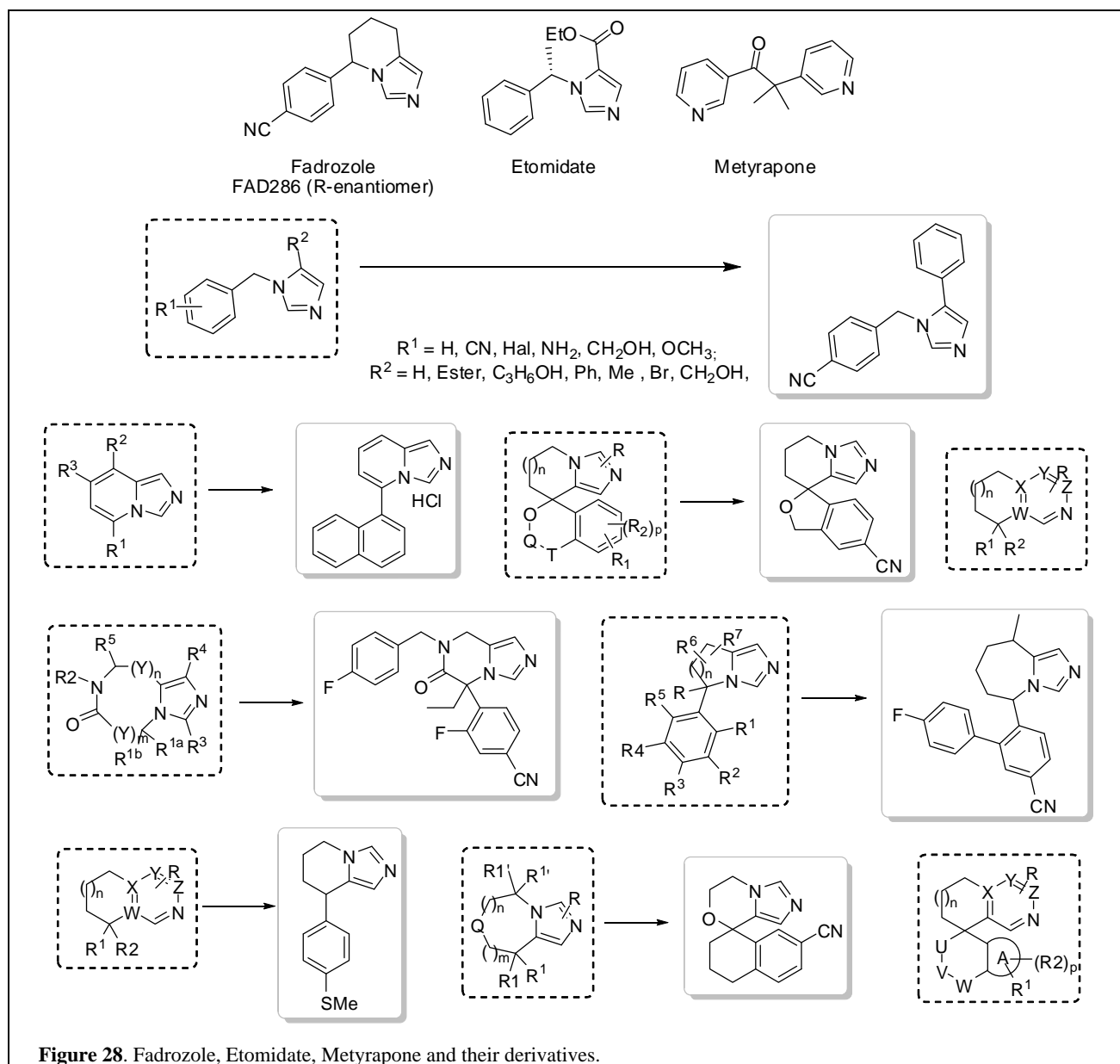
Early identified CYP11B2 inhibitors such as Fadrozole, Etomidate and Metyrapone (Figure 28) are very potent ($IC_{50} < 10$ nM), but lack of selectivity. Some of them even favor CYP11B1. As for compounds with chiral center, *R*- and *S*-enantiomers are proven to show different selectivity, for example: *R*-enantiomer of Fadrozole (FAD286) shows a selectivity factor (SF, $IC_{50\text{ CYP11B1}} / IC_{50\text{ CYP11B2}}$) of 20, whereas that of *S*-enantiomer is only 0.23. Moreover, recent *in vivo* studies elucidate that FAD286 can significantly reduce plasma aldosterone level,¹³⁹ and thus improve cardiac haemodynamics, as well as cardiac function in rats with heart failure.¹⁴⁰ Encouraged by the proof of conception, enormous modifications were carried out sustaining 1-benzyl-1*H*-imidazole — the common sub-structure of Fadrozole and Etomidate — as the fundamental scaffold. Four optimizing approaches were implemented: a) directly introducing substituents onto phenyl and / or imidazolyl moieties; b) replacing phenyl and / or imidazolyl with other aryl or N-containing heterocycle, respectively; c) fusing various cycles (aliphatic, aromatic or heterocycle) onto imidazolyl; d) inserting substituents onto the methylene bridge, which can further annulate with each other or phenyl group to yield spiral compounds. These approaches, which were employed solely or in combination lead to many potent CYP11B2 inhibitors.^{141,142}

1.3.4.II. Heterocycle Substituted Methylene Tetrahydronaphthalene or Dihydroindene

This is a series of potent ($IC_{50} < 10$ nM) and selective (SF > 100) CYP11B2 inhibitors originally identified by screening the focus library of inhibitors for other CYP enzymes (Figure 29). It is interesting that *Z*-isomers are more potent than corresponding *E*-isomer.^{143,144}

1.3.4.III. Pyridyl Naphthalenes and Indenes: Semi-unsaturation and Heteratom Inserting

Annulating the exocyclic double bond of pyridyl methylene dihydroindene into a new cycle condensing to the phenyl ring and removing the original aliphatic ring lead to pyridyl naphthalenes (Figure 30).^{145,146}



Although the resulting compounds are very potent and selective, they interfere with CYP1A2, which is an important hepatic CYP enzyme involved in the metabolism of many drugs. Since planer structure is an important feature of CYP1A2 substrates, it is feasible to reduce CYP1A2 inhibition of these compounds by increasing the flexibility of the whole molecule. Therefore, the naphthalene core was semi-unsaturated either at the left or the right side. Simultaneously, a ring size shrinkage was performed leading to indenenes (Figure 31).^{145,146} After careful optimization, the CYP1A2 inhibition of synthesized compounds is significantly reduced, whereas the potency and selectivity are increased at the same time.¹⁴⁷ Further modification by inserting heteratom into the molecule resulting in pyridyl indenenes¹⁴⁸ and dihydroquinolinones^{149,150} not only benefits inhibitory potency and selectivity, but also increases the water solubility and improves the

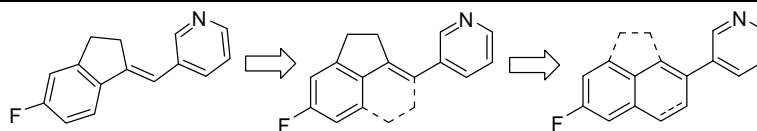


Figure 30. Design conception of pyridyl naphthalenes.

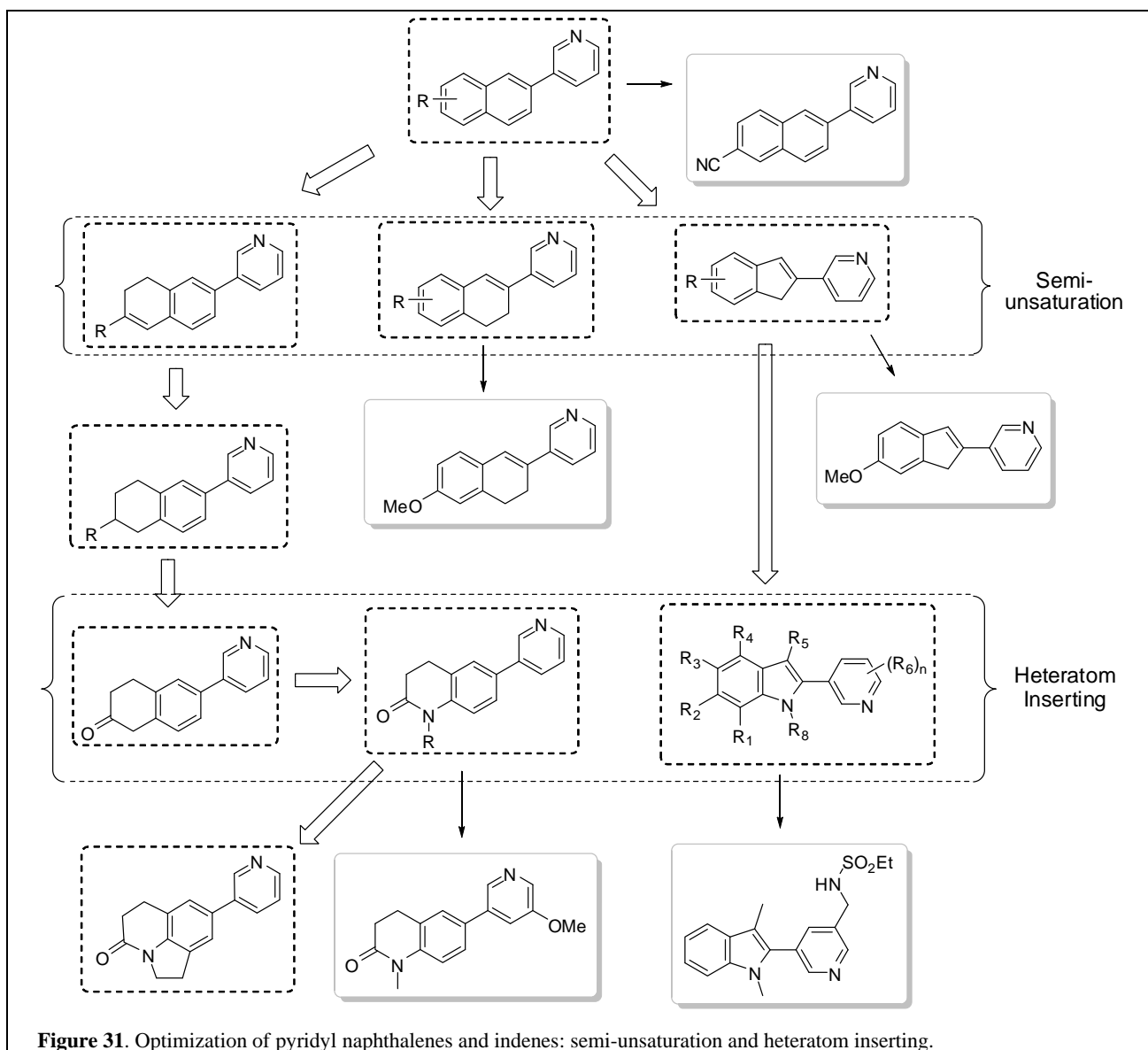


Figure 31. Optimization of pyridyl naphthalenes and indenes: semi-unsaturation and heteratom inserting.

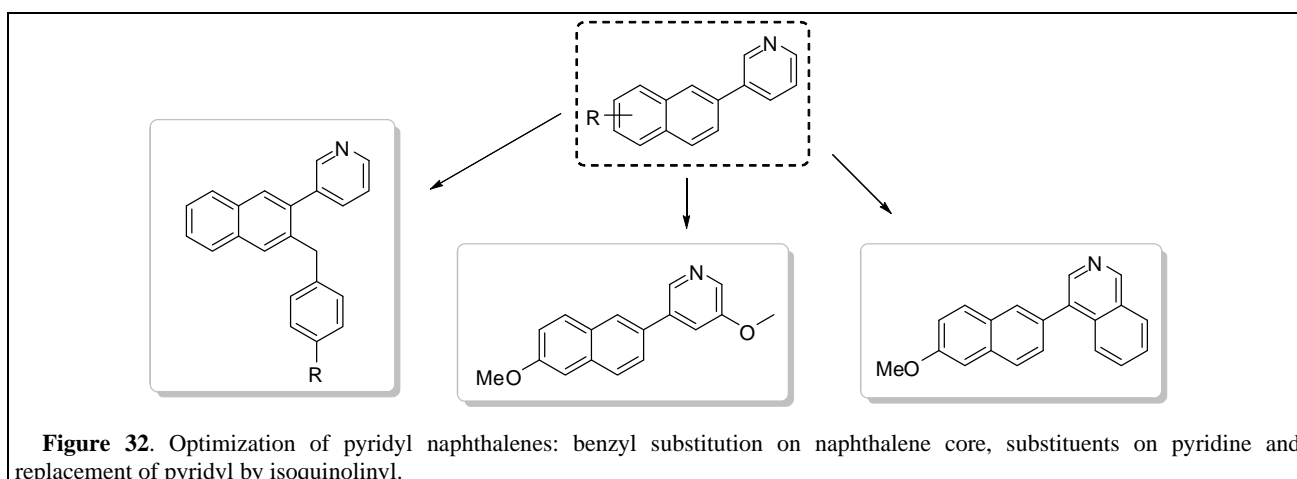


Figure 32. Optimization of pyridyl naphthalenes: benzyl substitution on naphthalene core, substituents on pyridine and replacement of pyridyl by isoquinolinyl.

pharmacokinetic properties.¹⁴⁹ The optimizations also provide information pertaining to the enzyme

hydrophobic pocket. It has been found there is an extra pocket near where the core placed, which can be utilized by a benzyl group (Figure 32).¹⁵⁰ Moreover, spar space is also identified around pyridyl, which is large enough to tolerate an additional direct connected or fused phenyl moiety.^{147,149,150} After such optimizations are applied, potent and selective CYP11B2 inhibitors with good pharmacokinetic properties are obtained, which are promising drug candidates for the treatment of diseases related to high aldosterone levels.

1.4 Dual Inhibition

The use of selective multi-target-directed ligands has already been proposed for the treatment of complicated diseases in order to enhance efficacy and to improve safety, for example, agents inhibiting angiotensin converting enzyme (ACE) and neutral endopeptidase (NEP) in the treatment of hypertension, multi-kinase inhibitors (MKI) with combined inhibition of vascular endothelial growth factor (VEGF), and platelet-derived growth factor (PDGF) for cancer therapy and dual binding site acetylcholinesterase inhibitors (AChEI) for Alzheimer's disease.¹⁵¹⁻¹⁵⁴ Compared to the traditional combinational application of two or more drugs, multi-target-directed agents can reduce the risk of drug-drug interactions and achieve better compliance.

1.4.1 Dual CYP17 / CYP11B1 Inhibition for Prostate Cancer Treatment

After the application of CAB, a major portion of patients becomes "castration resistant", which might be caused by androgen receptor mutations, such as T877A and W741C.⁵² These mutated androgen receptor can be activated by glucocorticoids, especially cortisol, and thus continue to stimulate cancer cell proliferation⁵³ thereby resulting in the collapse of CAB.

Moreover, since small cell anaplastic prostate carcinoma, which is usually concurrent with normal prostate adenocarcinoma, originates from neuro-endocrine cells, it is capable of ectopic ACTH production.¹⁵⁵ The elevated ACTH levels promote adrenals to synthesize and release high concentrations of cortisol leading to Cushing's syndrome,¹⁵⁶⁻¹⁵⁸ diabetes mellitus, osteoporosis, hypertension and obesity. For patients under CAB therapy, high cortisol levels, yet with a low concentration of androgen, probably induces the AR mutation exploiting cortisol as substrate; the high cortisol levels are therefore considered as a sign of PC progression in clinic.¹⁵⁶ Importantly, some patients die of severe infections largely due to the immunosuppression caused by the glucocorticoid.^{157,158}

Hence, for these patients the control of cortisol concentration is urgently needed. As the key step in the biosynthesis of this hormone is catalyzed by CYP11B1 (Figure 5), additional inhibition of this enzyme could be a substantial way to improve curative effects, relieve symptoms, and increase survival of prostate cancer patients.

Antimycotic Ketoconazole (Figure 16) has already been employed to treat prostate cancer patients with ectopic adrenocorticotrophic hormone syndrome¹⁵⁸ because it inhibits both androgen and corticosteroid — not only glucocorticoid but also mineralocorticoid — biosynthesis. However, the response was not satisfactory due to the weak potency of Ketoconazole (CYP17 IC₅₀ = 2780 nM). Metyrapone (Figure 28) as the

medication being employed in clinic for the treatment of Cushing's syndrome does not show enough selectivity over other steroidogenic CYP enzymes and therefore exhibits severe side effects. Accordingly it is not an appropriate candidate for combined application with CYP17 inhibitors. Therefore, it is necessary and urgent to design dual CYP17 / 11B1 inhibitors.

The application of CYP17 inhibitors with different selectivity profiles should adhere to the status of the patients. For normal patients, selective CYP17 inhibitors that do not interfere with other steroidogenic CYPs should be used to avoid side effects, whereas for patients with mutated androgen receptors or ectopic adrenocorticotrophic hormone syndrome, dual inhibitors of CYP17 and CYP11B1 are the best choice in the view of a personalized medicine.

1.4.2 Dual CYP19 / CYP11B2 Inhibition to Cure Cardiovascular Diseases in Breast Cancer Patients

In the western countries, breast cancer (BC) is the carcinoma with the highest morbidity in female. Although BC is still the second leading cause of death, the mortality is significantly reduced because of the cancer screening to identify cases in early stages¹⁵⁹ and, more importantly, the employment of adjuvant endocrine therapy. Endocrine therapy is based on the fact that estrogen stimulates the growth of "hormone sensitive" breast cancer, in which estrogen receptor (ER) and / or progesterone receptor (PgR) are expressed.¹⁶⁰ Therefore, deprivation of estrogen is a feasible treatment for the hormone sensitive BC, which accounts for more than 60% of all cases. Several decades ago, selective estrogen receptor modulators (SERM),¹⁶¹ such as Tamoxifen and Raloxifen (Figure 33), were introduced into the clinic. These SERMs competitively bind to ER antagonizing transcription and the subsequently mitogenic effects. However, the poor risk / benefit profiles prevented Tamoxifen from continuous application for more than five years. Moreover, severe toxicities such as endometrial cancer and thrombosis were observed.¹⁶² On the contrary, the third generation aromatase inhibitors (AI), such as, Anastrozole, Letrozole and Exemestane (Figure 33), exhibited better efficacy and tolerability compared to Tamoxifen, which rendered AIs to become the first choice as first-line and adjuvant therapy for postmenopausal women — the majority of breast cancer patients. Aromatase (CYP19) is the crucial enzyme catalyzing the final aromatization of steroidal A-ring in the biosynthesis of estrogen from corresponding androgen precursors: testosterone and androstenedione. Inhibition of CYP19 can totally block estrogen production and consequently prevent BC cells from proliferation. After the administration of the third generation AIs, the plasma estrogen concentration can even be reduced to an undetectable level.^{163,164} Several clinic trials demonstrated AIs as an adjuvant therapy significantly improved disease-free survival and relapse-free survival with the overall survival rate increased accordingly.¹⁶⁵⁻¹⁶⁸

However, it has been revealed that only around 40% of the patients, who did not survive, eventually died of BC,¹⁶⁹ which means a lot of people survive BC, yet perish of other diseases, especially patients older than 70 years old, among whom non-BC specific deaths accounted for 72% of total deaths.¹⁶⁹ Since cardiovascular diseases (CVD) have been identified as a statistically significant risk factor and a major cause of non-BC specific deaths,¹⁶⁹ it is necessary and urgent to manage CVD to prolong longevity of BC patients

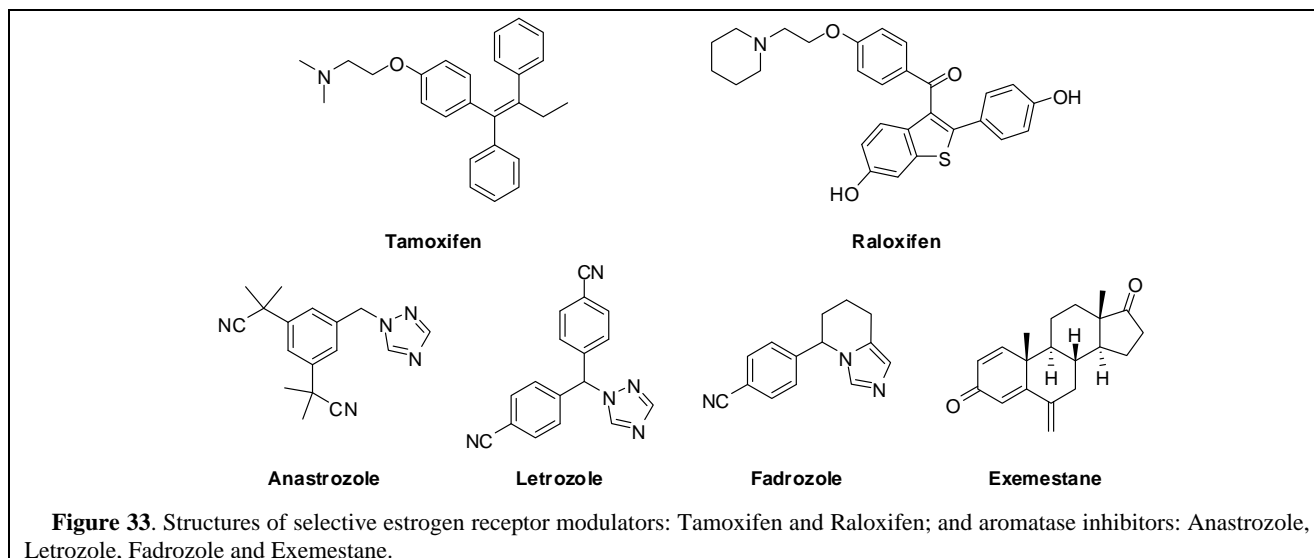


Figure 33. Structures of selective estrogen receptor modulators: Tamoxifen and Raloxifen; and aromatase inhibitors: Anastrozole, Letrozole, Fadrozole and Exemestane.

and to improve the overall survival.

Recently, estrogen has been proven to exhibit some protective effects on heart¹⁷⁰⁻¹⁷⁶ and kidney.¹⁷⁷ The administration of estrogen prevents the development of heart failure post-myocardial infarction¹⁷⁴ and attenuates ventricular hypertrophy and remodelling.^{175,176} Moreover, the fact that the incidences of CVD in post-menopausal women triple those of premenopausal women at the same age^{178,179} indicates the deficiency of estrogen is closely correlated with CVD. For post-menopausal BC patients under endocrine therapy, AIs further decrease the estrogen production to rather low levels leading to an even higher risk of CVD. The ischemic side effects observed in AIs clinic trials were considered as results of lipid metabolism dysfunction due to estrogen deficiency.¹⁸⁰⁻¹⁸⁵ This disturbance of lipid metabolism by AIs has been noticed and can be managed with antihyperlipidemic agents.^{182,183} However, the up-regulation of RAAS, especially aldosterone — another severe aftermath of estrogen deficiency^{186,187} and an important cause of CVD simultaneously — was still neglected. It has been established that the depletion of estrogen not only directly increases the circulating aldosterone level, but also augments the concentrations of other RAAS components, such as rennin, Ang II, ACE and the angiotensin type 1 receptor (AT1R), which further elevate aldosterone biosynthesis.¹⁸⁸⁻¹⁹³ Moreover, estrogen deficiency also increases the potassium plasma concentration resulting in promotion of aldosterone secretion in return.^{194,195} The consequent abnormality of high aldosterone level exhibits deleterious effects on kidney, vessels, brain and heart (Figure 24).

Therefore, reducing the high plasma aldosterone concentration rendered by estrogen deficiency is an effective treatment for the cardiovascular diseases in BC patients. Because aldosterone synthase (CYP11B2) catalyzing the conversion of 11-deoxycorticosterone to aldosterone is the key enzyme in aldosteron biosynthesis, the inhibition of CYP11B2 is a superior means to reduce the aldosterone levels. Since AIs as an adjuvant therapy have to be applied for at least 5 years and there are no selective CYP11B2 inhibitors in clinic use, it is therefore necessary to design selective dual inhibitors of CYP19 / 11B2.

2 Work Strategy

As described above, various steroidogenic CYP enzymes are promising targets for the treatment of some complicated diseases: CYP17 inhibition for prostates cancer, CYP19 inhibition for breast cancer, CYP11B2 inhibition for diseases related to high aldosterone levels, and CYP11B1 inhibition for Cushing's syndrome.

2.1 Inhibitors Design

2.1.1 General

2.1.1.I. Mechanism Inactivator or Reversible Inhibition via N–Fe Coordination

Although mechanism inactivators only inhibit the enzymes after being metabolized to give the reactive intermediates, which might be advantageous for the selectivity, the in vivo tests and clinical studies revealed that they are not effective enough.⁶⁶ On the contrary, reversible inhibition via N–Fe coordination is proven to be much more potent in vitro and vivo in blocking the production of corresponding steroidal hormones, especially some CYP19 inhibitors currently in clinical use, which could thus reduce the estrogen levels to under detectable limits. Therefore, the N–Fe coordination is implemented to design steroidogenic CYP enzymes inhibitors.

2.1.1.II. Steroidal or Non-steroidal

Although lots of steroidal inhibitors are very potent, especially Abiraterone for CYP17 inhibition, the potential drawback of these compounds can not be neglected: the relative short half life or poor bioavailability, the first pass effect when orally administered and the affinity toward steroid receptors which might result in side effect regardless acting as agonists or antagonists. These shortcomings render non-steroidal inhibitors more promising.

2.1.1.III. Multi-targeting and Selectivity

It has been found that almost all CYP enzymes inhibitors comprise two parts: N-containing heterocycle to interfere with the heme iron and hydrophobic core. This common feature provides the possibility of multi-targeting, but also denotes the selectivity as a challenging goal.

2.1.2 Combination of Ligand and Structure Approaches

The design of CYPs inhibitors mainly bases on the previously identified leads via the ligand approach. The SARs obtained in the early studies are employed as good guides. Systematic optimizations on all topological directions are performed to improve inhibitory potency and selectivity and also with the aim to probe amino acid residues surrounding. Moreover, since almost no crystal structures of human steroidogenic CYP enzymes are available (the first and only one solved is CYP19²), homology models of CYP17 and CYP11B2 are built based on multi-templates of CYP enzymes. After docking the synthesized compounds into the model, information of interactions between inhibitors and amino acids comprising the pocket is

obtained, which provide clues in further drug design.

2.1.3 Other Considerations: Drug-Like Properties, Solubility and Metabolic Stability

Besides pursuing the maximization of inhibitory potency, the drug-like properties are also considered when designing inhibitors. A principle on drug-like properties is known as “Lipinski's Rule of Five”, which is summarized from many orally active drugs and is an important guideline to design compounds with good pharmacokinetic properties, including absorption, distribution, metabolism and excretion. As a orally active compound, it contains no more than 5 hydrogen bond donors and no more than 10 hydrogen bond acceptors; the molecular weight is usually under 500 dalton and the octanol-water partition coefficient (log P) is less than 5. Furthermore, the water solubility is also taken into consideration due to it is important in drug formulation and absorption. Moieties or substituents might vulnerable to metabolism are concealed as well.

2.2 Syntheses

The design of synthetic routes follows “EOS” (easy of syntheses) principle trying to facilitate the future industrial production and reduce costs. For series of derivatives, common building blocks are used as frequently as possible, and diversification is attempted to achieve only in the last step.

2.3 Biological evaluation

The synthesized compounds are firstly tested for the inhibition of their targeting CYP enzyme(s). Only potent inhibitors ($IC_{50} < 100$ nM) will be further tested for the selectivity over other steroidogenic CYP enzymes (CYP17, CYP19, CYP11B1 and CYP11B2; sometimes CYP11A1 as well) and hepatic CYP enzymes (most frequently for CYP3A4, but CYP1A2, CYP2C9, CYP2D6, CYP2C19 as well). Subsequently, inhibition against enzymes from rat or other species is evaluated as the basis of in vivo test. As for in vivo studies, besides pharmacokinetic data obtained in health animals, the promising drug candidates are also evaluated in further disease models.

3 Results and Discussions

The design, syntheses and bio-evaluation of CYP17 inhibitors, CYP11B2 inhibitors as well as dual inhibitors of CYP17 / 11B1 and CYP19 / 11B2 are described in detail as following:

3.I Synthesis, Biological Evaluation and Molecular Modelling Studies of Methylene Imidazole Substituted Biaryls as Inhibitors of Human 17 α -Hydroxylase-17,20-lyase (CYP17) – Part II: Core Rigidification and Influence of Substituents at the Methylene Bridge

Qingzhong Hu, Matthias Negri, Kerstin Jahn-Hoffmann, Yan Zhuang, Sureyya Olgen, Marc Bartels, Ursula Müller-Vieira, Thomas Lauterbach, and Rolf W. Hartmann

This manuscript has been published as an article in
Bioorganic & Medicinal Chemistry **2008**, *16*, 7715–7727.

Paper I

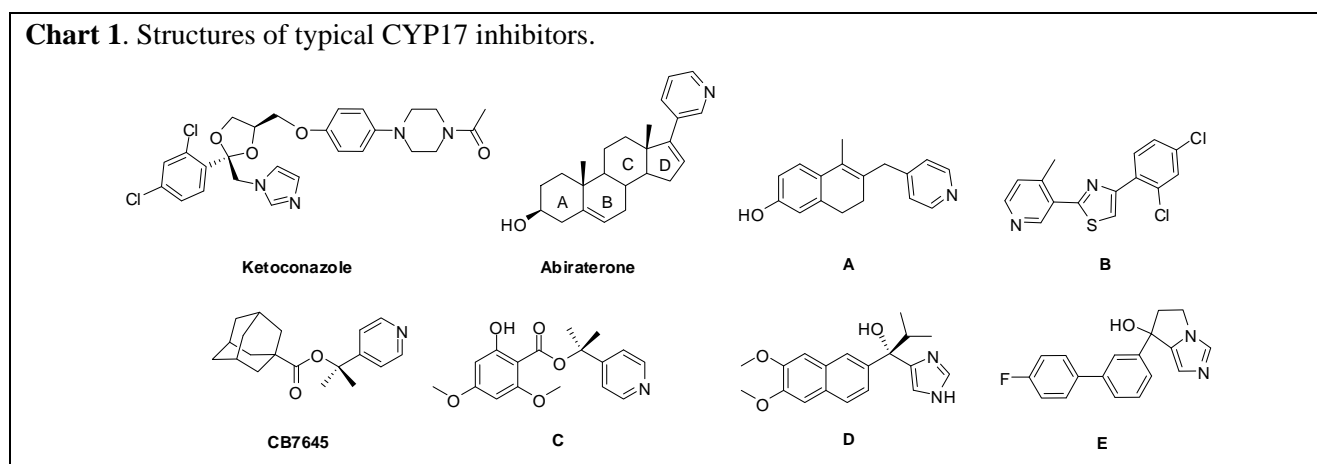
Abstract: Thirty-five novel substituted imidazolyl methylene biphenyls have been synthesised as CYP17 inhibitors for the potential treatment of prostate cancer. Their activities have been tested with recombinant human CYP17 expressed in *E. coli*. Promising compounds were tested for selectivity against CYP11B1, CYP11B2 and hepatic CYP enzymes 3A4, 1A2, 2B6, and 2D6. The core rigidified compounds (**30–35**) were the most active ones, being much more potent than Ketoconazole and reaching the activity of Abiraterone. However, they were not very selective. Another rather potent and more selective inhibitor (compound **23**, IC₅₀ = 345 nM) was further examined in rats regarding plasma testosterone levels and pharmacokinetic properties. Compared to the reference Abiraterone, **23** was more active in vivo, showed a longer plasma half-life (10 hours) and a higher bioavailability. Using our CYP17 homology protein model, docking studies with selected compounds were performed to study possible interactions between inhibitors and amino acid residues of the active site.

Keywords: prostate cancer, 17 α -hydroxylase-17,20-lyase (CYP17) inhibitors, pharmacokinetic studies, testosterone plasma concentrations.

1. Introduction

It has been illuminated that the growth of up to 80% of prostate carcinoma, the most common malignancy and cause of death for male elders, depends on androgen stimulation. Thus, inhibition of androgen formation or prevention of androgens unfolding activity will effectively prevent cancer cell proliferation. Currently the standard therapy for prostate carcinoma is the so called “combined androgen blockade” (CAB), which means orchidectomy or treatment with gonadotropin-releasing hormone (GnRH) analogues (chemical castration) combined with androgen receptor antagonists.¹ Anti-androgens are used to prevent adrenal androgens which are not affected by the former strategies from unfolding stimulatory effects. However, CAB often leads to resistance which can be associated with androgen receptor mutations. The mutated androgen receptor recognizes antagonists as agonists, and the efficiency of this therapy is whittled away. Total blockage of the androgen biosynthesis could be a more promising alternative, which brings CYP17 and its central role in the androgen biosynthesis into focus. CYP17, located in both testicular and adrenal tissue,² is the key enzyme catalyzing 17 α -hydroxylation and subsequent C17–C20 bond cleavage of pregnenolone and progesterone to form DHEA and androstenedione, which are then converted to testosterone and DHT.³

Chart 1. Structures of typical CYP17 inhibitors.

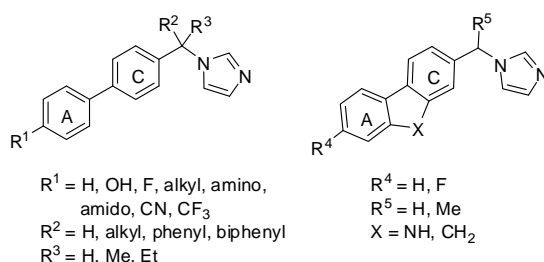


From Ketoconazole, the first medication which has been used clinically as CYP17 inhibitor, to Abiraterone which entered into phase II clinical trial very recently, several types of CYP17 inhibitors have been synthesised and tested (representative structures are shown in Chart 1). Almost all the inhibitors, steroidal or non-steroidal, are mimics of the natural substrates pregnenolone and progesterone. Although lots of steroidal inhibitors are very potent,⁴ especially Abiraterone,⁵ the potential drawback of these compounds should not be ignored: the relative short half-life or poor bioavailability,⁶ the first pass effect when orally administered⁷ and the affinity toward steroid receptors which might result in side effect no matter acting as agonists or antagonists. All of these shortcomings indicated the necessity to develop non-steroidal CYP17 inhibitors. In the past decade, a wide variety of non-steroidal compounds has been described, the most important of these were tetrahydronaphthalenes (A),⁸ *m*-pyridinyl substituted esters (CB7645 and C),⁹ 1*H*-imidazol-4-yl substituted alcohols (D and E)¹⁰ and 1-(*m*-pyridinyl)-3-phenyl substituted heterocycles (B).¹¹

Our group has reported a series of imidazolyl and triazolyl substituted biphenyls as potent CYP17 inhibitors.¹² Recently heterocyclic modifications of the core structure were performed with the more promising biphenyl methylene imidazoles. They have been published recently as part I of a study to further

improve biological properties.¹³ In the present paper modifications such as the introduction of different substituents at the methylene bridge as well as the A-ring and core rigidifications have been made leading to compounds **1–35** (general structures shown in Chart 2). Besides the syntheses and the determination of inhibitory activities toward human CYP17, the inhibitions of selected compounds against CYP11B1, CYP11B2 and hepatic CYP enzymes 3A4, 1A2, 2B6 and 2D6 are described. Furthermore, compound **23**, as the most selective inhibitor, was examined for its potency of reducing plasma testosterone concentration and its pharmacokinetic properties in rats. Moreover, molecular docking studies with both enantiomers of selected compounds, if existing, were carried out using our homology model of CYP17¹³ for getting a closer insight into the interaction between active site amino acids and the ligands.

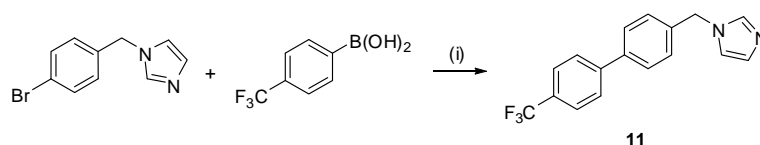
Chart 2. General structures of synthesised compounds **1–35**.



2. Chemistry

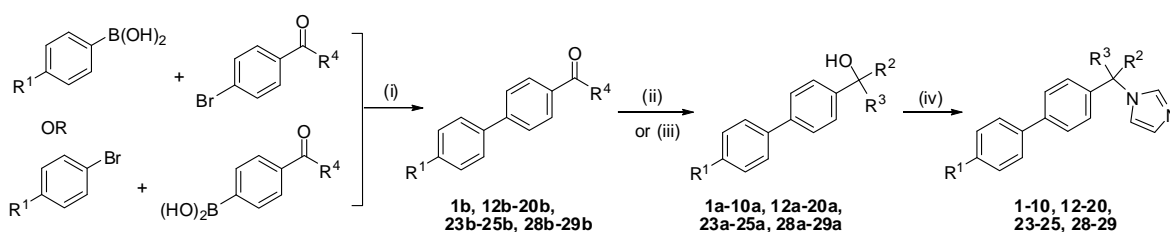
For the synthesis of compounds **1–10** and **12–35** (Scheme 1–7), basically the following strategy was used: the corresponding ketone or aldehyde intermediates were obtained commercially or synthesised by Suzuki coupling (Method C) from the corresponding bromides and boronic acids.¹⁴ Subsequently they were converted to the alcohols by reduction with NaBH_4 (Method D) or Grignard reaction (Method B). The

Scheme 1.^a



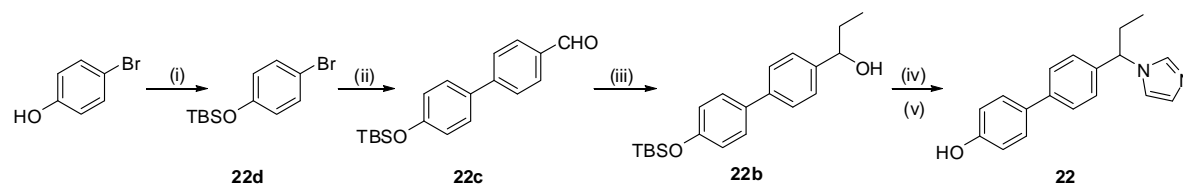
^a Reagents and conditions: (i) Method C: $\text{Pd}(\text{PPh}_3)_4$, Na_2CO_3 , toluene/ EtOH/ H_2O , reflux, 16h.

Scheme 2.^a

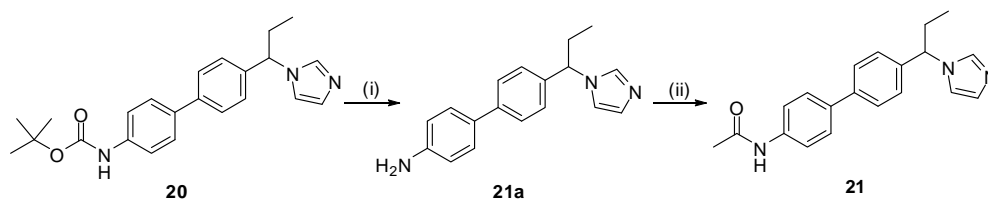


Compd.	R ¹	R ²	R ³	R ⁴	Compd.	R ¹	R ²	R ³	R ⁴	Compd.	R ¹	R ²	R ³	R ⁴
1	H	Et	H	H	9	H	phenyl	H	H	18	N(Et) ₂	Et	H	H
2	H	<i>n</i> -Pr	H	H	10	H	biphenyl	H	H	19	morpholino	Et	H	H
3	H	<i>i</i> -Pr	H	H	12	OCF ₃	Et	H	H	20	NHBoc	Et	H	H
4	H	<i>n</i> -Bu	H	H	13	SMe	Et	H	H	23	F	Et	H	Et
5	H	<i>i</i> -Pr	H	H	14	CN	Et	H	H	24	F	Me	Me	Me
6	H	<i>t</i> -Bu	H	H	15	Me	Et	H	Et	25	F	Et	Et	Et
7	H	cyclohexy	H	H	16	Et	Et	H	Et	28	F	CH=CH ₂	H	H
8	H	benzyl	H	H	17	N(Me) ₂	Et	H	H	29	H	CH=CH ₂	H	H

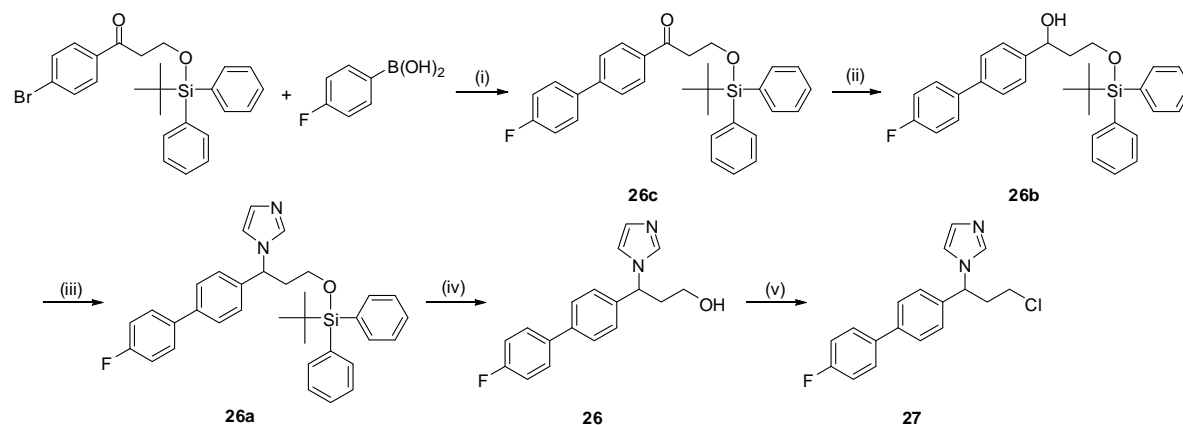
^a Reagents and conditions: (i) Method C: $\text{Pd}(\text{PPh}_3)_4$, Na_2CO_3 , toluene, reflux 6h. (ii) Method D, **15b–16b**, **23b**: NaBH_4 , MeOH. (iii) Method B, **1b**, **12b–14b**, **17b–20b**, **24b**, **25b**, **28b**, **29b**: corresponding Grignard reagent, THF. (iv) Method A: CDI, NMP.

Scheme 3.^a

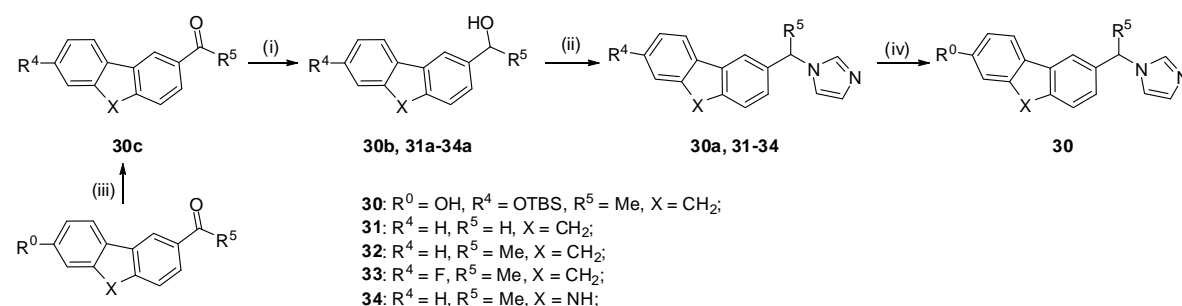
^a Reagents and conditions: (i) TBSCl, Imidazole. (ii) Method C: 4-formylphenylboronic acid, Pd(PPh₃)₄, Na₂CO₃, toluene, reflux 6h. (iii) Method B: EtMgBr, THF. (iv) Method A: CDI, NMP. (v) TBAF, THF, room temp.

Scheme 4.^a

^a Reagents and conditions: (i) TFA, DCM (ii) AcCl, N(Et)₃, DMAP, THF.

Scheme 5.^a

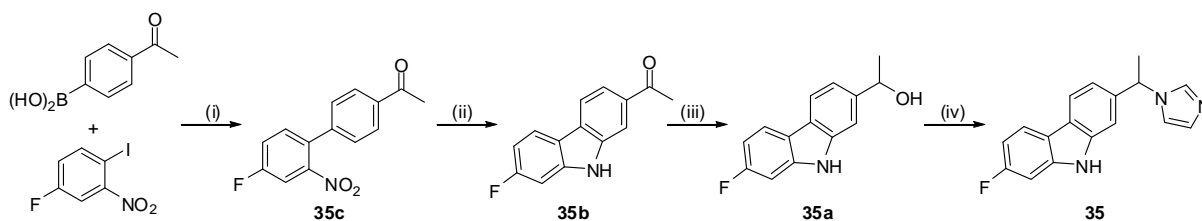
^a Reagents and conditions: (i) Method C: Pd(PPh₃)₄, Na₂CO₃, toluene, reflux 6h. (ii) Method D: NaBH₄, MeOH. (iii) Method A: CDI, NMP, reflux, 3h. (iv) TBAF, THF (v) SOCl₂, DCM.

Scheme 6.^a

^a Reagents and conditions: (i) Method D: NaBH₄, MeOH. (ii) Method A: CDI, NMP, reflux, 3h. (iii) TBSCl, imidazole. (iv) TBAF, THF.

alcohol intermediates were reacted with 1,1-carbonyl diimidazole (CDI) (Method A), in a S_NT reaction, to give the racemic mixtures of the desired products,¹⁵ which were tested for their inhibitory potencies without further separation. In the case of some sensitive intermediates, certain protecting groups were employed and subsequently removed: *tert*-butyldimethylsilyl (TBDMS) or *tert*-butyldiphenylsilyl (TBDPS) for hydroxy groups and *tert*-butoxycarbonyl (Boc) for amino groups. The conversion of the hydroxy compound **26** to the

chloro compound **27** was achieved using SOCl_2 (Scheme 5). In some cases, the carbazole core was constructed by ring closure of the *o*-nitro substituted biphenyl refluxed with phosphorous acid triethyl ester (Scheme 7). The only exception from this strategy was the synthesis of compound **11** (Scheme 1). This compound was simply prepared from 1-(4-bromobenzyl)-1*H*-imidazole and 4-trifluoromethylphenylboronic acid by means of Suzuki coupling (Method C).

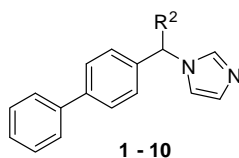
Scheme 7.^a

^a Reagents and conditions: (i) Method C: $\text{Pd}(\text{PPh}_3)_4$, Na_2CO_3 , toluene, reflux 6h. (ii) $\text{P}(\text{OEt})_3$, reflux. (iii) Method D: NaBH_4 , THF, MeOH. (iv) Method A: CDI, NMP, reflux, 3h.

3. Biological Results, Modelling Studies and Discussion

CYP17 inhibition of all compounds was evaluated using the 50,000 sediment after homogenation of *E. coli* expressing human CYP17 as well as cytochrome P450 reductase.^{12d} The assay was run with progesterone (25 μM) as substrate and NADPH as cofactor. Separation of substrate and product was accomplished by HPLC using UV detection.^{16a} IC_{50} values are presented in comparison to Ketoconazole and Abiraterone in Tables 1–4.

Table 1. Inhibition of CYP17 by compounds **1**–**10**



Compd	R ²	CYP17 IC ₅₀ [nM] ^b	Compd	R ²	CYP17 IC ₅₀ [nM] ^b
Ref. 1	Me	910	6	<i>t</i> -Bu	460
1	Et	450	7	Cyclohexyl	1050
2	<i>n</i> -Pr	580	8	Benzyl	780
3	<i>i</i> -Pr	310	9	Phenyl	790
4	<i>n</i> -Bu	300	10	Biphenyl	2300
5	<i>i</i> -Bu	2100			
KTZ ^a		2780	ABT ^a		72

^a **KTZ**: Ketoconazole; **ABT**: Abiraterone.

^b Concentration of inhibitors required to give 50% inhibition. The given values are mean values of at least three experiments. The deviations were within $\pm 10\%$.

Inheriting from **Ref. 1**,^{12b} the influence of different substituents on the methylene bridge was investigated (Table 1). From the inhibitory activity values, it becomes apparent that increasing the length of R² would largely influence the potency. The introduction of two-carbon alkyl substituents, like Et (**1**), and even more bulky ones like *i*-Pr (**3**) and *t*-Bu (**6**), increased the potency of the compounds compared to **Ref. 1** (IC₅₀ = 910 nM), resulting in inhibitors with IC₅₀ values in a range from 300 to 450 nM. Interestingly, the further

prolongation of the alkyl chain by another carbon atom led to moderate (**2**, R^2 : *n*-Pr, IC_{50} = 580 nM) or low active inhibitors (**5**, R^2 : *i*-Bu, IC_{50} = 2100 nM). However, adding another C atom to the alkyl R^2 gave again a very potent compound (**4**, R^2 : *n*-Bu, IC_{50} = 300 nM). Furthermore, it could be observed that the activity of the compounds with a bulky group was reduced dramatically as expected, like benzyl, phenyl (**8** and **9** with IC_{50} values around 800 nM), cyclohexyl (**7**, IC_{50} = 1050 nM) and biphenyl (**10**, IC_{50} = 2300 nM).

In the modelling studies, it was observed that all docked compounds showed two binding modes, named **BM1** and **BM2**, which were identified previously for other biaryl type inhibitors.^{13,17} These binding modes are different from the proposed substrate binding mode.¹⁸⁻¹⁹ In **BM1** the biaryl plane is oriented almost parallel to the I-helix and principally ligands bearing a R^1 -substituent were found in this mode (in Figure 1 compound **22** is taken as an example). The substituted A-ring is located next to a polar pocket¹⁸ delimited by Arg109, Lys231, His235 and Asp298 which tolerates different substitution patterns. On the other hand, in **BM2** the biaryl plane crosses the I-helix, avoiding the interaction with the polar pocket. It is a less permissive binding mode, which tolerates only planar ligands with an un- or fluorine substituted A-ring (compound **2** in Figure 1).

Nonetheless, for both binding orientations similar hydrophobic and π - π interactions can be observed,^{13,17} namely between the biphenyl core and Phe114 as well as between the biphenyl moiety and apolar parts of amino acids of the F-helix (Asn 202, Ile206) and I-helix (Gly301, Ala302, Val304, Glu305) (Figure 1).

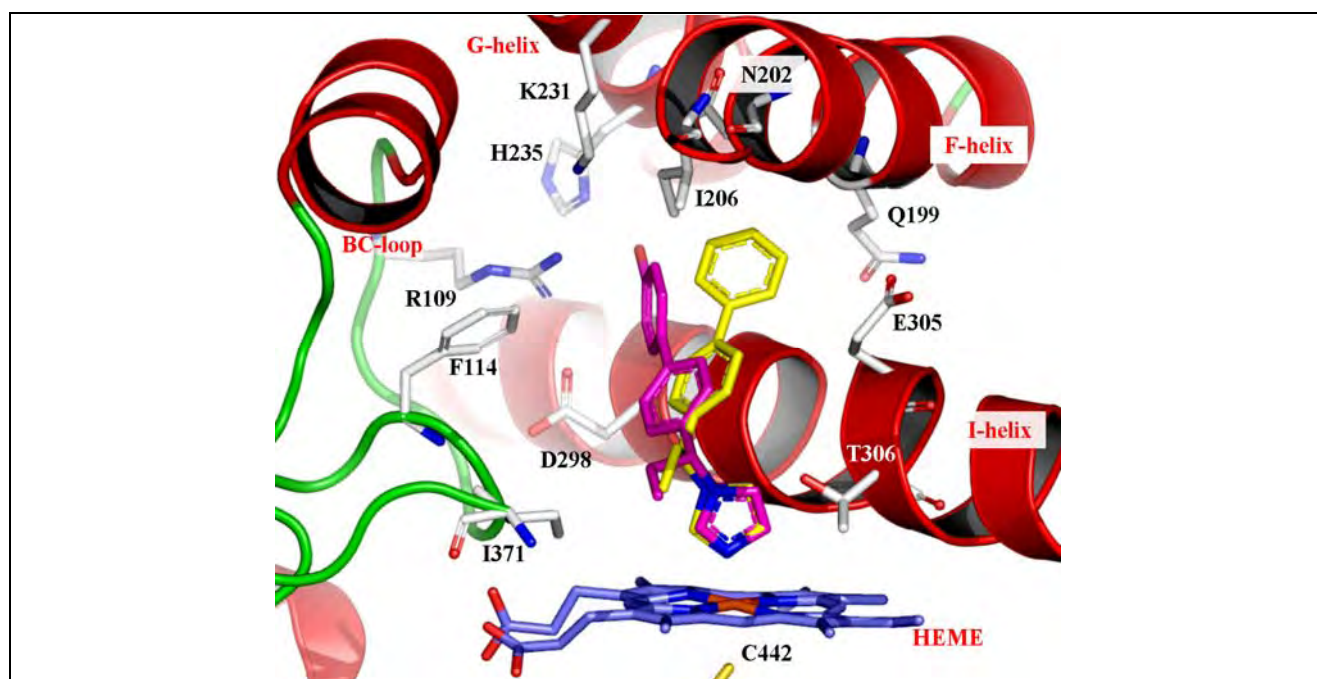
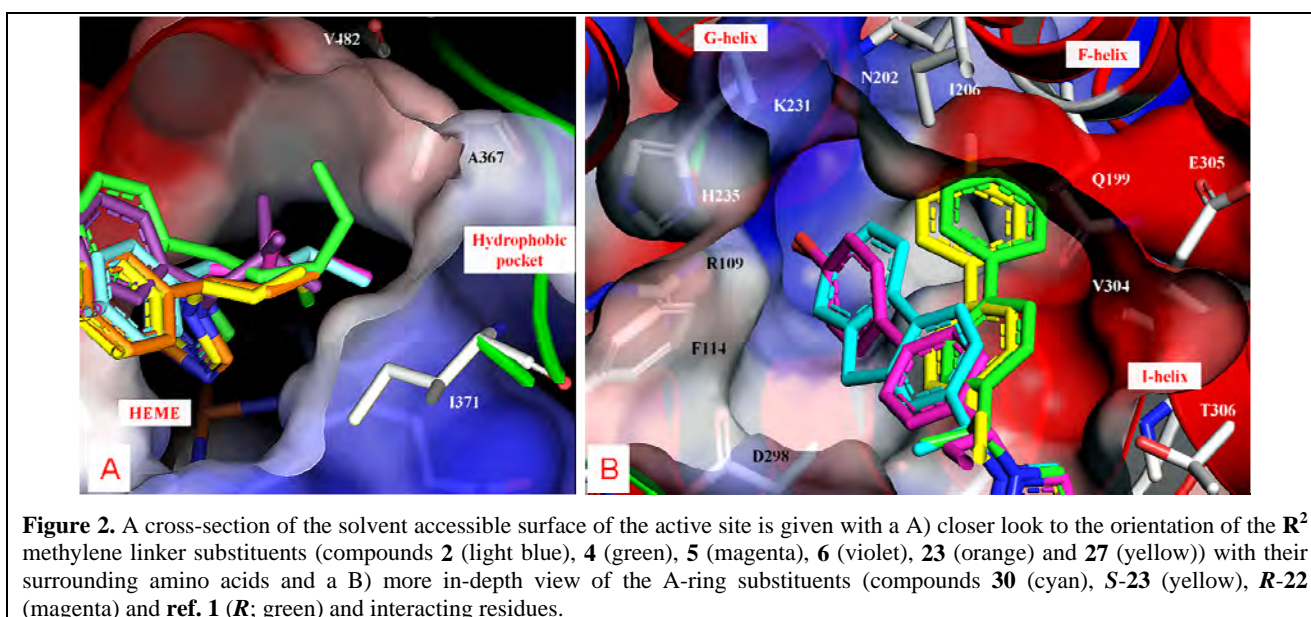


Figure 1. Presentation of the two found binding modes **BM1** and **BM2**, exemplified by compounds **22** (magenta, **BM1**) and **2** (yellow, **BM2**). Furthermore, heme, interacting residues and ribbon rendered tertiary structure of the active site are shown. Figures were generated with Pymol (<http://www.pymol.org>).

Compounds **1**, **2**, **4**, **5**, **6** and **Ref. 1** were docked into our CYP17 model with the aim of explaining the influence of the different R^2 substituents. For all *R*-enantiomers bearing a short alkyl substituent (Et, *i*-Pr, *t*-Bu or Me) at the methylene bridge, the preferred binding mode was **BM1**; whereas for the corresponding *S*-enantiomers, **BM2** seemed to be the most probable. Based on the requisites for each binding mode,^{13,17} both orientations seem to be possible for compounds **1**, **6** and **Ref. 1**. On the other hand, although poses in **BM2** could also be observed, the preferred orientations for compounds **2**, **4** and **5** seems to be **BM1**, regardless

which enantiomer was considered. This might be caused by the presence of a longer and bulkier substituent on the methylene bridge.

The results revealed an orientation of the R^2 group toward a tiny hydrophobic pocket, formed by amino acids Ala367-Pro368-Met369-Leu370-Ile371 (Figure 2A). Et, *i*-Pr and *t*-Bu substituents can undergo hydrophobic interactions with this apolar environment close to the heme without steric clashes due to their reduced length. However, for compounds **2** (*n*-Pr) and **5** (*i*-Bu) steric hindrance and hydrophobic repulsion perish the possibility of additional hydrophobic interactions, thus reducing their inhibitory potencies. As for compound **4**, the results indicate that the *n*-Bu group can interact not only with amino acids Ile371 and Ala367, like *n*-Pr does, but also with Val366, Pro368 and Val382 as additional contacts. This leads to the stabilization of its orientation, and makes it a potent inhibitor (Figure 2A).



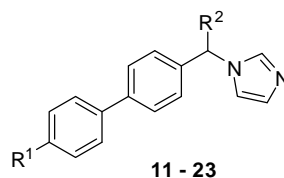
It can also be observed that different R^1 substituents on the A-ring show a strong influence on the activity of the imidazole substituted biphenyls. Exhibiting the same ethyl group at the methylene bridge, the A-ring substitution dispersed the inhibitory potency of the corresponding compounds strongly ranging from no to strong inhibition (Table 2). It becomes apparent that hydrophobic and electronegative groups in R^1 led to almost inactive compounds. However, when R^1 is a small polar substituent, capable of H-bond formation, the compounds turned out to be very active (**22**, $R^1 = OH$, $IC_{50} = 375$ nM; **23**, $R^1 = F$, $IC_{50} = 345$ nM).

Docking of both enantiomers of ligands **22** and **23** into the active site of our CYP17 model revealed **BM1** is preferred for *S*-**22**, *R*-**22** and *R*-**23**. There is obviously hydrogen bond formation between R^1 and the polar surrounding of Arg109, Asp298, Lys231 and His235 (Figure 2B). However, the *S*-enantiomer of compound **23** was found to bind in **BM2** as long as the small H-bond accepting fluorine group can interact with Gln199 and Asn202 (Figure 2B).

As it is known that fluorine compounds are more stable in vivo than hydroxy compounds, R^1 was sustained to be fluorine and the influence of substituents at the methylene bridge was further investigated (Table 3). Interestingly, the single ethyl group turned out to be the best, while twin alkyl substituted analogues (**24–25**) showed lower inhibitory potency than their single substituted analogues (**23**, **Ref. 2**). This

is obviously due to the steric clashes with amino acids of the I-helix kink and the reduced flexibility of these ligands. Moreover, the similar activity of compound **27** (2-chloroethyl, $IC_{50} = 756$ nM) and compound **2** (*n*-Pr) and the total loss of activity for the 2-hydroxyethyl analogue (**26**) demonstrate the necessity of a hydrophobic side chain on the methylene bridge.

Table 2. Inhibition of CYP17 by compounds **11–23**

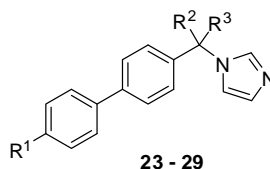


Compd	R ¹	R ²	CYP17 IC ₅₀ [nM] ^b	Compd	R ¹	R ²	CYP17 IC ₅₀ [nM] ^b
11	CF ₃	H	>5000	18	N(Et) ₂	Et	>>5000
12	OCF ₃	Et	>5000	19	morpholino	Et	2200
13	SMe	Et	3100	20	NHBoc	Et	1700
14	CN	Et	>5000	21	NHAc	Et	>5000
15	Me	Et	>5000	22	OH	Et	375
16	Et	Et	2000	23	F	Et	345
17	N(Me) ₂	Et	>>5000				
KTZ^a			2780	ABT^a			72

^a **KTZ**: Ketoconazole; **ABT**: Abiraterone.

^b Concentration of inhibitors required to give 50% inhibition. The given values are mean values of at least three experiments. The deviations were within ±10%.

Table 3. Inhibition of CYP17 by compounds **23–29**



Compd	R ¹	R ²	R ³	CYP17 IC ₅₀ [nM] ^b	Compd	R ¹	R ²	R ³	CYP17 IC ₅₀ [nM] ^b
Ref. 2	F	Me	H	1100	26	F	(CH ₂) ₂ OH	H	>5000
23	F	Et	H	345	27	F	(CH ₂) ₂ Cl	H	756
24	F	Me	Me	3800	28	F	CH=CH ₂	H	>5000
25	F	Et	Et	1300	29	H	CH=CH ₂	H	1400
KTZ^a				2780	ABT^a				72

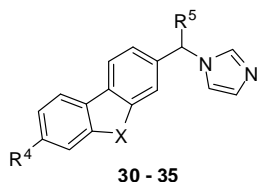
^a **KTZ**: Ketoconazole; **ABT**: Abiraterone.

^b Concentration of inhibitors required to give 50% inhibition. The given values are mean values of at least three experiments. The deviations were within ±10%.

Rigidification of the biphenyl core to form a carbazole or 9*H*-fluorene ring (Table 4) led to the most potent series of compounds (**30–35**). The planar conjugated scaffolds apparently contributed most to the inhibitory potency, probably due to the reduced degrees of freedom. Once again, inhibitors furnished with groups capable of forming hydrogen bonds turned out to be more active, with the hydroxy substituted 9*H*-fluorene analogue (**30**) being the most potent compound of this study ($IC_{50} = 99$ nM, 28 fold more potent than

Ketoconazole). Moreover, the importance of an alkyl substituent on the spacer has been demonstrated again, as can be seen from the higher activity of the methyl compound **32** showing IC_{50} of 112 nM (for this compound IC_{50} of 4 nM is reported²³) compared to the corresponding non-substituted analogue **31** (IC_{50} = 388 nM).

Table 4. Inhibition of CYP17 by compounds **30–35**

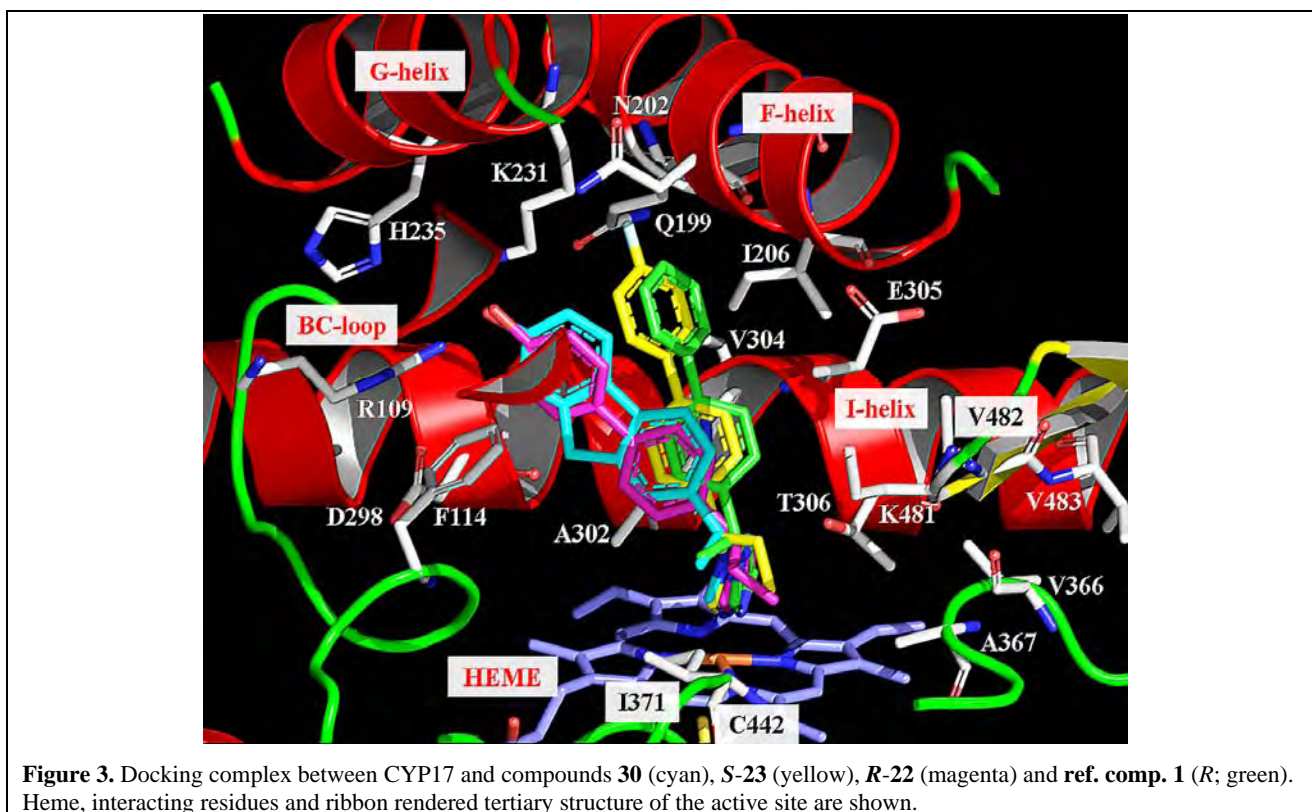


Compd	R ⁴	R ⁵	X	CYP17 IC ₅₀ [nM] ^b	Compd	R ⁴	R ⁵	X	CYP17 IC ₅₀ [nM] ^b
30	OH	Me	CH ₂	99	33	F	Me	CH ₂	168
31	H	H	CH ₂	388	34	H	Me	NH	282
32	H	Me	CH ₂	112 ^c	35	F	Me	NH	118
KTZ ^a				2780	ABT ^a				72

^a **KTZ**: Ketoconazole; **ABT**: Abiraterone.

^b Concentration of inhibitors required to give 50% inhibition. The given values are mean values of at least three experiments. The deviations were within $\pm 10\%$.

^c IC_{50} = 4 nM, reported in reference 23.



For the docking studies of selected compounds from Table 4 (**30**, **32** and **35**), similar results were achieved as obtained for the non-rigidified compounds. Two binding modes, **BM1** and **BM2**, were identified. The former seemed to be preferred, based on the internal energies of the docked inhibitors and the visual inspection of possible interactions, regardless which enantiomer was considered. The same H-bond interactions were found as described above (Figure 1, Figure 2B). Moreover, the poses were also

stabilized by the electrostatic interactions with carbon chain of Glu305 (Figure3).

The inhibition of selected compounds toward hepatic CYP enzymes was determined (Table 5), because of their important role in drug metabolism and drug-drug interaction. Although the compounds tested showed inhibition of CYP3A4, it was lower than that of Ketoconazole. Interestingly, compound **20** showed only little inhibition (52% at 1 μ M), possibly due to the bulky *t*-Boc amino group it bears. However, CYP1A2 inhibition shown by the test compounds was much higher than that of Ketoconazole. Compounds **23** and **27** showed good selectivity toward CYP2B6 and 2D6.

Table 5. Inhibition of hepatic CYP enzymes by selected compounds.

Compd	CYP % Inhibition ^b				Compd	CYP % Inhibition ^b			
	3A4	1A2	2B6	2D6		3A4	1A2	2B6	2D6
20	52	n.d. ^a	n.d. ^a	n.d. ^a	30	89	93	n.d. ^a	n.d. ^a
23	88	97	46	54	32	89	98	n.d. ^a	n.d. ^a
25	95	51	n.d.	n.d.	34	88	99	n.d. ^a	n.d. ^a
27	86	96	34	32	35	75	n.d.	n.d. ^a	n.d. ^a
KTZ^a	96	8	11	1	ABT^a	27	36	2	7

^a **KTZ**: Ketoconazole; **ABT**: Abiraterone; n.d.: not determined.

^b Inhibition at a concentration of 1 μ M; standard deviations were within $< \pm 5\%$; All the data are the mean values of at least 3 independent tests.

Furthermore, selectivity toward CYP11B1 and CYP11B2 — the most important steroidogenic enzymes being responsible for adrenal corticoid biosynthesis — has been determined as another criterion to decide which compound should be tested further *in vivo*. CYP11B1 catalyzes 11 β -hydroxylation in cortisol biosynthesis, whereas CYP11B2 is responsible for the final three steps (11 β -hydroxylation, 18-hydroxylation, and 18-oxidation) in aldosterone biosynthesis. Inhibition of these two enzymes could cause hyponatremia, hyperkalemia and a series of recessive disorders, such as adrenal hyperplasia and hypovolemic shock.²⁰ The most interesting compound of this series, **23** and **30**, were tested at a concentration of 0.2 μ M. As compound **23** showed less inhibition on both enzymes (11B2: 66%; 11B1: 66%, compound **30**: 11B1: 96%; 11B2: 98%), it was further tested in rats.

Table 6. Reduction of the plasma testosterone concentrations in rats by compound **23^a**

Compd	Relative plasma testosterone level (%) ^b					
	1h	2h	4h	6h	8h	24h
Control	143.1 \pm 13.3	76.4 \pm 13.3	81.4 \pm 24.6	109.6 \pm 31.7	90.6 \pm 22.8	80.6 \pm 21.0
23	16.5 \pm 5.7 ^d	11.7 \pm 5.0 ^d	13.9 \pm 8.0 ^d	13.9 \pm 7.1 ^d	13.4 \pm 6.2 ^d	36.7 \pm 27.4 ^d
ABT^e	92.5 \pm 43.1 ^d	44.0 \pm 14.7 ^d	43.5 \pm 12.4 ^d	43.3 \pm 12.8 ^c	35.6 \pm 9.7 ^d	476.0 \pm 238.6

^a Compound **23** was applied at a dose of 50 mg / kg body weight; Abiraterone was administrated as Abiraterone acetate (56 mg / kg body weight, equivalent to Abiraterone 50 mg / kg body weight). 5 to 6 intact adult male Wistar rats were employed for each treatment group; each sample was tested for 3 times.

^b The average plasma testosterone concentrations (1.81 ng / mL) at pre-treatment time points (-1, -0.5 and 0 h) were set to 100%. The values shown are the relative levels compared to the pre-treatment value.

^c $P < 0.05$. ^d $P < 0.01$. ^e **ABT**: Abiraterone.

The *in vivo* evaluation of compound **23**, including the ability of reducing plasma testosterone

concentration (Table 6) and the determination of pharmacokinetic properties (Table 7), was performed in male Wistar rats after oral application using Abiraterone as reference compound. The plasma concentrations of testosterone were determined by ELISA assay and plasma drug concentrations were measured using LC-MS. Although applied as acetate, only the signals of the free Abiraterone were monitored. It is obvious that both compounds significantly reduced the plasma testosterone concentration. It is striking that compound **23**, which was less active *in vitro*, was much more active *in vivo* than Abiraterone at each time point checked. Importantly, after 24 hours compound **23** still showed strong inhibitory activity, while Abiraterone exhibited at this time point plasma testosterone concentrations 6 fold higher than that of the untreated control. This activity profile can be explained by the pharmacokinetic properties of the compounds. Compound **23** exhibited a plasma half-life of 10 hours, while Abiraterone only showed 1.6 hours. The fact that Abiraterone had to be administrated as acetate prodrug, which is inactive as CYP17 inhibitor, could explain the reduced inhibitory activity of the steroidal compound. However, application of the acetate should prolong the plasma half-life having no influence on the AUC of the parent compound. The superiority of compound **23** becomes apparent by comparing the AUCs of the two compounds, leading to the conclusion that the bioavailability of compound **23** is much better.

Table 7. Pharmacokinetic properties of compound **23**^a

Compd	$t_{1/2z}(h)^b$	$t_{max}(h)^b$	$C_{max}(ng/mL)^b$	$AUC_{0-\infty}(ng \times h/mL)^b$	$Cl_{int}(l/kg/h)^b$
23	10.0	6.0	3288	70729	0.7
Abiraterone	1.6	2.0	592	4015	11.2

^a Compound **23** was applied at a dose of 50 mg / kg body weight; Abiraterone was administrated as Abiraterone acetate (56 mg / kg body weight, equivalent to Abiraterone 50 mg / kg body weight). 5 to 6 intact adult male Wistar rats were employed for each treatment group; each sample was tested for 3 times.

^b $t_{1/2z}$: terminal half-life; t_{max} : time of maximal concentration; C_{max} : maximal concentration; $AUC_{0-\infty}$: area under the curve; Cl_{int} : intrinsic hepatic clearance.

4. Conclusion

Herein, we reported the synthesis and evaluation of bioactivity of a series of substituted and core rigidified biphenyl methylene imidazoles as CYP17 inhibitors. We found clearer SAR for biphenyl type CYP17 inhibitors, comparing to previous work,¹²⁻¹³ that alkyl groups at the methylene bridge, if in suitable length, can strongly improve the inhibitory potency. Analogues substituted with polar substituents at the A-ring, capable of H-bond formation, always led to potent inhibitors. Besides, rigidification of the biphenyl core to form a carbazole or 9H-fluorene ring also significantly elevated the activity to give a series of CYP17 inhibitors more potent than previously reported,¹²⁻¹³ probably due to their planar conjugated scaffolds. Moreover, one of the best compounds *in vitro*, compound **23** showed potent activity *in vivo*, a long plasma half-life and a high bioavailability.

However, further structure modifications have to be performed with the aim of reducing the CYP1A2 inhibition — the enzyme responsible for the metabolism of approximately 10% of the prescription drugs — before a candidate for the treatment of prostate cancer can be propagated. Furthermore, because of being tested as racemic mixtures, it is likely that one enantiomer of compound **23** would be more potent and selective than the other. A separation of the enantiomers is presently being performed.

5. Experimental Section

5.1 CYP17 preparation and assay

Human CYP17 was expressed in *E. coli* (coexpressing human CYP17 and cytochrome P450 reductase) and the assay was performed as previously described.^{12d,16a}

5.2 Inhibition of hepatic CYP enzymes

The recombinantly expressed enzymes from baculovirus-infected insect microsomes (Supersomes) were used and the manufacturer's instructions (www.gentest.com) were followed.

5.3 Inhibition of CYP11B1 and CYP11B2

V79MZh cells expressing human CYP11B1 or CYP11B2 were incubated with [4-¹⁴C]-11-deoxycorticosterone as substrate. The assay was performed as previously described.^{16c-d}

5.4 *In vivo* study

The *in vivo* tests were performed with intact adult male Wistar rats (Harlan Winkelmann, Germany), 5 to 6 for each treatment group. These rats were cannulated with silicone tubing via the right jugular vein. Compound **23** was applied *p.o.* at 50 mg/kg body weight, while Abiraterone was administered as acetate at 56 mg/kg body weight (equivalent to Abiraterone at 50 mg/kg body weight). The concentrations of testosterone in the rat plasma were determined using the Testosterone ELISA (EIA - 1559) from DRG Instruments according to the manufacturer's instructions. The plasma drug levels were measured by LC-MS. Non-compartmental pharmacokinetic analysis of concentration *vs* time data was performed for each compound on the mean plasma level using a validated computer program (PK solution 2 software; Summit Research Services, Montrose, USA). Plasma concentrations below the limit of detection were assigned a value of zero.

5.5 Chemistry Section

General

Melting points were determined on a Mettler FP1 melting point apparatus and are uncorrected. IR spectra were recorded neat on a Bruker Vector 33FT-infrared spectrometer. ¹H and ¹³C NMR spectra were measured on a Bruker DRX-500 (500 MHz). Chemical shifts are given in parts per million (ppm), and TMS was used as an internal standard for spectra obtained. All coupling constants (*J*) are given in Hz. ESI (electrospray ionization) mass spectra were determined on a TSQ quantum (Thermo Electron Corporation) instrument. Elemental analyses were performed at the Department of Instrumental Analysis and Bioanalysis, Saarland University. The purities of the final compounds were controlled by Surveyor®-LC-system. Purities were greater than 98%. Column chromatography was performed using silica-gel 60 (50–200 μm), and reaction progress was determined by TLC analysis on Alugram® SIL G/UV₂₅₄ (Macherey-Nagel). Boronic acids and bromoaryls used as starting materials were commercially obtained (CombiBlocks, Chempur, Aldrich, Acros).

Method A: CDI reaction

To a solution of the corresponding alcohol (1 eq) in *N*-methylpyrrolidone (NMP) or acetonitrile (10 mL / mmol) was added CDI (5 eq). Then the solution was heated to reflux for 4 to 18 h. After cooling to ambient temperature, it was diluted with water (30 mL) and extracted with ethyl acetate (3 x 10 mL). The combined

organic phases were washed with brine, dried over MgSO_4 and evaporated under reduced pressure. Then the desired product was purified by chromatography on silica gel.

1-(1-Biphenyl-4-yl-propyl)-1H-imidazole, 1. Synthesised according to Method A using **1a** (0.50 g, 2.36 mmol) and CDI (1.91 g, 11.78 mmol); yield: 0.13 g (21%); yellow solid: mp 75–77 °C; $R_f = 0.31$ (DCM / MeOH, 10:1); δ_H (CDCl_3 , 500 MHz) 0.99 (t, $J = 7.5$ Hz, 3H, CH_3), 2.26–2.32 (m, 2H, CH_2), 5.09 (t, $J = 7.5$ Hz, 1H, CH), 6.99 (s, 1H), 7.11 (s, 1H), 7.25 (d, $J = 8.4$ Hz, 2H), 7.33–7.37 (m, 1H), 7.42–7.46 (m, 2H), 7.56 (d, $J = 8.4$ Hz, 2H), 7.58 (d, $J = 8.4$ Hz, 2H), 7.69 (s, 1H); MS (ESI): $m/z = 263$ [$\text{M}^+ + \text{H}$].

1-(1-Biphenyl-4-yl-butyl)-1H-imidazole, 2. Synthesised according to Method A using **2a** (0.50 g, 2.21 mmol) and CDI (1.79 g, 11.05 mmol); yield: 0.16 g (27%); brownish oil; $R_f = 0.29$ (DCM / MeOH, 10:1); δ_H (CDCl_3 , 500 MHz) 0.98 (t, $J = 7.5$ Hz, 3H, CH_3), 1.31–1.39 (m, 2H, CH_2), 2.14–2.28 (m, 2H, CH_2), 5.17 (t, $J = 7.5$ Hz, 1H, CH), 6.99 (s, 1H), 7.10 (s, 1H), 7.26 (d, $J = 8.0$ Hz, 1H), 7.34 (t, $J = 7.5$ Hz, 2H), 7.45 (dd, $J = 7.5, 8.4$ Hz, 2H), 7.54–7.57 (m, 4H), 7.66 (s, 1H); MS (ESI): $m/z = 277$ [$\text{M}^+ + \text{H}$].

1-(1-Biphenyl-4-yl-2-methyl-propyl)-1H-imidazole, 3. Synthesised according to Method A using **3a** (0.50 g, 2.36 mmol) and CDI (1.91 g, 11.78 mmol); yield: 0.20 g (33%); white solid: mp 124–125 °C; $R_f = 0.31$ (DCM / MeOH, 10:1); δ_H (CDCl_3 , 500 MHz) 0.95 (t, $J = 7.5$ Hz, 6H, $(\text{CH}_3)_2$), 2.56–2.65 (m, 1H, $\text{CH}(\text{Me})_2$), 4.67 (d, $J = 7.5$ Hz, 1H, CH), 7.05 (s, 1H), 7.07 (s, 1H), 7.32–7.38 (m, 3H), 7.42–7.45 (m, 2H), 7.55–7.58 (m, 4H), 7.67 (s, 1H); MS (ESI): $m/z = 277$ [$\text{M}^+ + \text{H}$].

1-(1-Biphenyl-4-yl-pentyl)-1H-imidazole, 4. Synthesised according to Method A using **4a** (0.50 g, 2.08 mmol) and CDI (1.69 g, 10.40 mmol); yield: 0.15 g (25%); brownish oil; $R_f = 0.30$ (DCM / MeOH, 10:1); δ_H (CDCl_3 , 500 MHz) 0.89 (t, $J = 7.5$ Hz, 3H, CH_3), 1.28–1.37 (m, 2H, CH_2), 1.39–1.43 (m, 2H, CH_2), 2.20–2.26 (m, 2H, CH_2), 5.14 (t, $J = 7.7$ Hz, 1H, CH), 6.99 (s, 1H), 7.12 (s, 1H), 7.26 (d, $J = 8.4$ Hz, 2H), 7.35–7.37 (m, 1H), 7.43 (dd, $J = 7.9, 8.4$ Hz, 2H), 7.54–7.57 (m, 4H), 7.68 (s, 1H); MS (ESI): $m/z = 291$ [$\text{M}^+ + \text{H}$].

1-(1-Biphenyl-4-yl-3-methyl-butyl)-1H-imidazole, 5. Synthesised according to Method A using **5a** (0.50 g, 2.08 mmol) and CDI (1.69 g, 10.40 mmol); yield: 0.16 g (27%); brownish oil; $R_f = 0.30$ (DCM / MeOH, 10:1); δ_H (CDCl_3 , 500 MHz) 0.96 (d, $J = 7.5$ Hz, 6H, $\text{C}(\text{CH}_3)_2$), 1.46–1.53 (m, 1H, $\text{CH}(\text{Me})_2$), 1.99–2.20 (m, 2H, CH_2), 5.14 (t, $J = 9.5$ Hz, 1H, CH), 6.99 (s, 1H), 7.09 (s, 1H), 7.25 (d, $J = 8.0$ Hz, 2H), 7.35–7.36 (m, 1H), 7.43 (dd, $J = 7.9, 8.4$ Hz, 2H), 7.54–7.57 (m, 4H), 7.65 (s, 1H); MS (ESI): $m/z = 291$ [$\text{M}^+ + \text{H}$].

1-(1-Biphenyl-4-yl-2,2-dimethyl-propyl)-1H-imidazole, 6. Synthesised according to Method A using **6a** (0.50 g, 2.08 mmol) and CDI (1.69 g, 10.40 mmol); yield: 0.15 g (25%); white solid: mp 150–151 °C; $R_f = 0.30$ (DCM / MeOH, 10:1); δ_H (CDCl_3 , 500 MHz) 1.07 (s, 9H, $\text{C}(\text{CH}_3)_3$), 4.92 (s, 1H, CH), 7.08 (s, 1H), 7.24 (s, 1H), 7.32–7.36 (m, 1H), 7.41–7.45 (m, 4H), 7.55–7.57 (m, 4H), 7.72 (s, 1H); MS (ESI): $m/z = 291$ [$\text{M}^+ + \text{H}$].

1-(1-Biphenyl-4-yl-cyclohexyl-methyl)-1H-imidazole, 7. Synthesised according to Method A using **7a** (0.50 g, 1.87 mmol) and CDI (1.52 g, 9.34 mmol); yield: 0.19 g (32%); white solid: mp 118–121 °C; $R_f = 0.32$ (DCM / MeOH, 10:1); δ_H (CDCl_3 , 500 MHz) 0.89–1.03 (m, 2H, cyclohexyl), 1.15–1.28 (m, 3H, cyclohexyl), 1.52–1.60 (m, 2H, cyclohexyl), 1.71–1.77 (m, 3H, cyclohexyl), 2.22–2.23 (m, 1H, cyclohexyl), 4.72 (t, $J = 10.1$ Hz, 1H, CH), 7.04 (s, 1H), 7.06 (s, 1H), 7.32–7.37 (m, 3H), 7.43 (dd, $J = 7.5, 8.8$ Hz, 2H), 7.54–7.57 (m, 4H), 7.63 (s, 1H); MS (ESI): $m/z = 317$ [$\text{M}^+ + \text{H}$].

1-(1-Biphenyl-4-yl-2-phenyl-ethyl)-1H-imidazole, 8. Synthesised according to Method A using **8a** (0.50

g, 1.82 mmol) and CDI (1.48 g, 9.11 mmol); yield: 0.14 g (23%); yellow solid: mp 99–101 °C [Ref: 98–100 °C²¹]; $R_f = 0.29$ (DCM / MeOH, 10:1); δ_H (CDCl₃, 500 MHz) 3.50 (d, $J = 7.5$ Hz, 2H, CH₂), 5.09 (t, $J = 7.5$ Hz, 1H, CH), 6.95 (s, 1H), 7.01 (d, $J = 8.0$ Hz, 2H), 7.06 (s, 1H), 7.22–7.24 (m, 3H), 7.28 (d, $J = 8.4$ Hz, 2H), 7.35–7.37 (m, 1H), 7.42–7.45 (m, 2H), 7.48 (s, 1H), 7.56–7.58 (m, 4H); MS (ESI): $m/z = 325$ [M⁺+H].

1-(1-Biphenyl-4-yl-2-phenyl-methyl)-1H-imidazole, 9. Synthesised according to Method A using **9a** (0.50 g, 1.92 mmol) and CDI (1.56 g, 9.60 mmol); yield: 0.07 g (12%); yellow oil; [Ref: mp 142 °C²²]; $R_f = 0.35$ (DCM / MeOH, 10:1); δ_H (CDCl₃, 500 MHz) 6.57 (s, 1H, CH), 6.89 (s, 1H), 7.13–7.19 (m, 5H), 7.35–7.38 (m, 4H), 7.42–7.47 (m, 3H), 7.56–7.59 (m, 4H); MS (ESI): $m/z = 311$ [M⁺+H].

1-(Bis-biphenyl-4-yl-methyl)-1H-imidazole, 10. Synthesised according to Method A using **10a** (0.50 g, 1.49 mmol) and CDI (1.21 g, 7.43 mmol); yield: 0.07 g (13%); yellow oil; [Ref: mp 120 °C²²]; $R_f = 0.37$ (DCM / MeOH, 10:1); δ_H (CDCl₃, 500 MHz) 6.95 (s, 1H), 7.16 (s, 1H), 7.21–7.23 (m, 4H), 7.35–7.38 (m, 2H), 7.43–7.47 (m, 4H), 7.55–7.61 (m, 10H); MS (ESI): $m/z = 387$ [M⁺+H].

1-(1-(4'-(Trifluoromethoxy)biphenyl-4-yl)propyl)-1H-imidazole, 12. Synthesised according to Method A using **12a** (0.50 g, 2.10 mmol) and CDI (2.00 g, 12.40 mmol); yield: 0.16 g (21%); brownish oil; $R_f = 0.51$ (DCM / MeOH, 95:5); δ_H (CDCl₃, 500 MHz) 0.99 (t, $J = 7.5$ Hz, 3H, CH₃), 2.26–2.32 (m, 2H, CH₂), 5.09 (t, $J = 7.5$ Hz, 1H, CH), 7.00 (s, 1H), 7.13 (s, 1H), 7.28–7.31 (m, 4H), 7.54–7.59 (m, 4H), 7.66 (s, 1H); δ_C (CDCl₃, 125 MHz) 11.1 (CH₃), 28.6 (CH₂), 63.0 (CH), 117.6 (CH), 119.5 (CF₃), 121.2 (CH), 127.0 (Im-C5), 127.5 (CH), 127.6 (CH), 128.4 (CH), 129.5 (C_q), 136.4 (C_q), 139.1 (C_q), 139.7, 139.8 (C_q), 148.8 (C_q); MS (ESI): $m/z = 347$ [M⁺+H].

1-(1-(4'-(Methylsulfonyl)biphenyl-4-yl)propyl)-1H-imidazole, 13. Synthesised according to Method A using **13a** (0.67 g, 2.6 mmol) and CDI (2.00 g, 12.40 mmol); yield: 0.12 g (15%); beige solid; $R_f = 0.44$ (DCM / MeOH, 95:5); δ_H (CDCl₃, 500 MHz) 0.96 (t, $J = 7.0$ Hz, 3H, CH₃), 2.24–2.28 (m, 2H, CH₂), 2.52 (s, 3H, SCH₃), 5.04 (t, $J = 7.0$ Hz, 1H, CH), 6.97 (s, 1H), 7.10 (s, 1H), 7.23–7.26 (m, 2H), 7.30–7.33 (m, 2H), 7.47–7.50 (m, 2H), 7.52–7.54 (m, 2H), 7.63 (s, 1H); δ_C (CDCl₃, 125 MHz) 11.1 (CH₃), 15.8 (SCH₃), 28.6 (CH₂), 63.0 (CH), 117.7 (Im-C4), 126.9 (CH), 127.0 (CH), 127.2 (CH), 127.4 (CH), 129.5 (C_q), 136.4 (C_q), 137.1 (C_q), 138.0 (C_q), 139.2 (CH), 140.4 (CH); MS (ESI): $m/z = 309$ [M⁺+H].

4'-(1-(1H-Imidazol-1-yl)propyl)biphenyl-4-carbonitrile, 14. Synthesised according to Method A using **14a** (0.46 g, 1.93 mmol) and CDI (1.5 g, 9.30 mmol); yield: 0.14 g (25%); brown oil; $R_f = 0.40$ (DCM/MeOH, 95:5); δ_H (CDCl₃, 500 MHz) 0.98 (t, $J = 7.0$ Hz, 3H, CH₃), 2.22–2.30 (m, 2H, CH₂), 5.08 (t, $J = 7.0$ Hz, 1H, CH), 6.97 (s, 1H), 7.10 (s, 1H), 7.29 (d, $J = 8.5$ Hz, 2H), 7.56 (d, $J = 8.5$ Hz, 2H), 7.61–7.68 (m, 3H), 7.73 (d, $J = 8.0$ Hz, 2H); δ_C (CDCl₃, 125 MHz) 11.1 (CH₃), 28.5 (CH₂), 62.9 (CH), 111.2 (C-4'), 117.6 (C-N), 118.7 (Im-C4), 127.2 (CH), 127.6 (CH), 129.6 (C_q), 132.6 (CH), 136.3 (C_q), 139.0 (CH), 140.9 (C_q), 144.7 (C_q); MS (ESI): $m/z = 288$ [M⁺+H].

1-(1-(4'-Methylbiphenyl-4-yl)propyl)-1H-imidazole, 15. Synthesised according to Method A using **15a** (0.57 g, 2.5 mmol) and CDI (2.0 g, 12.50 mmol); yield: 0.20 g (29%); yellow solid: mp 71–72 °C; $R_f = 0.26$ (EtOAc); δ_H (CDCl₃, 500 MHz) 0.88 (t, $J = 7.3$ Hz, 3H, CH₃), 2.16 (q, $J = 7.3$ Hz, 2H, CH₂), 2.30 (s, 3H, PhCH₃), 4.95 (t, $J = 7.3$ Hz, 1H, CH), 6.89 (s, 1H), 7.00 (s, 1H), 7.12–7.18 (m, 4H), 7.37 (d, $J = 8.2$ Hz, 2H), 7.45 (d, $J = 8.2$ Hz, 2H), 7.54 (s, 1H); δ_C (CDCl₃, 125 MHz) 11.1 (CH₃), 21.0 (PhCH₃), 28.5 (CH₂), 63.0 (CH), 117.6, 126.81, 126.86, 127.3, 129.5, 136.3, 137.3, 138.9, 140.9, 142.1; MS (ESI): $m/z = 277$ [M⁺+H].

1-(1-(4'-Ethylbiphenyl-4-yl)propyl)-1H-imidazole, 16. Synthesised according to Method A using **16a** (0.64 g, 2.6 mmol) and CDI (2.1 g, 13.12 mmol); yield: 0.14 g (18%); yellowish oil; $R_f = 0.30$ (EtOAc); δ_H (CDCl₃, 500 MHz) 0.89 (t, $J = 7.3$ Hz, 3H, CH₃), 1.20 (t, $J = 7.6$ Hz, 3H, CH₃), 2.18 (quint, $J = 7.3$ Hz, 2H, CH₂), 2.61 (q, $J = 7.6$ Hz, 2H, CH₂), 4.97 (t, $J = 7.3$ Hz, 1H, CH), 6.90 (s, 1H), 7.02 (s, 1H), 7.14–7.21 (m, 4H), 7.41 (d, $J = 8.2$ Hz, 2H), 7.47 (d, $J = 8.5$ Hz, 2H), 7.57 (s, 1H); δ_C (CDCl₃, 125 MHz) 10.1 (CH₃), 14.5 (CH₃), 27.5 (CH₂), 27.6 (CH₂), 62.1 (CH), 116.7, 125.9, 126.0, 126.4, 127.3, 128.3, 135.3, 136.7, 137.8, 140.0, 142.1; MS (ESI): $m/z = 291$ [M⁺+H].

[4'-(1H-Imidazol-1-yl-propyl)-biphenyl-4-yl]-dimethyl-amine, 17. Synthesised according to Method A using **17a** (0.59 g, 2.31 mmol) and CDI (0.56 g, 3.47 mmol); yield: 0.18 g (25%); white solid: mp 117–119 °C; $R_f = 0.33$ (DCM / MeOH, 20:1); δ_H (CDCl₃, 500 MHz) 0.95 (t, $J = 7.3$ Hz, 3H, CH₃), 2.24 (q, $J = 7.3, 7.6$ Hz, 2H, CH₂), 2.99 (s, 6H, N-CH₃), 5.01 (t, $J = 7.6$ Hz, 1H, CH), 6.78 (d, $J = 9.1$ Hz, 2H), 6.97 (s, 1H), 7.09 (s, 1H), 7.20 (d, $J = 8.5$ Hz, 2H), 7.47 (d, $J = 8.8$ Hz, 2H), 7.51 (d, $J = 8.2$ Hz, 2H), 7.62 (s, 1H); δ_C (CDCl₃, 125 MHz) 11.1 (CH₃), 28.6 (CH₂), 40.4 (N-CH₃), 63.0 (CH), 112.6, 117.6, 126.5, 126.8, 127.6, 129.4, 136.4, 137.7, 141.0, 150.1; MS (ESI): $m/z = 306$ [M⁺+H].

Diethyl-[4'-(1H-imidazol-1-yl-propyl)-biphenyl-4-yl]-amine, 18. Synthesised according to Method A using **18a** (0.70 g, 2.47 mmol) and CDI (0.61 g, 3.70 mmol); yield: 0.16 g (19%); white solid: mp 109–111 °C; $R_f = 0.33$ (DCM / MeOH, 20:1); δ_H (CDCl₃, 500 MHz) 0.95 (t, $J = 7.3$ Hz, 3H, CH₃), 1.19 (t, $J = 6.9$ Hz, 6H, NCH₃), 2.24 (q, $J = 7.3, 7.6$ Hz, 2H, CH₂), 3.39 (q, $J = 6.9$ Hz, 4H, NCH₂), 5.01 (t, $J = 7.6$ Hz, 1H, CH), 6.73 (d, $J = 9.1$ Hz, 2H), 6.97 (s, 1H), 7.09 (s, 1H), 7.19 (d, $J = 8.5$ Hz, 2H), 7.45 (d, $J = 8.8$ Hz, 2H), 7.50 (d, $J = 8.2$ Hz, 2H), 7.62 (s, 1H); δ_C (CDCl₃, 125 MHz) 11.1 (CH₃), 12.6 (NCH₃), 28.6 (CH₂), 44.3 (N-CH₂), 63.0 (CH), 111.8, 117.6, 126.3, 126.8, 127.7, 129.4, 136.4, 137.5, 141.1, 147.3; MS (ESI): $m/z = 334$ [M⁺+H].

4-[4'-(1H-Imidazol-1-yl-propyl)-biphenyl-4-yl]-morpholine, 19. Synthesised according to Method A using **19a** (0.70 g, 2.37 mmol) and CDI (0.58 g, 3.55 mmol); yield: 0.27 g (33%); white solid: mp 119–121 °C; $R_f = 0.17$ (DCM / MeOH, 20:1); δ_H (CDCl₃, 500 MHz) 0.95 (t, $J = 7.3$ Hz, 3H, CH₃), 2.24 (q, $J = 7.3, 7.6$ Hz, 2H, CH₂), 3.20 (t, $J = 4.7$ Hz, 4H), 3.86 (t, $J = 4.7$ Hz, 4H), 5.02 (t, $J = 7.6$ Hz, 1H, CH), 6.92–6.95 (m, 3H), 7.08 (s, 1H), 7.21 (d, $J = 8.5$ Hz, 2H), 7.49 (d, $J = 8.8$ Hz, 2H), 7.51 (d, $J = 8.5$ Hz, 2H), 7.61 (s, 1H); δ_C (CDCl₃, 125 MHz) 11.1 (CH₃), 28.5 (CH₂), 48.9, 62.9 (CH), 66.7, 115.6, 117.6, 126.7, 126.8, 127.6, 129.4, 131.5, 136.3, 138.3, 140.5, 150.6; MS (ESI): $m/z = 348$ [M⁺+H].

[4'-(1H-Imidazol-1-yl-propyl)-biphenyl-4-yl]-carbamic acid tert-butyl ester, 20. Synthesised according to Method A using **20a** (1.23 g, 3.75 mmol) and CDI (0.91 g, 5.63 mmol); yield: 0.33 g (23%); white solid: mp 204–206 °C; $R_f = 0.29$ (DCM / MeOH, 20:1); δ_H (CDCl₃, 500 MHz) 0.97 (t, $J = 7.3$ Hz, 3H, CH₃), 1.53 (s, 9H, *t*-Bu), 2.26 (q, $J = 7.3, 7.6$ Hz, 2H, CH₂), 5.04 (t, $J = 7.6$ Hz, 1H, CH), 6.57 (s, 1H, CONH), 6.97 (s, 1H), 7.09 (s, 1H), 7.24 (d, $J = 8.2$ Hz, 2H), 7.42 (d, $J = 8.5$ Hz, 2H), 7.51–7.53 (m, 4H), 7.62 (s, 1H); δ_C (CDCl₃, 125 MHz) 11.1 (CH₃), 28.3 (*t*-Bu), 28.6 (CH₂), 63.0 (CH), 118.8, 126.9, 127.1, 127.5, 129.5, 137.9, 138.8, 140.5; MS (ESI): $m/z = 378$ [M⁺+H].

1-[1-(4'-Fluoro-biphenyl-4-yl)-propyl]-1H-imidazole, 23. Synthesised according to Method A using **23a** (1.23 g, 5.34 mmol) and CDI (4.33 g, 26.70 mmol); yield: 0.52 g (35%); brown oil; $R_f = 0.6$ (DCM / MeOH, 95:5); δ_H (CDCl₃, 500 MHz) 0.97 (t, $J = 7.3$ Hz, 3H, CH₃), 2.27 (q, $J = 7.3, 7.6$ Hz, 2H, CH₂), 5.06 (t, $J = 7.6$

Hz, 1H, CH), 6.97 (s, 1H), 7.09–7.14 (m, 3H), 7.25 (d, $J = 8.9$ Hz, 2H), 7.51–7.53 (m, 4H), 7.62 (s, 1H); δ_C (CDCl₃, 125 MHz) 11.1 (CH₃), 28.6 (CH₂), 63.0 (CH), 115.6, 115.7, 117.7, 127.0, 127.4, 128.6, 128.7, 129.5, 136.4, 136.5, 139.3, 140.1, 161.6, 163.6; MS (ESI): $m/z = 281$ [M⁺+H].

1-(2-(4'-Fluorobiphenyl-4-yl)propan-2-yl)-1H-imidazole, 24. Synthesised according to Method A using **24a** (0.23 g, 1.0 mmol) and CDI (0.36 g, 2.20 mmol); yield: 0.05 g (19%); $R_f = 0.27$ (DCM / MeOH, 95:5); δ_H (CDCl₃, 500 MHz) 1.94 (s, 6H, CH₃), 6.94–6.96 (m, 1H), 7.10–7.15 (m, 5H), 7.47–7.36 (m, 4H), 7.67–7.69 (m, 1H); δ_C (CDCl₃, 125 MHz) 31.5 (CH₃), 60.3 (CH), 116.1, 117.0, 125.2, 127.3, 129.2, 132.6, 139.4, 145.4, 163.7; MS (ESI): $m/z = 281$ [M⁺+H].

1-(3-(4'-Fluorobiphenyl-4-yl)pentan-3-yl)-1H-imidazole, 25. Synthesised according to Method A using **25a** (0.26 g, 1.00 mmol) and CDI (0.36 g, 2.20 mmol); yield: 0.13 g (43%); $R_f = 0.33$ (DCM / MeOH, 95:5); δ_H (CDCl₃, 500 MHz) 0.75 (s, 6H, CH₃), 2.26–2.30 (q, 4H, CH₂), 6.84–6.86 (m, 1H), 7.08–7.09 (m, 1H), 7.10–7.13 (m, 2H), 7.17–7.20 (m, 2H), 7.48–7.55 (m, 4H), 7.62–7.63 (m, 1H); δ_C (CDCl₃, 125 MHz) 8.3 (CH₃), 30.5 (CH₂), 66.1 (CH), 116.3, 119.7, 127.6, 129.9, 136.2, 139.1, 142.8; MS (ESI): $m/z = 309$ [M⁺+H].

1-(1-(4'-Fluorobiphenyl-4-yl)allyl)-1H-imidazole, 28. Synthesised according to Method A using **28a** (1.14 g, 5.00 mmol) and CDI (1.80 g, 10.10 mmol); yield: 0.57 g (41%); $R_f = 0.27$ (DCM / MeOH, 95:5); δ_H (CDCl₃, 500 MHz) 4.73–4.74 (m, 2H, CH₂), 6.30–6.35 (m, 1H, CH), 6.54–6.57 (m, 1H, CH), 6.98 (s, 1H), 7.10–7.12 (m, 3H), 7.42–7.44 (m, 2H), 7.50–7.56 (m, 5H); δ_C (CDCl₃, 125 MHz) 49.3 (CH), 116.5, 124.9, 127.4, 128.6, 130.8, 133.2, 135.2, 137.0, 140.3, 161.7; MS (ESI): $m/z = 279$ [M⁺+H].

1-(1-(Biphenyl-4-yl)allyl)-1H-imidazole, 29. Synthesised according to Method A using **29a** (0.30 g, 1.00 mmol) and CDI (0.36 g, 2.20 mmol); yield: 0.09 g (32%); $R_f = 0.21$ (DCM / MeOH, 95:5); δ_H (CDCl₃, 500 MHz) 4.73–4.75 (m, 2H, CH₂), 6.30–6.35 (m, 1H, CH), 6.56–6.57 (m, 1H, CH), 6.98 (s, 1H), 7.12–7.13 (m, 1H), 7.34–7.37 (m, 1H), 7.43–7.46 (m, 4H), 7.56–7.60 (m, 5H); δ_C (CDCl₃, 125 MHz) 49.3 (CH), 119.4 (=CH₂), 123.8, 127.0, 129.4, 133.2, 134.5, 137.7, 140.9; MS (ESI): $m/z = 297$ [M⁺+H].

1-[(9H-Fluoren-2-yl)methyl]-1H-imidazole, 31. Synthesised according to Method A using **31a** (0.32 g, 1.63 mmol) and CDI (0.53 g, 3.26 mmol); yield: 0.16 g (40%); $R_f = 0.31$ (MeOH / EtOAc, 5:95); colourless solid: mp 183–185 °C; δ_H (CDCl₃, 500 MHz) 3.87 (s, 2H, CH₂), 5.18 (s, 2H), 6.94 (s, br, 1H), 7.11 (s, br, 1H), 7.19 (d, $J = 8.5$ Hz, 1H), 7.30–7.33 (m, 2H), 7.38 (dd, $J = 7.3, 7.6$ Hz, 1H), 7.54 (d, $J = 7.6$ Hz, 1H), 7.59 (s, br, 1H), 7.75 (d, $J = 7.9$ Hz, 1H), 7.77 (d, $J = 7.6$ Hz, 1H); δ_C (CDCl₃, 125 MHz) 36.8 (CH₂), 51.0 (CH₂), 119.3 (CH), 120.0 (CH), 120.2 (CH), 124.0 (CH), 125.1 (CH), 126.1 (CH), 126.8 (CH), 127.1 (CH), 129.7 (CH), 134.4 (C_q), 137.4 (CH), 140.9 (C_q), 141.9 (C_q), 143.3 (C_q), 144.1 (C_q); MS (ESI): $m/z = 247$ [M⁺+H].

1-((9H-Fluoren-2-yl)ethyl)-1H-imidazole, 32. Synthesised according to Method A using **32a** (1.00 g, 4.70 mmol) and CDI (1.53 g, 9.50 mmol); yield: 0.62 g (51%); $R_f = 0.58$ (MeOH / EtOAc, 5:95); light yellow solid: mp 109–110 °C [Ref: no mp reported²³]; δ_H (CDCl₃, 500 MHz) 1.90 (d, $J = 6.9$ Hz, 3H, CH₃), 3.86 (s, 2H, CH₂), 5.41 (q, $J = 6.9$ Hz, 1H, CH), 6.96 (t, $J = 1.3$ Hz, 1H), 7.10 (s, br, 1H), 7.17–7.19 (m, 1H), 7.29 (s, br, 1H), 7.31 (dd, $J = 1.3, 7.6$ Hz, 1H), 7.37 (t, $J = 7.8$ Hz, 1H), 7.53 (bd, $J = 7.6$ Hz, 1H), 7.63 (s, br, 1H), 7.74 (d, $J = 7.9$ Hz, 1H), 7.76 (d, $J = 7.6$ Hz, 1H); δ_C (CDCl₃, 125 MHz) 22.2 (CH₃), 36.9 (CH₂), 56.8 (CH), 118.0 (CH), 120.0 (CH), 120.1 (CH), 122.6 (CH), 124.8 (CH), 125.0 (CH), 126.8 (CH), 127.0 (CH), 129.2 (CH), 136.0 (CH), 139.9 (C_q), 140.9 (C_q), 141.8 (C_q), 143.3 (C_q), 144.0 (C_q); MS (ESI): $m/z = 261$

[M⁺+H].

1-[1-(7-Fluoro-9H-fluoren-2-yl)-ethyl]-1H-imidazole, 33. Synthesised according to Method A using **33a** (1.00 g, 4.38 mmol) and CDI (1.87 g, 1.16 mmol); yield: 0.44 g (36%); $R_f = 0.24$ (MeOH / EtOAc, 5:95); yellow oil; δ_H (CDCl₃, 500 MHz) 1.90 (d, $J = 6.9$ Hz, 3H, CH₃), 3.85 (s, 2H, CH₂), 5.41 (q, $J = 7.0$ Hz, 1H, CH), 6.96 (s, 1H), 7.05–7.09 (m, 2H), 7.18 (d, $J = 7.9$ Hz, 1H), 7.22 (dd, $J = 1.8, 8.6$ Hz, 1H), 7.28 (s, br, 1H), 7.63 (s, br, 1H), 7.67–7.70 (m, 2H); δ_C (CDCl₃, 125 MHz) 22.2 (CH₃), 36.9 (CH₂), 56.8 (CH), 112.4 (d, CH), 114.1 (d, CH), 118.0 (CH), 119.8 (CH), 120.9 (CH), 122.6 (CH), 125.0 (CH), 129.2 (CH), 136.0 (CH), 137.0 (C_q), 139.7 (C_q), 141.0 (C_q), 143.7 (C_q), 145.5 (C_q), 161.6 (C_q); MS (ESI): $m/z = 279$ [M⁺+H].

2-(1-Imidazol-1-yl-ethyl)-9H-carbazole, 34. Synthesised according to Method A using **34a** (0.22 g, 1.02 mmol) and CDI (0.33 g, 2.04 mmol); yield: 0.08 g (29%); [Ref: 157–158 °C²³]; $R_f = 0.40$ (MeOH / EtOAc, 5:95); δ_H (CDCl₃, 500 MHz) 1.90 (d, $J = 6.9$ Hz, 3H), 5.46 (q, $J = 6.9$ Hz, 1H), 6.97 (s, br, 1H), 7.05–7.07 (m, 2H), 7.11 (s, br, 1H), 7.22 (ddd, $J = 1.9, 6.4, 8.0$ Hz, 1H), 7.38–7.43 (m, 2H), 7.65 (s, br, 1H), 8.02 (d, $J = 8.5$ Hz, 1H), 8.05 (d, $J = 7.9$ Hz, 1H); δ_C (CDCl₃, 125 MHz) 22.4 (CH₃), 57.2 (CH), 108.0 (CH), 110.8 (CH), 117.3 (CH), 118.3 (CH), 119.4 (CH), 120.3 (CH), 120.5 (CH), 122.7 (C_q), 123.1 (C_q), 126.0 (CH), 128.8 (CH), 136.0 (CH), 139.2 (C_q), 140.0 (C_q), 140.2 (C_q); MS (ESI): $m/z = 262$ [M⁺+H].

2-(1-(1H-Imidazol-1-yl)ethyl)-7-fluoro-9H-carbazole, 35. Synthesised according to Method A using **35a** (0.30 g, 1.30 mmol) and CDI (0.42 g, 2.60 mmol); yield: 0.08 g (23%); $R_f = 0.11$ (EtOAc); δ_H (CDCl₃, 500 MHz) 1.93 (d, $J = 7.0$ Hz, 3H), 5.64 (q, $J = 7.0$ Hz, 1H), 6.90 (ddd, $J = 2.2, 8.5, 9.6$ Hz, 1H), 6.99 (t, $J = 1.3$ Hz, 1H), 7.07 (ddd, $J = 0.6, 1.6, 8.2$ Hz, 1H), 7.11 (dd, $J = 2.2, 9.6$ Hz, 1H), 7.18 (t, $J = 1.3$ Hz, 1H), 7.28 (d, $J = 1.6$ Hz, 1H), 7.80 (s, br, 1H), 7.96–7.99 (m, 2H); δ_C (CDCl₃, 125 MHz) 22.5 (CH₃), 58.6 (CH), 98.2 (d, CH), 107.9 (d, CH), 109.4 (CH), 118.6 (CH), 119.7 (CH), 120.6 (C_q), 121.1 (CH), 122.2 (CH), 123.8 (C_q), 128.9 (CH), 137.4 (CH), 140.4 (C_q), 142.2 (C_q), 142.8 (C_q), 163.5 (C_q); MS (ESI): $m/z = 280$ [M⁺+H].

Method B: Grignard reaction

Under exclusion of air and moisture a 1.0 M Grignard reagent (1.2 eq) solution in THF was added dropwise to a solution of the aldehyde or ketone (1 eq) in THF (12 mL / mmol). The mixture was stirred at room temperature overnight. Subsequently ethyl acetate (10 mL) and water (10 mL) were added and the organic phase was separated. The organic phase was extracted with water and brine, dried over Na₂SO₄, and evaporated under reduced pressure. The crude products were purified by flash chromatography on silica gel.

1-Biphenyl-4-yl-3-methyl-butan-1-ol, 5a. Synthesised according to Method B using Biphenyl-4-carbaldehyde (1.00 g, 5.48 mmol) and a 1.0 M iso-butyilmagnesiumbromide solution in THF (7.13 mL, 7.13 mmol); yield: 0.96 g (73%); $R_f = 0.28$ (PE / EtOAc, 5:1); δ_H (CDCl₃, 500 MHz) 0.97 (d, $J = 4.9$ Hz, 6H, CH₃), 1.51–1.58 (m, 1H, CH), 1.72 (s, br, 1H, OH), 1.75–1.81 (m, 2H, CH₂), 4.79 (t, $J = 2.7$ Hz, 1H, CH), 7.33 (t, $J = 7.5$ Hz, 1H), 7.43 (d, $J = 8.4$ Hz, 4H), 7.57 (d, $J = 8.4$ Hz, 4H); MS (ESI): $m/z = 241$ [M⁺+H].

1-[4'-(tert-Butyl-dimethyl-silanyloxy)-biphenyl-4-yl]-propan-1-ol, 22b. Synthesised according to method B using **22c** (3.30 g, 10.6 mmol) and 1.0 M EtMgBr (12.7 mL). Yield: 1.89 g (52%); $R_f = 0.40$ (PE / EtOAc, 9:1); δ_H (CDCl₃, 500 MHz) 0.23 (s, 6H), 0.95 (t, $J = 7.3$ Hz, 3H), 1.00 (s, 9H), 1.76–1.89 (m, 2H), 4.64 (t, $J = 6.6$ Hz, 1H), 6.90 (d, $J = 8.5$ Hz, 2H), 7.38 (d, $J = 8.5$ Hz, 2H), 7.46 (d, $J = 8.5$ Hz, 2H), 7.54 (d, $J = 8.5$ Hz, 2H); MS (ESI): $m/z = 344$ [M⁺+H].

3-(4'-Fluorobiphenyl-4-yl)pentan-3-ol, 25a. Synthesised according to Method B using **23b** (0.58 g, 2.53

mmol) and a 1.0 M ethylmagnesiumbromide solution in THF (25.0 mL, 25.0 mmol); yield: 0.58 g (89%); R_f = 0.28 (DCM); δ_H (CDCl₃, 500 MHz): 0.82 (s, 6H, CH₃), 1.68 (s, br, 1H, OH), 1.82–1.93 (m, 4H, CH₂), 7.10–7.14 (m, 2H), 7.43–7.45 (m, 2H), 7.51–7.58 (m, 4H); MS (ESI): m/z = 259 [M⁺+H].

Method C: Suzuki-Coupling

The corresponding brominated aromatic compound (1 eq) was dissolved in toluene (7 mL / mmol), an aqueous 2.0 M Na₂CO₃ solution (3.2 mL / mmol) and an ethanolic solution (3.2 mL / mmol) of the corresponding boronic acid (1.5-2.0 eq) were added. The mixture was deoxygenated under reduced pressure and flushed with nitrogen. After repeating this cycle several times Pd(PPh₃)₄ (4 mol%) was added and the resulting suspension was heated under reflux for 8 h. After cooling ethyl acetate (10 mL) and water (10 mL) were added and the organic phase was separated. The water phase was extracted with ethyl acetate (2 x 10 mL). The combined organic phases were washed with brine, dried over Na₂SO₄, filtered over a short plug of celite® and evaporated under reduced pressure. The compounds were purified by flash chromatography on silica gel.

1-((4'-(Trifluoromethyl)biphenyl-4-yl)methyl)-1H-imidazole, 11. Synthesised according to Method C using 1-(4-bromobenzyl)-1H-imidazole (0.24 g, 1.00 mmol) and 4-trifluoromethylphenylboronic acid (0.38 g, 2.00 mmol); yield: 0.24 g (80%); brown oil; R_f = 0.14 (EtOAc); δ_H (CDCl₃, 500 MHz) 5.17 (s, 2H, CH₂), 6.93 (s, br, 1H), 7.11 (s, br, 1H), 7.24 (d, J = 7.9 Hz, 2H), 7.57 (d, J = 7.9 Hz, 2H), 7.59 (s, br, 1H), 7.65 (d, J = 8.5 Hz, 2H), 7.68 (d, J = 8.5 Hz, 2H); δ_C (CDCl₃, 125 MHz) 50.4 (CH₂), 119.2 (CH), 123.1 (C_q), 125.2 (C_q), 125.7 (CH), 127.3 (CH), 127.7 (CH), 127.8 (CH), 129.8 (CH), 136.2 (C_q), 137.4 (CH), 139.7 (C_q), 143.8 (C_q); MS (ESI): m/z = 303 [M⁺+H].

1-(4'-Fluorobiphenyl-4-yl)propan-1-one, 23b. Synthesised according to Method C using 4-bromopropiophenone (1.23 g, 6.65 mmol) and 4-fluorophenylboronic acid (1.38 g, 6.47 mmol); yield: 1.20 g (79%); R_f = 0.45 (Hex / EtOAc, 10:1); δ_H (CDCl₃, 500 MHz) 1.24–1.27 (t, J = 7.3 Hz, 3H, CH₃), 3.01–3.06 (m, 2H, CH₂), 6.97–7.01 (m, 1H), 7.06–7.11 (m, 1H), 7.58–7.61 (m, 2H), 8.02–8.04 (m, 2H); MS (ESI): m/z = 229 [M⁺+H].

1-(4'-Fluoro-2'-nitrobiphenyl-4-yl)ethanone, 35c. Synthesised according to Method C using 4-fluoro-1-iodo-2-nitrobenzene (1.20 g, 4.50 mmol) and 4-acetylbenzeneboronic acid (1.48 g, 9.00 mmol); yield: 1.01 g (87%); R_f = 0.19 (petrolether / EtOAc, 10:1); δ_H (CDCl₃, 500 MHz) 2.64 (s, 3H, CH₃), 7.38 (d, J = 8.5 Hz, 2H), 7.39–7.41 (m, 1H), 7.43 (dd, J = 5.5, 8.5 Hz, 1H), 7.67 (dd, J = 2.5, 8.0 Hz, 1H), 8.01 (d, J = 8.5 Hz, 2H); δ_C (CDCl₃, 125 MHz) 26.6 (CH₃), 112.1 (d, CH), 119.9 (d, CH), 128.3 (CH), 128.7 (CH), 131.7 (C_q), 133.2 (CH), 136.8 (C_q), 141.3 (C_q), 161.6 (d, C_q), 197.4 (C_q); MS (ESI): m/z = 259 [M⁺-H].

Method D: Reduction with NaBH₄

To an ice-cooled solution of the corresponding aldehyde or ketone (1 eq) in methanol (5 mL / mmol) was added NaBH₄ (2 eq). Then the resulting mixture was heated to reflux for 30 minutes. After cooling to ambient temperature, the solvent was distilled off under reduced pressure. Subsequently water (10 mL) was added, and the resulting mixture was extracted with ethyl acetate (3 x 10 mL). The combined organic phases were washed with brine, dried over MgSO₄ and evaporated under reduced pressure. Then the desired product was purified by chromatography on silica gel.

1-(4'-Fluoro-biphenyl-4-yl)-propan-1-ol, 23a. Synthesised according to Method D using **22b** (1.20 g,

5.26 mmol) and NaBH₄ (0.30 g, 7.89 mmol); yield: 1.15 g (95%); the compound was directly used in the next step without further purification and characterization.

1-(9H-Carbazol-2-yl)ethanol, 34a. Synthesised according to Method D using 1-(9H-carbazol-2-yl)ethanone (0.50 g, 2.39 mmol) and NaBH₄ (0.16 g, 4.30 mmol); yield: 0.42 g (83%); *R_f* = 0.12 (petrolether / EtOAc, 5:1); light yellow solid: mp 192–194 °C; δ_H (CDCl₃, 500 MHz) 1.41 (d, *J* = 6.6 Hz, 3H, CH₃), 3.13 (s, br, 1H), 4.88 (q, *J* = 6.6 Hz, 1H), 7.03 (ddd, *J* = 1.2, 7.3, 7.9 Hz, 1H), 7.07 (dd, *J* = 1.6, 8.2 Hz, 1H), 7.22 (ddd, *J* = 1.2, 7.2, 8.2 Hz, 1H), 7.30 (dt, *J* = 1.0, 8.2 Hz, 1H), 7.37–7.39 (m, 1H), 7.85 (d, *J* = 8.2 Hz, 1H), 7.88 (d, *J* = 7.9 Hz, 1H), 9.62 (s, br, 1H); δ_C (CDCl₃, 125 MHz) 25.5 (CH₃), 69.9 (CH₂), 107.3 (CH), 110.4 (CH), 116.4 (CH), 118.4 (CH), 119.5 (CH), 119.6 (CH), 121.8 (C_q), 122.6 (C_q), 124.9 (CH), 139.7 (C_q), 139.8 (C_q), 144.4 (C_q); MS (ESI): *m/z* = 210 [M⁺-H].

1-(7-Fluoro-9H-carbazol-2-yl)ethanol, 35a. Synthesised according to Method D using **35b** (0.25 g, 1.12 mmol) and NaBH₄ (0.08 g, 2.02 mmol); yield: 0.21 g (82%); *R_f* = 0.19 (petrolether / EtOAc, 5:1); δ_H (CDCl₃, 500 MHz) 1.50 (d, *J* = 6.4 Hz, 3H), 4.94 (q, *J* = 6.4 Hz, 1H), 6.85 (ddd, *J* = 2.3, 8.5, 8.8 Hz, 1H), 7.08 (dd, *J* = 2.3, 9.8 Hz, 1H), 7.15 (dd, *J* = 1.2, 8.2 Hz, 1H), 7.43 (s, br, 1H), 7.91 (d, *J* = 8.5 Hz, 1H), 7.93 (dd, *J* = 5.5, 8.5 Hz, 1H); δ_C (CDCl₃, 125 MHz) 26.0 (CH₃), 71.5 (CH), 98.0 (d, CH), 107.5 (d, CH), 108.6 (CH), 118.2 (CH), 120.5 (CH), 120.8 (C_q), 121.8 (d, CH), 123.2 (C_q), 142.2 (C_q), 142.4 (C_q), 145.1 (C_q), 163.2 (d, C_q); MS (ESI): *m/z* = 212 [M⁺-OH].

4'-(1H-Imidazol-1-yl-propyl)-biphenyl-4-ylamine, 21a. To a solution of **20** (0.32 g, 0.85 mmol) in DCM (10 mL) was added TFA (0.63 mL, 8.5 mmol) slowly in an ice bath. Subsequently it was stirred at room temperature overnight. DCM (10 mL) and water (10 mL) were added and the organic phase was separated. The organic phase was extracted with water and brine, dried over Na₂SO₄, and evaporated under reduced pressure. The crude products were purified by flash chromatography on silica gel; yield: 0.22 g (95%); *R_f* = 0.35 (PE / EtOAc, 2:1); the compound was directly used in the next step without further purification and analysis.

N-[4'-(1H-Imidazol-1-yl-propyl)-biphenyl-4-yl]-acetamide, 21. To a solution of **21a** (0.07 g, 0.25 mmol) in THF (10 mL) were added DMAP (0.02 g, 0.13 mmol) and triethylamine (0.1 mL). After cooling to 0 °C in an ice bath, acetyl chloride was dropped into the reaction solution slowly. Then it was stirred in the ambient temperature overnight. After neutralized to pH = 7 with sodium bicarbonate in an ice bath, ethyl acetate (10 mL) and water (10 mL) were added and the organic phase was separated. The organic phase was extracted with water and brine, dried over Na₂SO₄, and evaporated under reduced pressure. The crude products were purified by flash chromatography on silica gel; yield: 0.33 g (23%); white solid: mp 221–223 °C; *R_f* = 0.27 (DCM / MeOH, 20:1); δ_H (CDCl₃, 500 MHz) 0.97 (t, *J* = 7.3 Hz, 3H, CH₃), 2.20 (s, 3H, CH₃CO), 2.26 (q, *J* = 7.3, 7.6 Hz, 2H, CH₂), 5.05 (t, *J* = 7.6 Hz, 1H, CH), 6.99 (s, 1H), 7.11 (s, 1H), 7.23 (d, *J* = 8.2 Hz, 2H), 7.49–7.58 (m, 6H), 7.72 (s, 1H); δ_C (CDCl₃, 125 MHz) 11.0 (CH₃), 24.6 (CH₃CO), 28.5 (CH₂), 63.2 (CH), 120.1, 126.9, 127.5, 127.5, 135.9, 137.6, 140.5, 168.4; MS (ESI): *m/z* = 320 [M⁺+H].

4'-(1H-Imidazol-1-yl-propyl)-biphenyl-4-ol, 22. To a solution of **22a** (0.85 g, 2.16 mmol) in anhydrous THF (20 mL) was added TBAF (2.4 mL, 2.4 mmol) and subsequently the solution was stirred at room temperature for 4 h. The reaction was terminated with the addition of methanol and the solvent was removed under reduced pressure. Then the desired product was purified by chromatography on silica gel. Yield: 0.22

g (37%); Yellow solid; $R_f = 0.21$ (Hex / EtOAc, 5:1); δ_H (DMSO- d_6 , 500 MHz) 0.82 (t, $J = 7.3$ Hz, 3H), 2.21 (m, 2H), 5.23 (t, $J = 7.3$ Hz, 1H), 6.82 (d, $J = 8.8$ Hz, 2H), 6.90 (s, 1H), 7.37 (d, $J = 8.5$ Hz, 2H), 7.46 (d, $J = 8.8$ Hz, 2H), 7.54 (d, $J = 8.5$ Hz, 2H), 7.82 (s, 1H), 9.55 (s, 1H); δ_C (DMSO- d_6 , 125 MHz) 10.9 (CH₃), 27.4 (CH₂), 61.5 (CH), 115.6 (CH), 117.7 (CH), 126.0 (CH), 127.1 (CH), 127.6 (CH), 128.4 (C_q), 130.3 (CH), 130.7 (C_q), 139.3 (CH), 139.5 (C_q), 157.1 (C_q); MS (ESI): $m/z = 279$ [M⁺+H].

3-(4'-Fluorobiphenyl-4-yl)-3-(1H-imidazol-1-yl)propan-1-ol, 26. 26a (0.241 g, 0.45 mmol) was dissolved by slowly adding dropwise to 15 mL THF and 1M TBAF (0.55 mL, 0.55 mmol) in THF. 1 hour later, according to TLC (DCM / methanol, 95:5) the deprotection was quantitative. The batch was diluted with a large quantity of ethyl acetate and extracted three times with water and once with brine, then dried over MgSO₄ and the solvent removed under reduced pressure. The crude product was subsequently purified by column chromatography; yield: 0.09 g (67%); $R_f = 0.34$ (DCM / MeOH, 9:1); δ_H (CDCl₃, 500 MHz) 2.43–2.49 (m, 2H, CH₂), 3.50–3.54 (m, 1H), 3.68–3.72 (m, 1H), 5.56–5.59 (q, 1H, CH), 6.98–6.99 (m, 1H), 7.08–7.09 (m, 1H), 7.13–7.14 (m, 2H), 7.26–7.29 (m, 2H), 7.48–7.51 (m, 4H), 7.56–7.57 (m, 1H); δ_C (CDCl₃, 125 MHz) 37.1 (CH₂), 50.5 (CH), 57.7 (CH₂-OH), 116.3, 127.6, 128.6, 129.8, 136.8, 137.2, 139.9, 140.0, 161.4; MS (ESI): $m/z = 297$ [M⁺+H].

1-(3-Chloro-1-(4'-fluorobiphenyl-4-yl)propyl)-1H-imidazole, 27. 26 (0.044 g, 0.148 mmol) was dissolved in 10 mL dry DCM and mixed with 13 μ L thionyl chloride. The batch was stirred for 2 hours at room temperature; according to the TLC control, the reaction was quantitative. The batch was diluted with a large quantity of DCM and water. The organic phase was separated off and extracted 5 times with water and once with brine, then dried over MgSO₄ and the solvent removed under reduced pressure; yield: 0.05 g (99%); $R_f = 0.63$ (DCM / MeOH, 9:1); δ_H (CDCl₃, 500 MHz) 2.87–2.97 (m, 2H, CH₂), 3.50–3.60 (m, 2H, CH₂Cl), 5.80–5.83 (m, 1H, CH), 7.11–7.16 (m, 2H), 7.16–7.17 (m, 1H), 7.35–7.37 (m, 1H), 7.49–7.53 (m, 4H), 7.58–7.60 (m, 2H), 9.51–9.53 (m, 1H); δ_C (CDCl₃, 125 MHz) 34.2 (CH₂), 41.4 (CH₂Cl), 61.8 (CH), 119.6, 122.9, 116.5, 128.4, 129.4, 135.7, 136.3, 137.6, 136.4, 142.5, 163.5; MS (ESI): $m/z = 315$ [M⁺+H].

1-(7-(tert-Butyldimethylsilyloxy)-9H-fluoren-2-yl)ethanone, 30c. Imidazole (0.17 g, 2.45 mmol) and 1-(7-hydroxy-9H-fluoren-2-yl)ethanone (0.50 g, 2.23 mmol) were dissolved in 20 mL DCM. Then tert-butyldimethylsilylchloride (0.37 g, 2.45 mmol) dissolved in 3 mL DCM were slowly added. The resulting mixture was stirred for 18 h at room temperature. Afterwards the mixture was extracted with water and brine. The organic phase was separated, dried over Na₂SO₄ and evaporated; yield: 0.58 g (77%); $R_f = 0.40$ (petrolether / EtOAc, 10:1); MS (ESI): $m/z = 339$ [M⁺+H].

7-(1-(1H-imidazol-1-yl)ethyl)-9H-fluoren-2-ol, 30. 30a (0.16 g, 0.40 mmol) was dissolved in 10 mL THF and 1M TBAF (0.41 mL, 0.41 mmol) solution in THF was added dropwise. After 1 hour according to TLC (DCM / methanol 95:5) the deprotection was quantitative. The batch was diluted with a large quantity of ethyl acetate and extracted three times with water and once with brine, then dried over MgSO₄ and the solvent removed under reduced pressure; yield: 0.10 g (90%); $R_f = 0.12$ (MeOH / EtOAc, 5:95); orange solid: mp 217–218 °C; δ_H (CDCl₃, 500 MHz) 1.81 (d, $J = 6.9$ Hz, 3H), 3.70 (s, 2H), 5.31 (q, $J = 6.9$ Hz, 1H), 6.77 (dd, $J = 2.2, 8.2$ Hz, 1H), 6.90 (s, 1H), 6.93 (s, 1H), 6.95 (s, 1H), 7.06 (d, $J = 7.9$ Hz, 1H), 7.18 (s, 1H), 7.50 (d, $J = 8.2$ Hz, 1H), 7.52 (d, $J = 7.9$ Hz, 1H), 7.55 (s, 1H); δ_C (CDCl₃, 125 MHz) 21.9 (CH₃), 36.6 (CH₂), 56.9 (CH), 112.0 (CH), 114.1 (CH), 118.1 (CH), 118.8 (CH), 120.6 (CH), 122.4 (CH), 124.7 (CH),

128.2 (CH), 132.8 (C_q), 135.6 (CH), 137.9 (C_q), 142.0 (C_q), 143.2 (C_q), 145.2 (C_q), 156.6 (C_q); MS (ESI): $m/z = 277$ [M⁺+H].

1-(7-Fluoro-9H-carbazol-2-yl)ethanone, 35b. 35c was dissolved in 3 mL P(OEt)₃ and refluxed for 16 h. The resulting mixture was directly purified using column chromatography; yield: 0.28 g (53%); $R_f = 0.13$ (petrolether / EtOAc, 5:1); δ_H (CDCl₃, 500 MHz) 2.54 (s, 3H), 6.79 (ddd, $J = 2.3, 8.6, 9.5$ Hz, 1H), 7.01 (dd, $J = 2.3, 9.6$ Hz, 1H), 7.65 (dd, $J = 1.6, 8.2$ Hz, 1H), 7.85 (dd, $J = 5.4, 8.5$ Hz, 1H), 7.87 (d, $J = 8.5$ Hz, 1H), 7.93 (dd, $J = 0.6, 1.6$ Hz, 1H), 10.53 (s, br, 1H); δ_C (CDCl₃, 125 MHz) 26.5 (CH₃), 97.4 (d, CH), 107.3 (d, CH), 110.9 (CH), 118.4 (C_q), 119.0 (CH), 119.2 (CH), 121.6 (d, CH), 126.2 (C_q), 133.6 (C_q), 139.7 (C_q), 142.0 (d, C_q), 162.2 (d, C_q), 197.8 (C_q); MS (ESI): $m/z = 227$ [M⁺+H].

Docking studies

All molecular modelling studies were performed on Intel(R) P4 CPU 3.00GHz running Linux Suse 10.1.

Ligands. The structures of the inhibitors were built with SYBYL 7.3.2 (Sybyl, Tripos Inc., St. Louis, Missouri, USA) and energy-minimized in MMFF94s force-field^{24a} as implemented in Sybyl. The resulting geometries for our compounds were then subjected to ab initio calculation employing the B3LYP functional^{24b-c} in combination with a 6-31G* basis set using the package Gaussian03 (Gaussian, Inc., Pittsburgh, PA, 2003).

Docking. Various inhibitors were docked into our CYP17 homology model by means of the GOLD v3.0.1 software.²⁵ Since it is known that non-steroidal inhibitors of CYP enzymes primary interact by complexation of the heme iron with their sp² hybridized nitrogen^{15c} a distance constraint of a minimum of 1.9 and a maximum of 2.5 Å between the nitrogen of the imidazole and the iron was set.

Ligands were docked in 50 independent genetic algorithm (GA) runs using GOLD. Heme iron was chosen as active-site origin, while the active site radius was set equal to 19 Å. The automatic active-site detection was switched on. A distance constraint of a minimum of 1.9 and a maximum of 2.5 Å between the sp²-hybridised nitrogen of the imidazole and the iron was set. Furthermore, some of the GOLDScore parameters were modified to improve the weight of hydrophobic interaction and of the coordination between iron and nitrogen. The genetic algorithm default parameters were set as suggested by the GOLD authors. On the other hand, the annealing parameters of fitness function were set at 3.5 Å for hydrogen bonding and 6.5 Å for Van der Waals interactions.

All 50 poses for each compound were clustered with ACIAP²⁶ and the representative structure of each significant cluster was selected. The quality of the docked representative poses was evaluated based on visual inspection of the putative binding modes of the ligands, as outcome of docking simulations and cluster analysis. Further the different interaction patterns were manually analyzed using Silver 1.1,^{25b} a program included for use with GOLD and used to post-process docking results.

Acknowledgement: The authors thank Ulrike E. Hille and Dr Carsten Jagusch for their help in the synthesis of some compounds, Maria-Christina Scherzberg for the IC₅₀ determination of some compounds. We also are grateful to Professor J. Hermans, Cardiovascular Research Institute, University of Maastricht, Netherlands, for providing us with V79MZh11B1 cells expressing human CYP11B1 and Professor R. Bernhardt, Saarland University, Germany, for making us V79MZh11B2 cells expressing human CYP11B2

available. This research was supported in part by the Fonds der Chemischen Industrie.

Supplementary data: The synthetic procedures and characterization of further intermediates and IR spectra of all compounds as well as the purities of final compounds by element analysis or HPLC can be found in the online version.

References

1. (a) Smith, J. A. *J. Urol.* **1987**, *137*, 1. (b) Crawford, E. D.; Eisenberger, M. A.; McLeod, D. G.; Spaulding, J. T.; Benson, R.; Dorr, F. A.; Blumstein, B. A.; Davis, M. A.; Goodman, P. J. *N. Engl. J. Med.* **1989**, *321*, 419.
2. Chung, B. C.; Picardo-Leonard, J.; Hanui, M.; Bienkowski, M.; Hall, P. F.; Shively, J. E.; Miller, W. L. *Proc. Natl. Acad. Sci. USA.* **1987**, *84*, 407.
3. (a) Swinney, M.; Mak, A. Y. *Biochem.* **1994**, *33*, 2185. (b) Akhtar, M.; Corina, D. L.; Miller, S. L.; Shyadehi, A. Z.; Wright, J. N. *Biochem.* **1994**, *33*, 4410.
4. (a) Hartmann, R. W.; Hector, M.; Haidar, M.; Ehmer, P. B.; Reichert, W.; Jose, J. *J. Med. Chem.* **2000**, *43*, 4266. (b) Hartmann, R. W.; Hector, M.; Wachall, B. G.; Paluszczak, A.; Palzer, M.; Huch, V.; Veith, M. *J. Med. Chem.* **2000**, *43*, 4437. (c) Njar, V. C. O.; Hector, M.; Hartmann, R. W. *Bioorg. Med. Chem.* **1996**, *4*, 1447.
5. (a) Potter, G. A.; Banie, S. E.; Jarman, M.; Rowlands, M. G. *J. Med. Chem.* **1995**, *38*, 2463. (b) Jarman, M.; Barrie, S. E.; Lera, J. M. *J. Med. Chem.* **1998**, *41*, 5375.
6. (a) Gambertoglio, J. G.; Amend, W. J. Jr; Benet, L. Z. *J. Pharmacokinet. Biopharm.* **1980**, *8*, 1. (b) Fotherby, K. *Contraception.* **1996**, *54*, 59. (c) Steiner, J. F. *Clin. Pharmacokinet.* **1996**, *30*, 16. (d) Hameed, A.; Brothwood, T.; Bouloux, P. *Curr. Opin. Investig. Drugs.* **2003**, *4*, 1213.
7. (a) Buster, J. E.; Casson, P. R.; Straughn, A. B.; Dale, D.; Umstot, E. S.; Chiamovi, N.; Abraham, G. E. *Am. J. Obstet. Gynecol.* **1992**, *166*, 1163. (b) Peterson, R. E. Metabolism of adrenal cortical steroids. In: Christy, N.P. editor. *The human adrenal cortex*. New York: Harper & Row, **1997**, pp. 87-189.
8. (a) Wächter, G. A.; Hartmann, R. W.; Sergejew, T.; Grün, G. L.; Ledergerber, D. *J. Med. Chem.* **1996**, *39*, 834. (b) Zhuang, Y.; Hartmann, R. W. *Archiv. Pharm.* **1998**, *331*, 36. (c) Zhuang, Y.; Hartmann, R. W. *Archiv. Pharm.* **1998**, *331*, 25. (d) Hartmann, R. W.; Wachall, B. WO9918075, 1998.
9. (a) Rowlands, M. G.; Barrie, S. E.; Chan, F.; Houghton, J.; Jarman, M.; McCague, R.; Potter, G. A. *J. Med. Chem.* **1995**, *38*, 4191. (b) Chan, F. C. Y.; Potter, G. A.; Barrie, S. E.; Haynes, B. P.; Rowlands, M. J.; Houghton, G.; Jarman, M. *J. Med. Chem.* **1996**, *39*, 3319.
10. (a) Matsunaga, N.; Kaku, T.; Itoh, T.; Tanaka, T.; Hara, T.; Miki, H.; Iwasaki, M.; Aono, T.; Yamaoka, M.; Kusaka, M.; Tasaka, A. *Bioorg. Med. Chem.* **2004**, *12*, 2251. (b) Matsunaga, N.; Kaku, T.; Ojida, A.; Tanaka, T.; Hara, T.; Yamaoka, M.; Kusaka, M.; Tasaka, A. *Bioorg. Med. Chem.* **2004**, *12*, 4313. (c) Tasaka, A.; Hitaka, T.; Matsunaga, N.; Kusaka, M.; Adachi, M.; Aoki, I.; Ojida, A. WO02040484, 2002.
11. (a) Bierer, D.; Mcclue, A.; Fu, W.; Achebe, F.; Ladouceur, G. H.; Burke, M. J.; Bi, C.; Hart, B.; Dumas, J.; Sibley, R.; Scott, W. J.; Johnson, J.; Asgari, D. WO03027085, 2003. (b) Ladouceur, G. H.; Burke, M. J.; Wong, W. C.; Bierer, D. WO03027094, 2003.
12. (a) Wachall, B. G.; Hector, M.; Zhuang, Y.; Hartmann, R. W. *Bioorg. Med. Chem.* **1999**, *7*, 1913. (b) Zhuang, Y.; Wachall, B. G.; Hartmann, R. W. *Bioorg. Med. Chem.* **2000**, *8*, 1245. (c) Leroux, F.; Hutschenreuter, T. U.; Charriere, C.; Scopelliti, R.; Hartmann, R. W. *Helv. Chim. Acta* **2003**, *86*, 2671. (d) Hutschenreuter, T. U.; Ehmer, P. E.; Hartmann, R. W. *J. Enzyme Inhib. Med. Chem.* **2004**, *19*, 17.
13. Jagusch, C.; Negri, M.; Hille, U. E.; Hu, Q.; Bartels, M.; Jahn-Hoffmann, K.; Pinto-Bazurco Mendieta, M. A. E.; Rodenwaldt, B.; Müller-Vieira, U.; Schmidt, D.; Lauterbach, T.; Recanatini, M.; Cavalli, A.; Hartmann, R. W. *Bioorg. Med. Chem.* **2008**, *16*, 1992.
14. Miyaura, N.; Suzuki, A. *Chem. Rev.* **1995**, *95*, 2457.
15. Tang, Y.; Dong, Y.; Vennerstrom, J. L. *Synthesis* **2004**, *15*, 2540.
16. (a) Ehmer, P. B.; Jose, J.; Hartmann, R. W. *J. Steroid Biochem. Mol. Biol.* **2000**, *75*, 57. (b) Hartmann, R. W.; Bayer, H.; Gruen, G. *J. Med. Chem.* **1994**, *37*, 1275. (c) Denner, K.; Bernhardt, R. Inhibition studies of steroid conversions mediated by human CYP11B1 and CYP11B2 expressed in cell cultures. In *Oxygen Homeostasis and Its Dynamics*; Ishimura, Y.; Shimada, H.; Suematsu, M., Eds.; Springer-Verlag: Tokyo-Berlin-Heidelberg-New York, 1998, pp 231-236. (d) Böttner, B.; Denner, K.; Bernhardt, R. *Eur. J. Biochem.* **1998**, *252*, 458.
17. Pinto-Bazurco Mendieta, M. A. E.; Negri, M.; Jagusch, C.; Hille, U. E.; Müller-Vieira, U.; Schmidt, D.; Hansen, K.; Hartmann, R. W. *Bioorg. Med. Chem. Lett.* **2008**, *18*, 267.
18. (a) Lin, D.; Zhang, L.; Chiao, E.; Miller, L. W. *Mol. Endocrinol.* **1994**, *8*, 392. (b) Auchus, R. J.; Miller, W. L. *Mol. Endocrinol.* **1999**, *13*, 1169.
19. Mathieu, A. P.; LeHoux, J.-G.; Auchus, R. J. *Biochim. Biophys. Acta* **2003**, *1619*, 291.
20. White, P. C.; Curnow, K. M.; Pascoe, L. *Endocr. Rev.* **1994**, *15*, 421.
21. Cuberes, M. R.; Moreno-Manas, M.; Trius, A. *Synthesis*, **1985**, *3*, 302.
22. Regel, E.; Draber, W.; Buechel, K. H.; Plempel, M. US4118487, 1978.
23. Okada, M.; Yoden, T.; Kawaminami, E.; Shimada, Y.; Ishihara, T.; Kudou, M. US5807880, 1994.
24. (a) Halgren, T. A. *J. Comput. Chem.* **1999**, *20*, 730. (b) Becke, A. D. *J. Chem. Phys.* **1993**, *98*, 5648. (c) Stevens, P. J.; Devlin, J. F.; Chabalowski, C. F.; Frisch, M. J. *J. Phys. Chem.* **1994**, *98*, 11623.
25. (a) Jones, G.; Willett, P.; Glen, R. C.; Leach, A. R.; Taylor, R. *J. Mol. Biol.* **1997**, *267*, 727. (b)

http://www.ccdc.cam.ac.uk/products/life_sciences/gold/

26. (a) Bottegoni, G.; Cavalli, A.; Recanatini, M. *J. Chem. Inf. Mod.* **2006**, *46*, 852. (b) Bottegoni, G.; Rocchia, W.; Recanatini, M.; Cavalli, A. *Bioinformatics*, **2006**, *22*, e58.

3.II The Role of Fluorine Substitution in Biphenyl Methylene Imidazole Type CYP17 Inhibitors for the Treatment of Prostate Carcinoma

Qingzhong Hu, Matthias Negri, Sureyya Olgen, and Rolf W. Hartmann

This manuscript has been published as an article in
ChemMedChem **2010**, 5, 899–910.

Paper II

Abstract: It has been illuminated that the growth of most prostate carcinoma depends on androgen stimulation. Therefore the inhibition of CYP17 to block androgen biosynthesis is regarded as a promising therapy. Based on our previously identified lead compound **Ref 1**, a series of fluorine substituted biphenyl methylene imidazoles were designed, synthesized and evaluated as CYP17 inhibitors, to elucidate the influence of fluorine on in vitro and in vivo activity. It has been found that meta- F substitution on the C-ring improved the activity, whereas *ortho*- substitution reduced the potency. Docking studies which were performed with our human CYP17 homology model suggest multi-polar interactions between fluorine and Arg109, Lys231, His235 and Glu305. As expected, introduction of fluorine also prolonged the plasma half-life. The SARs obtained confirm the reliability of the protein model and result in compound **9** (IC₅₀ = 131 nM) as strong CYP17 inhibitor showing potent activity in the rat, a high bioavailability and a long plasma half-life (12.8 hours).

Keywords: prostate cancer, CYP17 inhibitors, fluorine, pharmacokinetics, testosterone plasma concentrations.

Introduction

As the most common malignancy in male elders, prostate carcinoma also acts as a major cause of death.^[1] It has been illuminated that the growth of up to 80 % of prostate carcinoma depends on androgen stimulation. Therefore, segregation of tumour cells from androgen will effectively prevent cancer cell proliferation. Since more than 90 % of testosterone is produced in testes, orchidectomy or treatment with gonadotropin-releasing hormone (GnRH) analogues^[2] (chemical castration) are applied in clinic. As this therapy has no effect on the minor amount of androgen produced in the adrenals, androgen receptor antagonists are employed additionally. This is the current standard therapy for prostate carcinoma, the so called “combined androgen blockade” (CAB).^[3] However, CAB often leads to resistance which can be associated with androgen receptor mutations. The mutated androgen receptor recognizes antagonists and glucocorticoids as agonists, finally resulting in the collapse of CAB therapy.^[4]

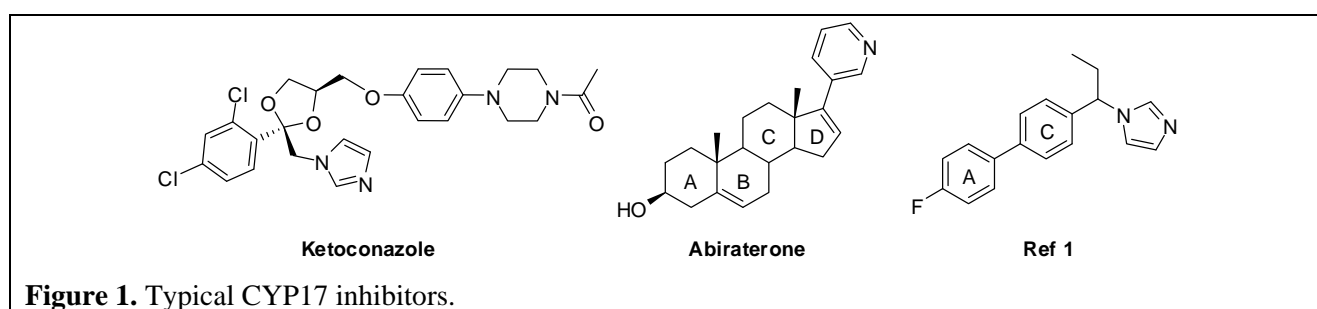
The shortcomings of CAB waken a more promising alternative: total blockage of androgen biosynthesis, which means inhibition of cytochrome P450-17 (17 α -hydroxylase-17,20-lyase, CYP17). CYP17 is one of six CYP enzymes involved in steroid biosynthesis. Like all CYP enzymes, CYP17 consists of a heme and an apoprotein moiety. Although all potent inhibitors interfere with the heme, which is common to CYP enzymes, by complexing its central iron ion, it is nevertheless possible to selectively inhibit these enzymes as has been demonstrated with CYP19 (aromatase, estrogen synthase)^[5] and CYP11B2 (aldosterone synthase).^[6] While aromatase inhibitors are already in clinical use,^[5a] the first highly potent and selective CYP11B2 inhibitors have been identified just recently,^[6] some of which are extremely selective.

CYP17, located in both testicular and adrenal tissue,^[7] is the key enzyme catalyzing the conversion of pregnenolone and progesterone to dehydroepiandrosterone (DHEA) and androstenedione, respectively. DHEA can be transformed into androstenedione by 3 β -HSD, which is subsequently converted into the most potent androgen dihydrotestosterone (DHT) in androgen target cells through two enzymatic steps catalyzed by 17 β -HSD1 or 3 and steroid 5 α -reductase (5 α R). Thus, inhibition of CYP17 could annihilate the androgen production both in testes and in adrenals. Furthermore, targeting genetically stable human tissue instead of cancer cells would avoid the resistance caused by mutation.

Ketoconazole (Figure 1), an antimycotic agent showing non-selective inhibition of CYP17, is the first medication which has been used clinically in treatment of prostate carcinoma. Although withdrawn because of side-effects, Ketoconazole shows good curative effects,^[8] which demonstrates the feasibility of prostate carcinoma treatment via CYP17 inhibition. Since then, in mimicry of the physiological substrates, many steroidal CYP17 inhibitors were synthesized by others^[9] and our group,^[10] including Abiraterone (Figure 1), which has entered into phase II clinical trial recently. However, the affinity of steroidal compounds toward steroid receptors, which often results in side effects no matter acting as agonists or antagonists, prompted us to develop non-steroidal CYP17 inhibitors.^[11, 12]

Our group has reported about series of biphenyl methylene imidazoles as potent CYP17 inhibitors.^[12] A promising lead compound 1-[1-(4'-fluoro-biphenyl-4-yl)-propyl]-1*H*-imidazole^[12g] (**Ref 1**, Figure 1) was identified in the optimization process. In the present investigation this compound was further modified to elevate potency, selectivity as well as pharmacokinetic properties. Since fluorine is known to be able to form

multi-polar interactions with several amino acids^[13e-1] and due to its capability to enhance metabolic stability, the biphenyl core was substituted with additional fluorine atoms leading to compounds **1–22**. Exchanging the 1-imidazolyl group by a 5-imidazolyl moiety while maintaining 4-fluoro-phenyl as A-ring, compounds **23–26** were subsequently obtained. Furthermore, besides determination of inhibitory activities toward human CYP17 in vitro, selected compounds were examined for their potency to reduce plasma testosterone concentration and for their pharmacokinetic properties in rats. Moreover, computational investigations were performed: molecular docking studies using our homology model of human CYP17^[12e] to elucidate the enzyme-inhibitor interactions and quantum mechanical studies to explore the influence of fluorine substitution on potency and pharmacokinetic properties of this type of CYP17 inhibitors.



Drug design

Fluorine, as the most electronegative atom, has been widely employed to prevent undesired metabolism because of the strong C-F bonds. Besides the increase of metabolic stability, fluorine can also improve other pharmacokinetic properties by means of influencing pKa, elevating lipophilicity and reducing plasma protein binding.^[13] Recently, multi-polar interactions between fluorine and some amino acid residues, responsible for the enhanced binding potency, have also been reported.^[13e-1] Based on these findings, fluorophilicity and fluorophobicity in protein active site have been discussed,^[13c, d] and systemic fluorine scan was recommended in drug discovery and lead optimization.

We found that fluorine substitution at the *para*- position of the A-ring could significantly increase the inhibitory potency of biphenyl methylene imidazole type CYP17 inhibitors, resulting in compound **Ref 1** (IC₅₀ = 345 nM).^[12g] Besides the complexation of the heme iron, recognized as the main anchor point for non-steroidal CYP inhibitors (first notified for CYP19 inhibitors^[5b-c]), by a heterocyclic nitrogen, polar interactions between this fluorine atom and the guanidinium side chain of Arg109 and the amino side chain of Lys231 were observed for **Ref 1** and considered as important for binding affinity^[12g] (Figure 2). The A-ring is presumably stabilized by a strong T-shaped arene quadrupole interaction with Phe114, a conformationally flexible residue responsible for dividing the CYP17 active site into two lobes. Furthermore, some more amino acid residues such as Asn, Arg or Gln were identified close to the A- or C-ring, which might provide the potential for additional fluorine substituents to form multi-polar interaction with H-X (where X = N, O, S)^[13h-1] and backbone C=O (in an orthogonal manner),^[13e-f] or even with the H-C_α.^[13c, 13g] Consequently, the following strategies to increase the inhibitory potency and the metabolic stability of **Ref 1** were applied: a) shifting the fluorine to other positions in the A-ring; b) additional introduction of fluorine atoms on the A- or C-ring in order to identify new interaction areas. Since these modifications change the molecular electrostatic potentials (MEP) of the compounds, the protein pocket surrounding of the C-ring was

scrutinized with the aim to identify potential interaction areas influenced by MEP variations, especially the backbone π -systems of amino acids such as Gly301-Ala302.

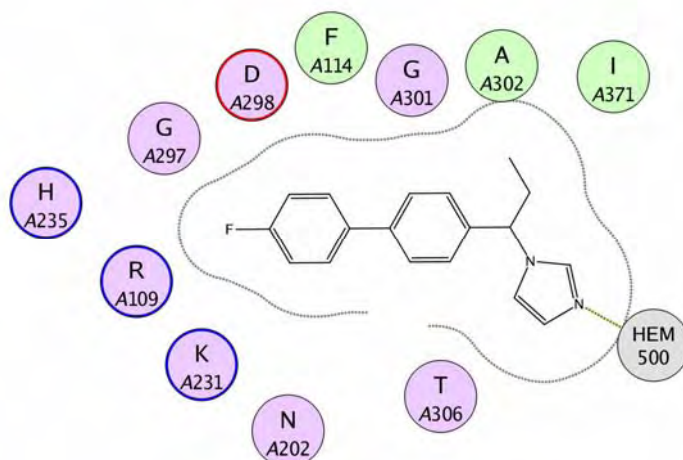


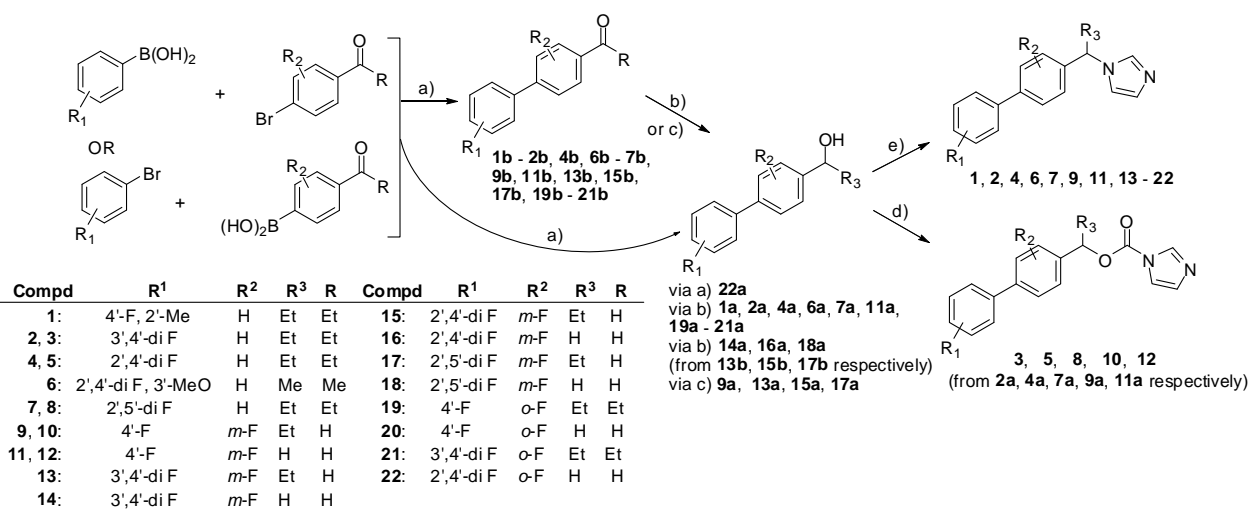
Figure 2. Amino acid residues surrounding **Ref 1**: Arg109 and Lys231 interact with the *para*-F on the A-ring. Some more amino acid residues around the A-ring or C-ring might form additional multi-polar interactions with further F substituents.

Results and Discussion

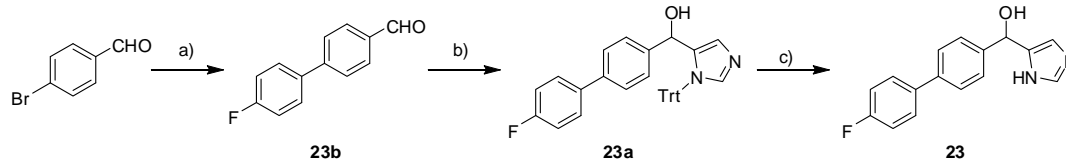
Chemistry

The syntheses of compounds **1–26** are shown in Schemes 1–3. For 1-imidazole analogues **1–22**, a general synthetic strategy was employed: ketone or aldehyde intermediates were obtained by means of Suzuki coupling (Method C) from the corresponding bromides and boronic acids.^[14] Subsequently they were converted to the alcohols by reduction with NaBH_4 (Method D) or Grignard reaction (Method B). The alcohol intermediates reacted with 1,1-carbonyl diimidazole (CDI) to give the racemic mixtures of the desired products, which were not separated into their enantiomers. Using different reaction conditions, such as solvent and reaction temperature, different products were obtained in this $\text{S}_\text{N}1$ reaction. After refluxing in NMP for 4 hours (Method A),^[15] biphenyl methylene imidazoles were obtained; whereas boiling in THF for

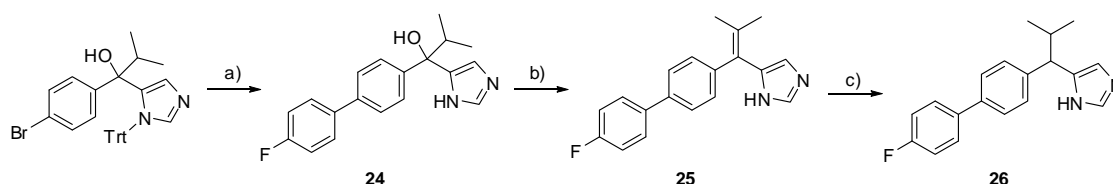
Scheme 1.^a



^a Reagents and conditions: Compounds were synthesized from the corresponding **a** or **b** intermediates unless annotated otherwise. a) Method C: $\text{Pd}(\text{PPh}_3)_4$, Na_2CO_3 , toluene, reflux, 6h. b) Method D: NaBH_4 , MeOH. c) Method B: EtMgBr , THF. d) Method E: CDI, THF, reflux, 4 days. e) Method A: CDI, NMP, reflux, 4h.

Scheme 2.^a

^a Reagents and conditions: a) Method C: 4-fluoro boronic acid, Pd(PPh₃)₄, Na₂CO₃, toluene, reflux, 6h. b) i. imidazole, n-BuLi, TrtCl, THF, 0 °C, 2h; ii. n-BuLi, *tert*-Bu-diMe-SiCl, THF, 0 °C, 2h; c. n-BuLi, **23b**, THF, room temp, 8h. c) pyridinium hydrochloride, MeOH, 60 °C, 4h.

Scheme 3.^a

^a Reagents and conditions: a) i. Method C: 4-fluoro boronic acid, Pd(PPh₃)₄, Na₂CO₃, toluene, reflux, 6h; ii. pyridinium hydrochloride, MeOH, 60 °C, 4h. b) HCl / *i*-PrOH, 80 °C, 2h. c) Pd(OH)₂, ethanol, THF, H₂, room temp, 3h.

4 days (Method E) gave imidazole-1-carboxylic acid biphenyl esters as major products. Distinguishing between these two products is easy as the chemical shifts of imidazole 2-H in biphenyl methylene imidazoles are around 7.6 ppm, whereas they are beyond 8.2 ppm in imidazole-1-carboxylic acid biphenyl esters.^[15] Moreover, the proton chemical shift of CH is 5.1 ppm in the biphenyl methylene imidazoles, whereas in the imidazole-1-carboxylic acid biphenyl esters it is 5.9 ppm. Additionally, the strong carbonyl signal in the IR spectra contributes to the identification of the latter class of compounds. For the synthesis of the 5-imidazole analogues (**23–26**) trityl was employed as protecting group for imidazole. The alcohol intermediates, commercially available or obtained by reaction of imidazolyl lithium with aldehyde, underwent elimination of the H₂O group in acidic environment to give the corresponding isopropylidene product, which was subsequently saturated by hydrogenation of the double bond.

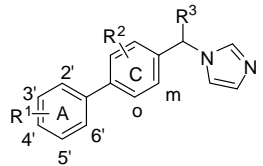
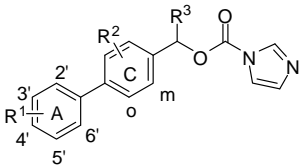
In vitro activity

CYP17 inhibition of all compounds was evaluated using the 50,000 sediment after homogenation of *E. coli* expressing human CYP17 as well as cytochrome P450 reductase.^[12d] The assay was run with progesterone as substrate and NADPH as cofactor. Separation of substrate and product was accomplished by HPLC using UV detection.^[16] IC₅₀ values are presented in comparison to Ketoconazole and Abiraterone in Tables 1–2.

It is striking that in the series of 1-imidazole compounds (**1–22**) a sharp structure activity relationship is observed. The analogues can be divided into 3 classes regarding the fluorine substitution on the C-ring, i.e. without F, *meta*-F and *ortho*-F (positions relative to the A-ring, Table 1).

It can be seen that, in the class of compounds without fluorine on the C-ring, additional substitution at the A-ring by fluorine, methyl or methoxy (**1, 2, 4, 6** and **7**), did not enhance the inhibitory activity compared to **Ref 1** (IC₅₀ = 345 nM). For example, extra fluorine substitution at *meta*- or *ortho*-position of the A-ring, resulting in 3',4'-di F (**2**) and 2',4'-di F (**4**) analogues, decreased activity somewhat (IC₅₀ = 803 and 985 nM, respectively). Interestingly, 2',5'-di F substitution (**7**) exhibited similar inhibitory potency (IC₅₀ = 956 nM) as seen with the 2',4'-di F analogue.

Table 1. Inhibition of CYP17 by compounds **1–22**.

		 Ref 1, 1-2, 4, 6-7, 9, 11, 13-22				 3, 5, 8, 10, 12								
Compd	R ¹	R ²	R ³	IC ₅₀ ^[a]	Compd	R ¹	R ²	R ³	IC ₅₀ ^[a]	Compd	R ¹	R ²	R ³	IC ₅₀ ^[a]
Ref 1	4'-F	H	Et	345	9	4'-F	<i>m</i> -F	Et	131	19	4'-F	<i>o</i> -F	Et	657
					10	4'-F	<i>m</i> -F	Et	4643					
					11	4'-F	<i>m</i> -F	H	2110	20	4'-F	<i>o</i> -F	H	2800
					12	4'-F	<i>m</i> -F	H	>5000					
1	4'-F, 2'-Me	H	Et	951										
2	3',4'-di F	H	Et	803	13	3',4'-di F	<i>m</i> -F	Et	305	21	3',4'-di F	<i>o</i> -F	Et	825
3	3',4'-di F	H	Et	>5000	14	3',4'-di F	<i>m</i> -F	H	>5000					
4	2',4'-di F	H	Et	985	15	2',4'-di F	<i>m</i> -F	Et	381					
5	2',4'-di F	H	Et	>5000	16	2',4'-di F	<i>m</i> -F	H	>5000	22	2',4'-di F	<i>o</i> -F	H	>5000
6	2',4'-di F, 3'-MeO	H	Me	>10000										
7	2',5'-di F	H	Et	956	17	2',5'-di F	<i>m</i> -F	Et	364					
8	2',5'-di F	H	Et	>5000	18	2',5'-di F	<i>m</i> -F	H	1640					
KTZ ^[b]				2780						ABT ^[b]				72

^[a] Concentration of inhibitors required to give 50 % inhibition. The mean values of at least three experiments are given in nM within ±10 % deviation.

^[b] **KTZ**: Ketoconazole; **ABT**: Abiraterone.

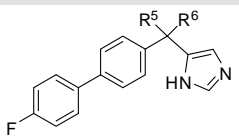
Importantly, the introduction of fluorine at the *meta*- position of the C-ring significantly increased the inhibitory potency. Compound **9** showed IC₅₀ of 131 nM, being 3 fold more potent than **Ref 1**. Similar improvements can be found for the other compounds in this class (**13**, **15** and **17**, IC₅₀ values around 350 nM) being 3 fold more potent than the corresponding compounds without F at the C-ring (**2**, **4** and **7**, respectively, IC₅₀ values around 900 nM). Moreover, it can be seen that the analogue with only one *para*-F at the A-ring (**9**) is more potent than other analogues with multi-F on the A-ring as mentioned above. A similar ranking of potency can be observed for multi-F analogues in this class of compounds too: the 3',4'-di F compound (**13**, IC₅₀ = 305 nM) being more potent than the others, e. g. the 2',5'-di F compound (**15**, IC₅₀ = 381 nM) and the 2',4'-di F compound (**17**, IC₅₀ = 364 nM).

On the contrary, *ortho*-F substitution at the C ring decreased activity. Compound **19** (IC₅₀ = 657 nM) was less potent than the corresponding analogues with *meta*-F (**9**, IC₅₀ = 131 nM) or without F (**Ref 1**, IC₅₀ = 345 nM). However, compound **19** exhibited stronger inhibition compared to compound **21** furnished with two fluorine substituents in 3',4'-position as expected.

Moreover, all imidazole-1-carboxylic acid biphenyl esters (**3**, **5**, **8**, **10** and **12**), which have been proven to be stable in incubation buffer by HPLC, were found to be inactive. This is probably due to the fact that these molecules are too large to fit into the binding pocket. Noteworthy is the importance of the ethyl substituent at the methylene bridge, as already reported,^[12g] i.e. that ethyl substitution results in more potent compounds compared to the corresponding non- or methyl substituted analogues.

Furthermore, 5-imidazole was employed instead of 1-imidazole leading to compounds **23–26** as shown in table 2. It is apparent that compounds with a hydroxy group substituted at the methylene bridge are inactive. Nonetheless, isopropyl substitution resulted in an active compound (**26**, IC₅₀ = 502 nM), which was, however, less potent compared to **Ref 1**. Surprisingly, the compound with an isopropylidene substitution (**25**) turned out to be very potent (IC₅₀ = 159 nM).

Table 2. Inhibition of CYP17 by compounds **23–26**.

							
Compd	R ⁵	R ⁶	IC ₅₀ ^[a]	Compd	R ⁵	R ⁶	IC ₅₀ ^[a]
23	OH	H	>>10000	25	<i>i</i> -Propylidene		159
24	OH	<i>i</i> -Pr	>5000	26	H	<i>i</i> -Pr	502
KTZ ^[b]			2780	ABT ^[b]			72

^[a] Concentration of inhibitors required to give 50 % inhibition. The mean values of at least three experiments are given in nM within ±10 % deviation.
^[b] **KTZ**: Ketoconazole; **ABT**: Abiraterone.

Finally, inhibition values of the most active compounds **9**, **13**, **15**, **17** and **25** toward the hepatic enzyme CYP3A4 were also determined, because of its important role in drug metabolism and drug-drug interaction. It turned out that the compounds tested showed only marginal inhibition (around 50 % at 10 μM), clearly lower than that shown by Ketoconazole (98 % at 10 μM).

Computational studies

Docking

Compounds **Ref 1**, **9**, **11**, **13**, **15**, **17** and **19**, both enantiomers if existing, were docked into the homology model of human CYP17^[12e] by means of two commercial docking softwares, GOLD_v4.0^[17] and FlexX 3.1.3,^[18] in order to elucidate their binding into the active site of the enzyme. The docking with GOLD was performed with both the scoring functions GOLDScore and ChemScore, while FlexX was used with the FlexX-Pharm module, with the iron of the heme chosen as pharmacophoric constraint. A clustering with ACIAP^[19] of all the docking poses of the three procedures resulted in one main, statistical predominant binding mode (**BM1**)^[12e] and two minor representative clusters. Interestingly, each of the latter two clusters solely consisted of either the *S*- (**BM2**)^[12e] or the *R*- (**BM-ABT**)^[12h] enantiomers respectively (Figure 3). This finding indicates that, together with the necessary perpendicular interaction angle between imidazole N and heme Fe to ensure sufficient coordination, the orientation of the hydrophobic pocket, which is occupied by the substituent on the methylene bridge, limits the pose distribution of different enantiomers. This geometrical restriction forces the *S*- enantiomers into **BM2** area and the *R*-enantiomers into **BM-ABT**. However, as the intersection of both areas, **BM1** is a better area for both enantiomers to bind.

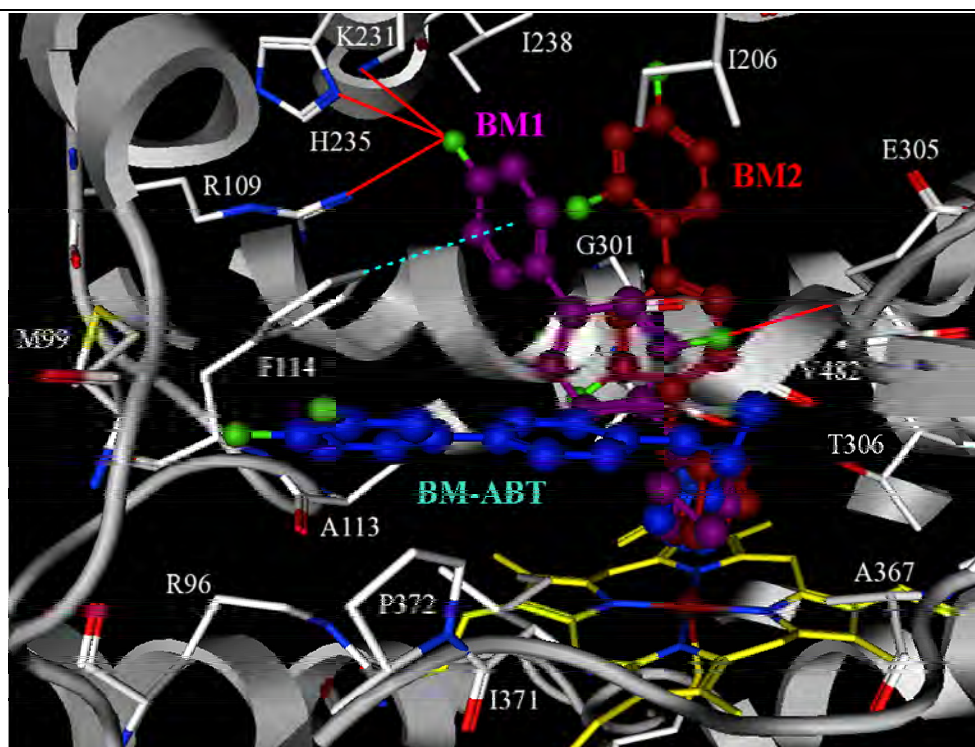


Figure 3. Presentation of the three main binding modes, exemplified by compounds **9** (magenta, **BM1**), **15** (red, **BM2**) and **13** (blue, **BM-ABT**). Heme, interacting residues and ribbon rendered tertiary structure of the active site are shown. Polar interactions are marked with red solid lines, whereas π - π stacking and metal complexation with cyan dotted lines. Figure was generated with MOE ([http:// www.chemcomp.com](http://www.chemcomp.com)).

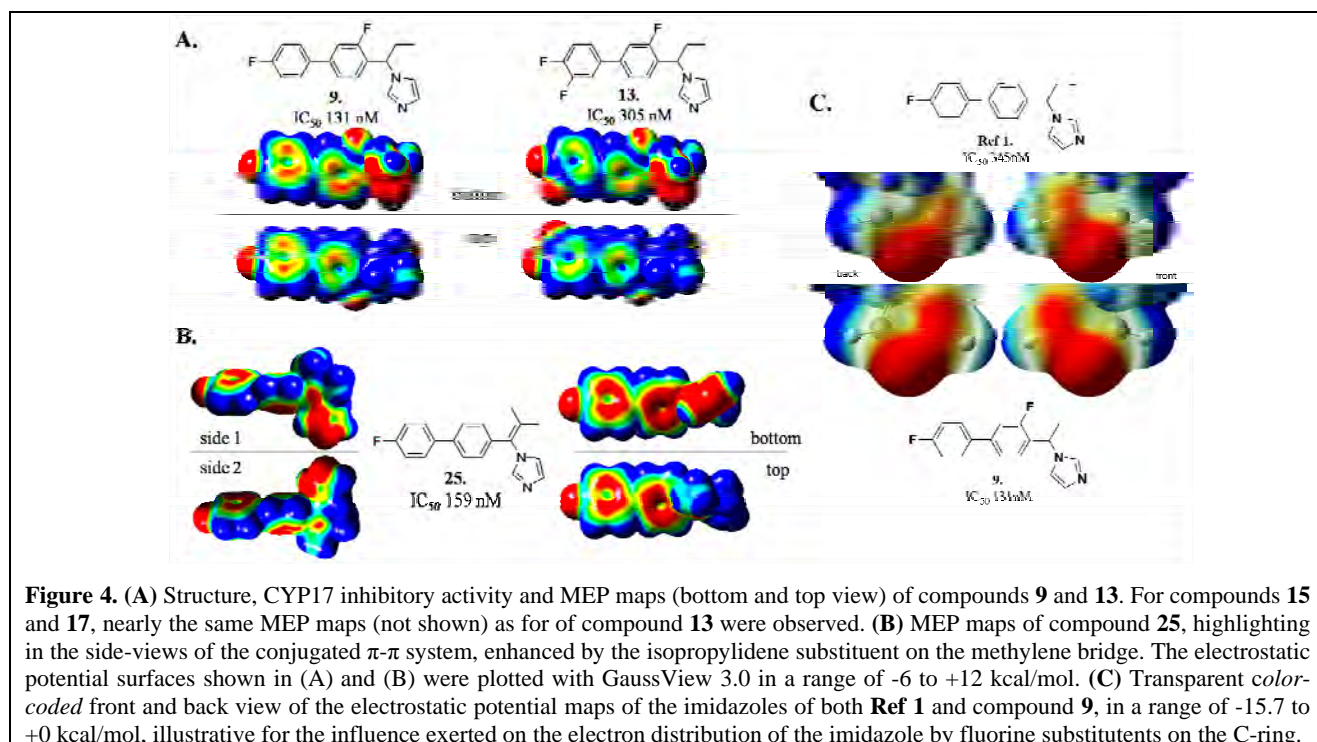
It can be observed for **BM1** that a conjugated scaffold orienting almost parallel to the I-helix is one of the key factors for high activity as previously described.^[12g] According to our docking studies this extended π -system obviously interacts not only with the π -system of the amino acid backbone in the I-helix (i.e. Gly301, Ala302, Gly303, Val304), but also with Phe114, which is oriented perpendicular toward the A-ring (Figure 3 **BM1**) to form a quadrupole-quadrupole interaction. More importantly, fluorine in the molecule showed

profound influence on the affinity for the enzyme. This can be explained by the obviously existing interactions of the *para*-F substituent with Arg109, Lys231 and His235 (Figure 3). When the fluorines were shifted to other positions in the A-ring resulting in 2',5'-di F analogues, a decrease of activities can be observed. Obviously, the interactions mentioned above can no longer be maintained. These observations nicely validate the reliability of our protein model. Furthermore, the elevated activity of C-ring *meta*-F substituted compounds can be explained by a multi-polar interaction between F and the N-H group of Glu305 (Figure 3) stabilizing the π - π interaction between the C-ring and the backbone π -system of Gly301-Ala302.

Additionally, a further flexible docking run was performed with GOLDv4.0-GOLDSCORE, with the side chains of Phe114, Arg109, Lys231, Asn202, Glu305, and Ile371 being set freely rotatable. Very similar results were observed as seen for the docking runs with the rigid side chains (data not shown).

MEP maps

To obtain an insight which physicochemical parameters might influence biological activity, the charge density distribution was considered and the molecular electrostatic potentials (MEPs) of selected compounds were determined. The geometry of these compounds (**Ref 1**, **2**, **9**, **13**, **15**, **17** and **25**) was optimized in the gas phase at the B3LYP/6-311++G** (d,p)^[20] level of density functional theory (DFT) by means of Gaussian 03.^[21] MEPs of electron density were plotted for every compound with GaussView 3.09.^[22]



The introduction of a second fluorine or the shift of fluorine into another position on the A-ring always leads to a reduction of the A-ring electron density, which can be clearly seen in the different MEP maps of compounds **9**, **13**, **15**, **17** and **25** (Figure 4A). This observation correlates with the different electron-withdrawing effects of the fluorine in *meta*- or *para*-position (σ values of +0.337 and +0.067, respectively). This reduction of electron density weakens the T-shaped interaction of the A-ring with Phe114, and consequently decreases the inhibitory potency of the compound.

The lower inhibitory potency of compounds with *ortho*-F substitution on the C-ring (**19** and **21**) might be due to the adverse effect that the fluorine exerts on the overall charge density of the biphenyl system by deforming the conjugated π - π system and by concentrating the electrons on the fluorine. However, for *meta*-F compounds (**9**, **13**, **15** and **17**) it seems that fluorine induces an increase in electron distribution on the imidazole ring, as visualized in the MEP maps of compounds **Ref 1** and **9** (Figure 4C), which is linked with an augmented inhibitory potency of the compounds. An analogous phenomenon was observed for compound **25**, where the isopropylidene strengthened the π - π system and extended the conjugation over the whole molecule (Figure 4B).

In vivo activity

The in vivo evaluation of the most potent compounds **9**, **13**, **15** and **17**, including the ability of reducing plasma testosterone concentration (Figure 5) and the determination of pharmacokinetic properties (Table 3) was performed in male Wistar rats after oral application. Abiraterone which was administered as acetate to improve its oral absorption and **Ref 1** were used as reference compounds. The plasma concentrations of testosterone were determined using an ELISA assay and plasma drug concentrations were measured using LC-MS. In the case of Abiraterone acetate only the signals of free Abiraterone were monitored, as the acetate is inactive as CYP17 inhibitor. As can be seen from Figure 5 all compounds significantly reduced the plasma testosterone concentration. It is striking at each time point investigated that all non-steroidal compounds, which were less active in vitro, exhibited higher activities in vivo than Abiraterone. After 24 hours,

Table 3. Pharmacokinetic properties of selected compounds ^[a]					
Compd	$t_{1/2z}$ (h) ^[b]	t_{max} (h) ^[b]	C_{max} (nM) ^[b]	C_{24h} (nM) ^[b]	AUC _{0-∞} (nM * h) ^[b]
9	12.8	2.0	3473	1528	80448
13	6.1	8.0	3496	1173	56114
15	4.2	6.0	2539	556	35091
17	2.2	1.0	458	187	2055
Ref 1	10.0	6.0	11729	4732	252297
Abiraterone	1.6	2.0	1694	253	11488

^[a] Compounds **Ref 1**, **9**, **13**, **15** and **17** were applied at a dose of 50 mg / kg body weight; Abiraterone was administrated as Abiraterone acetate (56 mg / kg body weight, equivalent to Abiraterone 50 mg / kg body weight). 5 to 6 intact adult male Wistar rats were employed for each treatment group; each sample was tested for 3 times.
^[b] $t_{1/2z}$: terminal half-life; t_{max} : time of maximal concentration; C_{max} : maximal concentration; C_{24h} : concentration at 24h; AUC_{0-∞}: area under the curve.

compound **9** and **Ref 1** still showed strong inhibitory activity, compounds **13** and **17** showed almost no inhibition, whereas compound **15** and Abiraterone exhibited an increase of testosterone levels above control at this time point, probably caused by feed-back stimulation. As expected this activity profile correlates to the pharmacokinetic properties of the compounds. Abiraterone exhibited a plasma half-life of only 1.6 hours, while the half-lives of other compounds are much longer (10 hours for **Ref 1** and 12.8 hours for **9**). Accordingly, the AUC values of the test compounds, except for compound **17**, are higher than for Abiraterone, indicating better bioavailability properties. Interestingly, the introduction of an additional fluorine into the C- ring of **Ref 1** prolongs plasma half-life (**9**), whereas introduction of further fluorine

atoms into the A-ring reduces half-lives strongly (**13**, **15** and **17**, half-lives between 2 to 6 hours). This observation is probably due to the electron withdrawing effects by multi F substitution. They significantly weaken the adjacent aromatic C-H bonds conferring them vulnerable to nucleophilic attacks.^[13m]

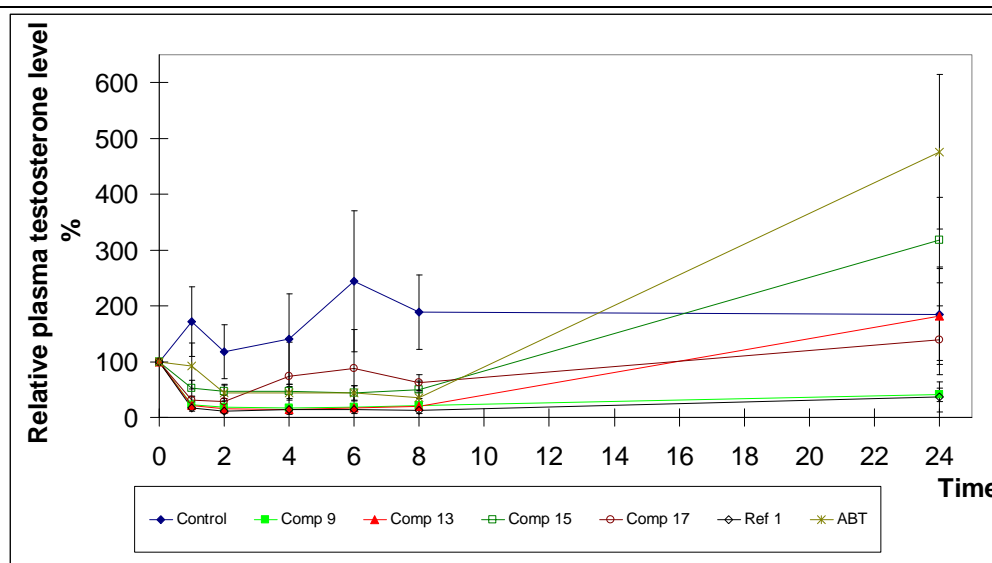


Figure 5. Reduction of the plasma testosterone concentrations in rats by selected compounds. Compounds **Ref 1**, **9**, **13**, **15** and **17** were applied at a dose of 50 mg / kg body weight; Abiraterone was administrated as Abiraterone acetate (56 mg / kg body weight, equivalent to Abiraterone 50 mg / kg body weight). 5 to 6 intact adult male Wistar rats were employed for each treatment group; each sample was tested for 3 times. The average plasma testosterone concentrations (1.97 ng / mL) at pre-treatment time points (-1, -0.5 and 0 h) were set to 100 %. The values shown are the relative levels compared to the pre-treatment value.

Conclusion

Herein, we reported the design, synthesis and bioactivity evaluation of a series of fluorine substituted biphenyl methylene imidazoles as CYP17 inhibitors. Fluorine substitution was found to show profound influence on the in vitro and in vivo activities, as well as the pharmacokinetic profiles.

It has been unveiled that fluorine in the *meta*-position of the C-ring increased the activity compared to the non-substituted analogues, whereas *ortho*-substitution reduced the potency. Compounds furnished with fluorine at the A-ring always followed the same activity ranking: 4'-F > 3',4'-di F > 2',5'-di F ≥ 2',4'-di F. Both the *R*- and *S*- enantiomers of the docked compounds predominantly adapt BM1 suggesting only a small difference in activity between these two enantiomers. The inspection of the docking poses revealed that the biphenyl moieties of both enantiomers are placed in the same area, interacting with Arg109 and Lys231, and their imidazolylmethylene group is located with only slight difference. The conformational flexibility of the latter group allows the ethyl substituents of both enantiomers to orient toward the hydrophobic pocket which is opposite to the I-helix and delimited by Ile371 and Ala367. Moreover, the biological data were well deciphered by docking studies and MEP mapping of selected compounds. The multi-polar interactions between the C-ring fluorine substituents and interacting amino acids residues significantly increased the binding affinities compared to the parent compound. The charge distribution difference on both the A- and the C-ring indicates π - π stacking (i.e. with both Phe114 and Gly301-Ala302), hydrophobic and Van der Waals interactions as determinants for activity. Furthermore, it could be demonstrated once again that fluorine substituted in an appropriate position, like in the C-ring, prolongs the plasma half life; in an unsuitable position, however, it decreases the $t_{1/2}$ value of the parent compound. This phenomenon might be

due to a decrease in metabolic stability and is interesting for further investigations in the future.

Finally, after the modification compound **9** is identified as strong CYP17 inhibitor showing potent activity *in vivo*, a high bioavailability and a long plasma half-life. Thus, Compound **9** appears to be an optimal candidate which after further structural optimization could be the first non-steroidal CYP17 inhibitor to be applied clinically. CYP17 inhibitors should be superior to the presently used GnRH analogues as mentioned above due to the fact that they reduce not only testicular but also adrenal androgen formation. Nevertheless, PC treatment could be further optimized by combining CYP17 inhibitors with inhibitors of androgen activation to DHT, catalyzed by 17β -HSD1^[23] and / or 17β -HSD3, as well as 5α -reductase.^[24]

Experimental Section

CYP17 preparation and assay

Human CYP17 was expressed in *E. coli* (coexpressing human CYP17 and cytochrome P450 reductase) and the assay was performed as previously described.^[12d, 16]

Inhibition of hepatic CYP enzymes

The recombinantly expressed enzymes from baculovirus-infected insect microsomes (Supersomes) were used and the manufacturer's instructions (www.gentest.com) were followed.

In vivo study

The *in vivo* tests were performed with intact adult male Wistar rats (Harlan Winkelmann, Germany), 5 to 6 for each treatment group. These rats were cannulated with silicone tubing via the right jugular vein. Compounds **9**, **13**, **15** and **17** were applied p.o. with doses of 50 mg / kg body weight, while Abiraterone was administrated as acetate 56 mg / kg body weight (equivalent to Abiraterone 50 mg / kg body weight). The concentrations of testosterone in the rat plasma were determined using the ELISA (EIA - 1559) from DRG Instruments according to the manufacturer's instructions. The plasma drug levels were measured by LC-MS. Non-compartmental pharmacokinetic analysis of concentration vs time data was performed for each compound on the mean plasma level using a validated computer program (PK solution 2 software; Summit Research Services, Montrose, USA). Plasma concentrations below the limit of detection were assigned a value of zero.

Chemistry Section

General

Melting points were determined on a Mettler FP1 melting point apparatus and are uncorrected. IR spectra were recorded neat on a Bruker Vector 33FT-infrared spectrometer. ¹H and ¹³C NMR spectra were measured on a Bruker DRX-500 (500 MHz). Chemical shifts are given in parts per million (ppm), and TMS was used as an internal standard for spectra. All coupling constants (*J*) are given in Hz. ESI (electrospray ionization) mass spectra were determined on a TSQ quantum (Thermo Electron Corporation) instrument. High resolution mass spectra were measured using LTQ Orbitrap (Thermo Electron Corporation) with positive ESI. The purities of the final compounds were controlled by Surveyor®-LC-system. Purities were greater than 98 %. Column chromatography was performed using silica-gel 60 (50–200 μm), and reaction progress was determined by TLC analysis on Alugram® SIL G/UV₂₅₄ (Macherey-Nagel). Boronic acids and bromoaryls used as starting materials were commercially obtained (CombiBlocks, Chempur, Aldrich, Acros

etc).

Method A: CDI reaction in NMP

To a solution of the corresponding alcohol (1 eq) in NMP or acetonitrile (10 mL / mmol) was added CDI (5 eq). Then the solution was heated to reflux for 4 to 18 h. After cooling to ambient temperature, it was diluted with water (30 mL) and extracted with ethyl acetate (3 x 10 mL). The combined organic phases were washed with brine, dried over MgSO₄ and evaporated under reduced pressure. Then the desired product was purified by chromatography on silica gel.

1-[1-(4'-Fluoro-2'-methyl-biphenyl-4-yl)-propyl]-1H-imidazole (1). Synthesized according to Method A using **1a** (0.15 g, 0.61 mmol) and CDI (0.20 g, 1.23 mmol); yield: 0.06 g (32 %); colorless oil; R_f = 0.27 (DCM / MeOH, 95:5); ¹H NMR (DMSO, 500 MHz) δ = 0.98 (t, J = 7.3 Hz, 3H, CH₃), 2.23 (s, 3H, CH₃), 2.24–2.30 (m, 2H, CH₂), 5.07 (t, J = 7.6 Hz, 1H, CH), 6.90–6.93 (m, 1H), 6.95–6.97 (m, 1H), 7.01 (s, 1H), 7.11 (s, 1H), 7.14 (dd, J = 6.0, 8.4 Hz, 1H), 7.22–7.26 (m, 4H), 7.67 ppm (s, 1H); ¹³C NMR (DMSO-*d*₆, 125 MHz) δ = 11.1 (CH₃), 20.5 (CH₃), 28.6 (CH₂), 63.2 (CH), 112.5, 112.6, 116.7, 116.9, 126.3, 129.7, 131.1, 131.1, 137.0, 137.6, 137.7, 138.9, 140.9, 161.1, 163.0 ppm; HRMS (ESI): calcd for C₁₉H₂₀FN₂ [M+H]⁺: 295.1611, found: 295.1607; MS (ESI): m/z = 295 [M⁺+H].

1-[1-(3',4'-Difluoro-biphenyl-4-yl)-propyl]-1H-imidazole (2). Synthesized according to Method A using **2a** (0.27 g, 1.09 mmol) and CDI (0.34 g, 2.06 mmol); yield: 0.09 g (27 %); colorless oil; R_f = 0.29 (DCM / MeOH, 95:5); ¹H NMR (CDCl₃, 500 MHz) δ = 0.98 (t, J = 7.3 Hz, 3H, CH₃), 2.23–2.31 (q, J = 7.3, 7.6 Hz, 2H, CH₂), 5.06 (t, J = 7.6 Hz, 1H, CH), 6.97–7.02 (m, 1H), 7.10–7.14 (m, 1H), 7.18–7.28 (m, 4H), 7.23–7.37 (m, 1H), 7.49 (m, 2H), 7.62–7.66 ppm (m, 1H, Im-2H); ¹³C NMR (CDCl₃, 125 MHz) δ = 11.3 (CH₃), 29.6 (CH₂), 63.0 (CH), 116.3, 117.5, 118.7, 123.2, 127.3, 130.5, 136.5, 137.4, 140.5, 151.3 ppm; HRMS (ESI): calcd for C₁₈H₁₇F₂N₂ [M+H]⁺: 299.1360, found: 299.1363; MS (ESI): m/z = 299 [M⁺+H].

1-[1-(2',4'-Difluorobiphenyl-4-yl)propyl]-1H-imidazole (4). Synthesized according to Method A using **4a** (0.27 g, 1.09 mmol) and CDI (0.34 g, 2.06 mmol); yield: 0.12 g (36 %); colorless oil; R_f = 0.34 (DCM / MeOH, 95:5); ¹H NMR (CDCl₃, 500 MHz) δ = 0.85 (t, J = 7.3 Hz, 3H, CH₃), 2.12–2.18 (m, 2H, CH₂), 4.96 (t, J = 7.6 Hz, 1H, CH), 6.77–6.85 (m, 2H), 6.87–6.90 (m, 1H), 6.99–7.02 (m, 1H), 7.13–7.15 (m, 2H), 7.23–7.28 (m, 1H), 7.35–7.37 (m, 2H), 7.62–7.68 ppm (m, 1H, Im-2H); ¹³C NMR (CDCl₃, 125 MHz) δ = 11.1 (CH₃), 29.3 (CH₂), 63.3 (CH), 104.5, 112.7, 117.8, 118.6, 124.6, 126.3, 130.2, 131.4, 135.7, 136.6, 140.3, 163.5 ppm; HRMS (ESI): calcd for C₁₈H₁₇F₂N₂ [M+H]⁺: 299.1360, found: 299.1352; MS (ESI): m/z = 299 [M⁺+H].

1-[1-(2',4'-Difluoro-3'-methoxybiphenyl-4-yl)ethyl]-1H-imidazole (6). Synthesized according to Method A using **6a** (0.30 g, 1.09 mmol) and CDI (0.34 g, 2.06 mmol); yield: 0.34 g (71 %); yellow oil; R_f = 0.30 (DCM / MeOH, 95:5); ¹H NMR (CDCl₃, 500 MHz) δ = 1.75 (d, J = 7.5 Hz, 3H, CH₃), 3.91 (s, 3H, OCH₃), 5.18–5.31 (q, J = 7.5 Hz, 1H, CH), 6.82–6.83 (m, 1H), 6.84–6.86 (m, 1H), 6.89–6.93 (m, 1H), 6.97–6.99 (m, 1H), 7.09–7.10 (m, 2H), 7.34–7.36 (m, 2H), 7.50–7.51 ppm (m, 1H, Im-2H); ¹³C NMR (CDCl₃, 125 MHz) δ = 21.1 (CH₃), 56.7 (CH), 62.5 (OCH₃), 112.3, 117.7, 123.9, 125.6, 127.8, 128.4, 134.1, 136.1, 141.6 ppm; HRMS (ESI): calcd for C₁₈H₁₇F₂N₂O [M+H]⁺: 315.1309, found: 315.1297; MS (ESI): m/z = 315 [M⁺+H].

1-[1-(2',5'-Difluorobiphenyl-4-yl)propyl]-1H-imidazole (7). Synthesized according to Method A using

7a (0.27 g, 1.09 mmol) and CDI (0.34 g, 2.06 mmol); yield: 0.13 g (41 %); colorless oil; $R_f = 0.38$ (DCM / MeOH, 95:5); $^1\text{H NMR}$ (CDCl_3 , 500 MHz) $\delta = 0.98$ (t, $J = 7.3$ Hz, 3H, CH_3), 2.26 (q, $J = 7.3, 7.6$ Hz, 2H, CH_2), 5.05 (t, $J = 7.6$ Hz, 1H, CH), 6.97–7.01 (m, 2H), 7.08–7.12 (m, 3H), 7.25–7.27 (m, 2H), 7.49–7.51 (m, 2H), 7.62–7.65 ppm (m, 1H, Im-2H); $^{13}\text{C NMR}$ (CDCl_3 , 125 MHz) $\delta = 11.3$ (CH_3), 29.6 (CH_2), 63.1 (CH), 116.8, 118.4, 126.5, 130.5, 135.4, 136.9, 140.0, 158.8, 160.7 ppm; HRMS (ESI): calcd for $\text{C}_{18}\text{H}_{17}\text{F}_2\text{N}_2$ $[\text{M}+\text{H}]^+$: 299.1360, found: 299.1351; MS (ESI): $m/z = 299$ $[\text{M}^++\text{H}]$.

1-[1-(3,4'-difluorobiphenyl-4-yl)propyl]-1H-imidazole (9). Synthesized according to Method A using **9a** (0.38 g, 1.53 mmol) and CDI (0.47 g, 2.88 mmol); yield: 0.08 g (17 %); yellow oil; $R_f = 0.38$ (DCM / MeOH, 95:5); $^1\text{H NMR}$ (CDCl_3 , 500 MHz) $\delta = 0.99$ (t, $J = 7.3$ Hz, 3H, CH_3), 2.21–2.31 (m, 2H, CH_2), 5.38 (t, $J = 7.5$ Hz, 1H, CH), 7.01 (s, 1H), 7.08 (s, 1H), 7.10–7.14 (m, 2H), 7.19–7.25 (m, 2H), 7.27–7.29 (m, 1H), 7.40–7.51 (m, 2H), 7.64 ppm (s, 1H, Im-2H); $^{13}\text{C NMR}$ (CDCl_3 , 125 MHz) $\delta = 11.3$ (CH_3), 28.6 (CH_2), 56.4 (CH), 114.5, 116.3, 118.0, 123.7, 126.6, 127.3, 128.9, 129.5, 130.9, 135.0, 136.5, 161.7, 163.4 ppm; $^{19}\text{F NMR}$ (CDCl_3 , 400 MHz) $\delta = -114.19$ (s, 1F), -117.98 ppm (s, 1F); HRMS (ESI): calcd for $\text{C}_{18}\text{H}_{17}\text{F}_2\text{N}_2$ $[\text{M}+\text{H}]^+$: 299.1360, found: 299.1352; MS (ESI): $m/z = 299$ $[\text{M}^++\text{H}]$.

1-[(3,4'-Difluorobiphenyl-4-yl)methyl]-1H-imidazole (11). Synthesized according to Method A using **11a** (0.28 g, 1.27 mmol) and CDI (0.41 g, 2.54 mmol); yield: 0.11 g (31 %); colorless oil; $R_f = 0.53$ (EtOAc / MeOH, 95:5); $^1\text{H NMR}$ (CDCl_3 , 500 MHz) $\delta = 5.20$ (s, 2H, CH_2), 6.98 (s, br, 1H), 7.10 (s, br, 1H), 7.11–7.16 (m, 3H), 7.26–7.31 (m, 2H), 7.50 (dd, $J = 5.4, 8.8$ Hz, 2H), 7.64 ppm (s, br, 1H, Im-2H); $^{13}\text{C NMR}$ (CDCl_3 , 125 MHz) $\delta = 44.4$ (CH_2), 114.2, 115.9, 119.2, 122.2, 123.1, 128.6, 129.6, 129.9, 135.3, 137.3, 142.9, 160.6, 162.9 ppm; HRMS (ESI): calcd for $\text{C}_{16}\text{H}_{13}\text{F}_2\text{N}_2$ $[\text{M}+\text{H}]^+$: 271.1047, found: 271.1039; MS (ESI): $m/z = 271$ $[\text{M}^++\text{H}]$.

1-[1-(3,3',4'-Trifluorobiphenyl-4-yl)propyl]-1H-imidazole (13). Synthesized according to Method A using **13a** (0.40 g, 1.70 mmol) and CDI (0.53 g, 3.20 mmol); yield: 0.11 g (20 %); colorless oil; $R_f = 0.35$ (DCM / MeOH, 95:5); $^1\text{H NMR}$ (CDCl_3 , 500 MHz) $\delta = 0.99$ (t, $J = 7.3$ Hz, 3H, CH_3), 2.22–2.33 (m, 2H, CH_2), 5.39 (t, $J = 7.6$ Hz, 1H, CH), 7.01 (s, 1H), 7.09 (s, 1H), 7.20–7.29 (m, 5H), 7.31–7.35 (m, 1H), 7.64 ppm (s, 1H, Im-2H); $^{13}\text{C NMR}$ (CDCl_3 , 125 MHz) $\delta = 11.3$ (CH_3), 28.6 (CH_2), 56.3 (CH), 114.5, 116.2, 118.4, 123.9, 127.5, 128.3, 130.5, 136.7, 149.4, 161.7 ppm; $^{19}\text{F NMR}$ (CDCl_3 , 400 MHz) $\delta = -117.56$ (s, 1F), -136.80 (d, $^3J_{\text{FF}} = -20.7$, 1F), -138.64 ppm (d, $^3J_{\text{FF}} = -20.7$, 1F); HRMS (ESI): calcd for $\text{C}_{18}\text{H}_{16}\text{F}_3\text{N}_2$ $[\text{M}+\text{H}]^+$: 317.1266, found: 317.1257; MS (ESI): $m/z = 317$ $[\text{M}^++\text{H}]$.

1-[(3,3',4'-trifluorobiphenyl-4-yl)methyl]-1H-imidazole (14). Synthesized according to Method A using **14a** (0.35 g, 1.67 mmol) and CDI (0.53 g, 3.20 mmol); yield: 0.10 g (23 %); white powder: mp 60–61 °C; $R_f = 0.26$ (DCM / MeOH, 95:5); $^1\text{H NMR}$ (CDCl_3 , 500 MHz) $\delta = 5.19$ (s, 2H, CH_2), 6.97 (s, 1H), 7.10 (s, 1H), 7.11–7.14 (m, 2H), 7.20–7.28 (m, 3H), 7.31–7.35 (m, 1H), 7.59 ppm (s, 1H, Im-2H); $^{13}\text{C NMR}$ (CDCl_3 , 125 MHz) 44.3 (CH_2), 114.9, 116.4, 118.6, 119.3, 123.9, 129.5, 136.8, 137.3, 141.4, 149.3, 151.7, 161.4 ppm; HRMS (ESI): calcd for $\text{C}_{16}\text{H}_{12}\text{F}_3\text{N}_2$ $[\text{M}+\text{H}]^+$: 289.0953, found: 289.0944; MS (ESI): $m/z = 289$ $[\text{M}^++\text{H}]$.

1-[1-(2',3,4'-Trifluorobiphenyl-4-yl)propyl]-1H-imidazole (15). Synthesized according to Method A using **15a** (0.27 g, 1.14 mmol) and CDI (0.35 g, 2.10 mmol); yield: 0.09 g (24 %); colorless oil; $R_f = 0.37$ (DCM / MeOH, 95:5); $^1\text{H NMR}$ (CDCl_3 , 500 MHz) $\delta = 0.99$ (t, $J = 7.3$ Hz, 3H, CH_3), 2.23–2.32 (m, 2H, CH_2), 5.40 (t, $J = 7.6$ Hz, 1H, CH), 6.89–6.97 (m, 2H), 7.02 (s, 1H), 7.08 (s, 1H), 7.19–7.27 (m, 3H), 7.34–

7.38 (m, 1H), 7.64 ppm (s, 1H, Im-2H); ^{13}C NMR (CDCl_3 , 125 MHz) δ = 11.3 (CH_3), 27.7 (CH_2), 56.2 (CH), 104.5, 112.7, 116.9, 117.7, 125.4, 127.0, 130.8, 136.5, 137.9, 160.3, 161.2 ppm; ^{19}F NMR (CDCl_3 , 400 MHz) δ = -109.86 (d, $^4J_{\text{FF}}$ = 8.0, 1F), -113.15 (d, $^4J_{\text{FF}}$ = 8.0, 1F), -118.03 ppm (s, 1F); HRMS (ESI): calcd for $\text{C}_{18}\text{H}_{16}\text{F}_3\text{N}_2$ $[\text{M}+\text{H}]^+$: 317.1266, found: 317.1257; MS (ESI): m/z = 317 $[\text{M}^++\text{H}]$.

1-[(2',3,4'-Trifluorobiphenyl-4-yl)methyl]-1H-imidazole (16). Synthesized according to Method A using **16a** (0.18 g, 0.76 mmol) and CDI (0.24 g, 1.51 mmol); yield: 0.09 g (42 %); orange oil; R_f = 0.52 (EtOAc / MeOH, 95:5); ^1H NMR (CDCl_3 , 500 MHz) δ = 5.20 (s, 2H, CH_2), 6.89–6.97 (m, 2H), 6.98 (s, br, 1H), 7.10 (s, br, 1H), 7.12 (dd, J = 7.9, 8.2 Hz, 1H), 7.24–7.27 (m, 2H), 7.36 (ddd, J = 6.4, 8.5, 8.8 Hz, 1H), 7.61 ppm (s, br, 1H, Im-2H); ^{13}C NMR (CDCl_3 , 125 MHz) δ = 44.3 (CH_2), 104.6, 111.8, 116.2, 119.2, 122.8, 123.3, 125.1, 129.4, 129.8, 131.1, 137.4, 159.2, 159.6, 161.2, 162.7 ppm; HRMS (ESI): calcd for $\text{C}_{16}\text{H}_{12}\text{F}_3\text{N}_2$ $[\text{M}+\text{H}]^+$: 289.0953, found: 289.0952; MS (ESI): m/z = 289 $[\text{M}^++\text{H}]$.

1-[1-(2',3,5'-Trifluorobiphenyl-4-yl)propyl]-1H-imidazole (17). Synthesized according to Method A using **17a** (0.40 g, 1.70 mmol) and CDI (0.53 g, 3.20 mmol); yield: 0.14 g (26 %); colorless oil; R_f = 0.38 (DCM / MeOH, 95:5); ^1H NMR (CDCl_3 , 500 MHz) δ = 0.99 (t, J = 7.3 Hz, 3H, CH_3), 2.23–2.32 (m, 2H, CH_2), 5.40 (t, J = 7.6 Hz, 1H, CH), 7.00–7.04 (m, 2H), 7.08–7.14 (m, 2H), 7.20–7.24 (m, 1H), 7.26–7.30 (m, 2H), 7.64 ppm (s, 1H, Im-2H); ^{13}C NMR (CDCl_3 , 125 MHz) δ = 11.3 (CH_3), 27.6 (CH_2), 56.3 (CH), 116.7, 117.9, 125.5, 127.0, 130.3, 136.7, 158.5, 159.7, 161.4 ppm; ^{19}F NMR (CDCl_3 , 400 MHz) δ = -117.81 (s, 1F), -118.39 (d, $^5J_{\text{FF}}$ = 17.7, 1F), -123.67 ppm (d, $^5J_{\text{FF}}$ = 17.7, 1F); HRMS (ESI): calcd for $\text{C}_{18}\text{H}_{16}\text{F}_3\text{N}_2$ $[\text{M}+\text{H}]^+$: 317.1266, found: 317.1257; MS (ESI): m/z = 317 $[\text{M}^++\text{H}]$.

1-[(2',3,5'-Trifluorobiphenyl-4-yl)methyl]-1H-imidazole (18). Synthesized according to Method A using **18a** (0.17 g, 0.71 mmol) and CDI (0.23 g, 1.43 mmol); yield: 0.09 g (45 %); light yellow solid: mp 125–126 °C; R_f = 0.48 (EtOAc / MeOH, 95:5); ^1H NMR (CDCl_3 , 500 MHz) δ = 5.21 (s, 2H, CH_2), 6.98 (s, br, 1H), 7.00–7.05 (m, 1H), 7.08–7.16 (m, 4H), 7.28–7.31 (m, 2H), 7.64 ppm (s, br, 1H, Im-2H); ^{13}C NMR (CDCl_3 , 125 MHz) δ = 44.4 (CH_2), 116.0, 116.4, 116.6, 117.4, 119.3, 125.1, 123.4, 129.5, 129.8, 137.1, 137.4, 156.5, 154.6, 158.7, 160.2 ppm; HRMS (ESI): calcd for $\text{C}_{16}\text{H}_{12}\text{F}_3\text{N}_2$ $[\text{M}+\text{H}]^+$: 289.0953, found: 289.0955; MS (ESI): m/z = 289 $[\text{M}^++\text{H}]$.

1-[1-(2,4'-Difluorobiphenyl-4-yl)propyl]-1H-imidazole (19). Synthesized according to Method A using **19a** (0.31 g, 1.22 mmol) and CDI (0.40 g, 2.46 mmol); yield: 0.11 g (31 %); colorless oil; R_f = 0.56 (EtOAc / MeOH, 95:5); ^1H NMR (CDCl_3 , 500 MHz) δ = 0.97 (t, J = 7.3 Hz, 3H), 2.21–2.27 (m, 2H), 5.04 (t, J = 7.7 Hz, 1H), 6.96–6.99 (m, 2H), 7.02 (dd, J = 1.9, 7.9 Hz, 1H), 7.11 (s, br, 1H), 7.12 (t, J = 8.6 Hz, 2H), 7.37 (t, J = 7.9 Hz, 1H), 7.47 (ddd, J = 1.3, 5.4, 8.8 Hz, 1H), 7.64 ppm (s, br, 1H, Im-2H); ^{13}C NMR (CDCl_3 , 125 MHz) δ = 11.0 (CH_3), 28.4 (CH_2), 62.5 (CH), 114.3, 115.4, 117.5, 122.4, 127.8, 129.6, 130.5, 131.0, 136.3, 141.8, 141.9, 159.6, 162.5 ppm; HRMS (ESI): calcd for $\text{C}_{18}\text{H}_{17}\text{F}_2\text{N}_2$ $[\text{M}+\text{H}]^+$: 299.1360, found: 299.1351; MS (ESI): m/z = 299 $[\text{M}^++\text{H}]$.

1-(2,4'-Difluoro-biphenyl-4-ylmethyl)-1H-imidazole (20). Synthesized according to Method A using **20a** (0.10 g, 0.44 mmol) and CDI (0.40 g, 2.46 mmol); yield: 0.05 g (42 %); white solid: mp 93–94 °C; R_f = 0.52 (EtOAc / MeOH, 95:5); ^1H NMR (CDCl_3 , 500 MHz) δ = 5.15 (s, 2H, CH_2), 6.90–6.98 (m, 3H), 7.11–7.13 (m, 2H), 7.25–7.27 (m, 3H), 7.36–7.39 (m, 1H), 7.60 ppm (s, 1H, Im-2H); ^{13}C NMR (CDCl_3 , 125 MHz) 50.0 (CH_2), 114.9, 115.1, 115.5, 119.3, 123.0, 129.9, 130.6, 130.7, 130.9, 131.2, 137.6, 158.8, 160.8, 161.6,

163.6 ppm; HRMS (ESI): calcd for $C_{16}H_{13}F_2N_2$ $[M+H]^+$: 271.1047, found: 271.1045; MS (ESI): $m/z = 271$ $[M^++H]$.

1-[1-(2,3',4'-Trifluorobiphenyl-4-yl)propyl]-1H-imidazole (21). Synthesized according to Method A using **21a** (0.28 g, 1.03 mmol) and CDI (0.34 g, 2.06 mmol); yield: 0.09 g (29 %); light brown oil; $R_f = 0.53$ (EtOAc / MeOH, 95:5); 1H NMR ($CDCl_3$, 500 MHz) $\delta = 0.97$ (t, $J = 7.4$ Hz, 3H), 2.20–2.28 (m, 2H), 5.04 (t, $J = 7.6$ Hz, 1H), 6.96–6.99 (m, 2H), 7.03 (dd, $J = 1.9, 7.9$ Hz, 1H), 7.11 (s, br, 1H), 7.18–7.23 (m, 2H), 7.31–7.34 (m, 1H), 7.35 (t, $J = 8.0$ Hz, 1H), 7.64 ppm (s, br, 1H, Im-2H); ^{13}C NMR ($CDCl_3$, 125 MHz) $\delta = 10.0$ (CH₃), 27.5 (CH₂), 61.5 (CH), 113.5, 116.4, 116.5, 117.0, 121.6, 124.0, 125.8, 128.7, 129.9, 130.8, 135.3, 141.5, 149.0, 149.2, 158.6 ppm; HRMS (ESI): calcd for $C_{18}H_{16}F_3N_2$ $[M+H]^+$: 317.1266, found: 317.1257; MS (ESI): $m/z = 317$ $[M^++H]$.

1-(2,2',4'-Trifluoro-biphenyl-4-ylmethyl)-1H-imidazole (22). Synthesized according to Method A using **22a** (0.10 g, 0.39 mmol) and CDI (0.40 g, 2.46 mmol); yield: 0.06 g (54 %); white solid: mp 112–113 °C; $R_f = 0.47$ (EtOAc / MeOH, 95:5); 1H NMR ($CDCl_3$, 500 MHz) $\delta = 5.21$ (s, 2H, CH₂), 6.90–6.98 (m, 4H), 7.02 (d, $J = 7.8$ Hz, 1H), 7.16 (s, 1H), 7.33–7.35 (m, 2H), 7.85 ppm (s, 1H, Im-2H); ^{13}C NMR ($CDCl_3$, 125 MHz) $\delta = 52.2$ (CH₂), 104.3, 111.5, 114.8, 119.4, 122.8, 129.1, 132.2, 132.2, 137.3, 138.3, 158.9, 161.0, 161.9, 162.0, 164.1 ppm; HRMS (ESI): calcd for $C_{16}H_{12}F_3N_2$ $[M+H]^+$: 289.0953, found: 289.0957; MS (ESI): $m/z = 289$ $[M^++H]$.

Method B: Grignard reaction

Under exclusion of air and moisture a 1.0 M EtMgBr (1.2 eq) solution in THF was added dropwise to a solution of the aldehyde or ketone (1 eq) in THF (12 mL / mmol). The mixture was stirred over night at room temperature. Then ethyl acetate (10 mL) and water (10 mL) were added and the organic phase was separated. The organic phase was extracted with water and brine, dried over Na_2SO_4 , and evaporated under reduced pressure. The crude products were purified by flash chromatography on silica gel.

Method C: Suzuki-Coupling

The corresponding brominated aromatic compound (1 eq) was dissolved in toluene (7 mL / mmol), an aqueous 2.0 M Na_2CO_3 solution (3.2 mL / mmol) and an ethanolic solution (3.2 mL / mmol) of the corresponding boronic acid (1.5–2.0 eq) were added. The mixture was deoxygenated under reduced pressure and flushed with nitrogen. After repeating this cycle several times $Pd(PPh_3)_4$ (4 mol%) was added and the resulting suspension was heated to reflux for 8 h. After cooling down, ethyl acetate (10 mL) and water (10 mL) were added and the organic phase was separated. The water phase was extracted with ethyl acetate (2 x 10 mL). The combined organic phases were washed with brine, dried over Na_2SO_4 , filtered over a short plug of celite® and evaporated under reduced pressure. The compounds were purified by flash chromatography on silica gel.

1-(4'-Fluorobiphenyl-4-yl)-1-(1H-imidazol-5-yl)-2-methylpropan-1-ol (24). Synthesized according to Method C using 1-(4-Bromophenyl)-2-methyl-1-(1-trityl-1H-imidazol-5-yl)propan-1-ol (0.50 g, 0.93 mmol) and 4-fluorophenyl boronic acid (0.23 mg, 1.63 mmol). After workup, the crude was stirred with pyridinium hydrochloride (0.17 g, 1.5 mmol) in MeOH (40 mL) at 60° C for 4 hours. Then the reaction was quenched by adding saturated $NaHCO_3$ aq (10 mL). After 20 mL EtOAc were added, the phases separated. The water phase was extracted 2 times with EtOAc (20 mL), the combined organic extracts were dried over Na_2SO_4

and concentrated under reduced pressure. The crude product was purified by flash chromatography; yield: 0.21 g (73 %); colorless oil; $R_f = 0.17$ (EtOAc / MeOH, 95:5); $^1\text{H NMR}$ (CDCl_3 , 500 MHz) $\delta = 0.82$ (d, $J = 6.8$ Hz, 3H), 0.98 (d, $J = 6.8$ Hz, 3H), 2.63–2.65 (m, 1H), 7.01 (s, 1H), 7.10 (dd, $J = 8.7, 8.8$ Hz, 2H), 7.49 (d, $J = 8.5$ Hz, 2H), 7.53 (dd, $J = 5.4, 8.7$ Hz, 2H), 7.58 (s, 1H), 7.62 ppm (d, $J = 8.3$ Hz, 2H); $^{13}\text{C NMR}$ (CDCl_3 , 125 MHz) $\delta = 17.3, 60.4, 77.7, 115.5, 115.6, 126.2, 126.4, 128.4, 128.5, 133.9, 136.9, 136.9, 138.3, 144.8, 161.4, 163.3$ ppm; HRMS (ESI): calcd for $\text{C}_{19}\text{H}_{20}\text{FN}_2\text{O}$ $[\text{M}+\text{H}]^+$: 311.1560, found: 311.1559; MS (ESI): $m/z = 311$ $[\text{M}^++\text{H}]$.

Method D: Reduction with NaBH_4

To an ice-cooled solution of the corresponding aldehyde or ketone (1 eq) in methanol (5 mL / mmol) was added NaBH_4 (2 eq). Then the resulting mixture was heated to reflux for 30 minutes. After cooling to ambient temperature, the solvent was distilled off under reduced pressure. Then water (10 mL) was added, and the resulting mixture was extracted with ethyl acetate (3 x 10 mL). The combined organic phases were washed with brine, dried over MgSO_4 and evaporated under reduced pressure. Then the desired product was purified by chromatography on silica gel.

Method E: CDI reaction in THF

To a solution of the corresponding alcohol (1 eq) in THF (10 mL / mmol) was added CDI (2 eq). Then the solution was heated to reflux at 70 °C for 4 days. After cooling to ambient temperature, the mixture was poured into water and extracted with CH_2Cl_2 (3 x 25 mL). The combined organic phases were washed with brine, dried over MgSO_4 and evaporated under reduced pressure. Then the desired product was purified by chromatography on silica gel.

Imidazole-1-carboxylic acid 1-(3',4'-difluoro-biphenyl-4-yl)-propyl ester (3). Synthesized according to Method E using **2a** (0.10 g, 0.42 mmol) and CDI (0.14 g, 0.83 mmol); yield: 0.09 g (37 %); white solid: mp 49–50 °C; $R_f = 0.29$ (DCM / MeOH, 95:5); $^1\text{H NMR}$ (CDCl_3 , 500 MHz) $\delta = 1.01$ (t, $J = 14.8$ Hz, 3H, CH_3), 2.01–2.21 (q, $J = 14.8, 15.5$ Hz, 2H, CH_2), 5.88 (t, $J = 15.5$ Hz, 1H, CH), 7.15 (s, 1H), 7.22–7.29 (m, 2H), 7.32–7.34 (m, 1H), 7.36–7.38 (m, 1H), 7.46 (d, $J = 8.2$ Hz, 2H), 7.54 (d, $J = 8.2$ Hz, 2H), 8.35 ppm (s, 1H, Im-2H); $^{13}\text{C NMR}$ (CDCl_3 , 125 MHz) $\delta = 9.9$ (CH_3), 28.9 (CH_2), 82.6 (CH), 115.9, 116.1, 117.5, 117.7, 122.4, 122.9, 123.0, 127.3, 127.4, 129.5, 137.8, 140.2, 149.0, 149.1, 151.2 ppm; HRMS (ESI): calcd for $\text{C}_{19}\text{H}_{17}\text{F}_2\text{N}_2\text{O}_2$ $[\text{M}+\text{H}]^+$: 343.1258, found: 343.1250; MS (ESI): $m/z = 343$ $[\text{M}^++\text{H}]$.

Imidazole-1-carboxylic acid 1-(2',4'-difluoro-biphenyl-4-yl)-propyl ester (5). Synthesized according to Method E using **4a** (0.21 g, 0.85 mmol) and CDI (0.28 g, 1.69 mmol); yield: 0.11 g (43 %); white solid: mp 76–77 °C; $R_f = 0.29$ (DCM / MeOH, 95:5); $^1\text{H NMR}$ (CDCl_3 , 500 MHz) $\delta = 1.01$ (t, $J = 14.8$ Hz, 3H, CH_3), 2.03–2.19 (q, $J = 14.8, 15.5$ Hz, 2H, CH_2), 5.87 (t, $J = 15.5$ Hz, 1H, CH), 6.89–7.06 (m, 2H), 7.09–7.11 (m, 1H), 7.36–7.40 (m, 1H), 7.45–7.48 (m, 3H), 7.52 (dd, $J = 1.6, 1.9$ Hz, 2H), 8.24 ppm (s, 1H, Im-2H); $^{13}\text{C NMR}$ (CDCl_3 , 125 MHz) $\delta = 9.9$ (CH_3), 28.9 (CH_2), 82.2 (CH), 104.4, 111.7, 117.2, 124.5, 126.8, 129.3, 130.7, 135.5, 136.9, 137.9, 148.0, 158.5, 1160.7, 161.4, 163.4, 171.2 ppm; HRMS (ESI): calcd for $\text{C}_{19}\text{H}_{17}\text{F}_2\text{N}_2\text{O}_2$ $[\text{M}+\text{H}]^+$: 343.1258, found: 343.1247; MS (ESI): $m/z = 343$ $[\text{M}^++\text{H}]$.

Imidazole-1-carboxylic acid 1-(2',5'-difluoro-biphenyl-4-yl)-propyl ester (8). Synthesized according to Method E using **7a** (0.12 g, 0.46 mmol) and CDI (0.15 g, 0.93 mmol); yield: 0.10 g (69 %); white solid: mp

77–78 °C; $R_f = 0.29$ (DCM / MeOH, 95:5); $^1\text{H NMR}$ (CDCl_3 , 500 MHz) $\delta = 1.01$ (t, $J = 14.8$ Hz, 3H, CH_3), 2.02–2.20 (q, $J = 14.8, 15.5$ Hz, 2H, CH_2), 5.88 (t, $J = 15.5$ Hz, 1H, CH), 6.93–7.02 (m, 1H), 7.09–7.15 (m, 3H), 7.46–7.48 (m, 3H), 7.52–7.55 (m, 2H), 8.23 ppm (s, 1H, Im-2H); $^{13}\text{C NMR}$ (CDCl_3 , 125 MHz) $\delta = 9.9$ (CH_3), 28.9 (CH_2), 82.2 (CH), 115.5, 116.7, 117.6, 126.9, 127.4, 129.4, 130.2, 135.3, 136.9, 138.4, 148.0, 154.7, 156.7, 157.8, 159.4 ppm; HRMS (ESI): calcd for $\text{C}_{19}\text{H}_{17}\text{F}_2\text{N}_2\text{O}_2$ $[\text{M}+\text{H}]^+$: 343.1258, found: 343.1250; MS (ESI): $m/z = 343$ $[\text{M}^++\text{H}]$.

Imidazole-1-carboxylic acid 1-(3,4'-difluoro-biphenyl-4-yl)-propyl ester (10). Synthesized according to Method E using **7a** (0.19 g, 0.75 mmol) and CDI (0.24 g, 1.50 mmol); yield: 0.10 g (69 %); colorless oil; $R_f = 0.29$ (DCM / MeOH, 95:5); $^1\text{H NMR}$ (CDCl_3 , 500 MHz) $\delta = 1.01$ (t, $J = 14.8$ Hz, 3H, CH_3), 2.02–2.20 (q, $J = 14.8, 15.5$ Hz, 2H, CH_2), 5.88 (t, $J = 15.5$ Hz, 1H, CH), 6.14 (s, 1H), 7.26–7.28 (m, 2H), 7.19–7.25 (m, 1H), 7.34–7.35 (m, 1H), 7.42–7.48 (m, 2H), 7.50–7.53 (m, 2H), 8.22 ppm (s, 1H, Im-2H); $^{13}\text{C NMR}$ (CDCl_3 , 125 MHz) $\delta = 9.7$ (CH_3), 28.1 (CH_2), 82.2 (CH), 114.3, 114.4, 115.8, 116.0, 117.2, 122.9, 128.1, 128.7, 135.3, 137.0, 159.3, 161.3, 161.9, 163.9, 171.1 ppm; HRMS (ESI): calcd for $\text{C}_{19}\text{H}_{17}\text{F}_2\text{N}_2\text{O}_2$ $[\text{M}+\text{H}]^+$: 343.1258, found: 343.1250; MS (ESI): $m/z = 343$ $[\text{M}^++\text{H}]$.

Imidazole-1-carboxylic acid 3,4'-difluoro-biphenyl-4-ylmethyl ester (12). Synthesized according to Method E using **11a** (0.26 g, 1.20 mmol) and CDI (0.39 g, 2.40 mmol); yield: 0.09 g (28 %); white solid: mp 220–221 °C; $R_f = 0.29$ (DCM / MeOH, 95:5); $^1\text{H NMR}$ (CDCl_3 , 500 MHz) $\delta = 5.33$ (s, 2H, CH_2), 7.07 (s, 1H), 7.12–7.15 (t, $J = 17.4$ Hz, 2H), 7.20 (s, 1H), 7.29 (d, $J = 11.0$ Hz, 1H), 7.33–7.35 (m, 2H), 7.49–7.52 (m, 2H), 8.32 ppm (s, 1H, Im-2H); $^{13}\text{C NMR}$ (CDCl_3 , 125 MHz) $\delta = 45.3$ (CH_2), 114.3, 115.9, 116.0, 121.1, 123.3, 126.7, 128.6, 128.7, 130.6, 130.7, 143.5, 143.6, 161.8, 162.0, 164.0 ppm; HRMS (ESI): calcd for $\text{C}_{17}\text{H}_{13}\text{F}_2\text{N}_2\text{O}_2$ $[\text{M}+\text{H}]^+$: 315.0945, found: 315.0943; MS (ESI): $m/z = 315$ $[\text{M}^++\text{H}]$.

(4'-Fluorobiphenyl-4-yl)(1H-imidazol-5-yl)methanol (23). A solution of **23a** (0.10 g, 0.20 mmol) in MeOH (5 mL) was stirred with pyridinium hydrochloride (35 mg, 0.30 mmol) at 60 °C for 4 hours. Then the reaction was quenched by adding saturated NaHCO_3 aq (10 mL), 20 mL EtOAc were added and the phases separated. The water phase was extracted 3 times with EtOAc (20 mL), the combined organic extracts were dried over Na_2SO_4 , and concentrated under reduced pressure. The crude product was purified by flash chromatography; yield: 0.05 g (91 %); colorless oil; $R_f = 0.19$ (EtOAc / MeOH, 95:5); $^1\text{H NMR}$ ($\text{CDCl}_3 + d_6$ -DMSO, 500 MHz) $\delta = 2.99$ (s, 1H), 5.84 (s, 1H), 6.87 (s, 2H), 7.02–7.06 (m, 2H), 7.41–7.47 ppm (m, 6H); $^{13}\text{C NMR}$ ($\text{CDCl}_3 + \text{DMSO}-d_6$, 125 MHz) $\delta = 71.2$ (COH), 115.8, 116.0, 116.4, 127.2, 127.9, 129.1, 129.4, 137.1, 138.6, 140.7, 142.3, 150.9, 162.1, 164.1 ppm; HRMS (ESI): calcd for $\text{C}_{16}\text{H}_{14}\text{FN}_2\text{O}$ $[\text{M}+\text{H}]^+$: 269.1090, found: 269.1088; MS (ESI): $m/z = 269$ $[\text{M}^++\text{H}]$.

5-(1-(4'-Fluorobiphenyl-4-yl)-2-methylprop-1-enyl)-1H-imidazole (25). Compound **24** (0.10 mg, 0.32 mol) was refluxed in an *i*-PrOH solution of HCl (10 mL, 3N) for 2 hours. Afterwards, the resulting solution was concentrated under reduced pressure and washed 3 times with Et_2O . No further purification was necessary; yield: 0.07 g (77 %); colorless oil; $R_f = 0.29$ (EtOAc / MeOH, 95:5); $^1\text{H NMR}$ (CDCl_3 , 500 MHz) $\delta = 1.80$ (s, 3H), 2.05 (s, 3H), 6.98 (s, 1H), 7.12 (dd, $J = 8.7, 8.8$ Hz, 2H), 7.19 (d, $J = 8.3$ Hz, 2H), 7.50 (d, $J = 8.3$ Hz, 2H), 7.54 (dd, $J = 5.3, 8.7$ Hz, 2H), 7.63 ppm (s, 1H); $^{13}\text{C NMR}$ (CDCl_3 , 125 MHz) $\delta = 22.7$ (CH_3), 23.1 (CH_3), 115.6, 115.8, 123.4, 125.2, 126.9, 128.5, 128.5, 129.8, 130.3, 132.6, 133.6, 133.7, 134.9, 136.6, 136.7, 136.7, 137.1, 138.8, 139.8, 160.9, 161.5 ppm; $^{19}\text{F NMR}$ (CDCl_3 , 400 MHz) $\delta = -115.56$ ppm (s, 1F);

HRMS (ESI): calcd for $C_{19}H_{18}FN_2$ $[M+H]^+$: 293.1454, found: 293.1455; MS (ESI): $m/z = 293$ $[M^+ + H]$.

5-(1-(4'-Fluorobiphenyl-4-yl)-2-methylpropyl)-1H-imidazole (26). Pearlman's catalyst (5 mg, 7.12 μ mol) and **25** (50 mg, 0.17 mmol) were prepared in EtOH and THF (2:1, 5mL) under H_2 atmosphere. The mixture was left stirring for 3 hours, then the catalyst was filtered off 3 times and the solution concentrated under reduced pressure. The obtained solid was washed 3 times with Et_2O . No further purification was necessary; yield: 50 mg (100%); yield: 0.07 g (77 %); colorless oil; $R_f = 0.29$ (EtOAc / MeOH, 95:5); 1H NMR ($CDCl_3$, 500 MHz) $\delta = 0.86$ (d, $J = 6.6$ Hz, 3H, CH_3), 0.99 (d, $J = 6.6$ Hz, 3H, CH_3), 3.60 (d, $J = 9.4$ Hz, 1H, CH), 6.90 (s, 1H), 7.09 (dd, $J = 8.7, 8.8$ Hz, 2H), 7.36 (d, $J = 8.2$ Hz, 2H), 7.45 (d, $J = 8.2$ Hz, 2H), 7.51 (dd, $J = 5.4, 8.7$ Hz, 2H), 7.55 ppm (s, 1H); ^{13}C NMR ($CDCl_3$, 125 MHz) $\delta = 21.2, 21.8, 32.5, 51.9, 115.4, 115.6, 123.1, 126.9, 128.4, 128.5, 128.9, 134.4, 137.1, 138.1, 142.4$ ppm; HRMS (ESI): calcd for $C_{19}H_{20}FN_2$ $[M+H]^+$: 295.1611, found: 295.1605; MS (ESI): $m/z = 295$ $[M^+ + H]$.

Docking studies

Ligands: All molecular modeling studies were performed on Intel(R) P4 CPU 3.00GHz running Linux CentOS5.2. The structures of the inhibitors were built with SYBYL 8 (Sybyl, Tripos Inc., St. Louis, Missouri, USA) and energy-minimized in MMFF94s force-field^[25] as implemented in Sybyl.

Docking: Molecular docking calculations were performed for various inhibitors of Table 1. Since the GOLD docking program allows flexible docking of the compounds, no conformational search was employed to the ligand structures. GOLD gave the best poses by a genetic algorithm (GA) search strategy. Ligands were docked in 50 independent genetic algorithm runs for each of the three GOLD-docking runs. Heme iron was chosen as active-site origin, while the radius was set equal to 19 Å. The automatic active-site detection was switched on. A distance constraint of a minimum of 1.9 and a maximum of 2.5 Å between the sp^2 -hybridised nitrogen of the imidazole and the iron was set. Additionally, the goldscore.p450_pdb parameters were used and some of the GOLDScore parameters were modified to improve the weight of hydrophobic interaction and of the coordination between iron and nitrogen. The genetic algorithm default parameters were set as suggested by the GOLD authors. On the other hand, the annealing parameters of fitness function were set at 3.5 Å for hydrogen bonding and 6.5 Å for Van der Waals interactions.

Analogously as for GOLD, no conformational search was performed prior docking with FlexX, since the ligands are docked according to an incremental fragment docking strategy. Standard parameter settings were used except for “base placement”, which was set on single interaction scan, and “chemical parameters”, in which the maximum overlap volume of the subroutine “clash handling” was set at a range of 3.6 Å. Additionally the “FlexX-Pharm” module was employed, setting the heme iron as an octahedral coordinating metal pharmacophore point. The very same iron atom was chosen as active site center and amino acid residues within 16 Å were considered as part of the active site.

All the poses resulting from three docking runs (GOLD-chemscore, GOLD-GOLDScore and FlexX) for each compound were clustered with ACIAP^[19] and the representative structure of each significant cluster was selected. After the docking simulations and cluster analysis were performed, the quality of the docked representative poses was evaluated based on visual inspection of the putative binding modes of the ligands. The latter were further evaluated by means of MOE (www.chemcompd.com) with its LigX module and evaluated by means of the various scoring functions (GOLDScore, CHEMScore and the empirical

FlexX Score).

MEP

For each docked compound geometry optimization was performed employing the B3LYP hybrid functional^[20] in combination with a 6-311++G (d,p) basis set using the package Gaussian03 (Gaussian, Inc., Pittsburgh, PA, 2003). The molecular electrostatic potential (MEP) maps were plotted using GaussView, version 3.0, the 3D molecular graphics package of Gaussian. These electrostatic potential surfaces were generated by mapping 6-311++G** electrostatic potentials onto surfaces of molecular electron density (isovalue = 0.004 electron/Å) and the ESP values on the surface color-coded ranging from -6 (red) to +12 (blue) kcal/mol.

Acknowledgement

The authors thank Dr. Ursula Müller-Vieira and Maria-Christina Scherzberg for the IC₅₀ determination, as well as Dr. Klaus Biemel for performing the in vivo test, and appreciate the help for synthesizing some compounds by Dr. Kerstin Jahn-Hoffmann, Dr. Mariano E. Pinto-Bazurco Mendieta and Dr. Marc Bartels, as well as the kind help from Professor Dr. Rolf Müller (Saarland University, Saarbrücken, Germany) in performing HSMS.

References

- [1] A. Jemal, R. Siegel, E. Ward, Y. Hao, J. Xu, T. Murray, M. J. Thun, *CA Cancer J. Clin.* **2008**, *58*, 71–96.
- [2] I. Huhtaniemi, H. Nikula, M.; Parvinen, S. Rannikko, *Am. J. Clin. Oncol.* **1988**, *11*, Suppl. 1, S11–15.
- [3] F. Labrie, A. Dupont, A. Belanger, L. Cusan, Y. Lacourciere, G. Monfette, J. G. Laberge, J. P. Emond, A. T. Fazekas, J. P. Raynaud, J. M. Husson, *Clin. Invest. Med.* **1982**, *5*, 267–275.
- [4] (a) T. Hara, J. Miyazaki, H. Araki, M. Yamaoka, N. Kanzaki, M. Kusaka, M. Miyamoto, *Cancer Res.* **2003**, *63*, 149–153. (b) X. Y. Zhao, P. J. Malloy, A. V. Krishnan, S. Swami, N. M. Navone, D. M. Peehl, D. Feldman, *Nature Medicine* **2000**, *6*, 703–706.
- [5] (a) C. I. Herold, K. L. Blackwell, *Clin. Breast Cancer.* **2008**, *8*, 50–64. (b) R. W. Hartmann, H. Bayer, G. Grün, *J. Med. Chem.* **1994**, *37*, 1275–81. (c) F. Leonetti, A. Favia, A. Rao, R. Aliano, A. Paluszczak, R. W. Hartmann, A. Carotti, *J. Med. Chem.* **2004**, *47*, 6792–6803. (d) M. Le Borgne, P. Marchand, M. Duflos, B. Delevoeye-Seiller, S. Piessard-Robert, G. Le Baut, R. W. Hartmann, M. Palzer, *Arch. Pharm. (Weinheim, Ger.)* **1997**, *330*, 141–145. (e) M. P. Leze, M. Le Borgne, P. Pinson, A. Paluszczak, M. Duflos, G. Le Baut, R. W. Hartmann, *Bioorg. Med. Chem. Lett.* **2006**, *16*, 1134–1137. (f) S. Gobbi, A. Cavalli, A. Rampa, F. Belluti, L. Piazzzi, A. Paluszczak, R. W. Hartmann, M. Recanatini, A. Bisi, *J. Med. Chem.* **2006**, *49*, 4777–4780. (g) A. Cavalli, A. Bisi, C. Bertucci, C. Rosini, A. Paluszczak, S. Gobbi, E. Giorgio, A. Rampa, F. Belluti, L. Piazzzi, P. Valenti, R. W. Hartmann, M. Recanatini, *J. Med. Chem.* **2005**, *48*, 7282–7289. (h) S. Castellano, G. Stefancich, R. Ragno, K. Schewe, M. Santoriello, A. Caroli, R. W. Hartmann, G. Sbardella, *Bioorg. Med. Chem.* **2008**, *16*, 8349–8358.
- [6] (a) S. Lucas, R. Heim, C. Ries, K. E. Schewe, B. Birk, R. W. Hartmann, *J. Med. Chem.* **2008**, *51*, 8077–8087. (b) S. Lucas, R. Heim, M. Negri, I. Antes, C. Ries, K. E. Schewe, A. Bisi, S. Gobbi, R. W. Hartmann, *J. Med. Chem.* **2008**, *51*, 6138–6149. (c) R. Heim, S. Lucas, C. M. Grombein, C. Ries, K. E. Schewe, M. Negri, U. Müller-Vieira, B. Birk, R. W. Hartmann, *J. Med. Chem.* **2008**, *51*, 5064–5074. (d) M. Voets, I. Antes, C. Scherer, U. Müller-Vieira, K. Biemel, S. Marchais-Oberwinkler, R. W. Hartmann, *J. Med. Chem.* **2006**, *49*, 2222–2231. (e) M. Voets, I. Antes, C. Scherer, U. Müller-Vieira, K. Biemel, C. Barassin, S. Marchais-Oberwinkler, R. W. Hartmann, *J. Med. Chem.* **2005**, *48*, 6632–6642. (f) S. Ulmschneider, U. Müller-Vieira, C. D. Klein, I. Antes, T. Lengauer, R. W. Hartmann, *J. Med. Chem.* **2005**, *48*, 1563–1575. (g) S. Ulmschneider, U. Müller-Vieira, M. Mitrenga, R. W. Hartmann, S. Oberwinkler-Marchais, C. D. Klein, M. Bureik, R. Bernhardt, I. Antes, T. Lengauer, *J. Med. Chem.* **2005**, *48*, 1796–1805.
- [7] B. C. Chung, J. Picardo-Leonard, M. Hanui, M. Bienkowski, P. F. Hall, J. E. Shively, W. L. Miller, *Proc. Natl. Acad. Sci. USA.* **1987**, *84*, 407–411.
- [8] (a) K. A. Harris, V. Weinberg, R. A. Bok, M. Kakefuda, E. J. Small, *J. Urol.* **2002**, *168*, 542–545. (b) J. Eklund, M. Kozloff, J. Vlamakis, A. Starr, M. Mariott, L. Gallot, B. Jovanovic, L. Schilder, E. Robin, M. Pins, R. C. Bergan, *Cancer* **2006**, *106*, 2459–2465.
- [9] (a) G. A. Potter, S. E. Banie, M. Jarman, M. G. Rowlands, *J. Med. Chem.* **1995**, *38*, 2463–2471. (b) J. P. Burkhart, C. A. Gates, M. E. Laughlin, R. J. Resvick, N. P. Peet, *Bioorg. Med. Chem.* **1996**, *4*, 1411–1420. (c) V. D. Handratta, T. S. Vasaitis, V. C. O. Njar, L. K. Gediya, R. Kataria, P. Chopra, D. Jr. Newman, R. Farquhar, Z. Guo, Y. Qiu, A. M. H. Brodie, *J. Med. Chem.* **2005**, *48*, 2972–2984. (d) V. C. O. Njar, K. Kato, I. P. Nnane, D. N. Grigoryev, B. J. Long, A. M. H. Brodie, *J. Med. Chem.* **1998**, *41*, 902–912.
- [10] (a) R. W. Hartmann, M. Hector, M. Haidar, P. B. Ehmer, W. Reichert, J. Jose, *J. Med. Chem.* **2000**, *43*, 4266–4277. (b) R.W. Hartmann, M. Hector, B. G. Wachall, A. Paluszczak, M. Palzer, V. Huch, M. Veith, *J. Med. Chem.* **2000**, *43*, 4437–4445. (c) V. C. O. Njar, M. Hector, R. W. Hartmann, *Bioorg. Med. Chem.* **1996**, *4*, 1447–1453. (d) S. Haidar, P. B. Ehmer, R. W.

- Hartmann, *Arch. Pharm. (Weinheim, Ger.)* **2001**, *334*, 373–374.
- [11] (a) G. A. Wächter, R. W. Hartmann, T. Sergejew, G. L. Grün, D. Ledergerber, *J. Med. Chem.* **1996**, *39*, 834–841. (b) F. C. Y. Chan, G. A. Potter, S. E. Barrie, B. P. Haynes, M. G. Rowlands, G. Houghton, M. Jarman, *J. Med. Chem.* **1996**, *39*, 3319–3323.
- [12] (a) B. G. Wachall, M. Hector, Y. Zhuang, R. W. Hartmann, *Bioorg. Med. Chem.* **1999**, *7*, 1913–1924. (b) Y. Zhuang, B. G. Wachall, R. W. Hartmann, *Bioorg. Med. Chem.* **2000**, *8*, 1245–1252. (c) F. Leroux, T. U. Hutschenreuter, C. Charriere, R. Scopelliti, R. W. Hartmann, *Helv. Chim. Acta* **2003**, *86*, 2671–2686. (d) T. U. Hutschenreuter, P. E. Ehmer, R. W. Hartmann, *J. Enzyme Inhib. Med. Chem.* **2004**, *19*, 17–32. (e) C. Jagusch, M. Negri, U. E. Hille, Q. Hu, M. Bartels, K. Jahn-Hoffmann, M. A. E. Pinto-Bazurco Mendieta, B. Rodenwaldt, U. Müller-Vieira, D. Schmidt, T. Lauterbach, M. Recanatini, A. Cavalli, R. W. Hartmann, *Bioorg. Med. Chem.* **2008**, *16*, 1992–2010. (f) M. A. E. Pinto-Bazurco Mendieta, M. Negri, C. Jagusch, U. E. Hille, U. Müller-Vieira, D. Schmidt, K. Hansen, R. W. Hartmann, *Bioorg. Med. Chem. Lett.* **2008**, *18*, 267–73. (g) Q. Hu, M. Negri, K. Jahn-Hoffmann, Y. Zhuang, S. Olgen, M. Bartels, U. Müller-Vieira, T. Lauterbach, R. W. Hartmann, *Bioorg. Med. Chem.* **2008**, *16*, 7715–7727. (h) M. A. E. Pinto-Bazurco Mendieta, M. Negri, C. Jagusch, U. Müller-Vieira, T. Lauterbach, R. W. Hartmann, *J. Med. Chem.* **2008**, *51*, 5009–5018. (i) U. E. Hille, Q. Hu, C. Vock, M. Negri, M. Bartels, U. Mueller-Vieira, T. Lauterbach, R. W. Hartmann, *Eur. J. Med. Chem.* **2009**, *44*, 2765–2775. (j) M. A. E. Pinto-Bazurco Mendieta, M. Negri, Q. Hu, U. E. Hille, C. Jagusch, K. Jahn-Hoffmann, U. Müller-Vieira, D. Schmidt, T. Lauterbach, R. W. Hartmann, *Arch. Pharm. (Weinheim, Ger.)* **2008**, *341*, 597–609. (k) U. E. Hille, Q. Hu, M. A. E. Pinto-Bazurco Mendieta, M. Bartels, C. A. Vock, T. Lauterbach, R. W. Hartmann, *C. R. Chim.* **2009**, *12*, 1117–1126.
- [13] (a) W. K. Hagmann, *J. Med. Chem.* **2008**, *51*, 4359–4369. (b) H. J. Böhm, D. Banner, S. Bendels, M. Kansy, B. Kuhn, K. Müller, U. Obst-Sander, M. Stahl, *ChemBioChem.* **2004**, *5*, 637–643. (c) K. Müller, C. Faeh, F. Diederich, *Science* **2007**, *317*, 1881–1886. (d) S. DiMagno, H. Sun, *Curr. Top. Med. Chem.* **2006**, *6*, 1473–1482. (e) R. Paulini, K. Müller, F. Diederich, *Angew. Chem., Int. Ed.* **2005**, *44*, 1788–1805. (f) J. A. Olsen, D. W. Banner, P. Seiler, U. O. Sander, A. D'Arcy, M. Stihle, K. Müller, F. Diederich, *Angew. Chem., Int. Ed.* **2003**, *42*, 2507–2511. (g) J. A. Olsen, D. W. Banner, P. Seiler, B. Wagner, T. Tschoop, U. Obst-Sander, M. Kansy, K. Müller, F. Diederich, *ChemBioChem* **2004**, *5*, 666–675. (h) F. Hof, D. M. Scofield, W. B. Schweizer, F. Diederich, *Angew. Chem., Int. Ed.* **2004**, *43*, 5056–5059. (i) E. S. Istvan, J. Deisenhofer, *Science*, **2001**, *292*, 1160–1164. (j) G. Phillips, D. D. Davey, K. A. Eagen, S. K. Koovakkat, A. Liang, H. P. Ng, M. Pinkerton, L. Trinh, M. Whitlow, A. M. Beatty, M. M. Morrissey, *J. Med. Chem.* **1999**, *42*, 1749–1756. (k) J. J. Parlow, A. M. Stevens, R. A. Stegeman, W. C. Stallings, R. G. Kurumbail, M. S. South, *J. Med. Chem.* **2003**, *46*, 4297–4312. (l) J. J. Parlow, R. G. Kurumbail, R. A. Stegeman, A. M. Stevens, W. C. Stallings, M. S. South, *J. Med. Chem.* **2003**, *46*, 4696–4701. (m) B. K. Park, N. R. Kitteringham, P. M. O'Neill, *Annu. Rev. Pharmacol. Toxicol.* **2001**, *41*, 443–470.
- [14] N. Miyaura, A. Suzuki, *Chem. Rev.* **1995**, *95*, 2457–2483.
- [15] Y. Tang, Y. Dong, J. L. Vennerstrom, *Synthesis* **2004**, *15*, 2540–2544.
- [16] P. B. Ehmer, J. Jose, R. W. Hartmann, *J. Steroid Biochem. Mol. Biol.* **2000**, *75*, 57–63.
- [17] a) G. Jones, P. Willett, R. C. Glen, A. R. Leach, R. Taylor, *J. Mol. Biol.* **1997**, *267*, 727–748. b) M. L. Verdonk, J. C. Cole, M. J. Hartshorn, C. W. Murray, R. D. Taylor, *Proteins* **2003**, *52*, 609–623.
- [18] a) B. Kramer, M. Rarey, T. Lengauer, *Proteins: Struct., Funct., and Gene.* **1999**, *37*, 228–241. b) FlexX trial Version 3.1.3; BioSolveIT GmbH, Sankt Augustin. <http://www.biosolveit.de/>
- [19] (a) G. Bottegoni, A. Cavalli, M. A. Recanatini, *J. Chem. Inf. Mod.* **2006**, *46*, 852–862. (b) G. Bottegoni, W. Rocchia, M. Recanatini, A. Cavalli, *Bioinformatics* **2006**, *22*, 58–65.
- [20] a) A. D. Becke, *J. Chem. Phys.* **1993**, *98*, 5648–5652; b) P. J. Stephens, F. J. Devlin, C. F. Chabalowski, M. J. Frisch, *J. Phys. Chem.* **1994**, *98*, 11623–11627.
- [21] M. J. Frisch, G. W. Trucks, H. B. Schlegel, G. E. Scuseria, M. A. Robb, J. R. Cheeseman, J. A. Jr. Montgomery, T. Vreven, K. N. Kudin, J. C. Burant, J. M. Millam, S. S. Lyengar, J. Tomasi, V. Barone, B. Mennucci, M. Cossi, G. Scalmani, N. Rega, G. A. Petersson, H. Nakatsuji, et al. Gaussian 03; Gaussian, Inc.: Pittsburgh, PA, 2004.
- [22] I. Dennington, K. T. Roy, J. Millam, K. Eppinnett, W. L. Howell, R. Gilliland, GaussView, version 3.0; Semichem Inc.: Shawnee Mission, KS, 2003.
- [23] (a) E. Bey, S. Marchais-Oberwinkler, M. Negri, P. Kruchten, A. Oster, T. Klein, A. Spadaro, R. Werth, M. Frotscher, B. Birk, R. W. Hartmann, *J. Med. Chem.* **2009**, *52*, 6724–6743. (b) P. Kruchten, R. Werth, E. Bey, A. Oster, S. Marchais-Oberwinkler, M. Frotscher, R. W. Hartmann, *J. Steroid Biochem. Mol. Biol.* **2009**, *114*, 200–206. (c) E. Bey, S. Marchais-Oberwinkler, R. Werth, M. Negri, Y. A. Al-Soud, P. Kruchten, A. Oster, M. Frotscher, B. Birk, R. W. Hartmann, *J. Med. Chem.* **2008**, *51*, 6725–6739. (d) S. Marchais-Oberwinkler, P. Kruchten, M. Frotscher, E. Ziegler, A. Neugebauer, U. Bhoga, E. Bey, U. Müller-Vieira, J. Messinger, H. Thole, R. W. Hartmann, *J. Med. Chem.* **2008**, *51*, 4685–4698. (e) M. Frotscher, E. Ziegler, S. Marchais-Oberwinkler, P. Kruchten, A. Neugebauer, L. Fetzer, C. Scherer, U. Müller-Vieira, J. Messinger, H. Thole, R. W. Hartmann, *J. Med. Chem.* **2008**, *51*, 2158–2169.
- [24] (a) F. Picard, T. Schulz, R. W. Hartmann, *Bioorg. Med. Chem.* **2002**, *10*, 437–448. (b) E. Baston, A. Paluszczak, R. W. Hartmann, *Eur. J. Med. Chem.* **2000**, *35*, 931–940. (c) W. Reichert, J. Jose, R. W. Hartmann, *Arch. Pharm. (Weinheim, Ger.)* **2000**, *333*, 201–204. (d) F. Picard, E. Baston, W. Reichert, R. W. Hartmann, *Bioorg. Med. Chem.* **2000**, *8*, 1479–1487. (e) E. Baston, R. W. Hartmann, *Bioorg. Med. Chem. Lett.* **1999**, *9*, 1601–1606.
- [25] T. A. Halgren, *J. Comput. Chem.* **1999**, *20*, 730–748.

3.III Replacement of Imidazolyl by Pyridyl in Biphenyl Methylenes Results in Selective CYP17 and Dual CYP17 / CYP11B1 Inhibitors for the Treatment of Prostate Cancer

Qingzhong Hu, Carsten Jagusch, Ulrike E. Hille, Jörg Haupenthal, and Rolf W. Hartmann

This manuscript has been accepted to be published as an article in
Journal of Medicinal Chemistry **2010**, 53, 5749–5758.

Paper III

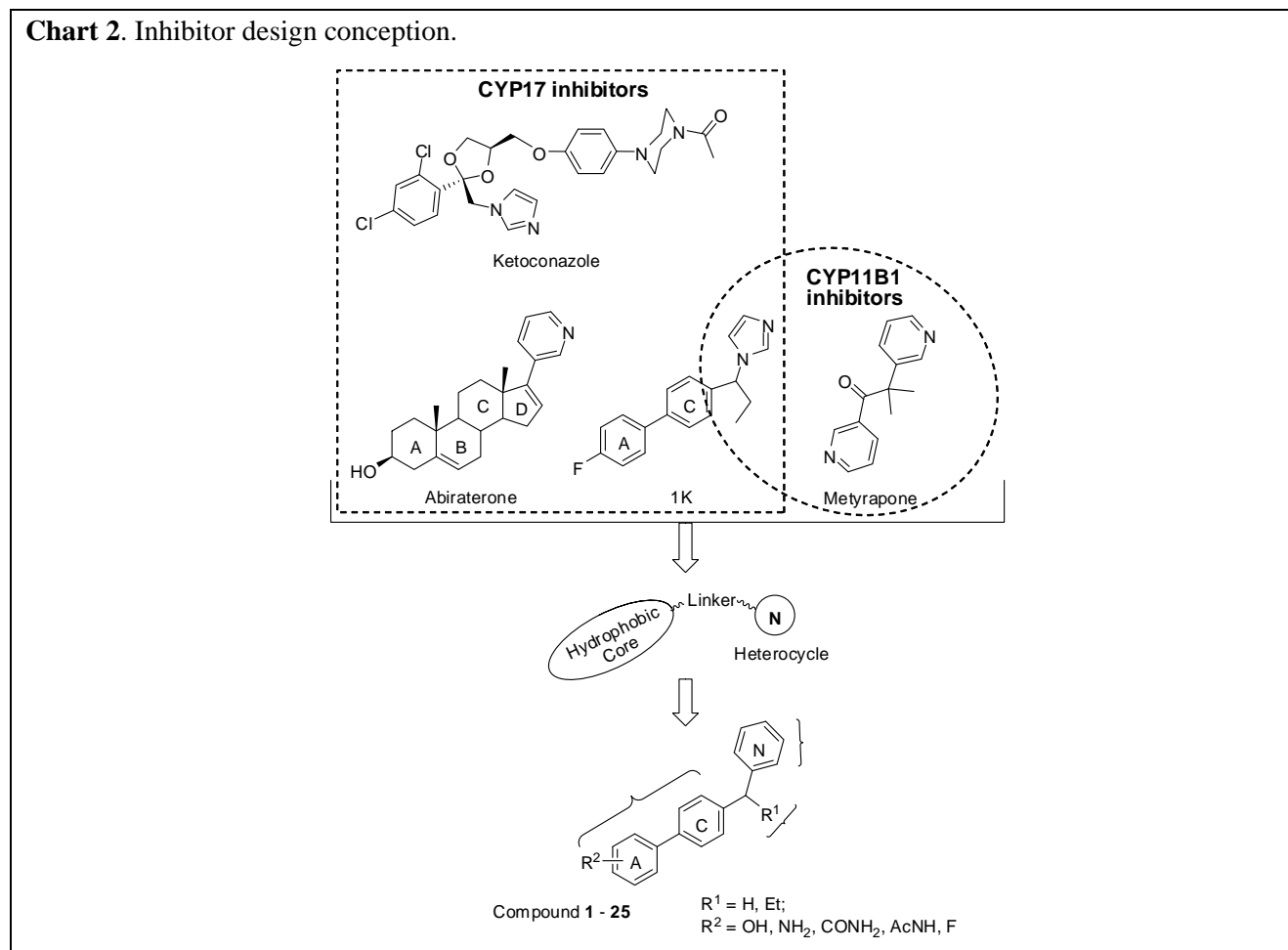
Abstract: Androgens are well known to stimulate prostate cancer (PC) growth. Thus, blockade of androgen production in testes and adrenals by CYP17 inhibition is a promising strategy for the treatment of PC. Moreover, many PC patients suffer from glucocorticoid overproduction and importantly mutated androgen receptors can be stimulated by glucocorticoids. In this study, the first dual inhibitor of CYP17 and CYP11B1 – the enzyme responsible for the last step in glucocorticoid biosynthesis – is described. A series of biphenyl methylene pyridines has been designed, synthesized and tested as CYP17 and CYP11B1 inhibitors. The most active compounds were also tested for selectivity against CYP11B2 (aldosterone synthase), CYP19 (aromatase) and hepatic CYP3A4. In detail, compound **6** was identified as a dual inhibitor of CYP17 / CYP11B1 (IC_{50} values of 226 and 287 nM) showing little inhibition of the other enzymes as well as compound **9** as a selective, highly potent CYP17 inhibitors ($IC_{50} = 52$ nM) exceeding Abiraterone in terms of activity and selectivity.

diabetes mellitus, osteoporosis, hypertension and obesity. High cortisol levels have also been considered as a sign of PC cell growth.^{8b} Importantly, some patients die of severe infections largely due to the immunosuppression caused by the glucocorticoid.^{8c-d} Hence, for these patients the control of cortisol concentration is urgently needed. As the key step in the biosynthesis of this hormone is catalyzed by CYP11B1 (Chart 1), additional inhibition of this enzyme could be a substantial way to improve curative effects, relieve symptoms and increase survival of prostate cancer patients.

Two decades ago, the first attempt to cure prostate cancer via CYP17 inhibition was described: the antimycotic Ketoconazole (Chart 2) was exploited as CYP17 inhibitor for the treatment of prostate cancer clinically.^{9a} Although curative response was observed,^{9b} Ketoconazole was withdrawn because of side effects associated with its poor selectivity against other steroidogenic and hepatic CYP enzymes. Later on, several steroidal inhibitors were designed based on endogenous substrates.¹⁰ Recently, Abiraterone^{11a} (Chart 2) entered into phase II and III clinical trials. Castration resistant patients showed good response to Abiraterone,^{11b} which confirms the superiority of prostate carcinoma treatment via CYP17 inhibition. However, the potential side effects might not be neglected which are caused by the affinity of steroidal scaffolds toward steroid receptors. Therefore, non-steroidal CYP17 inhibitors, such as heterocycle substituted tetrahydronaphthalenes,^{12a} adamantane-carboxylates^{12b} and biphenyls,¹³ attract more and more attention.

Our group has reported about several series of biphenyl methylene imidazoles¹³ as potent CYP17 inhibitors. All these compounds were designed based on the mechanism that the sp^2 hybrid nitrogen can coordinate with the heme iron, which was first^{14a} identified for aromatase (CYP19, estrogen synthase) inhibitors,¹⁴ and later was also proven to be valid for aldosterone synthase (CYP11B2)¹⁵ and CYP17 inhibitors.^{10, 12-13}

Although potent inhibitors, like 1K^{13e} (Chart 2, $IC_{50} = 131$ nM, for comparison: Abiraterone $IC_{50} = 72$ nM), were obtained after systematic modification on the biphenyl core and methylene bridge, activity and selectivity could possibly be further improved. Furthermore, compounds with additional CYP11B1 inhibition seemed feasible. After Abiraterone, 1K and Metyrapone (Chart 2) were superimposed using their heterocyclic N as a common atom, it is apparent that all of three compounds compose of three structural features: the hydrophobic core, an alkyl linker in between and a heterocycle containing N. Since Metyrapone is a CYP11B1 inhibitor, which has been applied in clinic to treat Cushing's syndrome for nearly half a century,¹⁶ and 1K also exhibits weak CYP11B1 inhibition, this common structural pattern might be the basis of dual inhibition, while the inhibitory potency toward each enzyme depends on the choice of the structural features. It is obvious that the steroidal scaffold of Abiraterone and the biphenyl core of 1K mate sterically. Nevertheless, the steroidal scaffold was avoided when choosing the hydrophobic core due to the potential affinities of steroidal structures for various steroidal receptors. As for Metyrapone, the nicotinoyl moiety occupies the same space as the steroidal C-ring. Since pyridyl as C-ring leads to a total loss of CYP17 inhibition,^{13d} the nicotinoyl moiety was replaced by a biphenyl moiety furnished with polar substituents. Moreover, a substituted methylene bridge, observed for these three inhibitors, was sustained, as we regard it to be crucial for inhibition of the two enzymes. Furthermore, inspired by the facts that pyridyl has already been successfully employed in other types of CYP17 inhibitors^{12a-b} leading to compounds being more potent

Chart 2. Inhibitor design conception.

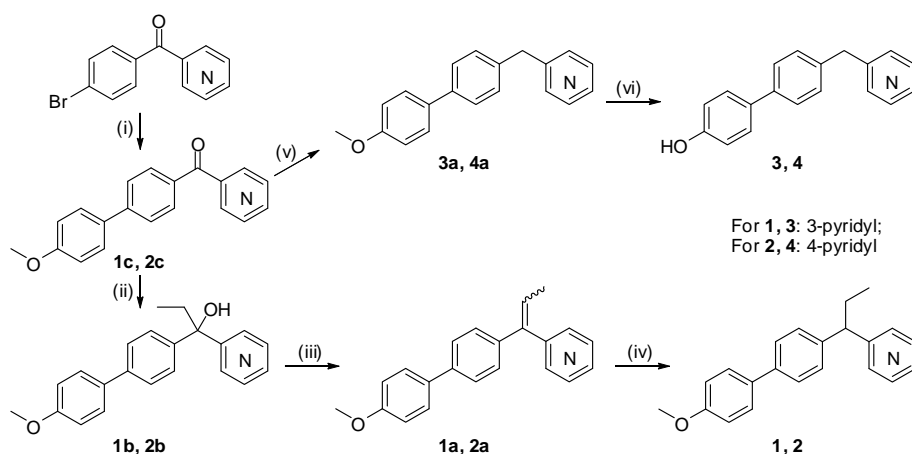
than the corresponding imidazoles,^{12a} and, importantly, that the pyridyl group is a common feature of CYP17 and CYP11B1 inhibitors, we replaced imidazole by pyridine. Accordingly, using this segmentation and hybridization procedure, biphenyl methylene pyridines were designed. Depending on the substituents at the core, these new compounds could be dual inhibitors of CYP17 and CYP11B1 or selective CYP17 inhibitors. This is because maximization of CYP17 inhibition was pursued as the first priority during the segment selection by choosing biphenyl instead of nicotinoyl, high inhibitory potency toward this enzyme should be the result, whereas inhibition toward CYP11B1 will largely depend on the substituents at the core.

As the first step, the effects of this design strategy on CYP17 inhibition were substantiated by comparing the imidazole, 3- and 4-pyridine analogues, i.e. **Ref. 1–2** and compounds **1–4** (Table 1). Encouraged by the positive results, more modifications on the A-ring were performed by introducing groups with different electrostatic potential, H-bond forming properties and various steric demand to improve both inhibition toward CYP17 and CYP11B1 (**5–25**, Tables 2–3). After determination of CYP17 inhibition, the most potent compounds were further tested for CYP11B1 inhibition and for selectivity against CYP11B2, CYP19 and hepatic CYP3A4.

Results

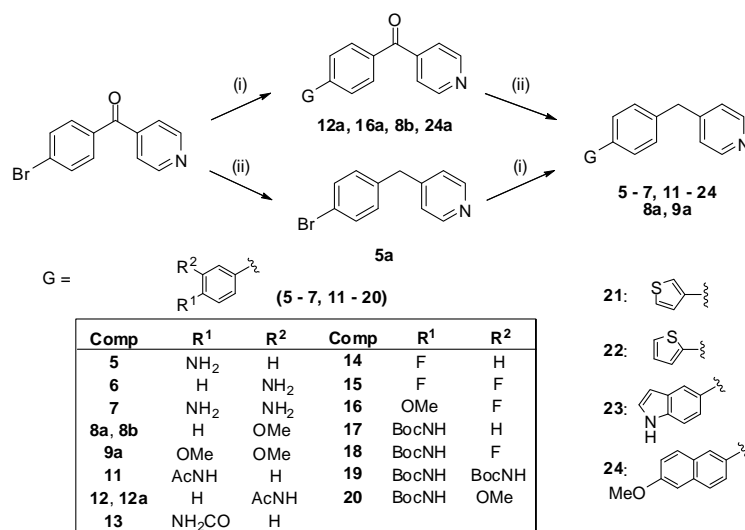
Chemistry. The synthesis of compounds **1–25** is shown in Schemes 1 and 2. A general strategy was employed starting from the corresponding (4-bromophenyl)-pyridyl-methanones, which are commercially available, but were easily prepared from bromobenzene and the corresponding nicotinic or isonicotinic acid

via Friedel-Crafts acylation. The starting material and the corresponding boronic acids were first reacted via Suzuki coupling to form the biaryl moieties, and then the ketone group was transferred by Wolff-Kishner reduction to afford the final methylene products. Subsequently, a more efficient strategy was used by first synthesizing the 4-bromobenzyl pyridine **5a** as a common building block, followed by introduction of the aryl ring via Suzuki coupling. For compounds **1** and **2** substituted with an ethyl rest on the methylene bridge, the ketone intermediates were reacted with ethylmagnesium bromide to give the corresponding alcohols **1b** and **2b**. After H₂O elimination in formic acid using Pd(OAc)₂ as catalyst, hydrogenation was performed to yield the final compounds. Moreover, the OH analogues **8–10** and **25** were obtained by ether cleavage of the corresponding methoxy compounds **8a**, **9a**, **16** and **24**, respectively, using boron tribromide.

Scheme 1.^a

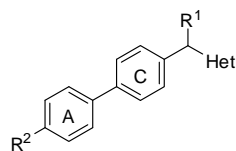
For **1**, **3**: 3-pyridyl;
For **2**, **4**: 4-pyridyl

^a Reagents and conditions: (i) Method A: Pd(OAc)₂, 4-methoxyphenylboronic acid, Na₂CO₃, TBAB, toluene, H₂O, ethanol, reflux, 6h. (ii) Method C: EtMgCl, THF; (iii) Method E: Pd(OAc)₂, HCOOH, reflux, 16h. (iv) Method F: Pd/C, H₂. (v) Method B: N₂H₄, KOH, ethylene glycol, reflux, 4h. (vi) Method D: BBr₃, DCM.

Scheme 2.^a

^a Reagents and conditions: (i) Method A: Pd(OAc)₂, corresponding boronic acid, Na₂CO₃, TBAB, toluene, H₂O, ethanol, reflux, 6h. (ii) Method B: N₂H₄, KOH, ethylene glycol, reflux, 4h.

CYP17 inhibition. Inhibitory activities of the synthesized compounds for CYP17 were determined using the 50,000g sediment after homogenation of *E.coli* expressing human CYP17 as well as cytochrome P450 reductase.^{17a} The assay was run with progesterone as substrate at high concentrations of 25 μM and NADPH as cofactor.^{13c} Separation of substrate and product was accomplished by HPLC using UV detection. IC₅₀

Table 1. Inhibition of CYP17 by compounds 1–4.**Ref. 1 - 2, 1 - 4**

Compd	R ¹	R ²	Heterocycles	IC ₅₀ [nM] ^b	Compd	R ¹	R ²	Heterocycles	IC ₅₀ [nM] ^b
Ref. 1	Et	OMe	1-Im	>5000	Ref. 2^c	H	OH	1-Im	>5000
1	Et	OMe	3-Py	>5000	3	H	OH	3-Py	4040
2	Et	OMe	4-Py	1610	4	H	OH	4-Py	248
MYP^a				>10000	KTZ^a				2780
ABT^a				72					

^a **MYP**: Metyrapone; **KTZ**: Ketoconazole; **ABT**: Abiraterone.

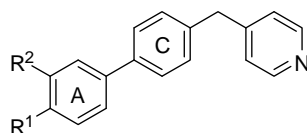
^b Concentration of inhibitors required to give 50 % inhibition. The given values are mean values of at least three experiments. The deviations were within ±10 %. The assay was run with human CYP17 expressed in *E. coli* using progesterone as substrate (25 μM).

^c **Ref. 1** was taken from reference 13a, where the inhibitory potency was test with human testicular microsome as 0.31 μM.

values are presented in comparison to Ketoconazole and Abiraterone in Tables 1–3.

To validate the possible benefits achieved after replacement of imidazolyl by pyridyl, the inhibitory potencies of imidazole, 3-pyridine and 4-pyridine analogues were compared. The SARs obtained from our previous work on biphenyl methylene imidazoles confirm that a) an ethyl group substituted on the methylene bridge elevates the inhibitory potency and b) H-bond forming groups such as hydroxy at 4-position of the A-ring increase the activity.^{13d-g} Taking these SARs into consideration, reference compounds **Ref. 1**^{13f} and **Ref. 2**^{13a} were chosen, each possessing one advantageous structural feature, ethyl or hydroxy, but showing low activity. Accordingly, the 3- and 4-pyridyl analogues were synthesized (Table 1). It becomes apparent that no matter which substituent furnished, the 3-pyridine analogues **1** and **3** showed similar inhibitory potencies compared to the reference compounds (IC₅₀ ≥ 5000 nM). However, the 4-pyridine analogue with an ethyl substituent on the methylene bridge exhibited IC₅₀ of 1610 nM, thus, being more potent than the corresponding imidazole analogue **Ref. 1** (IC₅₀ > 5000nM). The most active compound was the 4-pyridine analogue **4** furnished with hydroxy at the 4-position of the A-ring, showing IC₅₀ of 248 nM.

Encouraged by these results more compounds were designed based on the biphenyl methylene 4-pyridine scaffold (Table 2). It can be seen that the substituents at the A-ring showed a significant influence on the inhibitory potencies. The 4-amino substituted compound **5** showed IC₅₀ of 408 nM, whereas its 3-amino analogue **6** was even more potent (IC₅₀ = 226 nM). Interestingly, the 3, 4-diamino compound **7** exhibited potent activity with IC₅₀ in between (337 nM). Moreover, the hydroxy analogues were more potent than the amino derivatives. The 3-OH compound **8** was three fold more potent (IC₅₀ = 97 nM) compared to its corresponding NH₂ analogue, and to the 4-OH compound **4** (IC₅₀ = 248 nM). The 3,4-di OH compound **9** turned out to be the most potent one in this series with IC₅₀ of 52 nM, being even more potent than Abiraterone (IC₅₀ = 72 nM). The introduction of fluorine in 3-position of compound **4** resulting in compound **10** increased activity to 186 nM. The phenomenon that 3-substituted analogues are more potent than the corresponding 4-substituted compounds was also observed with the 4-acetamido compound **11** and its 3-analogue **12** (IC₅₀ = 876 nM). The retro-amide **13** (IC₅₀ = 1790 nM) showed a slightly increased potency

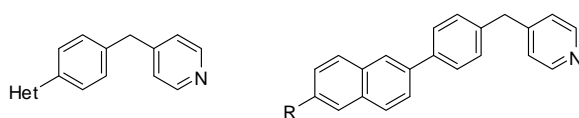
Table 2. Inhibition of CYP17 by compounds **5–20**.**5 - 20**

Compd	R ¹	R ²	IC ₅₀ [nM] ^b	Compd	R ¹	R ²	IC ₅₀ [nM] ^b
5	NH ₂	H	408	13	NH ₂ CO	H	1790
6	H	NH ₂	226	14	F	H	386
7	NH ₂	NH ₂	337	15	F	F	598
4	OH	H	248	16	OMe	F	3340
8	H	OH	97	17	BocNH	H	1370
9	OH	OH	52	18	BocNH	F	>10000
10	OH	F	186	19	BocNH	BocNH	>10000
11	AcNH	H	>5000	20	OMe	BocNH	>10000
12	H	AcNH	876	KTZ ^a			2780
MYP ^a			>10000	ABT ^a			72

^a **MYP**: Metyrapone; **KTZ**: Ketoconazole; **ABT**: Abiraterone.

^b Concentration of inhibitors required to give 50 % inhibition. The given values are mean values of at least three experiments. The deviations were within ±10 %. The assay was run with human CYP17 expressed in *E.coli* using progesterone as substrate (25 μM).

compared to compound **11**. As for fluorine derivatives introduction of additional F resulted in loss of inhibitory potency (**15**), which is in accordance with our previous findings,^{13g} while the compound with single fluorine in the 4-position of the A-ring (**14**) exhibited strong inhibition (IC₅₀ = 386 nM). Another interesting observation was the little activity of compounds **17** to **20** indicating that the Boc-amido group is not appropriate for highly active compounds, no matter introduced at the 3- or 4-position.

Table 3. Inhibition of CYP17 by compounds **21–25****21 - 23****24 - 25**

Compd	Het	R	IC ₅₀ [nM] ^b	Compd	Het	R	IC ₅₀ [nM] ^b
21	2-Thiophene		577	24		OMe	2000
22	3-Thiophene		647	25		OH	438
23	5-Indole		760	KTZ ^a			2780
MYP ^a			>10000	ABT ^a			72

^a **MYP**: Metyrapone; **KTZ**: Ketoconazole; **ABT**: Abiraterone.

^b Concentration of inhibitors required to give 50 % inhibition. The given values are mean values of at least three experiments. The deviations were within ±10 %. The assay was run with human CYP17 expressed in *E.coli* using progesterone as substrate (25 μM).

Finally, the A-ring phenyl group was exchanged by heterocycles and substituted naphthalenes (Table 3). The thiophene (**21** and **22**) and indole (**23**) compounds showed modest activity with IC₅₀ values around 600 nM. For the naphthalene analogues, the great influence of the substituent on the A-ring was again observed. The hydroxy derivative **25** showed rather potent inhibition (IC₅₀ = 438 nM), while the corresponding

methoxy derivative **24** was less active.

CYP11B1 inhibition. After it has been shown that the replacement of imidazolyl by pyridyl significantly increased the CYP17 inhibition, selected compounds (**4–10**, **12**, **14**, **15**, **21–23** and **25**) were examined for their CYP11B1 inhibition (Table 4). The inhibitory activities were determined in V79 MZh cells expressing human CYP11B1.^{17b-c} The V79 MZh cells were incubated with [¹⁴C]-deoxycorticosterone as substrate and the inhibitor in different concentrations. Product formation was monitored by HPTLC using a phosphoimager. It becomes apparent that the substituents on the A-ring also show profound influence on the inhibition of this enzyme. Compounds **4** and **6** exhibited rather strong effects with IC₅₀ values around 250 nM. Compounds **9** and **15** showed only weak or no inhibition (IC₅₀ values of 1400 and 4742 nM, respectively), thus, being rather selective inhibitors of CYP17, whereas all of the rest compounds **5**, **7**, **8**, **10**, **12**, **14**, **15**, **21–23** and **25** showed modest inhibition values between 300 and 930 nM.

Selectivity. The inhibition of CYP11B2 by selected potent compounds was determined as well using V79 MZh cells expressing human CYP11B2 (Table 4). CYP11B2 is the crucial enzyme responsible for the final steps in aldosterone biosynthesis (Chart 1). Inhibition of CYP11B2 could cause hyponatremia, hyperkalemia and a series of recessive disorders, such as adrenal hyperplasia and hypovolemic shock.^{18a} Selectivity over CYP11B2 is difficult to reach especially for the compounds inhibiting CYP11B1 because of the very high homology between these two enzymes of 93%. It can be seen that although compounds **8**, **10** and **15** exhibited strong inhibition toward CYP11B2 (IC₅₀ values around 250 nM), some compounds (**4**, **5**, **7**, **12**, **14** and **21–23**) showed modest inhibition with IC₅₀ values ranging from 300 to 800 nM, whereas other compounds (**6**, **9** and **25**) were very selective with IC₅₀ values around 1000 nM. Important is that compound **6** as a dual inhibitor of CYP17 and CYP11B1 exhibiting a selectivity factor of 3.2 between CYP11B1 and CYP11B2.

Table 4. Inhibition of CYP11B1, CYP11B2, CYP19 and CYP3A4 by selected compounds.

Comp	IC ₅₀ (nM) ^b				Comp	IC ₅₀ (nM) ^b			
	CYP11B1 ^c	CYP11B2 ^c	CYP19 ^d	CYP3A4 ^e		CYP11B1 ^c	CYP11B2 ^c	CYP19 ^d	CYP3A4 ^e
4	251	341	3070	3210	12	307	567	n.d. ^a	n.d. ^a
5	522	406	24500	2450	14	928	515	n.d. ^a	668
6	287	921	2830	1520	15	4742	273	n.d. ^a	n.d. ^a
7	902	367	>25000	n.d. ^a	21	422	331	n.d. ^a	n.d. ^a
8	342	261	663	538	22	415	796	n.d. ^a	n.d. ^a
9	1400	948	2440	7580	23	469	231	n.d. ^a	n.d. ^a
10	850	210	2693	896	25	627	1130	n.d. ^a	1140
MYP^a	15	72	>5000	n.d. ^a					
KTZ^a	127	67	>5000	57	ABT^a	1610	1750	>5000	2700

^a **MYP**: Metyrapone; **KTZ**: Ketoconazole; **ABT**: Abiraterone; n.d.: not determined.

^b Standard deviations were within < ±5 %; All the data are the mean values of at least 3 tests.

^c Hamster fibroblasts expressing human CYP11B1 or CYP11B2 are used with deoxycorticosterone as the substrate at a concentration of 100 nM.

^d Human placental CYP19 is used with androstenedione as the substrate at a concentration of 500 nM.

^e Recombinantly expressed enzyme from baculovirus-infected insect microsomes is used with 7-benzyloxy-trifluoromethyl coumarin as the substrate at a concentration of 50 μM.

Furthermore, the selectivity of these potent compounds toward CYP19 and hepatic CYP3A4 has also been tested as a criterion for safety (Table 4). CYP19 is the unique enzyme catalyzing the peripheral conversion of androgens to estrogens by hydroxylation and subsequent elimination of the C19 methyl group resulting in steroid A-ring aromatization. Estrogen deficiency causes osteoporosis, increased fracture risk^{17b} and memory loss.^{18c} Under CYP17 inhibition, there is a reduction of the estrogen plasma concentrations because the androgens, as substrates for estrogen formation, are decreased. A further reduction of estrogen levels by CYP19 inhibition would be detrimental. As can be seen, all the tested compounds except **8** showed no inhibition of CYP19 (IC₅₀ values above 2000 nM).

Besides, the important role of CYP3A4 in drug metabolism and drug-drug interaction has been addressed and the compounds have been tested for inhibition of this enzyme as well. Most of them showed weak or no inhibition of CYP3A4 (IC₅₀ > 1000 nM). Compounds **4** and **9** exhibited a better selectivity than Abiraterone (IC₅₀ values of 3210 nM and 7580 nM vs 2700 nM).

Discussion and Conclusion

The design concept applied in the present paper using the steroidal CYP17 inhibitor Abiraterone, the CYP11B1 inhibitor Metyrapone and our experience in non-steroidal biphenyl methylene based CYP17 inhibitors (including 1K) was successful. Exchange of the imidazolyl moiety by a 4-pyridyl rest led – depending on the substitution pattern at the A-ring – on the one hand to compound **9**, exceeding Abiraterone in activity and selectivity, and on the other hand to compound **6**, a dual inhibitor of CYP17 and CYP11B1.

The elevated inhibition of CYP17 caused by the novel pyridines compared to the corresponding imidazoles might be due to the prolonged distance between the *sp*² hybrid N and the methylene C. This elongation of the molecule places the H-bond forming groups at the A-ring closer to the amino acid residues, facilitating better H-bond formation. Moreover, it has been found that substituents on the A-ring showed profound influence on the inhibitory potency of both CYP17 and CYP11B1. Hydrogen bond forming groups, like OH and NH₂, significantly elevated CYP17 inhibition, probably due to the interaction with Arg109, Lys231, His235 and Asp298, similar as we described recently.^{13f} This finding indicates that imidazoles and pyridines may adopt the same binding mode in the enzyme pocket. Among them, OH analogues were found to be more potent than the corresponding NH₂ analogues (e.g. compounds **4** and **5** (IC₅₀ values of 248 nM and 408 nM), compounds **8** and **6** (IC₅₀ values of 97 nM and 226 nM) and compounds **9** and **7** (IC₅₀ values of 52 nM and 337 nM)), probably because the hydrogen bonds formed by O are stronger than the ones formed by N.¹⁹ Interestingly, *meta*-substituted analogues are more potent than the corresponding *para*-analogues. After methylation of OH (compounds **16** and **20**) or acylation of NH₂ (**11**, **12**, **17–20**), the inhibitory potency dropped along with the augment of bulk, which is probably due to the steric hindrance with His235, Arg109 and the proximal I-helix residues as described previously.^{13f}

Regarding the additional CYP11B1 inhibition we were aiming at in this study, the exchange of the nicotinoyl moiety from Metyrapone — because it leads to a loss of CYP17 inhibition — by a biphenyl moiety with small polar substituents was successful and resulted in compounds with dual, CYP17 and CYP11B1, inhibition. It was found that compounds **4–6**, **8** and **12** with one single H-bond donor showed potent to modest inhibition (IC₅₀ values ranged 250 to 350 nM, with compound **5** as an exception showing

IC₅₀ value of 522 nM), whereas H-bond acceptors or two donors resulted in rather weak inhibitors of CYP11B1 (compounds **7**, **9** and **10**; IC₅₀ values more than 800 nM). Since these compounds with differing CYP11B1 inhibition are potent CYP17 inhibitors, they are accordingly either dual inhibitors of CYP17 / 11B1 or selective CYP17 inhibitors.

The A-ring substituents also diversified the inhibitory potency toward the non-target enzyme CYP11B2. It was found that compounds with strong CYP11B1 inhibition were also associated with CYP11B2 inhibition. This is not surprising since homology between these two enzymes is more than 93%. As inhibition of CYP11B2 has to be avoided, the most interesting dual inhibitor in this study is compound **6** showing a selectivity factor of 3.2 regarding CYP11B1 and CYP11B2. For the application as a dual CYP17 / CYP11B1 inhibitor, this selectivity toward CYP11B2 is certainly not sufficient. However, compound **6** should be an interesting lead for further optimization. Since highly active and selective CYP11B2 inhibitors with *in vivo* activity^{15a} reaching selectivity factors of 1000^{15b} have been identified by our group for the treatment of congestive heart failure and myocardial fibrosis, we are confident that the selectivity of compound **6** can be further improved. Structure modifications are presently being performed.

The use of selective multi-target-directed ligands has already been proposed for the treatment of other diseases to enhance efficacy and to improve safety, for example agents inhibiting angiotensin converting enzyme (ACE) and neutral endopeptidase (NEP) in the treatment of hypertension, multi-kinase inhibitors (MKI) with combined inhibition of vascular endothelial growth factor (VEGF) and platelet-derived growth factor (PDGF) for cancer therapy and dual binding site acetylcholinesterase inhibitors (AChEI) for Alzheimer's disease.²⁰ Comparing to the traditional combinational application of two or more drugs, multi-target-directed agents can reduce the risk of drug-drug interactions and achieve better compliance. The conception of selective dual inhibition of CYP17 and CYP11B1 is a novel treatment for PC. There is indeed a high medical need in prostate cancer patients to combat elevated glucocorticoid levels and to prevent stimulation of mutated androgen receptors by glucocorticoids. CYP11B1 catalyzing the last step in cortisol biosynthesis is an ideal target to decrease corticosterone and cortisol production. However, there are no highly selective inhibitors of this enzyme described so far which could be used in a combination therapy with CYP17 inhibitors. Metyrapone is a compound not selective enough that inhibits other steroidogenic CYP enzymes and therefore shows severe side effects. Accordingly it is not an appropriate candidate for this purpose, although it has been used in the treatment of Cushing's syndrome for a long time. Another unselective compound, the antimycotic Ketoconazole has already been employed to treat prostate cancer patients with ectopic adrenocorticotropic hormone syndrome^{8d} because it inhibits both androgen and corticosteroid — not only glucocorticoid but also mineralocorticoid — biosynthesis. However, the response was not satisfactory due to the weak potency of Ketoconazole (CYP17 IC₅₀ = 2780 nM). Compound **6** should be a much better candidate than Ketoconazole showing a good dual inhibition of CYP17 and CYP11B1 with IC₅₀ values around 200 nM for both enzymes, a three fold selectivity of CYP11B1 over CYP11B2 and nearly no inhibition of CYP19 and CYP3A4. As selectivity for CYP11B2 should be further enhanced, compound **6** could be an ideal candidate for this optimization process.

Importantly, compound **9** showed an excellent selectivity with almost no inhibition of all other enzymes tested. It is highly active showing an IC₅₀ value of 52 nM. As in our experimental set-up with high substrate

concentrations, this value has to be ranked higher than similar IC₅₀ values obtained by other groups using much lower substrate concentrations. The fact that compound **9** not only shows strong inhibition of androgen formation (CYP17), but also does not block androgen conversion to estrogens (CYP19) provides maximally low androgen levels — a prerequisite for the therapeutic success. After validation *in vivo*, this compound could be a promising drug candidate for further development.

Based on the results of the present study we would like to propose a novel strategy for the treatment of prostate cancer: CYP17 inhibitors with different selectivity profiles according to the status of the patients should be applied. For normal patients, selective CYP17 inhibitors that do not interfere with other steroidogenic CYPs should be used to avoid side effects, whereas for patients with mutated androgen receptors or ectopic adrenocorticotrophic hormone syndrome, dual inhibitors of CYP17 and CYP11B1 are the best choice in the view of a personalized medicine.

Experimental Section

CYP17 preparation and assay

Human CYP17 was expressed in *E. coli*^{17a} (coexpressing human CYP17 and NADPH-P450 reductase) and the assay was performed as previously described.^{13c}

Inhibition of hepatic CYP3A4

The recombinantly expressed enzyme from baculovirus-infected insect microsomes (Supersomes) was used and the manufacturer's instructions (www.gentest.com) were followed.

Inhibition of CYP11B1 and CYP11B2

V79MZh cells expressing human CYP11B1 or CYP11B2 were incubated with [¹⁴C]-11-deoxycorticosterone as substrate. The assay was performed as previously described.^{17b-c}

Inhibition of CYP19

The inhibition of CYP19 was determined *in vitro* using human placental microsomes with [1β-³H]androstenedione as substrate.^{17d}

Chemistry Section

General

Melting points were determined on a Mettler FP1 melting point apparatus and are uncorrected. IR spectra were recorded neat on a Bruker Vector 33FT-infrared spectrometer. ¹H-NMR spectra were measured on a Bruker DRX-500 (500 MHz). Chemical shifts are given in parts per million (ppm), and TMS was used as an internal standard for spectra. All coupling constants (*J*) are given in Hz. ESI (electrospray ionization) mass spectra were determined on a TSQ quantum (Thermo Electron Corporation) instrument. The purities of the final compounds were controlled by Surveyor®-LC-system. Purities were greater than 95%. Column chromatography was performed using silica-gel 60 (50–200 μm), and reaction progress was determined by TLC analysis on Alugram® SIL G/UV₂₅₄ (Macherey-Nagel). Boronic acids and bromoaryls used as starting materials were commercially obtained (CombiBlocks, Chempur, Aldrich, Acros).

Method A: Suzuki-Coupling

The corresponding brominated aromatic compound (1 eq) was dissolved in toluene (7 mL / mmol), and an

aqueous 2.0 M Na₂CO₃ solution (3.2 mL / mmol), an ethanolic solution (3.2 mL / mmol) of the corresponding boronic acid (1.5–2.0 eq) and tetrabutylammonium bromide (1 eq) were added. The mixture was deoxygenated under reduced pressure and flushed with nitrogen. After having repeated this cycle several times Pd(OAc)₂ (5 mol%) was added and the resulting suspension was heated under reflux for 2–6 h. After cooling, ethyl acetate (10 mL) and water (10 mL) were added and the organic phase was separated. The water phase was extracted with ethyl acetate (2 x 10 mL). The combined organic phases were washed with brine, dried over Na₂SO₄, filtered over a short plug of celite® and evaporated under reduced pressure. The compounds were purified by flash chromatography on silica gel.

4'-(Pyridin-4-ylmethyl)biphenyl-4-amine (5). Synthesised according to Method A using **5a** (0.35 g, 1.41 mmol) and 4-aminophenyl boronic acid (0.29 g, 2.12 mmol); yield: 0.32 g (87%); white solid: mp 217–218 °C; *R*_f = 0.19 (DCM/MeOH, 20:1); δ_H (CD₃OD, 500 MHz) 4.04 (s, 2H), 6.77 (d, *J* = 8.5 Hz, 2H), 7.23 (d, *J* = 8.1 Hz, 2H), 7.29 (d, *J* = 5.9 Hz, 2H, Py 2,6-H), 7.36 (d, *J* = 8.5 Hz, 2H), 7.48 (d, *J* = 8.2 Hz, 2H), 8.40 (d, *J* = 6.1 Hz, 2H, Py 3,5-H); MS (ESI): *m/z* = 261 [M⁺+H].

4'-(Pyridin-4-ylmethyl)biphenyl-3-amine (6). Synthesised according to Method A using **5a** (0.30 g, 1.21 mmol) and 3-aminophenyl boronic acid (0.25 g, 1.81 mmol); yield: 0.26 g (83%); white solid: mp 79–80 °C; *R*_f = 0.45 (DCM/MeOH, 95:5); δ_H (CDCl₃, 500 MHz) 4.00 (s, 2H), 5.13 (s, 2H), 6.54 (dd, *J* = 2.2, 7.9 Hz, 1H), 6.74 (dd, *J* = 1.6, 7.6 Hz, 1H), 6.81 (t, *J* = 1.9 Hz, 1H), 7.07 (t, *J* = 7.9 Hz, 1H), 7.27 (d, *J* = 5.9 Hz, 2H), 7.30 (d, *J* = 8.2 Hz, 2H), 7.49 (d, *J* = 7.9 Hz, 2H), 8.46 (d, *J* = 5.9 Hz, 2H); MS (ESI): *m/z* = 261 [M⁺+H].

4'-(Pyridin-4-ylmethyl)biphenyl-3,4-diamine (7). Synthesised according to Method A using **5a** (0.35 g, 1.41 mmol) and 3,4-diaminophenyl boronic acid (0.32 g, 2.11 mmol); yield: 0.32 g (83%); white solid: mp 180–181 °C; *R*_f = 0.15 (DCM/MeOH, 20:1); δ_H (CDCl₃, 500 MHz) 3.48 (s, br, 4H, NH₂), 3.98 (s, 2H, CH₂), 6.76 (d, *J* = 8.2 Hz, 1H), 6.92–6.96 (m, 2H), 7.13 (d, *J* = 6.0 Hz, 2H), 7.18 (d, *J* = 8.2 Hz, 2H), 7.47 (d, *J* = 8.2 Hz, 2H), 8.50 (dd, *J* = 1.6, 6.0 Hz, 2H); MS (ESI): *m/z* = 276 [M⁺+H].

4-[(3',4'-Dimethoxybiphenyl-4-yl)methyl]pyridine (9a). Synthesised according to Method A using **5a** (0.31 g, 1.25 mmol) and 3,4-dimethoxyphenylboronic acid (0.34 g, 1.88 mmol); yield: 0.34 g, (90%). This compound was used directly in the next step without further purification and characterization.

4'-(Pyridin-4-ylmethyl)biphenyl-4-carboxamide (13). Synthesised according to Method A using **5a** (0.25 g, 1.01 mmol) and 4-carbamoylphenyl boronic acid (0.25 g, 1.51 mmol); yield: 0.26 g (89%); white solid: mp 241–242 °C; *R*_f = 0.21 (DCM/MeOH, 50:1); δ_H (CD₃OD, 500 MHz) 4.09 (s, 2H, CH₂), 7.09–7.11 (m, 4H), 7.64 (d, *J* = 7.9 Hz, 2H), 7.71 (d, *J* = 7.8 Hz, 2H), 7.94 (d, *J* = 8.1 Hz, 2H), 8.42 (d, *J* = 4.7 Hz, 2H, Py 3,5-H); MS (ESI): *m/z* = 289 [M⁺+H].

4-[(4'-Fluoro-biphenyl-4-yl)methyl]-pyridine (14). Synthesised according to Method A using **5a** (301 mg, 1.21 mmol) and 4-fluorophenyl boronic acid (254 mg, 1.82 mmol); yield: 168 mg (53%); white solid: mp 114–115 °C; *R*_f = 0.49 (DCM / MeOH, 95:5) δ_H (CDCl₃, 500 MHz) 3.96 (s, 2H), 7.03–7.07 (m, 2H), 7.12 (d, *J* = 5.4 Hz, 2H), 7.17 (d, *J* = 8.5 Hz, 2H), 7.43 (d, *J* = 8.2 Hz, 2H), 7.44–7.47 (m, 2H), 8.45 (d, *J* = 5.3 Hz, 2H); MS (ESI): *m/z* = 264 [M⁺+H]

4-[(3',4'-Difluorobiphenyl-4-yl)methyl]pyridine (15). Synthesised according to Method A using **5a** (0.125 g, 0.5 mmol) and 3,4-difluorophenyl boronic acid (0.21 g, 0.75 mmol); yield: 0.12 g (87%);

colourless oil; $R_f = 0.27$ (hexane/EtOAc, 1:1); δ_H (CDCl₃, 500 MHz) 3.93 (s, 2H), 7.05 (d, $J = 6.1$ Hz, 2H), 7.10–7.22 (m, 4H), 7.26–7.31 (m, 1H), 7.39 (d, $J = 8.2$ Hz, 2H), 8.44 (d, $J = 6.1$ Hz, 2H); MS (ESI): $m/z = 282$ [M⁺+H].

tert-Butyl 4'-(pyridin-4-ylmethyl)biphenyl-4-yl carbamate (17). Synthesised according to Method A using **5a** (0.30 g, 1.21 mmol) and 4-(*tert*-butoxycarbonylamino)phenyl boronic acid (0.43 g, 1.81 mmol); yield: 0.38 g (87%); white solid: mp 198–199 °C; $R_f = 0.26$ (DCM/MeOH, 50:1); δ_H (CD₃OD, 500 MHz) 1.53 (s, 9H, Boc), 4.05 (s, 2H, CH₂), 7.28–7.29 (m, 4H), 7.51–7.53 (m, 6H), 8.40 (d, $J = 4.9$ Hz, 2H); MS (ESI): $m/z = 361$ [M⁺+H].

4-[4-(Thiophen-2-yl)benzyl]pyridine (21). Synthesised according to Method A using **5a** (0.35 g, 1.41 mmol) and thiophen-2-yl boronic acid (0.27 g, 2.12 mmol); yield: 0.32 g (91%); white solid: mp 82–83 °C; $R_f = 0.26$ (DCM/MeOH, 50:1); δ_H (CD₃OD, 500 MHz) 4.00 (s, 2H, CH₂), 7.05 (dd, $J = 4.0, 4.6$ Hz, 1H), 7.22 (d, $J = 7.2$ Hz, 2H), 7.26 (d, $J = 4.6$ Hz, 2H), 7.33 (d, $J = 4.7$ Hz, 2H), 7.56 (d, $J = 7.9$ Hz, 2H), 8.40 (d, $J = 3.9$ Hz, 2H); MS (ESI): $m/z = 252$ [M⁺+H].

4-[4-(Thiophen-3-yl)benzyl]pyridine (22). Synthesised according to Method A using **5a** (0.35 g, 1.41 mmol) and thiophen-3-yl boronic acid (0.27 g, 2.12 mmol); yield: 0.31 g (90%); white solid: mp 97–98 °C; $R_f = 0.26$ (DCM/MeOH, 50:1); δ_H (CD₃OD, 500 MHz) 4.03 (s, 1H, CH₂), 7.24 (d, $J = 8.2$ Hz, 2H), 7.28 (d, $J = 6.0$ Hz, 2H), 7.43–7.45 (m, 2H), 7.60–7.63 (m, 3H), 8.40 (d, $J = 6.45$ Hz, 2H); MS (ESI): $m/z = 252$ [M⁺+H].

5-[4-(Pyridin-4-ylmethyl)phenyl]-1*H*-indole (23). Synthesised according to Method A using **5a** (0.30 g, 1.21 mmol) and 1*H*-indol-5-yl boronic acid (0.27 g, 2.12 mmol); yield: 0.30 g (87%); white solid: mp 170–171 °C; $R_f = 0.23$ (DCM/MeOH, 20:1); δ_H (CD₃OD, 500 MHz) 4.04 (s, 2H, CH₂), 6.48 (d, $J = 3.7$ Hz, 1H), 7.25–7.27 (m, 3H), 7.30 (d, $J = 5.9$ Hz, 2H), 7.35–7.37 (m, 1H), 7.42 (d, $J = 8.5$ Hz, 2H), 7.58 (d, $J = 8.2$ Hz, 2H), 7.76–7.78 (m, 1H), 8.40 (d, $J = 5.9$ Hz, 2H); MS (ESI): $m/z = 285$ [M⁺+H].

Method B: Wolff-Kishner-Reduction

To an ice-cooled solution of the appropriate ketone (10 mmol) in ethylene glycol (100 mL) was added hydrazine hydrate (70 mmol) and potassium hydroxide (10 mmol). Then the resulting mixture was heated to 150 °C for 1 hour. After cooling down, a further batch of potassium hydroxide (50 mmol) was added, and the mixture was heated to 210 °C for 2 hours. After cooling to ambient temperature, it was diluted with water (300 mL), and the resulting mixture was extracted with ethyl acetate (3 x 50 mL). The combined organic phases were washed with brine, dried over MgSO₄ and evaporated under reduced pressure. Then the desired product was purified by chromatography on silica gel.

4-(4-Bromobenzyl)pyridine (5a). Synthesised according to Method B using (4-bromophenyl)-pyridin-4-yl-methanone (0.39 g, 1.5 mmol); yield: 0.21 g (52%); amber oil; $R_f = 0.35$ (PE / EtOAc, 10:1); δ_H (CDCl₃, 500 MHz) 3.89 (s, 2H, CH₂), 7.02 (d, $J = 8.3$ Hz, 2H), 7.05 (d, $J = 5.9$ Hz, 2H), 7.41 (d, $J = 8.3$ Hz, 2H), 8.48 (d, $J = 5.9$ Hz, 2H); δ_C (CDCl₃, 125 MHz) 40.5 (CH₂), 120.5, 124.0, 130.6, 131.7, 137.7, 149.8; MS (ESI): $m/z = 249$ [M⁺+H].

***N*-(4'-Isonicotinoylbiphenyl-3-yl)acetamide (12).** Synthesised according to Method B using **12a** (0.32 g, 1.0 mmol); yield: 0.19 g (62%); yellowish solid: mp 123–124 °C; $R_f = 0.27$ (DCM/MeOH, 95:5); δ_H (DMSO-*d*₆, 500 MHz) 2.06 (s, 3H, CH₃), 4.00 (s, 2H, CH₂), 7.27 (d, $J = 5.9$ Hz, 2H), 7.29 (t, $J = 1.9$ Hz,

1H), 7.32–7.38 (m, 3H), 7.52–7.57 (m, 3H), 7.88 (t, $J = 1.9$ Hz, 1H), 8.47 (d, $J = 5.9$ Hz, 2H), 10.01 (s, 1H); MS (ESI): $m/z = 303$ [$M^+ + H$].

4-[(3'-Fluoro-4'-methoxybiphenyl-4-yl)methyl]pyridine (16). Synthesised according to Method B using **16a** (0.43 g, 1.38 mmol); yield: 0.37 g (91%); white solid: mp 98–99 °C; $R_f = 0.46$ (hexane/EtOAc, 1:1); δ_H (CDCl₃, 500 MHz) 3.84 (s, 3H), 3.91 (s, 2H), 6.93 (t, $J = 8.5$ Hz, 1H), 7.05 (d, $J = 6.3$ Hz, 2H), 7.14 (d, $J = 7.9$ Hz, 2H), 7.18–7.26 (m, 1H), 7.21 (s, 1H), 7.39 (d, $J = 7.9$ Hz, 2H), 8.43 (d, $J = 6.3$ Hz, 2H); MS (ESI): $m/z = 294$ [$M^+ + H$].

4-[4-(6-Methoxynaphthalen-2-yl)benzyl]pyridine (24). Synthesised according to Method B using **24a** (0.40 g, 1.18 mmol); yield: 0.34 g (89%); white solid; $R_f = 0.49$ (DCM/MeOH, 95:5); δ_H (CDCl₃, 500 MHz) 3.89 (s, 3H), 4.02 (s, 2H), 7.18 (dd, $J = 2.5, 8.8$ Hz, 1H), 7.29 (d, $J = 6.0$ Hz, 2H), 7.34 (d, $J = 2.5$ Hz, 1H), 7.37 (d, $J = 8.5$ Hz, 2H), 7.73 (d, $J = 8.2$ Hz, 2H), 7.77 (dd, $J = 1.9, 8.5$ Hz, 1H), 7.88 (d, $J = 8.8$ Hz, 2H), 8.11 (d, $J = 1.6$ Hz, 1H), 8.47 (d, $J = 6.0$ Hz, 2H); MS (ESI): $m/z = 326$ [$M^+ + H$].

Method C: Grignard reaction

Under exclusion of air and moisture a 1.0 M RMgBr (1.2 eq) solution in THF was added dropwise to a solution of the aldehyde or ketone (1 eq) in THF (12 mL / mmol). The mixture was stirred over night at rt. Then ethyl acetate (10 mL) and saturated ammonium chloride solution (10 mL) were added and the organic phase was separated. The organic phase was extracted with water and brine, dried over Na₂SO₄, and evaporated under reduced pressure. The crude products were purified by flash chromatography on silica gel.

Method D: Ether cleavage with BBr₃

To a solution of the corresponding ether (1 eq) in DCM (5 mL / mmol) at -78 °C was added 1 M borontribromide in DCM (5 eq). The resulting mixture was stirred at rt for 16 hours. Then water (25 mL) was added and the emulsion was stirred for further 30 minutes. The resulting mixture was extracted with ethyl acetate (3 x 25 mL). The combined organic phases were washed with brine, dried over Na₂SO₄ and evaporated under reduced pressure. Then the desired product was purified by chromatography on silica gel.

4-[(4'-Hydroxybiphenyl-4-yl)methyl]pyridine (4). Synthesised according to Method D using **4a** (0.38 g, 1.37 mmol) and 1 M BBr₃ solution in DCM (6.85 mL, 6.85 mmol); yield: 0.39 g (10%); white solid: mp 224–225 °C; $R_f = 0.24$ (DCM/MeOH, 95:5); δ_H (DMSO-*d*₆, 500 MHz) 3.97 (s, 2H), 6.83 (d, $J = 8.5$ Hz, 2H), 7.25–7.30 (m, 4H), 7.45 (d, $J = 8.5$ Hz, 2H), 7.50 (d, $J = 8.2$ Hz, 2H), 8.46 (d, $J = 5.9$ Hz, 2H), 9.52 (s, 1H); MS (ESI): $m/z = 262$ [$M^+ + H$].

4-[(3'-Hydroxybiphenyl-4-yl)methyl]pyridine (8). Synthesised according to Method D using **8a** (0.17 g, 0.62 mmol) and 1 M BBr₃ solution in DCM (3.10 mL, 3.10 mmol); yield: 0.10 g (62%); white solid: mp 153–154 °C; $R_f = 0.41$ (EtOAc/hexane, 4:1); δ_H (DMSO-*d*₆, 500 MHz) 3.99 (s, 2H), 6.74 (dd, $J = 2.5, 8.2$ Hz, 1H), 6.99 (t, $J = 2.1$ Hz, 1H), 7.04 (d, $J = 7.9$ Hz, 1H), 7.23 (t, $J = 7.9$ Hz, 1H), 7.28 (d, $J = 5.7$ Hz, 2H), 7.31 (d, $J = 8.2$ Hz, 2H), 7.53 (d, $J = 8.2$ Hz, 2H), 8.47 (d, $J = 5.7$ Hz, 2H), 9.50 (s, 1H); MS (ESI): $m/z = 262$ [$M^+ + H$].

4'-(Pyridin-4-ylmethyl)biphenyl-3,4-diol (9). Synthesised according to Method D using **9a** (0.26 g, 0.85 mmol) and 1 M BBr₃ solution in DCM (4.20 mL, 4.20 mmol); yield: 0.22 g (93%); white solid; $R_f = 0.55$ (DCM/MeOH, 10:1); δ_H (DMSO-*d*₆, 500 MHz) 3.97 (s, 2H), 6.79 (d, $J = 8.2$ Hz, 1H), 6.90 (dd, $J = 2.2, 8.2$ Hz, 1H), 7.00 (d, $J = 2.2$ Hz, 1H), 7.22–7.29 (m, 4H), 7.45 (d, $J = 8.2$ Hz, 2H), 8.46 (d, $J = 6.0$ Hz, 2H), 8.98

(s, 1H), 9.02 (s, 1H); MS (ESI): $m/z = 278 [M^+ + H]$.

3-Fluoro-4'-(pyridin-4-ylmethyl)biphenyl-4-ol (10). Synthesised according to Method D using **16** (0.18 g, 0.64 mmol) and 1 M BBr_3 solution in DCM (3.20 mL, 3.20 mmol); yield: 0.12 g (67%); white solid; mp 229–230 °C; $R_f = 0.16$ (DCM/MeOH, 19:1); δ_{H} (DMSO- d_6 , 500 MHz) 3.98 (s, 2H), 7.00 (t, $J = 8.8$ Hz, 1H), 7.25–7.31 (m, 5H), 7.44 (dd, $J = 2.2$ Hz, $^2J_{\text{HF}} = 12.9$ Hz, 1H), 7.55 (d, $J = 8.5$ Hz, 2H), 8.46 (d, $J = 5.9$ Hz, 2H), 9.95 (s, 1H); MS (ESI): $m/z = 280 [M^+ + H]$.

6-[4-(Pyridin-4-ylmethyl)phenyl]naphthalen-2-ol (25). Synthesised according to Method D using **24** (0.33 g, 1.00 mmol) and 1 M BBr_3 solution in DCM (3.00 mL, 3.00 mmol); yield: 0.25 g (80%); white solid; $R_f = 0.49$ (DCM/MeOH, 10:1); δ_{H} (DMSO- d_6 , 500 MHz) 4.00 (s, 2H, CH_2), 7.11 (dd, $J = 2.2, 8.8$ Hz, 1H), 7.14 (d, $J = 2.2$ Hz, 1H), 7.27 (d, $J = 6.0$ Hz, 2H), 7.34 (d, $J = 8.2$ Hz, 2H), 7.68–7.70 (m, 3H), 7.74 (d, $J = 8.8$ Hz, 1H), 7.82 (d, $J = 8.8$ Hz, 1H), 8.04 (s, 1H), 8.46 (d, $J = 6.0$ Hz, 2H), 9.80 (s, 1H); MS (ESI): $m/z = 312 [M^+ + H]$.

Method E: Dehydroxylation with HCOOH

Under exclusion of air and moisture the appropriate alcohol (1 mmol) was dissolved in formic acid (10 mL per mmol), $\text{Pd}(\text{OAc})_2$ (1 mol%) was added and the mixture was heated to reflux for 16 h. After cooling the reaction mixture, formic acid was distilled off and the mixture was neutralised using saturated sodium bicarbonate solution. Then the mixture was extracted with ethyl acetate (3 x 10 mL), the combined organic phases were washed with brine, dried over Na_2SO_4 , evaporated to dryness and purified using column chromatography.

Method F: Hydrogenation

A solution the corresponding alkene (1 mmol) in dry THF (15 mL / mmol) was treated with 10% Pd on charcoal (15 mg). The reaction vessel was repeatedly evacuated and flushed with hydrogen gas and left to stir at room temperature for 3 h, pressurized with 1 bar of H_2 . The resulting reaction mixture was filtered through a short plug of Celite, which was washed with THF (40 mL). The filtrates were concentrated on an oil pump und purified using column chromatography.

Acknowledgements

The authors thank Professor J. Hermans, Cardiovascular Research Institute, University of Maastricht, The Netherlands, for providing us with V79MZh11B1 cells expressing human CYP11B1 and Professor R. Bernhardt, Saarland University, Germany, for making the V79MZh11B2 cells expressing human CYP11B2 available to us.

Supporting Information Available: The synthetic procedures and characterization of compounds **1**, **2**, **3**, **11**, **18**, **19**, **20** and other intermediates as well as HPLC purities, ^{13}C -NMR and IR spectra of other final compounds. This material is available free of charge via the internet at <http://pubs.acs.org>.

References

1. Geller, J. Basis for hormonal management of advanced prostate cancer. *Cancer* **1993**, *71*, 1039–1045.
2. Huhtaniemi, I.; Nikula, H.; Parvinen, M.; Rannikko, S. Histological and functional changes of the testis tissue during GnRH agonist treatment of prostatic cancer. *Am. J. Clin. Oncol.* **1988**, *11*, Suppl. 1, S11–S15.
3. Labrie, F.; Dupont, A.; Belanger, A.; Cusan, L.; Lacourciere, Y.; Monfette, G.; Laberge, J. G.; Emond, J. P.; Fazekas, A. T.; Raynaud, J. P.; Husson, J. M. New hormonal therapy in prostatic carcinoma: combined treatment with LHRH agonist and an

- antiandrogen. *Clin. Invest. Med.* **1982**, *5*, 267–275.
- Hara, T.; Miyazaki, J.; Araki, H.; Yamaoka, M.; Kanzaki, N.; Kusaka, M.; Miyamoto, M. Novel mutations of androgen receptor: a possible mechanism of bicalutamide withdrawal syndrome. *Cancer Res.* **2003**, *63*, 149–153.
 - Zhao, X. Y.; Malloy, P. J.; Krishnan, A. V.; Swami, S.; Navone, N. M.; Peehl, D. M.; Feldman, D. Glucocorticoids can promote androgen-independent growth of prostate cancer cells through a mutated androgen receptor. *Nature Med.* **2000**, *6*, 703–706.
 - Chung, B. C.; Picardo-Leonard, J.; Hanui, M.; Bienkowski, M.; Hall, P. F.; Shively, J. E.; Miller, W. L. Cytochrome P450c17(steroid 17 α -hydroxylase/C17,20-lyase): cloning of human adrenal and testis cDNA indicates the same gene is expressed in both tissues. *Proc. Natl. Acad. Sci. USA.* **1987**, *84*, 407–411.
 - (a) Reed, A. B.; Parekh, D. J. The utility of 5- α reductase inhibitors in the prevention and diagnosis of prostate cancer. *Curr. Opin. Urol.* **2009**, *19*, 238–242. (b) Picard, F.; Schulz, T.; Hartmann, R. W. 5-Phenyl substituted 1-methyl-2-pyridones and 4'-substituted biphenyl-4-carboxylic acids: synthesis and evaluation as inhibitors of steroid-5 α -reductase type 1 and 2. *Bioorg. Med. Chem.* **2002**, *10*, 437–448. (c) Baston, E.; Paluszczak, A.; Hartmann, R. W. 6-Substituted 1H-quinolin-2-ones and 2-methoxy-quinolines: synthesis and evaluation as inhibitors of steroid 5 α reductases types 1 and 2. *Eur. J. Med. Chem.* **2000**, *35*, 931–940.
 - (a) Palmgren, J. S.; Karavadia, S. S.; Wakefield, M. R. Unusual and Underappreciated: Small Cell Carcinoma of the Prostate. *Semin. Oncol.* **2007**, *34*, 22–29. (b) Rajec, J.; Mego, M.; Sycova-mila, Z.; Obertova, J.; Brozmanova, K.; Mardiak, J. Paraneoplastic Cushing's syndrome as the first sign of progression of prostate cancer. *Bratisl lek Listy.* **2008**, *109*, 362–363. (c) Kataoka, K.; Akasaka, Y.; Nakajima, K.; Nagao, K.; Hara, H.; Miura, K.; Ishii, N. Cushing syndrome associated with prostatic tumor adrenocorticotropic hormone (ACTH) expression after maximal androgen blockade therapy. *Int. J. Urol.* **2007**, *14*, 436–439. (d) Hussein, W. I.; Kowalyk, S.; Hoogwerf, B. J. Ectopic adrenocorticotropic hormone syndrome caused by metastatic carcinoma of the prostate: therapeutic response to Ketoconazole. *Endocr. Pract.* **2002**, *8*, 381–384.
 - (a) Lamberts, S. W. J.; Uitterlinden, P.; De Jong, F. H. Rat prostatic weight regression in reaction to ketoconazole, cyproterone acetate, and RU 23908 as adjuncts to a depot formulation of gonadotropin-releasing hormone analog. *Cancer Res.* **1988**, *48*, 6063–6068. (b) Eklund, J.; Kozloff, M.; Vlamakis, J.; Starr, A.; Mariott, M.; Gallot, L.; Jovanovic, B.; Schilder, L.; Robin, E.; Pins, M.; Bergan, R. C. Phase II study of mitoxantrone and ketoconazole for hormone-refractory prostate cancer. *Cancer* **2006**, *106*, 2459–2465.
 - (a) Hartmann, R. W.; Hector, M.; Wachall, B. G.; Paluszczak, A.; Palzer, M.; Huch, V.; Veith, M. Synthesis and evaluation of 17-aliphatic heterocycle-substituted steroidal inhibitors of 17 α -hydroxylase/C₁₇₋₂₀-lyase (P450 17). *J. Med. Chem.* **2000**, *43*, 4437–4445. (b) Njar, V. C. O.; Hector, M.; Hartmann, R. W. 20-Amino and 20, 21-aziridinyl pregnene steroids: development of potent inhibitors of 17 α -hydroxylase/C_{17,20}-lyase (P450 17). *Bioorg. Med. Chem.* **1996**, *4*, 1447–1453. (c) Handratta, V. D.; Vasaitis, T. S.; Njar, V. C. O.; Gediya, L. K.; Kataria, R.; Chopra, P.; Newman, D. Jr.; Farquhar, R.; Guo, Z.; Qiu, Y.; Brodie, A. M. H. Novel C-17-heteroaryl steroidal CYP17 inhibitors/ antiandrogens: Synthesis, in vitro biological activity, pharmacokinetics, and antitumor activity in the LAPC4 human prostate cancer xenograft model. *J. Med. Chem.* **2005**, *48*, 2972–2984.
 - (a) Potter, G. A.; Barrie, S. E.; Jarman, M.; Rowlands, M. G. Novel steroidal inhibitors of human cytochrome P45017, (17 α -hydroxylase-C_{17,20}-lyase): potential agents for the treatment of prostatic cancer. *J. Med. Chem.* **1995**, *38*, 2463–2471. (b) Attard, G.; Reid, A. H. M.; A'Hern, R.; Parker, C.; Oommen, N. B.; Folkard, E.; Messiou, C.; Molife, L. R.; Maier, G.; Thompson, E.; Olmos, D.; Sinha, R.; Lee, G.; Dowsett, M.; Kaye, S. B.; Dearnaley, D.; Kheoh, T.; Molina, A.; de Bono, J. S. Selective inhibition of CYP17 with Abiraterone acetate is highly active in the treatment of castration-resistant prostate cancer. *J. Clin. Oncol.* **2009**, *27*, 3742–3748.
 - (a) Wächter, G. A.; Hartmann, R. W.; Sergejew, T.; Grün, G. L.; Ledergerber, D. Tetrahydronaphthalenes: Influence of heterocyclic substituents on inhibition of steroidogenic enzymes P450 arom and P450 17. *J. Med. Chem.* **1996**, *39*, 834–841. (b) Chan, F. C. Y.; Potter, G. A.; Barrie, S. E.; Haynes, B. P.; Rowlands, M. G.; Houghton, J.; Jarman, M. 3- and 4-pyridylalkyl adamantancarboxylates: inhibitors of human cytochrome P450 17 α (17 α -Hydroxylase/C_{17,20}-Lyase). Potential nonsteroidal agents for the treatment of prostatic cancer. *J. Med. Chem.* **1996**, *39*, 3319–3323.
 - (a) Wachall, B. G.; Hector, M.; Zhuang, Y.; Hartmann, R. W. Imidazole substituted biphenyls: a new class of highly potent and in vivo active inhibitors of P450 17 as potential therapeutics for treatment of prostate cancer. *Bioorg. Med. Chem.* **1999**, *7*, 1913–1924. (b) Leroux, F.; Hutschenreuter, T. U.; Charriere, C.; Scopelliti, R.; Hartmann, R. W. N-(4-biphenylmethyl)imidazoles as potential therapeutics for the treatment of prostate cancer: metabolic robustness due to fluorine substitution? *Helv. Chim. Acta* **2003**, *86*, 2671–2686. (c) Hutschenreuter, T. U.; Ehmer, P. E.; Hartmann, R. W. Synthesis of hydroxy derivatives of highly potent non-steroidal CYP 17 inhibitors as potential metabolites and evaluation of their activity by a non cellular assay using recombinant human enzyme. *J. Enzyme Inhib. Med. Chem.* **2004**, *19*, 17–32. (d) Jagusch, C.; Negri, M.; Hille, U. E.; Hu, Q.; Bartels, M.; Jahn-Hoffmann, K.; Pinto-Bazurco Mendieta, M. A. E.; Rodenwaldt, B.; Müller-Vieira, U.; Schmidt, D.; Lauterbach, T.; Recanatini, M.; Cavalli, A.; Hartmann, R. W. Synthesis, biological evaluation and molecular modeling studies of methyleneimidazole substituted biaryls as inhibitors of human 17 α -hydroxylase-17,20-lyase (CYP17) – Part I: heterocyclic modifications of the core structure. *Bioorg. Med. Chem.* **2008**, *16*, 1992–2010. (e) Hu, Q.; Negri, M.; Jahn-Hoffmann, K.; Zhuang, Y.; Olgen, S.; Bartels, M.; Müller-Vieira, U.; Lauterbach, T.; Hartmann, R. W. Synthesis, biological evaluation, and molecular modeling studies of methylene imidazole substituted biaryls as inhibitors of human 17-hydroxylase-17,20-lyase (CYP17)-Part II: Core rigidification and influence of substituents at the methylene bridge. *Bioorg. Med. Chem.* **2008**, *16*, 7715–7727. (f) Hille, U. E.; Hu, Q.; Vock, C.; Negri, M.; Bartels, M.; Müller-Vieira, U.; Lauterbach, T.; Hartmann, R. W. Novel CYP17 inhibitors: Synthesis, biological evaluation, structure-activity relationships and modeling of methoxy- and hydroxy-substituted methyleneimidazolyl biphenyls. *Eur. J. Med. Chem.* **2009**, *44*, 2765–2775. (g) Hu, Q.; Negri, M.; Olgen, S.; Hartmann, R. W. The role of fluorine substitution in biphenyl methylene imidazole type CYP17 inhibitors for the treatment of prostate carcinoma. *ChemMedChem* **2010**, *5*, 899–910.
 - (a) Hartmann, R. W.; Bayer, H.; Grün, G. Aromatase inhibitors. Syntheses and structure-activity studies of novel pyridyl-substituted indanones, indans, and tetralins. *J. Med. Chem.* **1994**, *37*, 1275–1281. (b) Leonetti, F.; Favia, A.; Rao, A.; Aliano, R.; Paluszczak, A.; Hartmann, R. W.; Carotti, A. Design, synthesis, and 3D QSAR of novel potent and selective aromatase inhibitors. *J. Med. Chem.* **2004**, *47*, 6792–6803. (c) Le Borgne, M.; Marchand, P.; Duflos, M.; Delevoye-Seiller, B.; Piessard-Robert, S.; Le Baut, G.; Hartmann, R. W.; Palzer, M. Synthesis and in vitro evaluation of 3-(1-azolylmethyl)-1H-indoles and 3-(1-azoly1-1-phenylmethyl)-1H-indoles as inhibitors of P450 arom. *Arch. Pharm. (Weinheim, Ger.)* **1997**, *330*, 141–145. (d)

- Gobbi, S.; Cavalli, A.; Rampa, A.; Belluti, F.; Piazzini, L.; Paluszczak, A.; Hartmann, R. W.; Recanatini, M.; Bisi, A. Lead optimization providing a series of flavone derivatives as potent nonsteroidal inhibitors of the cytochrome P450 aromatase enzyme. *J. Med. Chem.* **2006**, *49*, 4777–4780.
15. (a) Lucas, S.; Heim, R.; Ries, C.; Schewe, K. E.; Birk, B.; Hartmann, R. W. In vivo active aldosterone synthase inhibitors with improved selectivity: lead optimization providing a series of pyridine substituted 3,4-dihydro-1H-quinolin-2-one derivatives. *J. Med. Chem.* **2008**, *51*, 8077–8087. (b) Lucas, S.; Heim, R.; Negri, M.; Antes, I.; Ries, C.; Schewe, K. E.; Bisi, A.; Gobbi, S.; Hartmann, R. W. Novel aldosterone synthase inhibitors with extended carbocyclic skeleton by a combined ligand-based and structure-based drug design approach. *J. Med. Chem.* **2008**, *51*, 6138–6149. (c) Ulmschneider, S.; Müller-Vieira, U.; Klein, C. D.; Antes, I.; Lengauer, T.; Hartmann, R. W. Synthesis and evaluation of (pyridylmethylene)tetrahydronaphthalenes/-indanes and structurally modified derivatives: potent and selective inhibitors of aldosterone synthase. *J. Med. Chem.* **2005**, *48*, 1563–1575. (d) Ulmschneider, S.; Müller-Vieira, U.; Mitrenga, M.; Hartmann, R. W.; Oberwinkler-Marchais, S.; Klein, C. D.; Bureik, M.; Bernhardt, R.; Antes, I.; Lengauer, T. Synthesis and evaluation of imidazolylmethylene tetrahydronaphthalenes and imidazolylmethyleneindanes: potent inhibitors of aldosterone synthase. *J. Med. Chem.* **2005**, *48*, 1796–1805.
16. Temple, T. E.; Liddle, G. W. Inhibitors of adrenal steroid biosynthesis. *Annu. Rev. pharmacol.* **1970**, *10*, 199–218.
17. (a) Ehmer, P. B.; Jose, J.; Hartmann, R. W. Development of a simple and rapid assay for the evaluation of inhibitors of human 17 α -hydroxylase-C(17,20)-lyase (P450c17) by coexpression of P450c17 with NADPH-cytochrome-P450-reductase in *Escherichia coli*. *J. Steroid Biochem. Mol. Biol.* **2000**, *75*, 57–63. (b) Denner, K.; Doehmer, J.; Bernhardt, R. Cloning of CYP11B1 and CYP11B2 from normal human adrenal and their functional expression in COS-7 and V79 chinese hamster cells. *Endocr. Res.* **1995**, *21*, 443–448. (c) Ehmer, P. B.; Bureik, M.; Bernhardt, R.; Müller, U.; Hartmann, R. W. Development of a test system for inhibitors of human aldosterone synthase (CYP11B2): Screening in fission yeast and evaluation of selectivity in V79 cells. *J. Steroid Biochem. Mol. Biol.* **2002**, *81*, 173–179. (d) Hartmann, R. W.; Batzl, C. Aromatase inhibitors. Synthesis and evaluation of mammary tumor inhibiting activity of 3-alkylated 3-(4-aminophenyl)piperidine-2,6-diones. *J. Med. Chem.* **1986**, *29*, 1362–1369.
18. (a) White, P. C.; Curnow, K. M.; Pascoe, L. Disorders of steroid 11 β -hydroxylase isozymes. *Endocr. Rev.* **1994**, *15*, 421–38. (b) Vandenput, L.; Ohlsson, C. Estrogens as regulators of bone health in men. *Nat. Rev. Endocrinol.* **2009**, *5*, 437–43. (c) Hill, R. A.; Boon, W. C. Estrogens, brain, and behavior: lessons from knockout mouse models. *Semin. Reprod. Med.* **2009**, *27*, 218–228.
19. Eigen, M. Structures of biomolecules. In *Introduction to molecular biophysics*; Tuszynski, J.; Kurzynski, M., Eds; CRC Press LLC: Boca Raton-London-New York-Washington, D.C., **2003**, pp 52–59.
20. (a) Richard, M.; Zoran, R. Designed multiple ligands. An emerging drug discovery paradigm. *J. Med. Chem.* **2005**, *48*, 6523–6543. (b) Andrea, C.; Laura, B. M.; Anna, M.; Michela, R.; Vincenzo, T.; Maurizio, R.; Carlo, M. Multi-target-directed ligands to combat neurodegenerative diseases. *J. Med. Chem.* **2008**, *51*, 347–372. (c) Marco, R.; Chiara, U. Polysulfated/sulfonated compounds for the development of drugs at the crossroad of viral infection and oncogenesis. *Curr. Pharm. Des.* **2009**, *15*, 2946–2957. (d) Richard, M. Selectively nonselective kinase inhibition: striking the right balance. *J. Med. Chem.* **2010**, *53*, 1413–1437.

3.IV Isopropylidene Substitution Increases Activity and Selectivity of Biphenyl Methylene 4-Pyridine Type CYP17 Inhibitors

Qingzhong Hu, Lina Yin, Carsten Jagusch, Ulrike E. Hille, and Rolf W. Hartmann

This manuscript has been accepted to be published as an article in
Journal of Medicinal Chemistry **2010**, 53, 5049–5053.

Paper IV

Abstract: CYP17 inhibition is a promising therapy for prostate cancer (PC) because proliferation of 80 % of PC depends on androgen stimulation. Introduction of *i*-propylidene substituents onto the linker of biphenyl methylene 4-pyridines resulted in several strong CYP17 inhibitors, which were more potent and selective, regarding CYP 11B1, 11B2, 19 and 3A4, than the drug candidate Abiraterone.

Introduction

Prostate cancer (PC) is the carcinoma with the highest incidence in male, and it accounts for a quarter of cancer related deaths each year. Few patients in early stages can be cured by local therapy, like prostatectomy or radiotherapy, the majority, especially the ones with metastases, are treated with hormone therapy. Due to severe side effects, chemotherapy is usually reserved as the last choice. Hormone therapy is based on the finding that up to 80% of PCs depend on androgen stimulation for proliferation. Early attempts to suppress androgen production by estrogen application were soon replaced by orchidectomy and later by administration of gonadotropin-releasing hormone (GnRH) analogues.¹ GnRH analogues unfold their activity via the hypothalamic, pituitary and gonadal axis resulting in an annihilation of testicular androgen production. However, adrenal androgen formation is not affected. Although approximately 90% of androgens are no longer produced and the plasma testosterone concentration is reduced below 50 ng/dL, androgen levels (testosterone and subsequently dihydrotestosterone, DHT) in the prostate are higher and maintain cancer cell growth.²⁻³ This accumulation is due to the presence of androgen receptor (AR) and steroidogenic enzymes which convert adrenal steroids into testosterone and DHT.³⁻⁴ Hence, AR antagonists (anti-androgens) are employed in combination with GnRH analogues to prevent adrenal androgens from unfolding activity.⁵ This is the current standard therapy, the so called “combined androgen blockade” (CAB). However, long term application of antagonists induce mutations of AR which renders the receptor to be activated by the anti-androgenic drug⁶ or by endogenous glucocorticoids⁷ resulting in resistance to CAB.

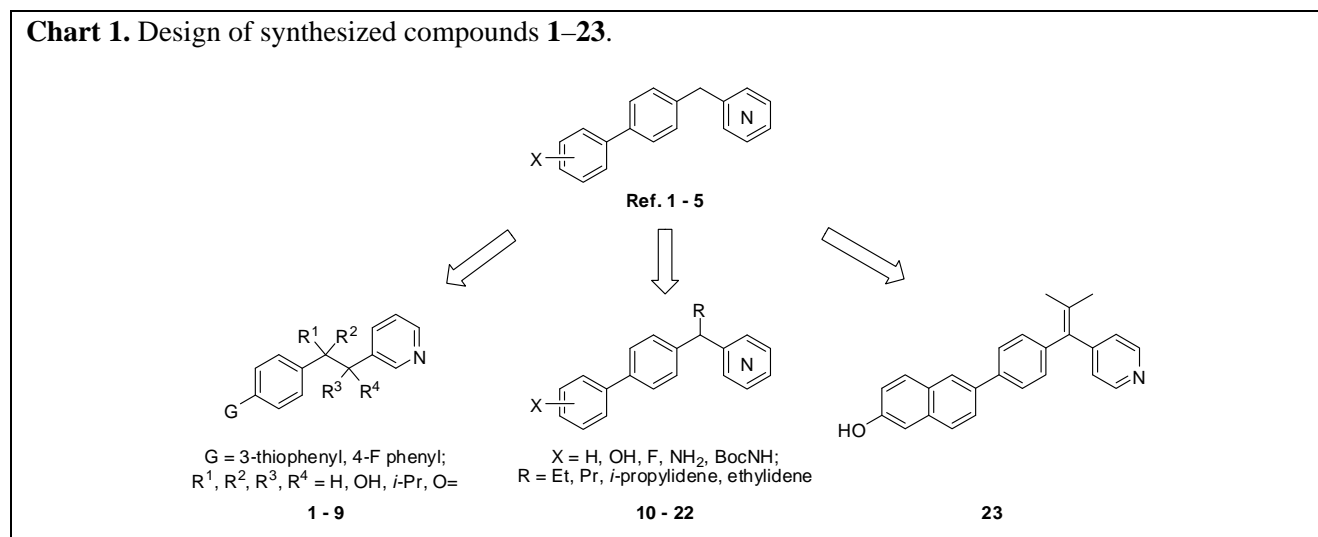
To avoid the stimulation, the inhibition of 17 α -hydroxylase-17,20-lyase (CYP17) was proposed as a superior alternative to CAB. CYP17 catalyzes not only the testicular but also the adrenal conversion of pregnenolone and progesterone to the weak androgens DHEA and androstenedione, respectively. Moreover, recent observations suggest that there is also CYP17 activity in prostate cancer cells.⁶ Testosterone subsequently formed from these two weak androgens is in the prostate converted to DHT, which is the most potent androgen. This final step of androgen activation can be inhibited by 5 α -reductase (5 α R) inhibitors.⁸ However, CYP17 inhibition should be a better strategy than 5 α R inhibition as it totally blocks not only androgen biosynthesis in testes and adrenals, but also intracellular androgen formation in the cancer cell.

The benefit of PC treatment via CYP17 inhibition was shown by the off-label administration of the antimycotic Ketoconazole.⁹ However, Ketoconazole had to be withdrawn because of severe hepatic toxicity resulting from its non-selective inhibition of other CYP enzymes. Nevertheless, as it has been demonstrated by the success of aromatase (CYP19)¹⁰ and more recently aldosterone synthase (CYP11B2) inhibitors,¹¹ high selectivity can be achieved. As for CYP17, Abiraterone¹² is an outstanding example of a potent and selective inhibitor among the steroidal compounds synthesized.¹³ This compound exhibited significant anti-tumour effects in patients diagnosed as “castration resistant” in phase II and III clinical trials.^{12b} However, the potential affinity of steroidal scaffolds for steroid receptors, which often results in side effects no matter acting as agonists or antagonists, prompted the development of non-steroidal CYP17 inhibitors.¹⁴

Our group has designed and synthesized several series of biphenyl methylene heterocycles¹⁵ as CYP17 inhibitors, in which some imidazoles were found to be very potent.^{15a-f} During further optimization, it has been revealed that the replacement of imidazolyl by 4-pyridyl significantly improved potency and selectivity,

whereas 3-pyridyl analogues exhibited similar activity as imidazoles.^{15g} For the imidazoles, we had observed that small alkyl groups, especially ethyl, significantly increase inhibitory potency, while bulkier substituents reduce activity.^{15c} This observation inspired us to perform a thorough study on the influence of the linker between the biphenyl and pyridyl moieties, which is described in this article. Besides freely rotatable alkyl groups, ethylidene and *i*-propylidene, which rigidify the conformation of the whole molecule, were also inserted onto the methylene bridge (compounds **10–22**, Chart 1). Because different interaction angles between sp² hybrid N and heme Fe might account for the disparity in potency between 3- and 4-pyridines, further modifications, such as prolonging the bridge and inserting various substitutions onto the bridge, were performed on the 3-pyridyl scaffold (compounds **1–9**, Chart 1). Furthermore, optimizations of the A-ring by exchanging phenyl to naphthyl or thiophenyl were also casted resulting in, for example, compound **23**. In the following, we also describe the selectivity of selected compounds against CYP11B1, CYP11B2, CYP19 and hepatic CYP enzyme 3A4 to evaluate safety.

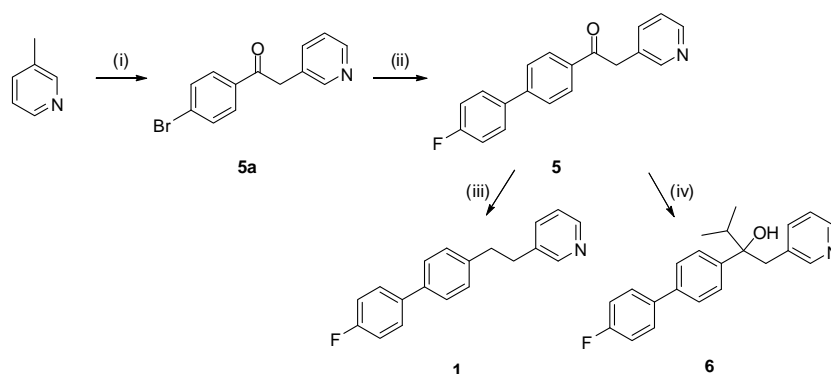
Chart 1. Design of synthesized compounds **1–23**.



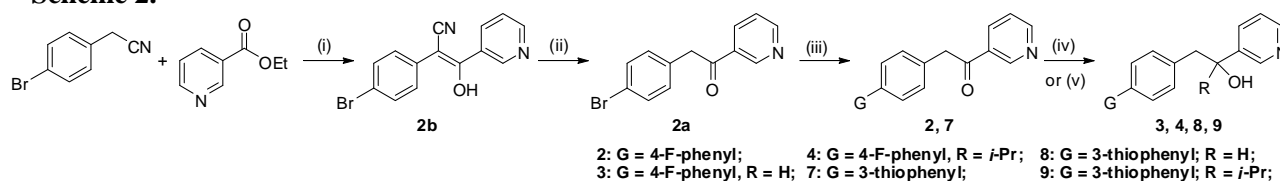
Results and Discussion

Chemistry. The synthetic routes for the preparation of compounds **1–23** are shown in Scheme 1–4. For the syntheses of the compounds with the two-membered linker between the biphenyl and pyridine moieties, the corresponding 4-bromophenyl-pyridin-3-yl ethanones **2a** and **5a** were prepared as building blocks. These bromo compounds were coupled with the corresponding boronic acids via Suzuki coupling to yield the ketones **2**, **5** and **7**, which were then converted to the alcohols **3**, **4**, **6**, **8** and **9** via Grignard reaction or reduced by Wolff-Kishner reduction to give compound **1** (Scheme 1 and 2).

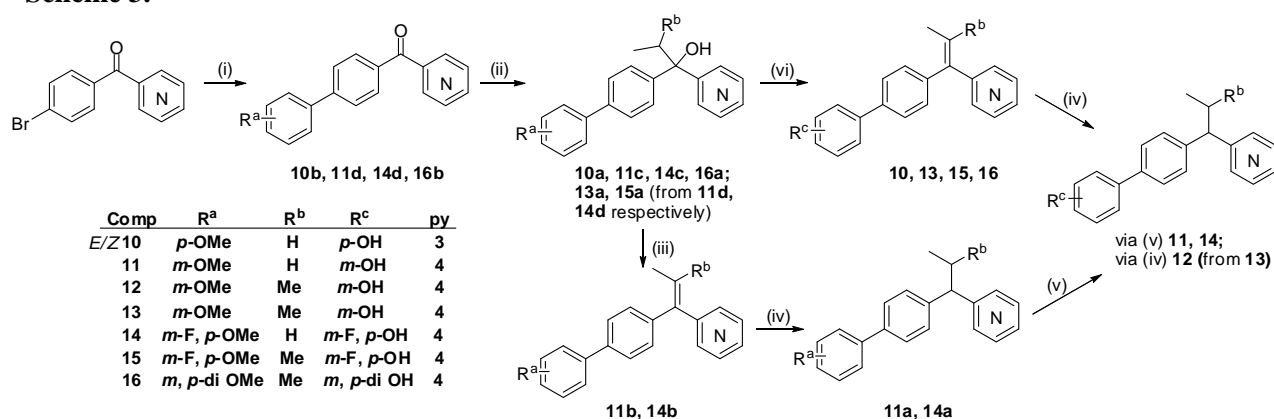
Similarly, the syntheses of the biphenyl methylene pyridines started from (4-bromophenyl)-pyridyl-methanones, which were subjected to Suzuki coupling and Grignard reaction to form the corresponding alcohol intermediates. After elimination of a H₂O molecule under acidic conditions, the alcohols were converted to the enyl pyridines **10**, **13**, **15** and **16**. The hydrogenation of the double bond led to saturated analogues **11**, **12** and **14** (Scheme 3). Subsequently, a more efficient strategy was employed by synthesizing 4-(1-(4-bromophenyl)-2-methylprop-1-enyl)pyridine **17a** as a common building block, followed by introduction of the aryl ring via Suzuki reaction. Via this route, the final compounds **17–23** were conveniently obtained (Scheme 4).

Scheme 1.^a

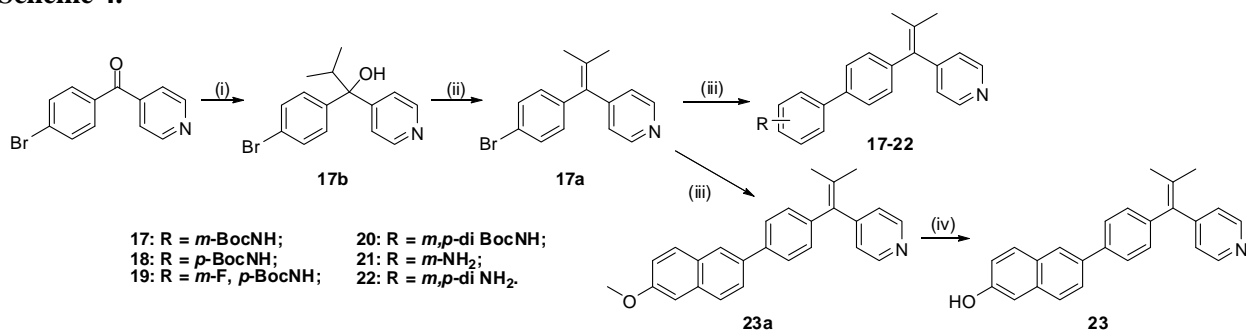
^a Reagents and conditions: (i) 3-picoline, LDA, HMPA, THF, methyl 4-bromobenzoate, rt, 2h. (ii) Method A: Pd(OAc)₂, 4-fluorophenyl boronic acid, TBAB, Na₂CO₃, EtOH, toluene, 110 °C, 4 h. (iii) NaOH, N₂H₄·H₂O, diethyleneglycol, 200 °C, 3h. (iv) Method B: *i*-PrMgCl, THF, room temp, 8h.

Scheme 2.^a

^a Reagents and conditions: (i) Na, EtOH; (ii) HBr, reflux 16h. (iii) Method A: Pd(PPh₃)₄, Na₂CO₃, toluene, reflux 6h. (iv) Method B, for 4, 9: *i*-PrMgBr, THF. (v) Method C, for 3, 8: NaBH₄, MeOH.

Scheme 3.^a

^a Reagents and conditions: Compounds were synthesized from the corresponding a, b, c or d intermediates unless annotated otherwise. (i) Method A: Pd(OAc)₂, corresponding boronic acid, TBAB, EtOH, Na₂CO₃ aq, toluene, 110 °C, 4 h. (ii) Method B: *i*-PrMgCl or EtMgCl, THF, rt, 8h. (iii) Method D: HCOOH, Pd(OAc)₂, reflux, 16h; (iv) Method E: H₂, Pd/C, THF, rt, 3h. (v) Method F: BBr₃, DCM. (vi) Method G: HBr, reflux, 4h.

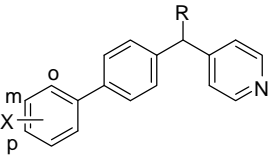
Scheme 4.^a

^a Reagents and conditions: (i) Method B: *i*-PrMgCl, THF, room temp, 8h. (ii) Method G: HBr, reflux, 4h. (iii) Method A: Pd(OAc)₂, corresponding boronic acid, TBAB, EtOH, Na₂CO₃ aq, toluene, 110 °C, 4 h. (iv) Method F: BBr₃, DCM.

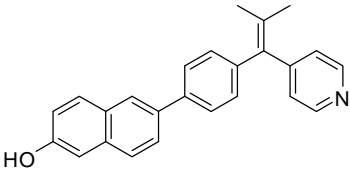
CYP17 inhibitory activity. Inhibition of CYP17 by the synthesized compounds was determined using the

50,000 sediment after homogenation of *E.coli* co-expressing human CYP17 and cytochrome P450 reductase.^{16a} The assay was run with progesterone (25 μ M) as substrate and NADPH as cofactor.^{15a} Separation of substrate and product was accomplished by HPLC using UV detection. IC₅₀ values are presented in comparison to Ketoconazole, Abiraterone and reference compounds **24–28**^{15g} in Table 1. All 3-pyridyl compounds (detailed structures can be found in Scheme 1 and 2) were only weakly active (IC₅₀ > 5000 nM), no matter furnished with a two membered linker (**1–9**) or ethylidene substituted methylene (**10**).

Table 1. Inhibition of CYP17 by compounds **11 – 23** and reference compounds **24 – 28**.



11 - 22, 24 - 28



23

Compd	X	R	IC ₅₀ [nM] ^b
24 ^c	<i>m</i> -OH	H	97
11	<i>m</i> -OH	Et	189
12	<i>m</i> -OH	<i>i</i> -Pr	783
13	<i>m</i> -OH	<i>i</i> -Propylidene	56
25 ^c	<i>m</i> -F, <i>p</i> -OH	H	186
14	<i>m</i> -F, <i>p</i> -OH	Et	343
15	<i>m</i> -F, <i>p</i> -OH	<i>i</i> -Propylidene	75
26 ^c	<i>m</i> , <i>p</i> -di OH	H	52
16	<i>m</i> , <i>p</i> -di OH	<i>i</i> -Propylidene	37
17	<i>m</i> -BocNH	<i>i</i> -Propylidene	1458
18	<i>p</i> -BocNH	<i>i</i> -Propylidene	493
19	<i>m</i> -F, <i>p</i> -BocNH	<i>i</i> -Propylidene	852
20	<i>m</i> , <i>p</i> -di BocNH	<i>i</i> -Propylidene	>10000
27 ^c	<i>m</i> -NH ₂	H	226
21	<i>m</i> -NH ₂	<i>i</i> -Propylidene	38
28 ^c	<i>m</i> , <i>p</i> -di NH ₂	H	337
22	<i>m</i> , <i>p</i> -di NH ₂	<i>i</i> -Propylidene	75
23			62
KTZ ^a			2780
ABT ^a			72

^a **KTZ**: Ketoconazole; **ABT**: Abiraterone.

^b Concentration of inhibitors required to give 50 % inhibition. The given values are mean values of at least three experiments. The deviations were within ± 10 %. The assay was run with human CYP17 expressed in *E.coli* using progesterone as substrate (25 μ M).

^c Reference compounds **24 – 28** were taken from reference 15g.

On the contrary, the 4-pyridyl compounds were potent CYP17 inhibitors and the substituents on the methylene bridge showed profound influence on the inhibitory potency. It is apparent that for the A-ring *m*-OH analogues, the introduction of an ethyl (**11**) and a propyl (**12**) group decreased activities to 189 and 783

nM, respectively, compared to the corresponding non-substituted reference compound **24** ($IC_{50} = 97$ nM). However, the *i*-propylidene substitution increased activity to 56 nM. A similar observation can be made for the A-ring *m*-F, *p*-OH series: the ethyl compound **14** is less potent than the non-substituted reference compound **25** (IC_{50} values of 343 nM vs 186 nM), whereas the *i*-propylidene compound **15** once again was the most active one exhibiting IC_{50} of 75 nM. More examples for the enhancement of inhibitory potency rendered by *i*-propylidene were observed with the remaining couples: the di-OH analogues (reference compound **26** and **16**: IC_{50} values of 52 nM vs 37 nM), the amines (reference compound **27** and **21**: IC_{50} values of 226 nM vs 38 nM) and the di-amino compounds (reference compound **28** and **22**: IC_{50} values of 337 nM vs 75 nM). The change in geometry from sp^3 to sp^2 leading to a planar compound with less conformational flexibility is a plausible explanation for the observed increase in activity. Moreover, the conjugation of the biphenyl moiety and the pyridyl ring facilitated by *i*-propylidene increases the electron density in the hetero-aromat, which might additionally contribute to the enhanced affinity to the enzyme. In our previous studies on biphenyl methylene imidazoles, introduction of an ethyl group into the methylene bridge was found to significantly increase activity.^{15c} The opposite impact of ethyl exhibited with the pyridines presented in this paper compared to those imidazoles is probably due to the longer distance between the sp^2 hybrid N and the methylene group in the pyridines, which might prevent the ethyl group from binding into the hydrophobic pocket.^{15c} Furthermore, Boc-amido was again^{15g} proven to be not tolerated: the corresponding analogues **17–20** showed modest to no inhibition of CYP17 (IC_{50} values ranging from 493 nM to more than 10,000 nM). Besides the introduction of *i*-propylidene, the exchange of the A-ring from phenyl to 6-OH naphthyl also led to a highly potent CYP17 inhibitor, compound **23** ($IC_{50} = 62$ nM).

Selectivity. As a criterion to evaluate safety, the inhibition values of the most potent CYP17 inhibitors – all of them *i*-propylidene compounds – toward CYP11B1, CYP11B2 and CYP19 were determined (Table 2). CYP11B1 and CYP11B2 catalyze the crucial final steps in cortisol and aldosterone biosynthesis, respectively. Inhibition of these enzymes could lead to hyponatremia, hyperkalemia, adrenal hyperplasia and hypovolemic shock.^{17a} CYP19 catalyzes the formation of estrogens, which have been proven to be capable of reducing the incidence of heart disease.^{17b} Furthermore, estrogen deficiency resulting from CYP19 inhibition causes osteoporosis, increased fracture risk and memory loss.^{17c} It can be seen that all the *i*-propylidene analogues tested are much more selective compared to the corresponding non-substituted compounds. For CYP11B1, only weak inhibition (IC_{50} values around 2000 to 3000 nM for compounds **13** and **15**) or no inhibition (IC_{50} values more than 5000 nM for compounds **16**, **21–23**) was observed, which makes these compounds superior to Abiraterone ($IC_{50} = 1610$ nM). A similar selectivity pattern was achieved for CYP11B2: most of the tested compounds did not interfere with this enzyme with IC_{50} values more than 3000 nM (**13**, **21** and **23**). The only exception was compound **15** exhibiting weak inhibition with IC_{50} of 1870 nM, which is comparable to Abiraterone ($IC_{50} = 1750$ nM). Compounds **16** and **22** were less selective with IC_{50} values around 1000 nM. Regarding CYP19, all of the tested compounds **13**, **15**, **16** and **21–23** showed no inhibition with IC_{50} values more than 5000 nM. Furthermore, the inhibition of the hepatic CYP enzyme 3A4 was also determined, because it accounts for most of the drug metabolism and is therefore to a high extent involved in drug-drug interactions. Although compounds **13** and **16** were less selective showing IC_{50} values around 500 to 700 nM, compounds **21** and **22** exhibited only weak inhibition with IC_{50} values around 1500

nM. The most selective compound **15** exhibited almost no inhibition of CYP3A4 with IC₅₀ of more than 17600 nM, which is much better than the drug candidate Abiraterone (IC₅₀ = 2700 nM).

Table 2. Selectivity profiles of selected compounds toward CYP11B1, CYP11B2, CYP19 and CYP3A4.

Compd	IC ₅₀ (nM) ^b			
	CYP11B1 ^c	CYP11B2 ^c	CYP19 ^d	CYP3A4 ^e
24 ^f	342	261	663	538
13	3100	3450	12000	730
25 ^f	351	110	1670	896
15	2000	1870	5750	17650
26 ^f	1400	948	2440	7580
16	37470	974	9500	464
27 ^f	287	921	2830	1520
21	7300	3830	5060	1330
28 ^f	502	368	24560	n.d. ^a
22	7180	1130	49500	1770
23	5060	49500	48700	n.d. ^a
KTZ ^a	127	67	>50000	57
ABT ^a	1610	1750	>50000	2700

^a **KTZ**: Ketoconazole; **ABT**: Abiraterone; n.d.: not determined.

^b Standard deviations were within < ±5 %; All the data are mean values of at least three tests.

^c Hamster fibroblasts expressing human CYP11B1 or CYP11B2 are used with deoxycorticosterone as the substrate at a concentration of 100 nM.

^d Human placental CYP19 is used with androstenedione as the substrate at a concentration of 500 nM.

^e Microsomal fraction of recombinantly expressed enzyme from baculovirus-infected insect is used with 7-benzoyloxy-trifluoro methyl coumarin as the substrate at a concentration of 50 μM.

^f Reference compounds **24** – **28** were taken from reference 15g.

Conclusion

CYP17 inhibition is a promising therapy for prostate cancer because it blocks not only the androgen biosyntheses in testes and adrenals, but also intracellular androgen formation in the cancer cell.³⁻⁴ Biphenyl methylene heterocycles, especially pyridines, have been proven to be potent CYP17 inhibitors.¹⁵ In the present study, modifications of the linker between biphenyl and pyridine moieties were described. Variations on the 3-pyridyl scaffold, such as prolongation of the linker and introduction of different substituents onto the bridge, resulted in only weak inhibitors. On the contrary, modifications of 4-pyridyl analogues led to potent and selective CYP17 inhibitors. The differing substituents on the methylene bridge had a profound influence on the inhibitory potency: flexible alkyl groups reduced activity, whereas conformation rigidifying *i*-propylidene groups significantly improved activity and selectivity. Among the nine *i*-propylidene substituted biphenyl methylene 4-pyridines synthesized, six compounds (**13**, **15**, **16**, **21**, **22** and **23**, IC₅₀ values between 37 and 75 nM) were more potent than or comparable to the drug candidate Abiraterone (IC₅₀ = 72 nM). Most of these potent compounds also exhibited better selectivity profiles toward CYP11B1, CYP11B2, CYP19 and hepatic CYP3A4 than the parent compounds and Abiraterone. Thus, this study presents an example that a single substituent can be the key for selectivity among several CYP enzymes.

Several compounds of this investigation can be considered as promising drug candidates after further validation in vivo.

Experimental Section

General

Melting points were determined on a Mettler FP1 melting point apparatus and are uncorrected. IR spectra were recorded neat on a Bruker Vector 33FT-infrared spectrometer. ¹H-NMR spectra were measured on a Bruker DRX-500 (500 MHz). Chemical shifts are given in parts per million (ppm), and TMS was used as an internal standard. All coupling constants (*J*) are given in Hz. ESI (electrospray ionization) mass spectra were determined on a TSQ quantum (Thermo Electron Corporation) instrument. The purities of the final compounds were controlled by Surveyor®-LC-system. Purities were greater than 95 %. Column chromatography was performed using silica-gel 60 (50-200 μm), and reaction progress was determined by TLC analysis on Alugram® SIL G/UV₂₅₄ (Macherey-Nagel).

Method A: Suzuki-Coupling (see Supporting Information for details)

4'-[2-Methyl-1-(pyridin-4-yl)prop-1-enyl]biphenyl-3-amine (21). Synthesized according to Method A using **17a** (0.50 g, 1.74 mmol) and 3-aminophenylboronic acid (0.36 g, 2.60 mmol); yield: 0.39 g (75 %); white solid; mp 131–132 °C; *R*_f = 0.21 (DCM / MeOH, 20:1); δ_H (CDCl₃, 500 MHz) 1.85 (s, 3H, CH₃), 1.86 (s, 3H, CH₃), 3.73 (s, br, 2H, NH₂), 6.66 (dd, *J* = 2.1, 7.8 Hz, 1H), 6.90 (t, *J* = 2.0 Hz, 1H), 6.98 (dt, *J* = 1.4, 7.9 Hz, 1H), 7.09 (dd, *J* = 1.6, 6.1 Hz, 2H), 7.14 (d, *J* = 8.3 Hz, 2H), 7.21 (t, *J* = 7.8 Hz, 1H), 7.49 (d, *J* = 8.3 Hz, 2H), 8.51 (dd, *J* = 1.6, 6.0 Hz, 2H); MS (ESI): *m/z* = 301 [M⁺+H].

Method B: Grignard reaction (see Supporting Information for details)

1-(4-Bromophenyl)-2-methyl-1-(pyridin-4-yl)propan-1-ol (17b). Synthesized according to Method B using (4-bromophenyl)(pyridin-4-yl)methanone (2.00 g, 7.63 mmol) and 2.0 M *i*-propylmagnesium chloride solution in THF (4.20 mL, 8.39 mmol); yield: 1.35 g (58 %); amble oil; δ_H (CDCl₃, 500 MHz) 0.84 (d, *J* = 6.7 Hz, 3H, CH₃), 0.88 (d, *J* = 6.7 Hz, 3H, CH₃), 2.79 (q, *J* = 6.7 Hz, 1H, CH), 3.25 (s, br, 1H, OH), 7.36–7.42 (m, 6H), 8.41 (d, *J* = 6.1 Hz, 2H); MS (ESI): *m/z* = 307 [M⁺+H].

Method C: Reduction with NaBH₄ (see Supporting Information for details)

Method D: Dehydroxylation with HCOOH (see Supporting Information for details)

Method E: Hydrogenation (see Supporting Information for details)

Method F: Ether cleavage with BBr₃ (see Supporting Information for details)

6-[4-(2-Methyl-1-pyridin-4-yl-propenyl)-phenyl]-naphthalen-2-ol (23). Synthesized according to Method F using **23a** (0.25 g, 0.68 mmol) and 1M BBr₃ in DCM (2.05 mL, 2.05 mmol); yield: 0.18 g (73 %); yellow oil; *R*_f = 0.52 (DCM / MeOH, 19:1); δ_H (DMSO-*d*₆, 500 MHz) 1.98 (s, 3H, CH₃), 2.02 (s, 3H, CH₃), 7.19 (d, *J* = 8.2 Hz, 2H), 7.31 (d, *J* = 8.5 Hz, 1H), 7.65 (d, *J* = 6.4 Hz, 2H), 7.72 (d, *J* = 8.2 Hz, 2H), 7.72 (d, *J* = 8.5 Hz, 2H), 7.83 (dd, *J* = 1.8, 8.5 Hz, 1H), 8.00 (d, *J* = 1.8 Hz, 1H), 8.14 (d, *J* = 8.5 Hz, 1H), 8.60 (d, *J* = 6.4 Hz, 2H); MS (ESI): *m/z* = 352 [M⁺+H].

Method G: Dehydroxylation and ether cleavage with HBr (see Supporting Information for details)

4-[1-(4-Bromophenyl)-2-methylprop-1-enyl]pyridine (17a). Synthesized according to Method G using **17b** (1.00 g, 3.27 mmol); yield: 0.89 g (95 %); white solid; *R*_f = 0.21 (DCM / MeOH, 10:1); δ_H (CDCl₃, 500

MHz) 1.85 (s, 3H, CH₃), 1.86 (s, 3H, CH₃), 7.09 (dd, *J* = 1.6, 6.1 Hz, 2H), 7.14 (d, *J* = 8.3 Hz, 2H), 7.49 (d, *J* = 8.3 Hz, 2H), 8.51 (dd, *J* = 1.6, 6.0 Hz, 2H); MS (ESI): *m/z* = 289 [M⁺+H].

Acknowledgements

The authors thank Professor J. Hermans (Cardiovascular Research Institute, University of Maastricht, The Netherlands) and Professor R. Bernhardt (Saarland University, Germany) for providing us with V79MZh11B1 and V79MZh11B2 cells respectively.

Supporting Information Available: The synthetic procedures, characterization and HPLC purities of the rest intermediates and final compounds, as well as the biological assays for CYP17, CYP11B1, CYP11B2, CYP19 and CYP3A4. This material is available free of charge via the internet at <http://pubs.acs.org>.

References

1. Huhtaniemi, I.; Nikula, H.; Parvinen, M.; Rannikko, S. Histological and functional changes of the testis tissue during GnRH agonist treatment of prostatic cancer. *Am. J. Clin. Oncol.* **1988**, *11*, S11–S15.
2. Titus, M. A.; Schell, M. J.; Lih, F. B.; Tomer, K. B.; Mohler, J. L. Testosterone and dihydrotestosterone tissue levels in recurrent prostate cancer. *Clin. Cancer Res.* **2005**, *11*, 4653–4657.
3. Stanbrough, M.; Bubley, G. J.; Ross, K.; Golub, T. R.; Rubin, M. A.; Penning, T. M.; Febbo, P. G.; Balk, S. P. Increased expression of genes converting adrenal androgens to testosterone in androgen-independent prostate cancer. *Cancer Res.* **2006**, *66*, 2815–2825.
4. (a) Montgomery, R. B.; Mostaghel, E. A.; Vessella, R.; Hess, D. L.; Kalhorn, T. F.; Higano, C. S.; True, L. D.; Nelson, P. S. Maintenance of intratumoral androgens in metastatic prostate cancer: A mechanism for castration-resistant tumor growth. *Cancer Res.* **2008**, *68*, 4447–4454. (b) Holzbeierlein, J.; Lal, P.; La Tulippe, E.; Smith, A.; Satagopan, J.; Zhang, L.; Ryan, C.; Smith, S.; Scher, H.; Scardino, P.; Reuter, V.; Gerald, W. L. Gene expression analysis of human prostate carcinoma during hormonal therapy identifies androgen-responsive genes and mechanisms of therapy resistance. *Am. J. Pathol.* **2004**, *164*, 217–227.
5. Labrie, F.; Dupont, A.; Belanger, A.; Cusan, L.; Lacourciere, Y.; Monfette, G.; Laberge, J. G.; Emond, J. P.; Fazekas, A. T.; Raynaud, J. P.; Husson, J. M. New hormonal therapy in prostatic carcinoma: combined treatment with LHRH agonist and an antiandrogen. *Clin. Invest. Med.* **1982**, *5*, 267–275.
6. Hara, T.; Miyazaki, J.; Araki, H.; Yamaoka, M.; Kanzaki, N.; Kusaka, M.; Miyamoto, M. Novel mutations of androgen receptor: a possible mechanism of bicalutamide withdrawal syndrome. *Cancer Res.* **2003**, *63*, 149–153.
7. Zhao, X. Y.; Malloy, P. J.; Krishnan, A. V.; Swami, S.; Navone, N. M.; Peehl, D. M.; Feldman, D. Glucocorticoids can promote androgen-independent growth of prostate cancer cells through a mutated androgen receptor. *Nature Med. (N. Y., NY, U. S.)* **2000**, *6*, 703–706.
8. (a) Reed, A. B.; Parekh, D. J. The utility of 5- α reductase inhibitors in the prevention and diagnosis of prostate cancer. *Curr. Opin. Urol.* **2009**, *19*, 238–242. (b) Picard, F.; Schulz, T.; Hartmann, R. W. 5-Phenyl substituted 1-methyl-2-pyridones and 4'-substituted biphenyl-4-carboxylic acids: synthesis and evaluation as inhibitors of steroid-5 α -reductase type 1 and 2. *Bioorg. Med. Chem.* **2002**, *10*, 437–448. (c) Baston, E.; Paluszczak, A.; Hartmann, R. W. 6-Substituted 1H-quinolin-2-ones and 2-methoxy-quinolines: synthesis and evaluation as inhibitors of steroid 5 α reductases types 1 and 2. *Eur. J. Med. Chem.* **2000**, *35*, 931–940.
9. Harris, K. A.; Weinberg, V.; Bok, R. A.; Kakefuda, M.; Small, E. J. Low dose ketoconazole with replacement doses of hydrocortisone in patients with progressive androgen independent prostate cancer. *J. Urol.* **2002**, *168*, 542–545.
10. (a) Leonetti, F.; Favia, A.; Rao, A.; Aliano, R.; Paluszczak, A.; Hartmann, R. W.; Carotti, A. Design, synthesis, and 3D QSAR of novel potent and selective aromatase inhibitors. *J. Med. Chem.* **2004**, *47*, 6792–6803. (b) Le Borgne, M.; Marchand, P.; Duflos, M.; Delevoye-Seiller, B.; Piessard-Robert, S.; Le Baut, G.; Hartmann, R. W.; Palzer, M. Synthesis and in vitro evaluation of 3-(1-Azolylmethyl)-1H-indoles and 3-(1-azoly1-1-phenylmethyl)-1H-indoles as inhibitors of P450 arom. *Arch. Pharm. (Weinheim, Ger.)* **1997**, *330*, 141–145. (c) Gobbi, S.; Cavalli, A.; Rampa, A.; Belluti, F.; Piazzzi, L.; Paluszczak, A.; Hartmann, R. W.; Recanatini, M.; Bisi, A. Lead optimization providing a series of flavone derivatives as potent nonsteroidal inhibitors of the cytochrome P450 aromatase enzyme. *J. Med. Chem.* **2006**, *49*, 4777–4780. (d) Castellano, S.; Stefancich, G.; Ragno, R.; Schewe, K.; Santoriello, M.; Caroli, A.; Hartmann, R. W.; Sbardella, G. CYP19 (aromatase): exploring the scaffold flexibility for novel selective inhibitors. *Bioorg. Med. Chem.* **2008**, *16*, 8349–8358.
11. (a) Lucas, S.; Heim, R.; Ries, C.; Schewe, K. E.; Birk, B.; Hartmann, R. W. In vivo active aldosterone synthase inhibitors with improved selectivity: lead optimization providing a series of pyridine substituted 3,4-dihydro-1H-quinolin-2-one derivatives. *J. Med. Chem.* **2008**, *51*, 8077–8087. (b) Lucas, S.; Heim, R.; Negri, M.; Antes, I.; Ries, C.; Schewe, K. E.; Bisi, A.; Gobbi, S.; Hartmann, R. W. Novel aldosterone synthase inhibitors with extended carbocyclic skeleton by a combined ligand-based and structure-based drug design approach. *J. Med. Chem.* **2008**, *51*, 6138–6149. (c) Heim, R.; Lucas, S.; Grombein, C. M.; Ries, C.; Schewe, K. E.; Negri, M.; Müller-Vieira, U.; Birk, B.; Hartmann, R. W. Overcoming undesirable CYP1A2 inhibition of pyridynaphthalene-type aldosterone synthase inhibitors: influence of heteroaryl derivatization on potency and selectivity. *J. Med. Chem.* **2008**, *51*, 5064–5074. (d) Ulmschneider, S.; Müller-Vieira, U.; Klein, C. D.; Antes, I.; Lengauer, T.; Hartmann, R. W. Synthesis and evaluation of (pyridylmethylene) tetrahydronaphthalenes/-indanes and structurally modified derivatives: potent and selective inhibitors of aldosterone synthase. *J. Med. Chem.* **2005**, *48*, 1563–1575. (e) Ulmschneider, S.; Müller-Vieira, U.; Mitrenga, M.; Hartmann, R. W.; Oberwinkler-Marchais, S.; Klein, C. D.; Bureik, M.; Bernhardt, R.; Antes, I.

- Lengauer, T. Synthesis and evaluation of imidazolylmethylene tetrahydronaphthalenes and imidazolylmethylene indanes: potent inhibitors of aldosterone synthase. *J. Med. Chem.* **2005**, *48*, 1796–1805.
12. (a) Potter, G. A.; Barrie, S. E.; Jarman, M.; Rowlands, M. G. Novel steroidal inhibitors of human cytochrome P45017, (17 α -hydroxylase-C_{17,20}-lyase): potential agents for the treatment of prostatic cancer. *J. Med. Chem.* **1995**, *38*, 2463–2471. (b) Attard, G.; Reid, A. H. M.; Yap, T. A.; Raynaud, F.; Dowsett, M.; Settatee, S.; Barrett, M.; Parker, C.; Martins, V.; Folkard, E.; Clark, J.; Cooper, C. S.; Kaye, S. B.; Dearnaley, D.; Lee, G.; de Bono, J. S. Phase I clinical trial of a selective inhibitor of CYP17, Abiraterone acetate, confirms that castration-resistant prostate cancer commonly remains hormone driven. *J. Clin. Oncol.* **2008**, *26*, 4563–4571.
13. (a) Hartmann, R. W.; Hector, M.; Haidar, M.; Ehmer, P. B.; Reichert, W.; Jose, J. Synthesis and evaluation of novel steroidal oxime inhibitors of P450 17 (17 α -hydroxylase/C_{17,20}-lyase) and 5 α -reductase types 1 and 2. *J. Med. Chem.* **2000**, *43*, 4266–4277. (b) Njar, V. C. O.; Kato, K.; Nnane, I. P.; Grigoryev, D. N.; Long, B. J.; Brodie, A. M. H. Novel 17-azoly steroids, potent inhibitors of human cytochrome 17 α -hydroxylase-C_{17,20}-lyase (P450 17 α): Potential agents for the treatment of prostate cancer. *J. Med. Chem.* **1998**, *41*, 902–912.
14. Wächter, G. A.; Hartmann, R. W.; Sergejew, T.; Grün, G. L.; Ledergerber, D. Tetrahydronaphthalenes: Influence of heterocyclic substituents on inhibition of steroidogenic enzymes P450 arom and P450 17. *J. Med. Chem.* **1996**, *39*, 834–841.
15. (a) Hutschenreuter, T. U.; Ehmer, P. E.; Hartmann, R. W. Synthesis of hydroxy derivatives of highly potent non-steroidal CYP 17 inhibitors as potential metabolites and evaluation of their activity by a non cellular assay using recombinant human enzyme. *J. Enzyme Inhibit. Med. Chem.* **2004**, *19*, 17–32. (b) Jagusch, C.; Negri, M.; Hille, U. E.; Hu, Q.; Bartels, M.; Jahn-Hoffmann, K.; Pinto-Bazurco Mendieta, M. A. E.; Rodenwaldt, B.; Müller-Vieira, U.; Schmidt, D.; Lauterbach, T.; Recanatini, M.; Cavalli, A.; Hartmann, R. W. Synthesis, biological evaluation and molecular modeling studies of methyleneimidazole substituted biaryls as inhibitors of human 17 α -hydroxylase-17,20-lyase (CYP17) – Part I: heterocyclic modifications of the core structure. *Bioorg. Med. Chem.* **2008**, *16*, 1992–2010. (c) Hu, Q.; Negri, M.; Jahn-Hoffmann, K.; Zhuang, Y.; Olgen, S.; Bartels, M.; Müller-Vieira, U.; Lauterbach, T.; Hartmann, R. W. Synthesis, biological evaluation, and molecular modeling studies of methyleneimidazole substituted biaryls as inhibitors of human 17 α -hydroxylase-17,20-lyase (CYP17)-Part II: Core rigidification and influence of substituents at the methylene bridge. *Bioorg. Med. Chem.* **2008**, *16*, 7715–7727. (d) Leroux, F.; Hutschenreuter, T. U.; Charriere, C.; Scopelliti, R.; Hartmann, R. W. N-(4-biphenylmethyl)imidazoles as potential therapeutics for the treatment of prostate cancer: metabolic robustness due to fluorine substitution? *Helv. Chim. Acta* **2003**, *86*, 2671–2686. (e) Hille, U. E.; Hu, Q.; Vock, C.; Negri, M.; Bartels, M.; Müller-Vieira, U.; Lauterbach, T.; Hartmann, R. W. Novel CYP17 inhibitors: Synthesis, biological evaluation, structure-activity relationships and modeling of methoxy- and hydroxy-substituted methyleneimidazolyl biphenyls. *Eur. J. Med. Chem.* **2009**, *44*, 2765–2775. (f) Hu, Q.; Negri, M.; Olgen, S.; Hartmann, R. W. The role of fluorine substitution in biphenyl methylene imidazole type CYP17 inhibitors for the treatment of prostate carcinoma. *ChemMedChem.* **2010**, *5*, 899–910. (g) Hu, Q.; Jagusch, C.; Hille, U. E.; Hauptenthal, J.; Hartmann, R. W. Replacement of imidazolyl by pyridyl in biphenyl methylenes results in selective CYP17 and dual CYP17 / CYP11B1 inhibitors for the treatment of prostate cancer. *J. Med. Chem.* 2010, In Press.
16. (a) Ehmer, P. B.; Jose, J.; Hartmann, R. W. Development of a simple and rapid assay for the evaluation of inhibitors of human 17 α -hydroxylase-C(17,20)-lyase (P450c17) by coexpression of P450c17 with NADPH-cytochrome-P450-reductase in *Escherichia coli*. *J. Steroid Biochem. Mol. Biol.* **2000**, *75*, 57–63. (b) Denner, K.; Doehmer, J.; Bernhardt, R. Cloning of CYP11B1 and CYP11B2 from normal human adrenal and their functional expression in COS-7 and V79 chinese hamster cells. *Endocr. Res.* **1995**, *21*, 443–448. (c) Ehmer, P. B.; Bureik, M.; Bernhardt, R.; Müller, U.; Hartmann, R. W. Development of a test system for inhibitors of human aldosterone synthase (CYP11B2): Screening in fission yeast and evaluation of selectivity in V79 cells. *J. Steroid Biochem. Mol. Biol.* **2002**, *81*, 173–179. (d) Hartmann, R. W.; Batzl, C. Aromatase inhibitors. Synthesis and evaluation of mammary tumor inhibiting activity of 3-alkylated 3-(4-aminophenyl)piperidine-2,6-diones. *J. Med. Chem.* **1986**, *29*, 1362–1369.
17. (a) White, P. C.; Curnow, K. M.; Pascoe, L. Disorders of steroid 11 β -hydroxylase isozymes. *Endocr. Rev.* **1994**, *15*, 421–38. (b) Booth, E. A.; Marchesi, M.; Kilbourne, E. J.; Lucchesi, B. R. 17 β -estradiol as a receptor-mediated cardioprotective agent. *J. Pharmacol. Exp. Ther.* **2003**, *307*, 395–401. (c) Vandenput, L.; Ohlsson, C. Estrogens as regulators of bone health in men. *Nat. Rev. Endocrinol.* **2009**, *5*, 437–43.

3.V Selective Dual Inhibitors of CYP19 and CYP11B2: Targeting Cardiovascular Diseases Hiding in the Shadow of Breast Cancer

Qingzhong Hu, Lina Yin, and Rolf W. Hartmann

This manuscript will be submitted to
Journal of Medicinal Chemistry

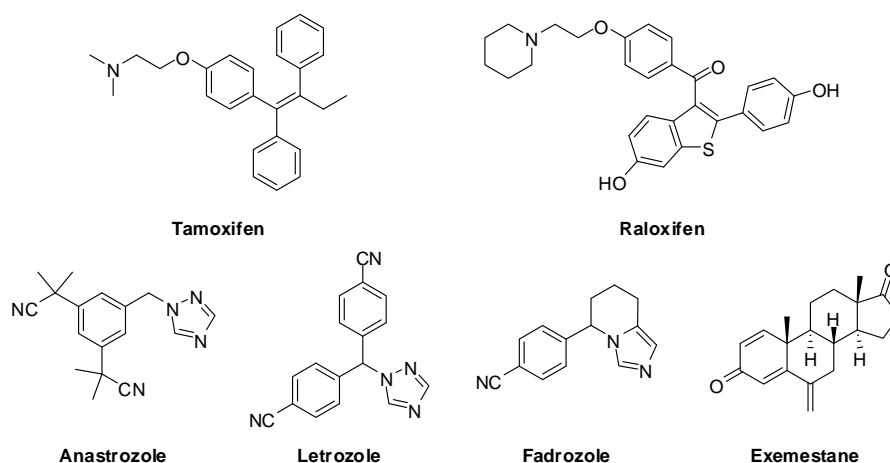
Paper V

Abstract: It is well known that postmenopausal women are in high risk of cardiovascular diseases because of the estrogen deficiency. As for the postmenopausal breast cancer patients, this risk is much higher due to inhibition of estrogen biosyntheses in peripheral tissue by aromatase inhibitors applied. Since deficiency of estrogen results in significantly elevated aldosterone level, which is a major cause of cardiovascular diseases, dual inhibition of CYP19 and CYP11B2 is a promising treatment for breast cancer and the coinstantaneous cardiovascular diseases. By combination of important structural features of CYP19 and CYP11B2 inhibitors, selective dual inhibitors were successfully obtained as compounds **9** and **11** with IC_{50} values around 50 and 20 nM toward CYP19 and CYP11B2, respectively. These compounds also showed good selectivity against CYP11B1 with selectivity factors around 50 and no interference with CYP17. Moreover, due to the different influence on SAR toward different enzymes by the optimization, selective CYP11B2 inhibitors (**1–6** and **16**) were achieved as well, with IC_{50} values less than 10 nM, selectivity factors ($IC_{50\text{ CYP11B1}} / IC_{50\text{ CYP11B2}}$) arranged from 50 to 170 over CYP11B1 and no inhibition of CYP19 and CYP17. Another compound **13** turned out to be a selective CYP19 inhibitor with IC_{50} value of 22 nM and selectivity factors more than 35 for the other enzymes.

Introduction

Breast cancer (BC) is the carcinoma with the highest morbidity in female in western countries. Although BC is still the second leading cause of death, the mortality is significantly reduced because of the cancer screening to identify cases in early stages¹ and, more importantly, the employment of adjuvant endocrine therapy. Endocrine therapy is based on the fact that estrogen stimulates the growth of “hormone sensitive” breast cancer, in which estrogen receptor (ER) and / or progesterone receptor (PgR) are expressed.² Therefore, deprivation of estrogen is a feasible treatment for the hormone sensitive BC, which accounts for more than 60 % of all cases. Several decades ago, selective estrogen receptor modulators (SERM),³ such as Tamoxifen and Raloxifen (Chart 1), were introduced into the clinic. These SERMs competitively bind to ER antagonizing transcription and subsequently mitogenic effects. However, the poor risk / benefit profiles prevented Tamoxifen from continuous application of more than five years and severe toxicities such as endometrial cancer and thrombosis were observed.⁴ On the contrary, the third generation aromatase inhibitors (AI), for example: Anastrozole, Letrozole and Exemestane (Chart 1), exhibited better efficacy and tolerability compared to Tamoxifen, which rendered AIs to become the first choice as first-line and adjuvant therapy for postmenopausal women — the majority of breast cancer patients. Aromatase (CYP19) is the crucial enzyme catalyzing the final aromatization of steroidal A-ring in the biosynthesis of estrogen from corresponding androgen precursors: testosterone and androstenedione. Inhibition of CYP19 can totally block estrogen production and consequently prevent BC cells from proliferation. After the administration of the third generation AIs, the plasma estrogen concentration can even be reduced to undetectable level.⁵ Several clinic trials demonstrated AIs as adjuvant therapy significantly improved disease-free survival and relapse-free survival with the overall survival increased accordingly.⁶

Chart 1. Structures of selective estrogen receptor modulators: Tamoxifen and Raloxifen; and aromatase inhibitors: Anastrozole, Letrozole, Fadrozole and Exemestane.



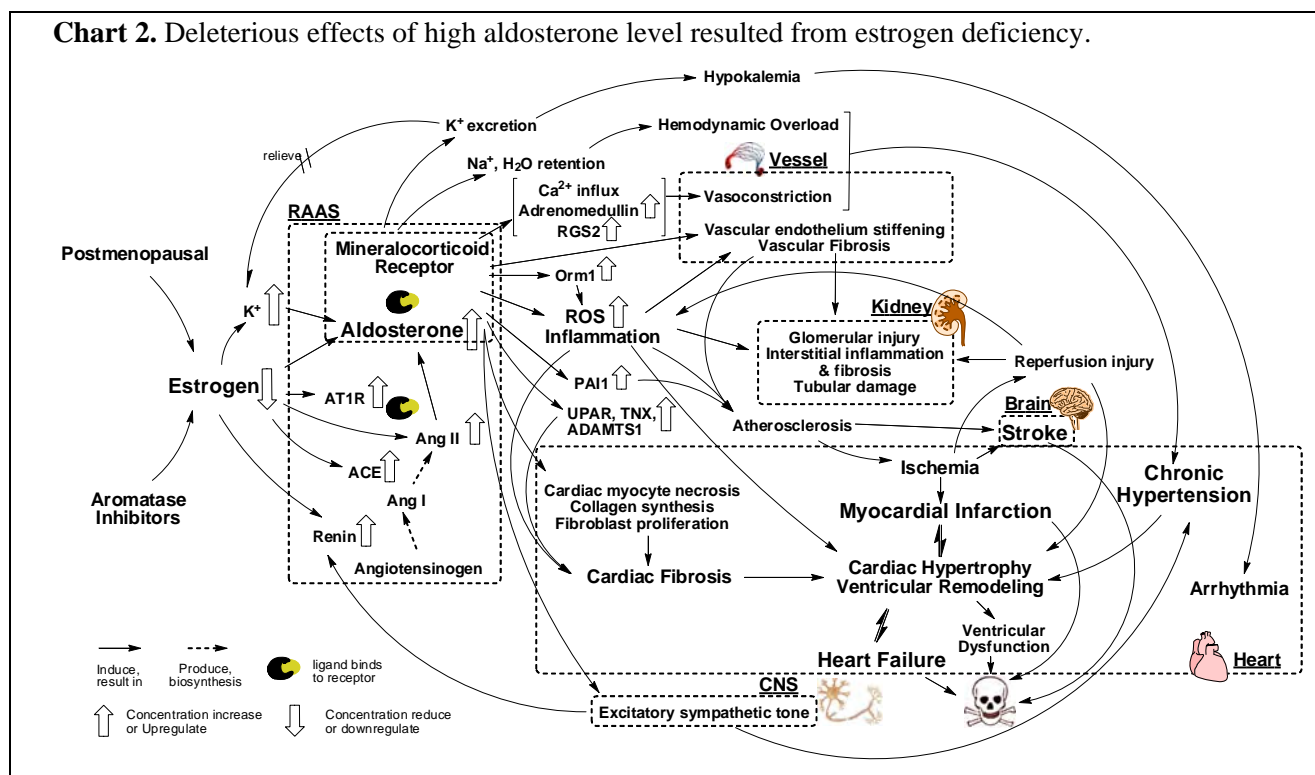
However, it has been unveiled that only around 40% of the BC patients' deaths are eventually caused by BC.⁷ A lot of people survived BC but died of other diseases, especially cardiovascular diseases (CVD).⁷ Therefore it is necessary and urgent to manage CVD to prolong longevity of BC patients and to improve the overall survival.

Recently, estrogen has been proven to exhibit some protective effects on heart⁸ and kidney.⁹ The administration of estrogen prevents the development of heart failure post-myocardial infarction^{8e} and attenuates ventricular hypertrophy and remodelling.^{8f-g} Moreover, the incidences of CVD in post-menopause women triple those of premenopausal women at the same age,¹⁰ which indicates the deficiency of estrogen is closely correlated with CVD. Regarding post-menopause BC patients under endocrine therapy, AIs further decrease the estrogen production leading to even higher risk of CVD. The ischemic side effects observed in AIs clinic trials were considered as results of lipid metabolism dysfunction caused by estrogen deficiency.¹¹ This disturbance of lipid metabolism by AIs has been noticed and can be managed with antihyperlipidemic agents.^{11e-f} However, the up-regulation of renin-angiotensin-aldosterone system (RAAS), especially aldosterone, was still neglected. It has been established that the depletion of estrogen not only directly increases circulating aldosterone level, but also augments the concentrations of other RAAS components (Chart 2). Elevated levels of renin, angiotensin II (Ang II), angiotensin converting enzyme (ACE) and angiotensin type 1 receptor (AT1R) further stimulate aldosterone biosynthesis.¹³ Moreover, estrogen deficiency also increases the potassium plasma concentration resulting in the promotion of aldosterone secretion.¹⁴

The resulted high aldosterone levels exhibit deleterious effects on kidney, vessels, brain and the severest on heart (Chart 2).^{15a} After excessive aldosterone binds to mineralocorticoid receptor (MR) in renal collecting ducts, sodium and water are retained leading to the increase of blood volume and subsequently chronic hypertension.^{15b-c} This pathological process is accompanied with hypokalemia due to the over-excretion of potassium, which sometimes leads to arrhythmia.^{15d} Moreover, aldosterone increases intracellular calcium concentration of vascular smooth muscle cells^{15e-f} and up-regulates the expression of adrenomedullin and regulator of G protein signaling-2 (RGS2)^{15g} leading to vasoconstriction. The persisting tension of vascular together with the excitatory sympathetic tone irritated by excessive aldosterone^{15h} exacerbates chronic hypertension. Another deleterious effect that aldosterone exhibits on vessels is the induction of vascular fibrosis and vascular endothelium stiffening,¹⁵ⁱ which is mediated by reactive oxygen species (ROS)^{15j} and inflammation.^{15k-n} The resulted atherosclerosis^{15o} is a high risk factor for stroke and ischemia related myocardial infarction (MI) that lead to disability and death. The subsequent reperfusion after ischemia can further stimulate inflammation, and together with renal vascular fibrosis lead to glomerular injury, tubular damage and interstitial fibrosis.^{15p-q} Furthermore, excessive aldosterone causes cardiac myocyte necrosis, collagen synthesis and fibroblast proliferation resulting in cardiac fibrosis and increase of myocardial stiffness.^{15r-t} During these pathological processes, some genes closely related to cardiac fibrosis, such as tenascin-X (TNX), urokinase plasminogen activator receptor (UPAR) and a disintegrin and metalloprotease with thrombospondin motifs (ADAMTS1), are also over-expressed within the induction of aldosterone.^{15g} Subsequently, cardiac hypertrophy and ventricular remodelling happen as further structural deterioration with functional degradation.^{15u} Some more factors as consequences of high aldosterone levels are also involved in ventricular remodelling, such as ROS, inflammation, chronic hypertension, reperfusion injury and MI.^{15v-x} The ventricular remodeling causes diastolic dysfunction, diminishes contractile capability, reduces stroke volume and ultimately results in heart failure, which often leads to sudden death.

Therefore, reducing the high plasma aldosterone concentration rendered by estrogen deficiency is an effective treatment for the cardiovascular diseases in BC patients. Because aldosterone synthase (CYP11B2) catalyzing the conversion of 11-deoxycorticosterone to aldosterone is the key enzyme in aldosterone biosynthesis, the inhibition of CYP11B2 is a superior means to reduce aldosterone level. Since AIs as adjuvant therapy have to be applied for at least 5 years and there are no selective CYP11B2 inhibitors in clinic use, it is necessary to design selective dual inhibitors of CYP19 and CYP 11B2. This kind of multi-target-directed agents^{16,17} can not only improve the patient compliance, but also avoid possible drug-drug interaction. In this study, after integration of CYP19 inhibitors' important structural features into CYP11B2 inhibitors, a series of pyridyl dihydroquinolinone derivatives were designed and synthesized leading to compounds 1–19. The inhibition of these compounds toward CYP11B2 and CYP19 are presented with Fadrozole (Chart 1) as a reference, which is a potent CYP19 inhibitor showing unselective inhibition toward 11 β -hydroxylase (CYP11B1) and CYP11B2. Furthermore, the selectivity of these compounds against CYP11B1 and 17 α -hydroxylase-17,20-lyase (CYP17), which are the crucial enzymes in the biosynthesis of glucocorticoid and androgen respectively, are also determined as safety criteria.

Chart 2. Deleterious effects of high aldosterone level resulted from estrogen deficiency.

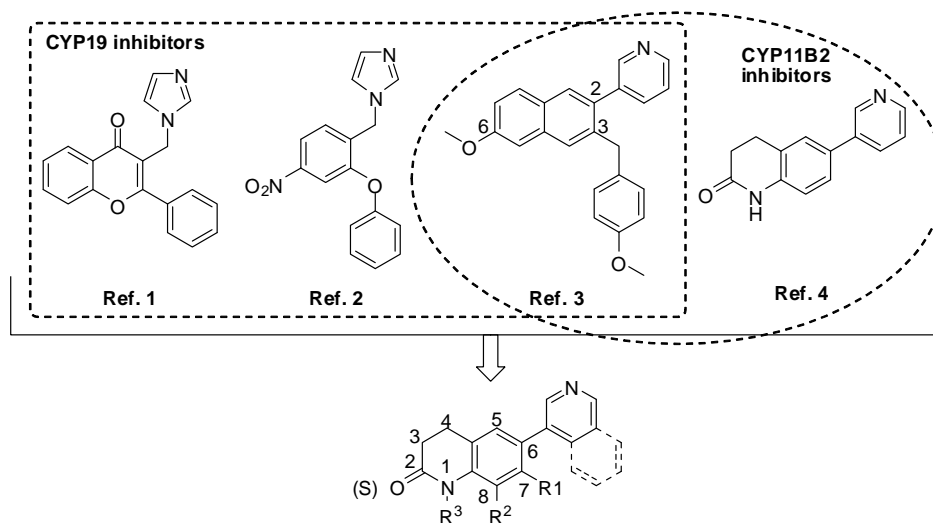


Dual inhibitors design conception

Besides Anastrozole and Letrozole — the CYP19 inhibitors in clinic use, a lot of potent non-steroidal CYP19 inhibitors have been designed and synthesized.¹⁸ Almost all these inhibitors are based on the mechanism that the *sp*² hybrid nitrogen coordinates with the heme iron resulting in the inhibition of this enzyme in a reversible manner.^{18a} Since all CYP enzymes contain heme iron as catalysis centre, inhibitors toward other steroidogenic enzymes, such as CYP17¹⁹ and CYP11B2,²⁰ have also been designed according to this mechanism.

Two potent CYP19 inhibitors have been employed in the design of dual inhibitors: **Ref. 1** (Chart 3, CYP19 $IC_{50} = 71$ nM)^{18b} with the imidazolyl furnishing on flavone scaffold, and **Ref. 2** (Chart 3, CYP19 $IC_{50} = 12$ nM)^{18c} with a phenyl core substituted by phenoxy group next to the imidazolyl-methyl moiety. Three important structural features can be noticed in these two potent CYP19 inhibitors: heterocycle providing sp^2 hybrid N (imidazolyl), aromatic hydrophobic core (chromenone or benzene) and aryl substituent nearby. Besides, a suitable linker between aryl substituent and the core as well as the groups furnished on the core are also considered to significantly influence the potency. This was demonstrated by **Ref. 3** (Chart 3),^{20b} which is one of a series of potent CYP11B2 inhibitors. All the compounds in that series contain these three structural features described above, but only **Ref. 3** exhibited potent CYP19 inhibition (CYP19 $IC_{50} = 38$ nM) because of the methoxyl substitution at the 6 position of the naphthalene core.^{20b} Therefore, to design the dual inhibitors of CYP19 and CYP11B2, we selected 6-(pyridin-3-yl)-3,4-dihydroquinolin-2(1H)-one (**Ref. 4**, Chart 3),^{20a} which is a highly potent and selective CYP11B2 inhibitor (CYP11B2 $IC_{50} = 28$ nM) showing no interference with CYP19, as the template for CYP11B2 inhibition and tried to introduce important structural features of CYP19 inhibitors into this template. **Ref. 4** is already composed of two structural features important for CYP19 inhibition: a) 3-pyridyl as N containing heterocycle and b) dihydroquinolinone as aromatic core. The presence of ketone mimicking 6-methoxyl of **Ref. 3** as hydrogen bond acceptor fulfilled another precondition of potent CYP19 inhibition. Therefore, hydrophobic groups were further introduced to the 7- or 8-position of the core including aryl, halogen and alkyl in various sizes. When substituted at 7-position, an oxygen was exploited as the linker, similar to **Ref. 2**, because of the SAR observed previously that bulky groups furnishing next to pyridyl significantly reduce the CYP11B2 inhibition.^{20a} Furthermore, bioisostere exchange of ketone O to S, methylation of amide and replacement of pyridyl by isoquinolinyl were performed as well aiming to improve the inhibitory potency toward both enzymes.

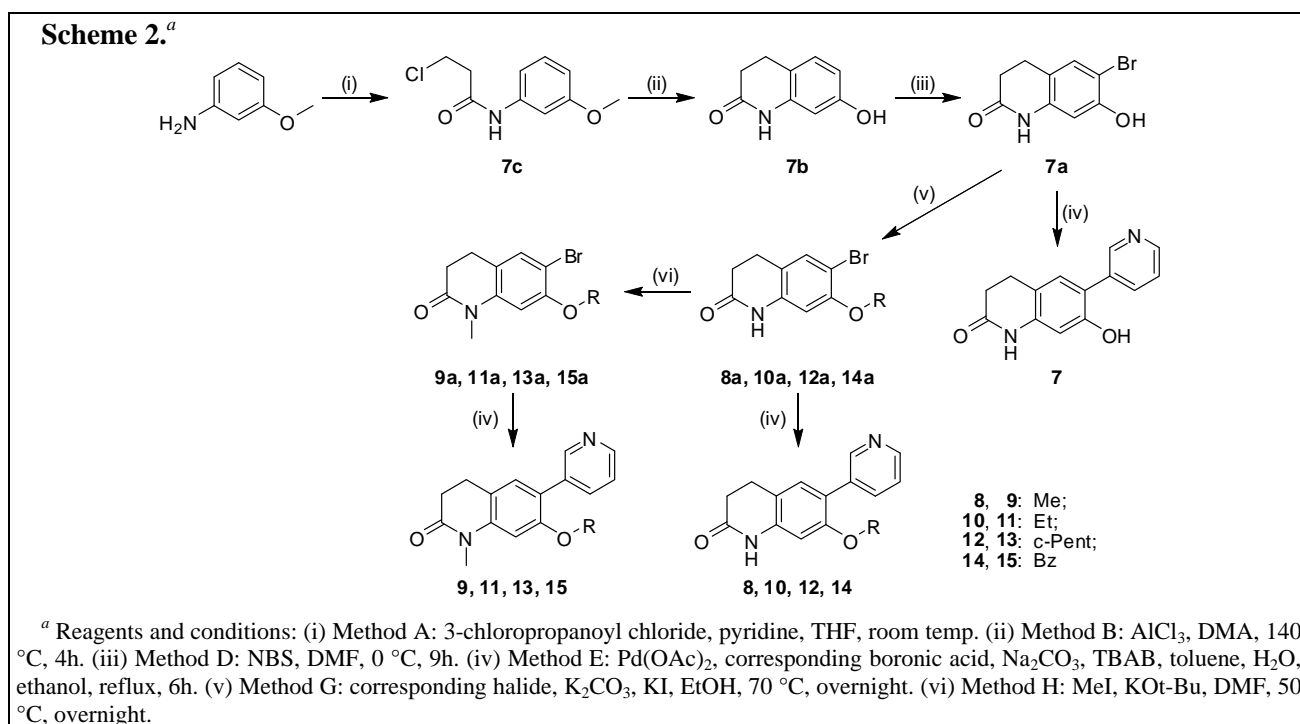
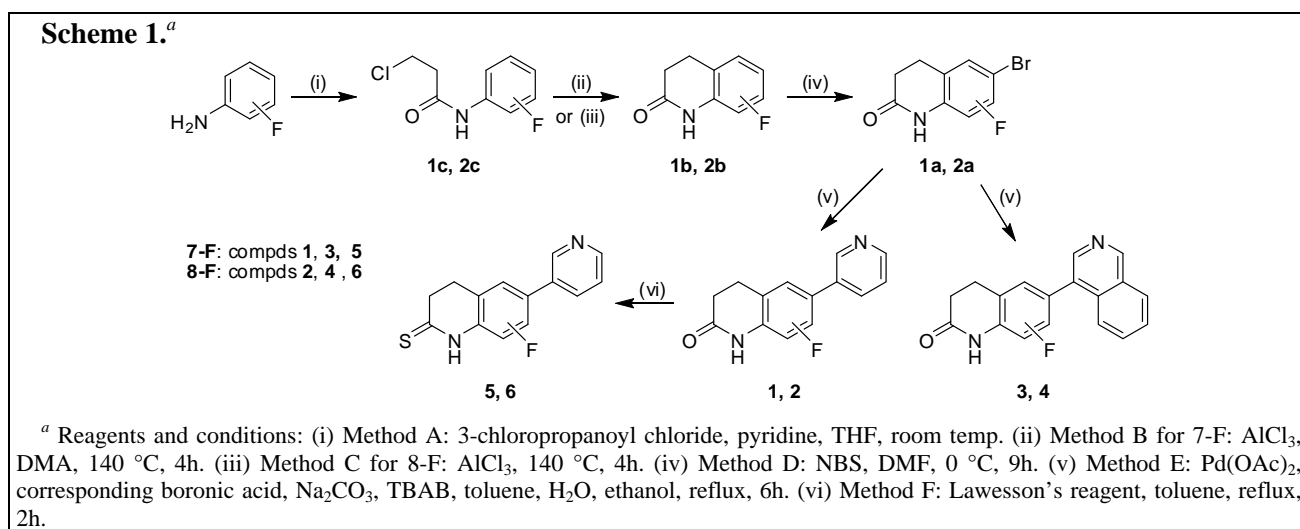
Chart 3. Design of heterocyclic dihydroquinolinones as dual CYP19 / CYP11B2 inhibitors.



Results and Discussion

Chemistry. The synthesis of compounds **1–19** is shown in Schemes 1–3. Firstly, the substituted 3,4-dihydroquinolin-2(1H)-one cores **1b**, **2b**, **7b** and **16c** were built from the corresponding anilines after amidation with 3-chloropropanoyl chloride and then cyclization via Friedel-Craft alkylation. For 8-

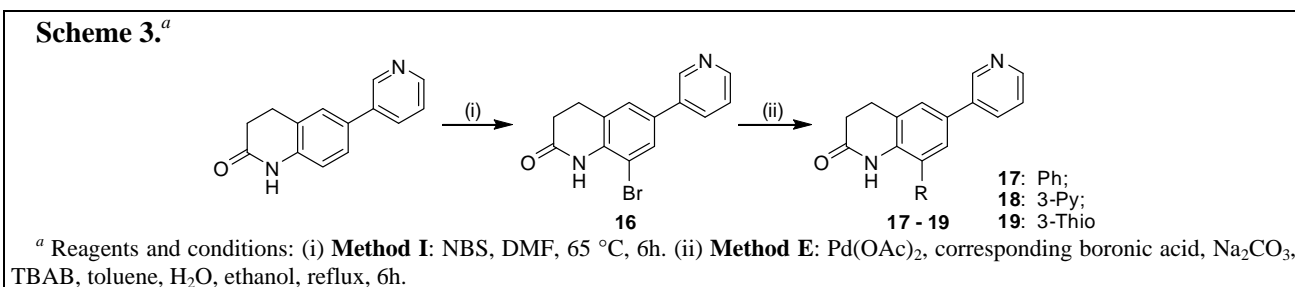
substituted analogues, Friedel-Craft reactions were performed without solvent; whereas *N,N*-dimethyl acetamide (DMA) was employed for 7-substituted derivatives to suppress the side reactions. During



the Friedel-Craft alkylation, methoxyl group was cleaved simultaneously to afford hydroxyl intermediate **7b**. Secondly, 6-position specified bromination was achieved with *N*-bromosuccinimide (NBS) in an ice bath, which was followed by Suzuki coupling with respective pyridyl or isoquinolyl boronic acids leading to compounds **1–4** and **7**. Further derivatives **5, 6** and **8–15** were obtained after sulphuration of ketone with Lawesson's reagent and alkylation of phenol or amide, which were applied either after or before Suzuki coupling respectively. As for 8-substituted analogues, 6-(pyridin-3-yl)-3,4-dihydroquinolin-2(1*H*)-one was prepared similarly as described above as a common intermediate, which after 8-position specified bromination gave compound **16**. Further aryl groups were then introduced via another Suzuki coupling reaction resulting in desired compounds **17–19**.

Inhibition of CYP19, CYP11B2 and CYP11B1. Inhibitory activity of the synthesized compounds toward CYP19 was determined using human placental microsomes with [1β -³H]androstenedione as substrate,^{21d}

whereas V79MZh cells expressing human CYP11B2 were employed for CYP11B2 tests with [^{14}C]-11-deoxycorticosterone as substrate.^{21b-c} Since CYP11B1 and CYP11B2 exhibit more than 93% of homology and inhibition of CYP11B1 results in cortisol deficiency, the selectivity toward CYP11B1 was also examined for safety in a similar procedure described for CYP11B2, except for V79MZh cells expressing human CYP11B1 as the source of enzyme.^{21b-c} The IC_{50} values of the synthesized compounds toward these three enzymes are presented in Table 1 in comparison with Fadrozole.



It can be seen that regardless of the substituting position, the introduction of small, strong electron-withdrawn group fluorine increased CYP11B2 inhibition compared to the non-substituted analogue **Ref. 4** from 28 nM to around 10 nM. However, the resulted compounds **1** and **2** showed no improvement of the CYP19 inhibition. Although the selectivity against CYP11B1 was reduced compared to **Ref. 4**, these compounds are still quit selective with the selectivity factors (SF, $\text{IC}_{50} \text{CYP11B1} / \text{IC}_{50} \text{CYP11B2}$) around 150. Moreover, the replacement of pyridyl by isoquinolinyl led to compounds **3** and **4** with further elevated CYP11B2 inhibitory potency of below 1 nM and good selectivity over CYP11B1 (SF of 91 and 50, respectively). Nevertheless, this fusing of extra phenyl to pyridyl paid the cost of total loss of CYP19 inhibition indicating no more spar space near the heme of this enzyme. Similar phenomenon was observed for the bioisostere exchange of ketone O to S (compounds **5** and **6**), the enhanced CYP11B2 inhibition was accompanied by the deterioration of selectivity against CYP11B1 (SF of 61 and 87) and the total loss of CYP19 inhibition.

On the contrary, the hydroxy substitution at the 7-position (compound **7**) slightly improved CYP19 inhibition, but decreased CYP11B2 inhibitory potency to about 300 nM and selectivity to 38. After alkylation of this hydroxy with groups in different sizes, great influence was shown. It can be observed that as the bulk of substituents swelling, the inhibition of the corresponding compounds toward CYP19 increased from 450–500 nM (compounds **8** and **10** with methoxyl and ethoxyl, respectively) to 162 nM (compound **12** with cyclopentyloxy), and finally to 35 nM (compound **14** with benzyloxy). Simultaneously, the inhibitory activity of these compounds toward CYP11B2 largely dropped. Compound **8** (methoxyl) exhibited IC_{50} of 268 nM, whereas 673 nM for compound **10** (ethoxyl) and 1700 nM for compound **12** (cyclopentyloxy). Surprisingly, benzyloxy analogue **14** turned out to be a potent CYP11B2 inhibitor with IC_{50} of 22 nM probably due to a different binding mode. The inhibition toward CYP11B1 followed the same trend. However, it seemed that CYP11B1 are less sensitive to the bulky augments compared to CYP11B2, therefore significant reduction of selectivity was observed with SF less than 10 for these compounds. Nevertheless, further methylation of amide N dramatically improved the inhibition toward CYP19 and CYP11B2 as well as the selectivity against CYP11B1. It is apparent that after amide methylation the methoxyl (**9**) and ethoxyl (**11**) analogues exhibited 10 fold more potent inhibition toward CYP19 than their

Table 1. Inhibition of CYP11B1, CYP11B2 and CYP19 by compounds **1–19**.

	1 - 2, 7 - 19, Ref. 1			3 - 4	5 - 6		
	R ¹	R ²	R ³	CYP19 IC ₅₀ nM ^{b,d}	CYP11B2 IC ₅₀ nM ^{b,c}	CYP11B1 IC ₅₀ nM ^{b,c}	SF ^e
Ref. 4	H	H	H	>5000	28.0	6747.0	241
1	F	H	H	4819.4	10.7	1306.0	122
2	H	F	H	5750.0	8.6	1454.0	168
3	F	H	H	>10000	0.59	53.6	91
4	H	F	H	>10000	0.24	12.1	50
5	F	H	H	>10000	7.8	471.9	61
6	H	F	H	>10000	2.7	236.9	87
7	OH	H	H	3073.4	312	11940	38
8	OMe	H	H	447.4	267.6	2867.0	9
9	OMe	H	Me	49.2	18.5	1098.5	59
10	OEt	H	H	488.0	673.7	3737.3	5.5
11	OEt	H	Me	47.5	19.1	789.8	41
12	O-c-Pent	H	H	161.8	1702.6	1077.3	0.6
13	O-c-Pent	H	Me	22.2	759.4	1166.7	1.5
14	OBz	H	H	35.1	21.5	43.8	2
15	OBz	H	Me	11.4	177.5	139.4	0.8
16	H	Br	H	2901.3	11.8	1421.8	120
17	H	Ph	H	394.2	1166.7	16170	13.9
18	H	3-Py	H	953.5	1097.4	4087.2	3.7
19	H	3-Thio	H	275.0	208.1	4588.9	22
FDZ^a				52.0	0.8	6.3	8.3

^a **FDZ**: Fadrozole.^b Concentration of inhibitors required to give 50 % inhibition. Standard deviations were within $\pm 5\%$; All the data are the mean values of at least 3 tests.^c Hamster fibroblasts expressing human CYP11B1 or CYP11B2 are used with deoxycorticosterone as the substrate at a concentration of 100 nM.^d Human placental CYP19 is used with androstenedione as the substrate at a concentration of 500 nM.^e SF: selective factor = $IC_{50\text{CYP11B1}} / IC_{50\text{CYP11B2}}$.

precursors (**8** and **10**, respectively) with IC_{50} values about 50 nM. The inhibitory activity of CYP11B2 was also significantly increased to less than 20 nM. Important is their selectivity over CYP11B1 was promoted to 59 and 41 respectively at the same time. Therefore, via optimizing combination of introducing small alkoxy groups at the 7-position and amide methylation, the desired dual inhibitors of CYP19 / 11B2 were successfully obtained with good selectivity over CYP11B1. When the alkoxy substituent was more bulky (**13**, cyclopentyloxy), regarding the CYP11B2 inhibition, the promotion of activity rendered by amide

methylation could hardly neutralize the deterioration from the augment of bulk. As the inhibition toward CYP19 was increased to 22 nM, this compound turned out to be a selective CYP19 inhibition with selectivity of 35 and 53 ($IC_{50\text{ CYP19}} / IC_{50\text{ CYP11B2 or CYP11B1}}$) over CYP11B2 and CYP11B1, respectively. As for the benzyloxyl analogues (**14** and **15**), which were believed to bind in a different mode to CYP11B, the methylation of amide significantly decreased the inhibition of CYP11B to around 150 nM. Since compound **15** showed potent inhibition toward CYP19 ($IC_{50} = 11$ nM), this compound was considered as selective CYP19 inhibitor with around 15 fold of selectivity against CYP11B2 and CYP11B1.

Furthermore, the influence of substituents at the 8-position was also investigated. The bromo analogue **16** turned out to be a potent selective CYP11B2 inhibitor exhibiting IC_{50} of 11 nM and SF of 120 over CYP11B1. However, this compound showed only weak inhibition of CYP19 ($IC_{50} = 2900$ nM). The introduction of aryl groups (**17** with phenyl and **18** with 3-pyridyl) increased CYP19 inhibition with the potency toward CYP11B2 reduced accordingly. It is notable that unlike its bioisostere phenyl, 3-thiophenyl group in smaller bulk rendered compound **19** as a modest dual inhibitor of CYP19 / 11B2 (IC_{50} values of 275 nM and 208 nM, respectively) with modest SF of 22 over CYP11B1.

Selectivity. The inhibition of CYP17 by synthesized compounds was also determined as a criterion to evaluate safety because this enzyme is crucial in the biosynthesis of androgen. It turned out all compounds exhibited IC_{50} values more than 10000 nM (data not shown) indicating no interference with CYP17.

Conclusions

Although AIs as BC treatment are successful, they together with menopausal significantly reduced estrogen concentration to prevent BC cells proliferation, the estrogen deficiency also results in elevation of aldosterone levels, sometimes not in plasma but inside the heart and other target organs. The abnormally high aldosterone level exerts deleterious effects on kidney, vessels, brain and the severest on heart. These damages, such as asymptomatic left ventricular dysfunction, may exist long before the clinical syndrome appears and sudden death happens. Therefore it is urgent to find a convenient way to cope with breast cancer and the coinstantaneous cardiovascular diseases. Since AIs as adjuvant therapy have to be administered for long time, the compliance of the patients is another advantage of dual inhibition of CYP19 and CYP11B2, besides reduced risk of drug-drug interactions.

The approach of combining important structural features of CYP19 and CYP11B2 inhibitors to design dual inhibitors is demonstrated to be successful. Modifications exhibits various influence on SARs toward different enzymes. It has been found that introduction of halogen, bioisostere exchange of ketone O to S and replacement of pyridyl by isoquinolinyll significantly increased CYP11B2 inhibitory potency. Nevertheless, the resulted compounds (**1-6** and **16**) showed weak to no inhibition of CYP19, CYP11B1 and CYP17, which rendered them as selective CYP11B2 inhibitors ($IC_{50} < 10$ nM). Moreover, the bulky augment of alkoxy groups at the 7-position largely elevated CYP19 inhibition, however, reduced CYP11B2 inhibition and selectivity over CYP11B1. On the contrary, methylation of amide led to increase of inhibitory toward all of these three enzymes. After balancing the different influence on SARs, selective dual inhibitors were successfully obtained as compounds **9** and **11** with IC_{50} values around 50 and 20 nM toward CYP19 and CYP11B2, respectively. These compounds also showed good selectivity against CYP11B1 with selectivity

factors around 50 and no interference with CYP17. In the same procedure, compound **13** was identified as a selective CYP19 inhibitor with IC_{50} value of 22 nM and selectivity factors more than 35 for the other enzymes. The dual inhibitors **9** and **11** are promising treatment for BC patients with risk of CVD after further evaluation in vivo.

Experimental Section

Inhibition of CYP11B1 and CYP11B2

V79MZh cells expressing human CYP11B1 or CYP11B2 were incubated with [^{14}C]-11-deoxycorticosterone as substrate. The assay was performed as previously described.^{21b-c}

Inhibition of CYP19

The inhibition of CYP19 was determined in vitro using human placental microsomes with [3H]androstenedione as substrate.^{21d}

Inhibition of CYP17

Human CYP17 was expressed in *E. coli*^{19a} (coexpressing human CYP17 and NADPH-P450 reductase) and the assay was performed with progesterone as substrate at high concentrations of 25 μ M as previously described.^{21d}

Chemistry Section

General

Melting points were determined on a Mettler FP1 melting point apparatus and are uncorrected. IR spectra were recorded neat on a Bruker Vector 33FT-infrared spectrometer. 1H -NMR spectra were measured on a Bruker DRX-500 (500 MHz). Chemical shifts are given in parts per million (ppm), and TMS was used as an internal standard for spectra obtained. All coupling constants (J) are given in Hz. ESI (electrospray ionization) mass spectra were determined on a TSQ quantum (Thermo Electron Corporation) instrument. The purities of the final compounds were controlled by Surveyor®-LC-system. Purities were greater than 95 %. Column chromatography was performed using silica-gel 60 (50-200 μ m), and reaction progress was determined by TLC analysis on Alugram® SIL G/UV₂₅₄ (Macherey-Nagel).

Method A: Amidation

To the corresponding aniline (1.0 eq.) solution in dry THF (10 mL / mmol) was added pyridine (1.5 eq.) before the mixture was cooled to 0 °C in an ice bath. Then, 3-chloropropanoyl chloride (1.1 eq.) was dropped in carefully. After the addition, the reaction mixture was warmed to ambient temperature and stirred overnight. THF was then removed by reduced pressure, and the residues were taken up with ethyl acetate (10 mL) and water (10 mL). After extraction of the water phase for 3 times with ethyl acetate (10 mL), the organic phases were combined, washed with brine, dried over Na_2SO_4 , and evaporated under reduced pressure to give the crude product. The compounds were then purified by flash chromatography on silica gel.

Method B: Friedel-Craft alkylation in DMA

To the cold mixture of corresponding 3-chloro-*N*-phenylpropanamides (1.0 eq.) and $AlCl_3$ (5.0 eq.) was dropped in DMA (1.0 eq.). Then the reaction mixture was heated to 140 °C for 4 hours. After cooling down to ambient temperature, the black mixture was worked up with ethyl acetate (20 mL) and ice water (20 mL).

After extraction of the water phase for 3 times with ethyl acetate (10 mL), the organic phases were combined, washed with brine, dried over Na₂SO₄, and evaporated under reduced pressure to give the crude product. The compounds were then purified by flash chromatography on silica gel.

7-Fluoro-3,4-dihydro-1H-quinolin-2-one (1b). Synthesized according to Method b using **1c** (0.35 g, 1.74 mmol); yield: 0.15 g (53%); white solid; $R_f = 0.29$ (DCM/MeOH, 100:1); δ_H (CDCl₃, 500 MHz) 2.64 (t, $J = 7.8$ Hz, 2H, CH₂), 2.94 (t, $J = 7.8$ Hz, 2H, CH₂), 6.90–6.99 (m, 3H), 7.83 (s, br, 1H, NH); MS (ESI): $m/z = 166$ [M⁺+H].

Method C: Friedel-Craft alkylation neat

The mixture of corresponding 3-chloro-*N*-phenylpropanamides (1.0 eq.) and AlCl₃ (5.0 eq.) was heated to 140 °C for 4 hours. After cooling down to ambient temperature, the black mixture was worked up with ethyl acetate (20 mL) and ice water (20 mL). After extraction of the water phase for 3 times with ethyl acetate (10 mL), the organic phases were combined, washed with brine, dried over Na₂SO₄, and evaporated under reduced pressure to give the crude product. The compounds were then purified by flash chromatography on silica gel.

8-Fluoro-3,4-dihydro-1H-quinolin-2-one (2b). Synthesized according to Method C using **2C** (0.35 g, 1.41 mmol); yield: 0.24 g (82%); white solid; $R_f = 0.28$ (DCM/MeOH, 100:1); δ_H (CDCl₃, 500 MHz) 2.66 (t, $J = 7.8$ Hz, 2H, CH₂), 3.01 (t, $J = 7.8$ Hz, 2H, CH₂), 6.57 (dd, $J = 2.5$ Hz, $^3J_{HF} = 9.3$ Hz, 1H), 6.67 (ddd, $J = 2.5$, 8.4 Hz, $^3J_{HF} = 8.5$ Hz, 1H), 7.09 (dd, $J = 8.2$ Hz, $^4J_{HF} = 6.0$ Hz, 1H), 7.83 (s, br, 1H, NH); MS (ESI): $m/z = 166$ [M⁺+H].

Method D: Selective bromination at 6-position

To the solution of corresponding dihydroquinolinone (1.0 eq.) in DMF (5 mL / mmol) cooling in an ice bath was dropped in NBS (1.1 eq.) solution in DMF (2 mL / mmol). The addition lasted for 3 hours, and then the reaction mixture was hold at 0 °C for another 6 hours before extraction with ethyl acetate (20 mL) and water (20 mL). After extraction of the water phase for 3 times with ethyl acetate (10 mL), the organic phases were combined, washed with brine, dried over Na₂SO₄, and evaporated under reduced pressure to give the crude product. The compounds were then purified by flash chromatography on silica gel.

6-Bromo-8-fluoro-3,4-dihydro-1H-quinolin-2-one (2a). Synthesized according to Method D using **2b** (0.50 g, 3.02 mmol) and NBS (0.54 g, 3.02 mmol); yield: 0.63 g (85%); white solid; $R_f = 0.29$ (DCM/MeOH, 100:1); δ_H (CDCl₃, 500 MHz) 2.65 (t, $J = 7.5$ Hz, 2H, CH₂), 2.99 (t, $J = 7.7$ Hz, 2H, CH₂), 7.12 (s, 1H), 7.16 (dd, $J = 1.9$ Hz, $^3J_{HF} = 9.6$ Hz, 1H), 7.88 (s, br, 1H, NH); MS (ESI): $m/z = 244$ [M⁺+H].

6-Bromo-7-hydroxy-3,4-dihydro-1H-quinolin-2-one (7a). Synthesized according to Method D using **7b** (0.47 g, 2.88 mmol) and NBS (0.51 g, 2.88 mmol); yield: 0.61 g (87%); white solid; $R_f = 0.25$ (DCM/MeOH, 20:1); δ_H (CDCl₃, 500 MHz) 2.38 (t, $J = 7.5$ Hz, 2H, CH₂), 2.75 (t, $J = 7.7$ Hz, 2H, CH₂), 6.53 (s, 1H), 7.24 (s, 1H), 10.05 (s, br, 1H, NH); MS (ESI): $m/z = 242$ [M⁺+H].

Method E: Suzuki-Coupling

The corresponding brominated aromatic compound (1.0 eq.) was dissolved in toluene (7 mL / mmol), and an aqueous 2.0 M Na₂CO₃ solution (3.2 mL / mmol), an ethanolic solution (3.2 mL / mmol) of the corresponding boronic acid (1.5-2.0 eq.) and tetrabutylammonium bromide (1.0 eq) were added. The mixture was deoxygenated under reduced pressure and flushed with nitrogen. After having repeated this cycle several

times Pd(OAc)₂ (5 mol%) was added and the resulting suspension was heated under reflux for 2-6 h. After cooling, ethyl acetate (10 mL) and water (10 mL) were added and the organic phase was separated. The water phase was extracted with ethyl acetate (2 x 10 mL). The combined organic phases were washed with brine, dried over Na₂SO₄, filtered over a short plug of celite® and evaporated under reduced pressure. The compounds were purified by flash chromatography on silica gel.

7-Fluoro-6-pyridin-3-yl-3,4-dihydro-1H-quinolin-2-one (1). Synthesized according to Method E using **1a** (0.35 g, 1.43 mmol) and pyridin-3-ylboronic acid (0.21 g, 1.72 mmol); yield: 0.32 g (91%); white solid: mp 230–231 °C; *R*_f = 0.23 (DCM/MeOH, 50:1); δ_H (CDCl₃, 500 MHz) 2.70 (t, *J* = 7.8 Hz, 2H, CH₂), 3.02 (t, *J* = 7.8 Hz, 2H, CH₂), 6.69 (d, ³*J*_{HF} = 10.8 Hz, 1H), 7.23 (d, ⁴*J*_{HF} = 7.9 Hz, 1H), 7.35 (ddd, *J* = 0.7, 4.9, 8.0 Hz, 1H), 7.83 (dt, *J* = 2.2, 7.9 Hz, 1H), 8.60 (dd, *J* = 1.6, 4.8 Hz, 1H), 8.76 (d, *J* = 2.2 Hz, 1H), 8.92 (s, br, 1H, NH); MS (ESI): *m/z* = 243 [M⁺+H].

8-Fluoro-6-pyridin-3-yl-3,4-dihydro-1H-quinolin-2-one (2). Synthesized according to Method E using **2a** (0.35 g, 1.43 mmol) and pyridin-3-ylboronic acid (0.21 g, 1.72 mmol); yield: 0.29 g (87%); white solid: mp 204–205 °C; *R*_f = 0.21 (DCM/MeOH, 50:1); δ_H (CDCl₃, 500 MHz) 2.72 (t, *J* = 7.8 Hz, 2H, CH₂), 3.10 (t, *J* = 7.8 Hz, 2H, CH₂), 7.20 (s, 1H), 7.21 (dd, *J* = 1.6 Hz, ³*J*_{HF} = 11.0 Hz, 1H), 7.36 (dd, *J* = 4.8, 7.9 Hz, 1H), 7.76 (s, br, 1H, NH), 7.81 (dt, *J* = 2.2, 7.9 Hz, 1H), 8.60 (dd, *J* = 1.5, 4.8 Hz, 1H), 8.80 (d, *J* = 2.2 Hz, 1H); MS (ESI): *m/z* = 243 [M⁺+H].

7-Fluoro-6-isoquinolin-4-yl-3,4-dihydro-1H-quinolin-2-one (3). Synthesized according to Method E using **5a** (0.35 g, 1.43 mmol) and isoquinolin-4-ylboronic acid (0.30 g, 1.72 mmol); yield: 0.39 g (93%); white solid: mp 283–284 °C; *R*_f = 0.25 (DCM/MeOH, 50:1); δ_H (CDCl₃, 500 MHz) 2.73 (t, *J* = 7.2 Hz, 2H, CH₂), 3.03 (t, *J* = 7.3 Hz, 2H, CH₂), 6.74 (d, ³*J*_{HF} = 9.8 Hz, 1H), 7.21 (d, ⁴*J*_{HF} = 7.4 Hz, 1H), 7.64 (ddd, *J* = 0.7, 4.9, 8.0 Hz, 1H), 7.69–7.70 (m, 2H), 8.05 (d, *J* = 8.0 Hz, 1H), 8.48 (s, 1H), 8.62 (s, br, 1H, NH), 9.29 (s, 1H); MS (ESI): *m/z* = 293 [M⁺+H].

8-Fluoro-6-isoquinolin-4-yl-3,4-dihydro-1H-quinolin-2-one (4). Synthesized according to Method E using **5a** (0.35 g, 1.43 mmol) and isoquinolin-4-ylboronic acid (0.30 g, 1.72 mmol); yield: 0.35 g (88%); white solid: mp 202–203 °C; *R*_f = 0.26 (DCM/MeOH, 50:1); δ_H (CDCl₃, 500 MHz) 2.75 (t, *J* = 7.9 Hz, 2H, CH₂), 3.11 (t, *J* = 7.9 Hz, 2H, CH₂), 7.13 (s, 1H), 7.17 (dd, *J* = 1.5 Hz, ³*J*_{HF} = 10.7 Hz, 1H), 7.44–7.56 (m, 1H), 7.54–7.73 (m, 2H), 7.75 (s, br, 1H, NH), 7.90 (d, *J* = 8.5 Hz, 1H), 8.10 (d, *J* = 8.0 Hz, 1H), 8.45 (s, 1H), 9.26 (s, 1H); MS (ESI): *m/z* = 293 [M⁺+H].

7-Methoxy-1-methyl-6-pyridin-3-yl-3,4-dihydro-1H-quinolin-2-one (9). Synthesized according to Method E using **9a** (0.50 g, 1.85 mmol) and pyridin-3-ylboronic acid (0.22 g, 2.22 mmol); yield: 0.46 g (93%); white solid: mp 207–208 °C; *R*_f = 0.19 (DCM/MeOH, 50:1); δ_H (CDCl₃, 500 MHz) 2.62 (t, *J* = 7.9 Hz, 2H, CH₂), 2.83 (t, *J* = 7.9 Hz, 2H, CH₂), 3.35 (s, 3H, NCH₃), 3.79 (s, 3H, OCH₃), 6.56 (s, 1H), 7.01 (s, 1H), 7.25 (ddd, *J* = 0.7, 5.3, 8.3 Hz, 1H), 7.76 (dt, *J* = 2.0, 8.0 Hz, 1H), 8.46 (dd, *J* = 1.6, 4.8 Hz, 1H), 8.68 (d, *J* = 1.7 Hz, 1H); MS (ESI): *m/z* = 269 [M⁺+H].

7-Ethoxy-1-methyl-6-pyridin-3-yl-3,4-dihydro-1H-quinolin-2-one (11). Synthesized according to Method E using **11a** (0.50 g, 1.76 mmol) and pyridin-3-ylboronic acid (0.26 g, 2.11 mmol); yield: 0.43 g (86%); white solid: mp 217–218 °C; *R*_f = 0.20 (DCM/MeOH, 50:1); δ_H (CDCl₃, 500 MHz) 1.35 (t, *J* = 6.9 Hz, 3H, CH₃), 2.66 (t, *J* = 7.9 Hz, 2H, CH₂), 2.88 (t, *J* = 7.9 Hz, 2H, CH₂), 3.38 (s, 3H, NCH₃), 4.04 (q, *J* =

6.9 Hz, 2H, OCH₂), 6.61 (s, 1H), 7.11 (s, 1H), 7.30 (ddd, $J = 0.7, 4.9, 7.9$ Hz, 1H), 7.84 (dt, $J = 2.0, 7.9$ Hz, 1H), 8.50 (dd, $J = 1.6, 4.8$ Hz, 1H), 8.76 (d, $J = 1.7$ Hz, 1H); MS (ESI): $m/z = 283$ [M⁺+H].

7-Cyclopentyloxy-1-methyl-6-pyridin-3-yl-3,4-dihydro-1H-quinolin-2-one (13). Synthesized according to Method E using **13a** (0.50 g, 1.54 mmol) and pyridin-3-ylboronic acid (0.23 g, 1.85 mmol); yield: 0.42 g (85%); colorless oil; $R_f = 0.23$ (DCM/MeOH, 50:1); δ_H (CDCl₃, 500 MHz) 1.52–1.89 (m, 8H, c-Pent), 2.67 (t, $J = 7.9$ Hz, 2H, CH₂), 2.88 (t, $J = 7.9$ Hz, 2H, CH₂), 3.38 (s, 3H, NCH₃), 4.75 (sept, $J = 2.8$ Hz, 1H, OCH), 6.62 (s, 1H), 7.11 (s, 1H), 7.29 (ddd, $J = 0.7, 5.3, 7.9$ Hz, 1H), 7.81 (dt, $J = 1.9, 7.9$ Hz, 1H), 8.50 (dd, $J = 1.5, 4.8$ Hz, 1H), 8.72 (d, $J = 1.8$ Hz, 1H); MS (ESI): $m/z = 322$ [M⁺+H].

7-Benzyloxy-1-methyl-6-pyridin-3-yl-3,4-dihydro-1H-quinolin-2-one (15). Synthesized according to Method E using **15a** (0.50 g, 1.44 mmol) and pyridin-3-ylboronic acid (0.21 g, 1.73 mmol); yield: 0.45 g (90%); white solid: mp 209–210 °C; $R_f = 0.23$ (DCM/MeOH, 50:1); δ_H (CDCl₃, 500 MHz) 2.67 (t, $J = 7.9$ Hz, 2H, CH₂), 2.89 (t, $J = 7.9$ Hz, 2H, CH₂), 3.33 (s, 3H, NCH₃), 5.09 (s, 2H, bz CH₂), 6.67 (s, 1H), 7.14 (s, 1H), 7.29–7.38 (m, 6H, bz), 7.87 (dt, $J = 1.9, 8.0$ Hz, 1H), 8.53 (dd, $J = 1.6, 4.9$ Hz, 1H), 8.78 (d, $J = 1.8$ Hz, 1H); MS (ESI): $m/z = 345$ [M⁺+H].

6-Pyridin-3-yl-8-thiophen-3-yl-3,4-dihydro-1H-quinolin-2-one (19). Synthesized according to Method E using **16** (0.47 g, 1.55 mmol) and thiophen-3-ylboronic acid (0.24 g, 1.86 mmol); yield: 0.39 g (83%); white solid: mp 235–236 °C; $R_f = 0.35$ (DCM/MeOH, 50:1); δ_H (CDCl₃, 500 MHz) 2.71 (t, $J = 7.9$ Hz, 2H, CH₂), 3.11 (t, $J = 7.9$ Hz, 2H, CH₂), 7.18 (dd, $J = 1.2, 4.9$ Hz, 1H), 7.34–7.38 (m, 2H), 7.40 (s, 2H), 7.52 (dd, $J = 4.8, 4.9$ Hz, 1H), 7.66 (s, br, 1H, NH), 7.85 (dt, $J = 1.8, 8.0$ Hz, 1H), 8.58 (dd, $J = 1.5, 4.9$ Hz, 1H), 8.83 (d, $J = 2.1$ Hz, 1H); MS (ESI): $m/z = 307$ [M⁺+H].

Method F: Sulphuration with Lawesson's reagent

To the suspension of the corresponding dihydroquinolinone (1.0 eq.) in toluene (5 mL / mmol) was added Lawesson's reagent (1.5 eq.). After reflux for 2 hours, toluene was distilled off to give the crude product, which was then purified by flash chromatography on silica gel.

7-Fluoro-6-pyridin-3-yl-3,4-dihydro-1H-quinoline-2-thione (5). Synthesized according to Method F using **1** (0.35 g, 1.44 mmol); yield: 0.28 g (76%); light yellow solid: mp 245–246 °C; $R_f = 0.22$ (DCM/MeOH, 50:1); δ_H (DMSO, 500 MHz) 2.85 (t, $J = 7.8$ Hz, 2H, CH₂), 2.99 (t, $J = 7.8$ Hz, 2H, CH₂), 7.02 (d, $^3J_{HF} = 11.5$ Hz, 1H), 7.49 (ddd, $J = 0.7, 4.9, 8.0$ Hz, 1H), 7.50 (d, $^4J_{HF} = 8.2$ Hz, 1H), 7.95 (dt, $J = 2.0, 7.9$ Hz, 1H), 8.58 (dd, $J = 1.6, 4.8$ Hz, 1H), 8.74 (s, 1H), 12.33 (s, br, 1H, NH); MS (ESI): $m/z = 258$ [M⁺+H].

8-Fluoro-6-pyridin-3-yl-3,4-dihydro-1H-quinoline-2-thione (6). Synthesized according to Method F using **2** (0.35 g, 1.44 mmol); yield: 0.30 g (81%); light yellow solid: mp 229–230 °C; $R_f = 0.22$ (DCM/MeOH, 50:1); δ_H (DMSO, 500 MHz) 2.91 (t, $J = 7.8$ Hz, 2H, CH₂), 3.00 (t, $J = 7.8$ Hz, 2H, CH₂), 7.47 (ddd, $J = 0.7, 4.9, 8.0$ Hz, 1H), 7.52 (s, 1H), 7.59 (dd, $J = 1.9$ Hz, $^3J_{HF} = 11.7$ Hz, 1H), 8.10 (dt, $J = 1.7, 8.0$ Hz, 1H), 8.56 (dd, $J = 1.5, 4.7$ Hz, 1H), 8.92 (d, $J = 1.7$ Hz, 1H), 12.16 (s, br, 1H, NH); MS (ESI): $m/z = 258$ [M⁺+H].

Method G: Alkylation of phenol

The suspension of K₂CO₃ (2.0 eq.) and 6-bromo-7-hydroxy-3,4-dihydroquinolin-2(1H)-one (1.0 eq.) in dry ethanol (5 mL / mmol) was refluxed for 2 hours before KI (0.05 eq.) and the corresponding halide (2.0 eq.)

were added. Then the white suspension was boiling overnight. After cooling down to ambient temperature, ethanol was removed with reduced pressure and the residue was taken up with ethyl acetate (20 mL) and water (20 mL). After extraction of the water phase for 3 times with ethyl acetate (10 mL), the organic phases were combined, washed with brine, dried over Na₂SO₄, and evaporated under reduced pressure to give the crude product. The compounds were then purified by flash chromatography on silica gel.

Method H: Alkylation of amide

The suspension of potassium *t*-butanolate (2.0 eq.) and corresponding dihydroquinolinone (1.0 eq.) in dry DMF (5 mL / mmol) was heated to 50 °C for 2 hours before KI (0.05 eq.) and the iodomethane (2.0 eq.) were added. Then the white suspension was boiling overnight. After cooling down to ambient temperature, the reaction mixture was diluted with ethyl acetate (20 mL) and water (20 mL). After extraction of the water phase for 3 times with ethyl acetate (10 mL), the organic phases were combined, washed with brine, dried over Na₂SO₄, and evaporated under reduced pressure to give the crude product. The compounds were then purified by flash chromatography on silica gel.

Method I: Selective bromination at 8-position

To the solution of corresponding dihydroquinolinone (1.0 eq.) in DMF (5 mL / mmol) was dropped in NBS (1.1 eq.) solution in DMF (2 mL / mmol) at 65 °C. The addition lasted for 3 hours, and then the reaction mixture was hold at 65 °C for another 3 hours before extraction with ethyl acetate (20 mL) and water (20 mL). After extraction of the water phase for 3 times with ethyl acetate (10 mL), the organic phases were combined, washed with brine, dried over Na₂SO₄, and evaporated under reduced pressure to give the crude product. The compounds were then purified by flash chromatography on silica gel.

8-Bromo-6-pyridin-3-yl-3,4-dihydro-1H-quinolin-2-one (16). Synthesized according to Method I using 6-(pyridin-3-yl)-3,4-dihydroquinolin-2(1H)-one (0.50 g, 2.23 mmol) and NBS (0.40 g, 2.23 mmol); yield: 0.61 g (90%); white solid: mp 175–176 °C; $R_f = 0.25$ (DCM/MeOH, 50:1); δ_H (CDCl₃, 500 MHz) 2.70 (t, $J = 7.9$ Hz, 2H, CH₂), 3.09 (t, $J = 7.9$ Hz, 2H, CH₂), 7.35–7.37 (m, 2H), 7.64 (d, $J = 1.8$ Hz, 1H), 7.81 (dt, $J = 1.8, 7.9$ Hz, 1H), 7.84 (s, br, 1H, NH), 8.61 (dd, $J = 1.5, 5.4$ Hz, 1H), 8.79 (d, $J = 1.8$ Hz, 1H); MS (ESI): $m/z = 303$ [M⁺+H].

Acknowledgements

The authors appreciate Christina Zimmer, Jeannine Jung and Jannine Ludwig for the help in determination of bioactivity, and thank Professor J. Hermans (Cardiovascular Research Institute, University of Maastricht, The Netherlands) and Professor R. Bernhardt (Saarland University, Germany) for providing us with V79MZh11B cells expressing human CYP11B1 and CYP11B2, respectively.

Supporting Information Available: The synthetic procedures and characterization of compounds **7**, **8**, **10**, **12**, **14**, **17**, **18** and rest intermediates as well as HPLC purities, ¹³C-NMR and IR spectra of all final compounds. This material is available free of charge via the internet at <http://pubs.acs.org>.

References

1. Puliti, D.; Miccinesi, G.; Collina, N.; De Lisi, V.; Federico, M.; Ferretti, S.; Finarelli, A. C.; Foca, F.; Mangone, L.; Naldoni, C.; Petrella, M.; Ponti, A.; Segnan, N.; Sigonal, A.; Zarcone, M.; Zorzi, M.; Zappa, M.; Paci, E.; the IMPACT Working Group. Effectiveness of service screening: a case-control study to assess breast cancer mortality reduction. *Brit. J. Cancer* **2008**, *99*,

- 423–427.
2. Miller, W. R. Endocrine treatment for breast cancers: biological rationale and current progress. *J. Steroid Biochem. Mol. Biol.* **1990**, *37*, 467–480.
 3. Wang, T.; You, Q.; Huang, F. S.; Xiang, H. Recent advances in selective estrogen receptor modulators for breast cancer. *Mini Rev. Med. Chem.* **2009**, *9*, 1191–1201.
 4. Perez, E. A. Safety profiles of tamoxifen and the aromatase inhibitors in adjuvant therapy of hormone-responsive early breast cancer. *Ann. Oncol.* **2007**, *18*, viii26–viii35.
 5. (a) Jurgen, G.; Ben, H.; Gun, A.; Mitch, D.; Per Eystein, L. Influence of letrozole and anastrozole on total body aromatization and plasma estrogen levels in postmenopausal breast cancer patients evaluated in a randomized, cross-over study. *J. Clin. Oncol.* **2002**, *20*, 751–757. (b) Jurgen, G.; Nick, K.; Gun, A.; Giorgio, O.; Enrico, D. S.; Per Eystein, L.; Mitch, D. In vivo inhibition of aromatization by exemestane, a novel irreversible aromatase inhibitor, in postmenopausal breast cancer patients. *Clin. Cancer Res.* **1998**, *4*, 2089–2093.
 6. (a) Goss, P. E.; Ingle, J. N.; Martino, S.; Robert, N. J.; Muss, H. B.; Piccart, M. J.; Castiglione, M.; Tu, D.; Shepherd, L. E.; Pritchard, K. I.; Livingston, R. B.; Davidson, N. E.; Norton, L.; Perez, E. A.; Abrams, J. S.; Cameron, D. A.; Palmer, M. J.; Pater, J. L. Randomized trial of Letrozole following Tamoxifen as extended adjuvant therapy in receptor-positive breast cancer: Updated findings from NCIC CTG MA.17. *J. Natl. Cancer Inst.* **2005**, *97*, 1262–1271. (b) Coombes, R. C.; Kilburn, L. S.; Snowdon, C. F.; Paridaens, R.; Coleman, R. E.; Jones, S. E.; Jassem, J.; Van de Velde, C. J.; Delozier, T.; Alvarez, I.; Del Mastro, L.; Ortmann, O.; Diedrich, K.; Coates, A. S.; Bajetta, E.; Holmberg, S. B.; Dodwell, D.; Mickiewicz, E.; Andersen, J.; Lonning, P. E.; Cocconi, G.; Forbes, J.; Castiglione, M.; Stuart, N.; Stewart, A.; Fallowfield, L. J.; Bertelli, G.; Hall, E.; Bogle, R. G.; Carpentieri, M.; Colajori, E.; Subar, M.; Ireland, E.; Bliss, J. M. Survival and safety of exemestane versus tamoxifen after 2–3 years' tamoxifen treatment (Intergroup Exemestane Study): a randomised controlled trial. *Lancet* **2007**, *369*, 559–570. (c) Baum, M.; Budzar, A. U.; Cuzick, J.; Forbes, J.; Houghton, J. H.; Klijn, J. G.; Sahmoud, T. Anastrozole alone or in combination with tamoxifen versus tamoxifen alone for adjuvant treatment of postmenopausal women with early breast cancer: first results of the ATAC randomised trial. *Lancet* **2002**, *359*, 2131–2139. (d) Thurlimann, B.; Keshaviah, A.; Coates, A. S.; Mouridsen, H.; Mauriac, L.; Forbes, J. F.; Paridaens, R.; Castiglione-Gertsch, M.; Gelber, R. D.; Rabaglio, M.; Smith, I.; Wardley, A.; Price, K. N.; Goldhirsch, A. A comparison of letrozole and tamoxifen in postmenopausal women with early breast cancer. *N. Engl. J. Med.* **2005**, *353*, 2747–2757. (e) Coates, A. S.; Keshaviah, A.; Thurlimann, B.; Mouridsen, H.; Mauriac, L.; Forbes, J. F.; Paridaens, R.; Castiglione-Gertsch, M.; Gelber, R. D.; Colleoni, M.; Lang, I.; Del Mastro, L.; Smith, I.; Chirgwin, J.; Nogaret, J. M.; Pienkowski, T.; Wardley, A.; Jakobsen E. H.; Price, K. N.; Goldhirsch, A. Five years of letrozole compared with tamoxifen as initial adjuvant therapy for postmenopausal women with endocrine-responsive early breast cancer: update of study BIG 1-98. *J. Clin. Oncol.* **2007**, *25*, 486–492. (f) Boccardo, F.; Rubagotti, A.; Puntoni, M.; Guglielmini, P.; Amoroso, D.; Fini, A.; Paladini, G.; Mesiti, M.; Romeo, D.; Rinaldini, M.; Scali, S.; Porpiglia, M.; Benedetto, C.; Restuccia, N.; Buzzi, F.; Franchi, R.; Massidda, B.; Distante, V.; Amadori, D.; Sismondi, P. Switching to Anastrozole versus continued Tamoxifen of early breast cancer: preliminary results of the italian tamoxifen anastrozole trial. *J. Clin. Oncol.* **2005**, *23*, 5138–5147. (g) Boccardo, F.; Rubagotti, A.; Guglielmini, P.; Fini, A.; Paladini, G.; Mesiti, M.; Rinaldini, M.; Scali, S.; Porpiglia, M.; Benedetto, C.; Restuccia, N.; Buzzi, F.; Franchi, R.; Massidda, B.; Distante, V.; Amadori, D.; Sismondi, P. Switching to anastrozole versus continued tamoxifen treatment of early breast cancer. Updated results of the Italian tamoxifen anastrozole (ITA) trial. *Ann. Oncol.* **2006**, *17*, vii10–vii14. (h) Jakesz, R.; Jonat, W.; Gnant, M.; Mittlboeck, M.; Greil, R.; Tausch, C.; Hilfrich, J.; Kwasny, W.; Menzel, C.; Samonigg, H.; Seifert, M.; Gademann, G.; Kaufmann, M.; Wolfgang, J. Switching of postmenopausal women with endocrine-responsive early breast cancer to anastrozole after 2 years' adjuvant tamoxifen: combined results of ABCSG trial 8 and ARNO 95 trial. *Lancet* **2005**, *366*, 455–462. (i) Goss, P. E.; Ingle, J. N.; Martino, S.; Robert, N. J.; Muss, H. B.; Piccart, M. J.; Castiglione, M.; Tu, D.; Shepherd, L. E.; Pritchard, K. I.; Livingston, R. B.; Davidson, N. E.; Norton, L.; Perez, E. A.; Abrams, J. S.; Therasse, P.; Palmer, M. J.; Pater, J. L. A randomized trial of letrozole in postmenopausal women after five years of tamoxifen therapy for early-stage breast cancer. *N. Engl. J. Med.* **2003**, *349*, 1793–1802. (j) Goss, P. E.; Ingle, J. N.; Martino, S.; Robert, N. J.; Muss, H. B.; Piccart, M. J.; Castiglione, M.; Tu, D.; Shepherd, L. E.; Pritchard, K. I.; Livingston, R. B.; Davidson, N. E.; Norton, L.; Perez, E. A.; Abrams, J. S.; Cameron, D. A.; Palmer, M. J.; Pater, J. L. Efficacy of Letrozole extended adjuvant therapy according to estrogen receptor and progesterone receptor status of the primary tumor: national cancer institute of canada clinical trials group MA.17. *J. Clin. Oncol.* **2007**, *25*, 2006–2011.
 7. Chapman, J. W.; Meng, D.; Shepherd, L.; Parulekar, W.; Ingle, J. N.; Muss, H. B.; Palmer, M.; Yu, C.; Goss, P. E. Competing causes of death from a randomized trial of extended adjuvant endocrine therapy for breast cancer. *J. Natl. Cancer Inst.* **2008**, *100*, 252–260.
 8. (a) Wang, Y.; Wang, Q.; Zhao, Y.; Gong, D.; Wang D.; Li, C.; Zhao, H. Protective effects of estrogen against reperfusion arrhythmias following severe myocardial ischemia in rats. *Circ. J.* **2010**, *74*, 634–643. (b) Merchenthaler, I.; Dellovade, T. L.; Shughrue, P. J. Neuroprotection by estrogen in animal models of global and focal ischemia. *Ann. N. Y. Acad. Sci.* **2003**, *1007*, 89–100. (c) Booth, E. A.; Marchesi, M.; Kilbourne, E. J.; Lucchesi, B. R. 17 β -Estradiol as a receptor-mediated cardioprotective agent. *J. Pharmacol. Exp. Ther.* **2003**, *307*, 395–401. (d) Jazbutyte, V.; Arias-Loza, P. A.; Hu, K.; Widder, J.; Govindaraj, V.; von Poser-Klein, C.; Bauersachs, J.; Fritzscheier, K. H.; Hegele-Hartung, C.; Neyses, L.; Ertl, G.; Pelzer, T. Ligand-dependent activation of ER β lowers blood pressure and attenuates cardiac hypertrophy in ovariectomized spontaneously hypertensive rats. *Cardiovasc. Res.* **2008**, *77*, 774–781. (e) Beer, S.; Reincke, M.; Kral, M.; Callies, F.; Ströer, H.; Dienesch, C.; Steinhauer, S.; Ertl, G.; Allolio, B.; Neubauer, S. High-dose 17 β -estradiol treatment prevents development of heart failure post-myocardial infarction in the rat. *Basic Res. Cardiol.* **2007**, *102*, 9–18. (f) Gardner, J. D.; Murray, D. B.; Voloshenyuk, T. G.; Brower, G. L.; Bradley, J. M.; Janicki, J. S. Estrogen attenuates chronic volume overload induced structural and functional remodeling in male rat hearts. *Am. J. Physiol. Heart Circ. Physiol.* **2010**, *298*, H497–H504. (g) Donaldson, C.; Eder, S.; Baker, C.; Aronovitz, M. J.; Weiss, A. D.; Hall-Porter, M.; Wang, F.; Ackerman, A.; Karas, R. H.; Molkenstin, J. D.; Patten, R. D. Estrogen attenuates left ventricular and cardiomyocyte hypertrophy by an estrogen receptor dependent pathway that increases calcineurin degradation. *Circ. Res.* **2009**, *104*, 265–275.
 9. Arias-Loza, P. A.; Muehlfelder, M.; Elmore, S. A.; Maronpot, R.; Hu, K.; Blode, H.; Hegele-Hartung, C.; Fritzscheier, K. H.; Ertl, G.; Pelzer, T. Differential effects of 17 β -estradiol and of synthetic progestins on aldosterone-salt-induced kidney disease. *Toxicol. Pathol.* **2009**, *37*, 969–982.
 10. (a) American Heart Association. Heart disease and stroke statistics: 2004 update. Dallas, TX: American Heart Association;

2003. (b) Witteman, J. C.; Grobbee, D. E.; Kok, F. J.; Hofman, A.; Valkenburg, H. A. Increased risk of atherosclerosis in women after the menopause. *Br. Med. J.* **1989**, *298*, 642–644.
11. (a) Nabholz, J. M.; Gligorov, J. Cardiovascular safety profiles of aromatase inhibitors: a comparative review. *Drug Saf.* **2006**, *29*, 785–801. (b) Pritchard, K. I.; Abramson, B. L. Cardiovascular health and aromatase inhibitors. *Drugs* **2006**, *66*, 1727–1740. (c) Cuppone, F.; Bria, E.; Verma, S.; Pritchard, K. I.; Gandhi, S.; Carlini, P.; Milella, M.; Nistico, C.; Terzoli, E.; Cognetti, F.; Giannarelli, D. Do adjuvant aromatase inhibitors increase the cardiovascular risk in postmenopausal women with early breast cancer? *Cancer* **2008**, *112*, 260–267. (d) Bundred, N. J. The effects of aromatase inhibitors on lipids and thrombosis. *Br. J. Cancer* **2005**, *93*, S23–S27. (e) Ewer, M. S.; Glück, S. A woman's heart. The impact of adjuvant endocrine therapy on cardiovascular health. *Cancer* **2009**, *115*, 1813–1826. (f) Healey Bird, B. R. J.; Swain, S. M. Cardiac toxicity in breast cancer survivors: review of potential cardiac problems. *Clin. Cancer Res.* **2008**, *14*, 14–24.
12. (a) Macova, M.; Armando, I.; Zhou, J.; Baiardi, G.; Tyurmin, D.; Larrayoz-Roldan, I. M.; Saavedra, J. M. Estrogen reduces aldosterone, upregulates adrenal angiotensin II AT2 receptors and normalizes adrenomedullary Fra-2 in ovariectomized rats. *Neuroendocrinology* **2008**, *88*, 276–286. (b) Hoshi-Fukushima, R.; Nakamoto, H.; Imai, H.; Kanno, Y.; Ishida, Y.; Yamanouchi, Y.; Suzuki, H. Estrogen and angiotensin II interactions determine cardio-renal damage in Dahl salt-sensitive rats with heart failure. *Am. J. Nephrol.* **2008**, *28*, 413–423.
13. (a) Castelli, W. P. Cardiovascular disease in women. *Am. J. Obstet. Gynecol.* **1988**, *158*, 1553–1560. (b) Fischer, M.; Baessler, A.; Schunkert, H. Renin angiotensin system and gender differences in the cardiovascular system. *Cardiovasc. Res.* **2002**, *53*, 672–677. (c) Roesch, D. M.; Tian, Y.; Zheng, W.; Shi, M.; Verbalis, J. G.; Sandberg, K. Estradiol attenuates angiotensin-induced aldosterone secretion in ovariectomized rats. *Endocrinology* **2000**, *141*, 4629–4636. (d) Chappell, M. C.; Gallagher, P. E.; Averill, D. B.; Ferrario, C. M.; Brosnihan, K. B. Estrogen or the AT1 antagonist olmesartan reverses the development of profound hypertension in the congenic mRen2.Lewis rat. *Hypertension* **2003**, *42*, 781–786. (e) Harrison-Bernard, L. M.; Schulman, I. H.; Raij, L. Post-ovariectomy hypertension is linked to increased renal AT1 receptor and salt sensitivity. *Hypertension* **2003**, *42*, 1157–1163. (f) Krishnamurthi, K.; Verbalis, J. G.; Zheng, W.; Wu, Z.; Clerch, L. B.; Sandberg, K. Estrogen regulates angiotensin AT1 receptor expression via cytosolic proteins that bind to the 5' leader sequence of the receptor mRNA. *Endocrinology* **1999**, *140*, 5435–5438.
14. (a) Zheng, W.; Shi, M.; Yoo, S. E.; Ji, H.; Roesch, D. M. Estrogens contribute to a sex difference in plasma potassium concentration: a mechanism for regulation of adrenal angiotensin receptors. *Gender Med.* **2006**, *3*, 43–53. (b) Ji, H.; Zheng, W.; Falconetti, C.; Roesch, D. M.; Mulroney, S. E.; Sandberg, K. 17 β -Estradiol deficiency reduces potassium excretion in an angiotensin type 1 receptor-dependent manner. *Am. J. Physiol. Heart Circ. Physiol.* **2007**, *293*, H17–H22.
15. (a) Gekle, M.; Grossmann, C. Actions of aldosterone in the cardiovascular system: the good, the bad, and the ugly? *Eur. J. Physiol.* **2009**, *458*, 231–246. (b) Duprez, D. A. Aldosterone and the vasculature: mechanisms mediating resistant hypertension. *J. Clin. Hypertension* **2007**, *9*, 13–18. (c) Rahmouni, K.; Barthelmebs, M.; Grima, M.; Imbs, J. L.; De Jong, W. Brain mineralocorticoid receptor control of blood pressure and kidney function in normotensive rats. *Hypertension* **1999**, *33*, 1201–1206. (d) Humphreys, M. Potassium disturbances and associated electrocardiogram changes. *Emerg. Nurse* **2007**, *15*, 28–34. (e) Romagnoli, P.; Rossi, F.; Guerrini, L.; Quirini, C.; Santemma, V. Aldosterone induces contraction of the resistance arteries in man. *Atherosclerosis* **2003**, *166*, 345–349. (f) Schmidt, B. M. W.; Sammer, U.; Fleischmann, I.; Schlaich, M.; Delles, C.; Schmieder, R. E. Rapid nongenomic effects of aldosterone on the renal vasculature in humans. *Hypertension* **2006**, *47*, 650–655. (g) Fejes-Tóth, G.; Náráy-Fejes-Tóth, A. Early aldosterone-regulated genes in cardiomyocytes: clues to cardiac remodeling? *Endocrinology* **2007**, *148*, 1502–1510. (h) Lal, A.; Veinot, J. P.; Leenen, F. H. H. Critical role of CNS effects of aldosterone in cardiac remodeling post-myocardial infarction in rats. *Cardiovasc. Res.* **2004**, *64*, 437–447. (i) Leibovitz, E.; Ebrahimian, T.; Paradis, P.; Schiffrin, E. L. Aldosterone induces arterial stiffness in absence of oxidative stress and endothelial dysfunction. *J. Hypertens.* **2009**, *27*, 2192–2200. (j) Fiebeler, A.; Luft, F. C. The mineralocorticoid receptor and oxidative stress. *Heart Fail. Rev.* **2005**, *10*, 47–52. (k) Joffe, H. V.; Adler, G. K. Effect of aldosterone and mineralocorticoid receptor blockade on vascular inflammation. *Heart Fail. Rev.* **2005**, *10*, 31–37. (l) Brown, N. J. Aldosterone and vascular inflammation. *Hypertension* **2008**, *51*, 161–167. (m) Fiebeler, A.; Muller, D. N.; Shagdarsuren, E.; Luft, F. C. Aldosterone, mineralocorticoid receptors, and vascular inflammation. *Curr. Opin. Nephrol. Hypertens.* **2007**, *16*, 134–142. (n) Weber, K. T. From inflammation to fibrosis: a stiff stretch of highway. *Hypertension* **2004**, *4*, 716–719. (o) Rader, D. J.; Daugherty, A. Translating molecular discoveries into new therapies for atherosclerosis. *Nature* **2008**, *451*, 904–913. (p) Blasi, E. R.; Rocha, R.; Rudolph, A. E.; Blomme, E. A.; Polly, M. L.; McMahon, E. G. Aldosterone/salt induces renal inflammation and fibrosis in hypertensive rats. *Kidney Int.* **2003**, *63*, 1791–1800. (q) Cortinovis, M.; Perico, N.; Cattaneo, D.; Remuzzi, G. Aldosterone and progression of kidney disease. *Ther. Adv. Cardiovasc. Dis.* **2009**, *3*, 133–143. (r) Zannad, F.; Radauceanu, A. Effect of MR blockade on collagen formation and cardiovascular disease with a specific emphasis on heart failure. *Heart Fail. Rev.* **2005**, *10*, 71–78. (s) Weber, K. T.; Brilla, C. G.; Campbell, S. E.; Guarda, E.; Zhou, G.; Sriram, K. Myocardial fibrosis: role of angiotensin II and aldosterone. *Basic Res. Cardiol.* **1993**, *88*, 107–124. (t) Brilla, C. G.; Zhou, G.; Matsubara, L.; Weber, K. T. Collagen metabolism in cultured adult rat cardiac fibroblasts: response to angiotensin II and aldosterone. *J. Mol. Cell. Cardiol.* **1994**, *26*, 809–820. (u) Qin, W.; Rudolph, A. E.; Bond, B. R.; Rocha, R.; Blomme, E. A. G.; Goellner, J. J.; Funder, J. W.; McMahon, E. G. Transgenic model of aldosterone-driven cardiac hypertrophy and heart failure. *Circ. Res.* **2003**, *93*, 69–76. (v) Felder, R. B. Mineralocorticoid receptors, inflammation and sympathetic drive in a rat model of systolic heart failure. *Exp. Physiol.* **2009**, *95*, 19–25. (w) Nicoletti, A.; Michel, J. B. Cardiac fibrosis and inflammation: interaction with hemodynamic and hormonal factors. *Cardiovasc. Res.* **1999**, *41*, 532–543. (x) Rodríguez-Sinovas, A.; Abdallah, Y.; Piper, H. M.; Garcia-Dorado, D. Reperfusion injury as a therapeutic challenge in patients with acute myocardial infarction. *Heart Fail. Rev.* **2007**, *12*, 207–216.
16. Lawrence Woo, L. W.; Sutcliffe, O. B.; Bubert, C.; Grasso, A.; Chander, S. K.; Purohit, A.; Reed, M. J.; Potter, B. V. L. First dual aromatase-steroid sulfatase inhibitors. *J. Med. Chem.* **2003**, *46*, 3193–3196.
17. (a) Richard, M.; Zoran, R. Designed multiple ligands. An emerging drug discovery paradigm. *J. Med. Chem.* **2005**, *48*, 6523–6543. (b) Andrea, C.; Laura, B. M.; Anna, M.; Michela, R.; Vincenzo, T.; Maurizio, R.; Carlo, M. Multi-target-directed ligands to combat neurodegenerative diseases. *J. Med. Chem.* **2008**, *51*, 347–372. (c) Richard, M. Selectively nonselective kinase inhibition: striking the right balance. *J. Med. Chem.* **2010**, *53*, 1413–1437.
18. (a) Hartmann, R. W.; Bayer, H.; Grün, G. Aromatase inhibitors. Syntheses and structure-activity studies of novel pyridyl-substituted indanones, indans, and tetralins. *J. Med. Chem.* **1994**, *37*, 1275–81. (b) Gobbi, S.; Cavalli, A.; Rampa, A.; Belluti, F.; Piazzi, L.; Paluszczak, A.; Hartmann, R. W.; Recanatini, M.; Bisi, A. Lead optimization providing a series of flavone derivatives

- as potent nonsteroidal inhibitors of the cytochrome P450 aromatase enzyme. *J. Med. Chem.* **2006**, *49*, 4777–4780. (c) Gobbi, S.; Zimmer, C.; Belluti, F.; Rampa, A.; Hartmann, R. W.; Recanatini, M.; Bisi, A. Novel highly potent and selective nonsteroidal aromatase inhibitors: synthesis, biological evaluation and structure-activity relationships investigation. *J. Med. Chem.* **2006**, *49*, 5347–5351. (d) Le Borgne, M.; Marchand, P.; Duflos, M.; Delevoye-Seiller, B.; Piessard-Robert, S.; Le Baut, G.; Hartmann, R. W.; Palzer, M. Synthesis and in vitro evaluation of 3-(1-azolylmethyl)-1H-indoles and 3-(1-azoly-1-phenylmethyl)-1H-indoles as inhibitors of P450 arom. *Arch. Pharm. (Weinheim, Ger.)* **1997**, *330*, 141–145. (e) Woo, L. W. L.; Jackson, T.; Putey, A.; Cozier, G.; Leonard, P.; Acharya, K. R.; Chander, S. K.; Purohit, A.; Reed, M. J.; Potter, B. V. L. Highly Potent First Examples of Dual Aromatase-Steroid Sulfatase Inhibitors based on a Biphenyl Template. *J. Med. Chem.* **2010**, *53*, 2155–2170. (f) Leze, M. P.; Le Borgne, M.; Pinson, P.; Paluszczak, A.; Duflos, M.; Le Baut, G.; Hartmann, R. W. Synthesis and biological evaluation of 5-[(aryl)(1H-imidazol-1-yl)methyl]-1H-indoles: potent and selective aromatase inhibitors. *Bioorg. Med. Chem. Lett.* **2006**, *16*, 1134–1137. (g) Gobbi, S.; Cavalli, A.; Negri, M.; Schewe, K. E.; Belluti, F.; Piazzini, L.; Hartmann, R. W.; Recanatini, M.; Bisi, A. Imidazolylmethylbenzophenones as highly potent aromatase inhibitors. *J. Med. Chem.* **2007**, *50*, 3420–3422. (h) Leonetti, F.; Favia, A.; Rao, A.; Aliano, R.; Paluszczak, A.; Hartmann, R. W.; Carotti, A. Design, synthesis, and 3D QSAR of novel potent and selective aromatase inhibitors. *J. Med. Chem.* **2004**, *47*, 6792–6803.
19. (a) Hutschenreuter, T. U.; Ehmer, P. E.; Hartmann, R. W. Synthesis of hydroxy derivatives of highly potent non-steroidal CYP 17 Inhibitors as potential metabolites and evaluation of their activity by a non cellular assay using recombinant human enzyme. *J. Enzyme Inhib. Med. Chem.* **2004**, *19*, 17–32. (b) Hu, Q.; Negri, M.; Jahn-Hoffmann, K.; Zhuang, Y.; Olgen, S.; Bartels, M.; Müller-Vieira, U.; Lauterbach, T.; Hartmann, R. W. Synthesis, biological evaluation, and molecular modeling studies of methylene imidazole substituted biaryls as inhibitors of human 17 α -hydroxylase-17,20-lyase (CYP17)-Part II: Core rigidification and influence of substituents at the methylene bridge. *Bioorg. Med. Chem.* **2008**, *16*, 7715–7727. (c) Hille, U. E.; Hu, Q.; Vock, C.; Negri, M.; Bartels, M.; Müller-Vieira, U.; Lauterbach, T.; Hartmann, R. W. Novel CYP17 inhibitors: Synthesis, biological evaluation, structure-activity relationships and modeling of methoxy- and hydroxy-substituted methyleneimidazolyl biphenyls. *Eur. J. Med. Chem.* **2009**, *44*, 2765–2775. (d) Hu, Q.; Negri, M.; Olgen, S.; Hartmann, R. W. The role of fluorine substitution in biphenyl methylene imidazole type CYP17 inhibitors for the treatment of prostate carcinoma. *ChemMedChem.* **2010**, In Press. DOI: 10.1002/cmdc.201000065. (e) Hu, Q.; Jagusch, C.; Hille, U. E.; Hauptenthal, J.; Hartmann, R. W. Replacement of imidazolyl by pyridyl in biphenyl methylenes results in selective CYP17 and dual CYP17 / CYP11B1 inhibitors for the treatment of prostate cancer. *J. Med. Chem.* **2010**, In Press. (f) Hu, Q.; Yin, L.; Jagusch, C.; Hille, U. E.; Hartmann, R. W. Isopropylidene Substitution Increases Activity and Selectivity of Biphenyl Methylene 4-Pyridine Type CYP17 Inhibitors. *J. Med. Chem.* **2010**, In Press.
20. (a) Lucas, S.; Heim, R.; Ries, C.; Schewe, K. E.; Birk, B.; Hartmann, R. W. In vivo active aldosterone synthase inhibitors with improved selectivity: lead optimization providing a series of pyridine substituted 3,4-dihydro-1H-quinolin-2-one derivatives. *J. Med. Chem.* **2008**, *51*, 8077–8087. (b) Lucas, S.; Heim, R.; Negri, M.; Antes, I.; Ries, C.; Schewe, K. E.; Bisi, A.; Gobbi, S.; Hartmann, R. W. Novel aldosterone synthase inhibitors with extended carbocyclic skeleton by a combined ligand-based and structure-based drug design approach. *J. Med. Chem.* **2008**, *51*, 6138–6149. (c) Heim, R.; Lucas, S.; Grombein, C. M.; Ries, C.; Schewe, K. E.; Negri, M.; Müller-Vieira, U.; Birk, B.; Hartmann, R. W. Overcoming undesirable CYP1A2 inhibition of pyridyl-naphthalene-type aldosterone synthase inhibitors: influence of heteroaryl derivatization on potency and selectivity. *J. Med. Chem.* **2008**, *51*, 5064–5074. (d) Voets, M.; Antes, I.; Scherer, C.; Müller-Vieira, U.; Biemel, K.; Marchais-Oberwinkler, S.; Hartmann, R. W. Synthesis and evaluation of heteroaryl-substituted dihydronaphthalenes and indenones: potent and selective inhibitors of aldosterone synthase (CYP11B2) for the treatment of congestive heart failure and myocardial fibrosis. *J. Med. Chem.* **2006**, *49*, 2222–2231. (e) Voets, M.; Antes, I.; Scherer, C.; Müller-Vieira, U.; Biemel, K.; Barassin, C.; Marchais-Oberwinkler, S.; Hartmann, R. W. Heteroaryl-substituted naphthalenes and structurally modified derivatives: selective inhibitors of CYP11B2 for the treatment of congestive heart failure and myocardial fibrosis. *J. Med. Chem.* **2005**, *48*, 6632–6642. (f) Ulmschneider, S.; Müller-Vieira, U.; Klein, C. D.; Antes, I.; Lengauer, T.; Hartmann, R. W. Synthesis and evaluation of (pyridylmethylene) tetrahydronaphthalenes/-indanes and structurally modified derivatives: potent and selective inhibitors of aldosterone synthase. *J. Med. Chem.* **2005**, *48*, 1563–1575. (g) Ulmschneider, S.; Müller-Vieira, U.; Mitrenga, M.; Hartmann, R. W.; Oberwinkler-Marchais, S.; Klein, C. D.; Bureik, M.; Bernhardt, R.; Antes, I.; Lengauer, T. Synthesis and evaluation of imidazolylmethylene tetrahydronaphthalenes and imidazolylmethyleneindanes: potent inhibitors of aldosterone synthase. *J. Med. Chem.* **2005**, *48*, 1796–1805.
21. (a) Ehmer, P. B.; Jose, J.; Hartmann, R. W. Development of a simple and rapid assay for the evaluation of inhibitors of human 17 α -hydroxylase-C(17,20)-lyase (P450c17) by coexpression of P450c17 with NADPH-cytochrome-P450-reductase in *Escherichia coli*. *J. Steroid Biochem. Mol. Biol.* **2000**, *75*, 57–63. (b) Denner, K.; Doehmer, J.; Bernhardt, R. Cloning of CYP11B1 and CYP11B2 from normal human adrenal and their functional expression in COS-7 and V79 chinese hamster cells. *Endocr. Res.* **1995**, *21*, 443–448. (c) Ehmer, P. B.; Bureik, M.; Bernhardt, R.; Müller, U.; Hartmann, R. W. Development of a test system for inhibitors of human aldosterone synthase (CYP11B2): Screening in fission yeast and evaluation of selectivity in V79 cells. *J. Steroid Biochem. Mol. Biol.* **2002**, *81*, 173–179. (d) Hartmann, R. W.; Batzl, C. Aromatase inhibitors. Synthesis and evaluation of mammary tumor inhibiting activity of 3-alkylated 3-(4-aminophenyl)piperidine-2,6-diones. *J. Med. Chem.* **1986**, *29*, 1362–1369.

3.VI Novel Heterocycle Substituted 4,5-Dihydro-[1,2,4]triazolo[4,3-a]quinolines as Potent and Selective Aldosterone Synthase Inhibitors for the Treatment of Related Cardiovascular Diseases

Qingzhong Hu, Lina Yin, and Rolf W. Hartmann

This manuscript will be submitted to

Journal of Medicinal Chemistry

Paper VI

Abstract: Excessive aldosterone exhibits various deleterious effects on vessels, heart, kidney and central nervous system. It is closely related to cardiac fibrosis, congestive heart failure, chronic hypertension, myocardial infarction and stroke, which often lead to disability and sudden death. The inhibition of CYP11B2, the crucial enzyme in aldosterone biosynthesis, is a promising and superior therapy for these diseases related compared to the ACE inhibitors and MR antagonists. Based on our previously identified CYP11B2 inhibitors, a series of novel heterocycle substituted 4,5-dihydro-[1,2,4]triazolo[4,3-a]quinolines were designed, synthesized and bio-evaluated. The study leads to many potent and highly selective CYP11B2 inhibitors, especially compound **24** ($IC_{50} = 4.2$ nM, selectivity factor ($IC_{50\text{ CYP11B1}} / IC_{50\text{ CYP11B2}} = 422$). This compound is considered as a promising drug candidate after further evaluation in vivo.

Introduction

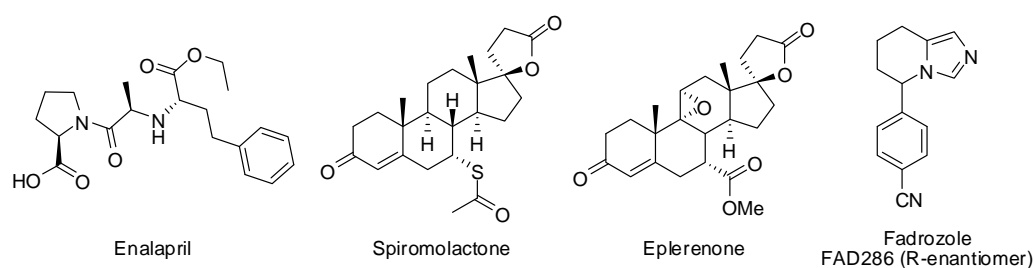
Aldosterone has been considered only as the mineralocorticoid in circulation to regulate electrolyte and fluid homeostasis for a long time since its discovery in 1953.¹ It is widely accepted that after the binding of aldosterone to mineralocorticoid receptor (MR)^a in epithelial cells of renal collecting duct, the conformation of MR is changed. This renders MR to migrate into the cell nucleus and finally to activate gene transcription modulating the activity of amiloride-sensitive epithelial sodium channel (ENaC). As results, sodium and water are retained leading to the increase of blood volume and consequently elevated blood pressure. Nevertheless, recent studies revealed that aldosterone elicits some additional, non-classic effects on vessels, heart, kidney and central nervous system. There are reports that the biosyntheses of aldosterone also takes place in other target organs like heart and vessels.^{2,3} Normally, the secretion of aldosterone is strictly regulated by the negative feedback loop of renin-angiotensin-aldosterone system (RAAS), as well as the concentration of potassium and adrenocorticotrophic hormone (ACTH). Any disturbances of the balance will result in the abnormality of aldosterone level. High aldosterone concentration exhibits various deleterious effects on its target organs, the severest on heart.⁴ Aldosterone is a potent pro-inflammation factor⁵ and is capable of inducing reactive oxygen species (ROS).⁶ These effects result in vascular fibrosis and vascular endothelium stiffening⁷ and are thought to be closely related to atherosclerosis,⁸ which is a high risk factor for stroke and ischemia related myocardial infarction (MI) that lead to disability and death. Aldosterone also promotes calcium influx into smooth muscle cells,⁹ up-regulates the expression of adrenomedullin and regulator of G protein signaling-2 (RGS2)¹⁰ and engenders excitatory sympathetic tone¹¹ after acting on CNS. These effects lead to vasoconstriction and, together the blood volume increase mentioned above, finally result into chronic hypertension. Furthermore, excessive aldosterone causes cardiac myocyte necrosis, collagen synthesis and fibroblast proliferation resulting in cardiac fibrosis and increase of myocardial stiffness.¹² These damages are mediated in part via the expression of some genes closely related to cardiac fibrosis, for example: tenascin-X (TNX), urokinase plasminogen activator receptor (UPAR) and a disintegrin and metalloprotease with thrombospondin motifs (ADAMTS1).¹⁰ Consequently, cardiac hypertrophy and ventricular remodelling result as the outcome of severe cardiac fibrosis. Inflammation, chronic hypertension, reperfusion injury, myocardial infarction and some other events stimulated by excessive aldosterone all contribute to this pathological process.¹³ The ventricular remodeling causes diastolic dysfunction, diminishes contractile capability, reduces stroke volume and ultimately results in congestive heart failure (CHF), which often leads to sudden death. Besides heart, high aldosterone level causes renal vascular fibrosis, glomerular injury, tubular damage and interstitial fibrosis as well.¹⁴

Hence, the control of the high aldosterone level is necessary and urgent for the patients with related diseases. Since ACTH involves in the production and release of other adrenal steroids, it is not suitable for this purpose. On the contrary, two different approaches to suppress the RAAS components are employed in clinic: angiotensin converting enzyme (ACE) inhibitors and MR antagonists. ACE inhibitors, such as enalapril (Chart 1), block the biosyntheses of angiotensin II (Ang II) and the subsequent aldosterone. Since ACE inhibitors relieve the vasoconstriction irrigated by Ang II and aldosterone, they are exploited in the treatment of hypertension and CHF. However, the long-term plasma aldosterone level is only slightly

influenced by the application of ACE inhibitors, which is known as “aldosterone escape”,¹⁵ probably due to the complicated regulation mechanism of aldosterone biosyntheses. As for MR antagonists, such as spironolactone and eplerenone (Chart 1), although several clinical trails have demonstrated their improvement on morbidity and mortality of heart failure, adverse effects like gynaecomastia and hyperkalemia are common.¹⁶ Moreover, MR antagonists leave high level of aldosterone unaffected, which can leads to further exacerbation of heart dysfunction in a MR independent non-genomic manner.¹⁷ Given these facts, the inhibition of aldosterone synthase (CYP11B2) is expected as a superior therapy for these diseases.

CYP11B2 is a mitochondrial cytochrome P450 enzyme, which is crucial in aldosterone production due to the consecutive three steps from 11-deoxycorticosterone (DOC) to aldosterone depends on its catalysis. Recent in vivo studies in rats proved that CYP11B2 inhibitors, for example FAD286 (*R*-enantiomer of the aromatase inhibitor Fadrozole, Chart 1), can significantly reduce the plasma aldosterone levels,¹⁸ and hence improve cardiac haemodynamics as well as cardiac function in rats with heart failure.¹⁹

Chart 1. Structures of ACE inhibitor Enalapril, MR antagonists Spiromolactone and Eplerenone and CYP11B2 inhibitor Fadrozole.



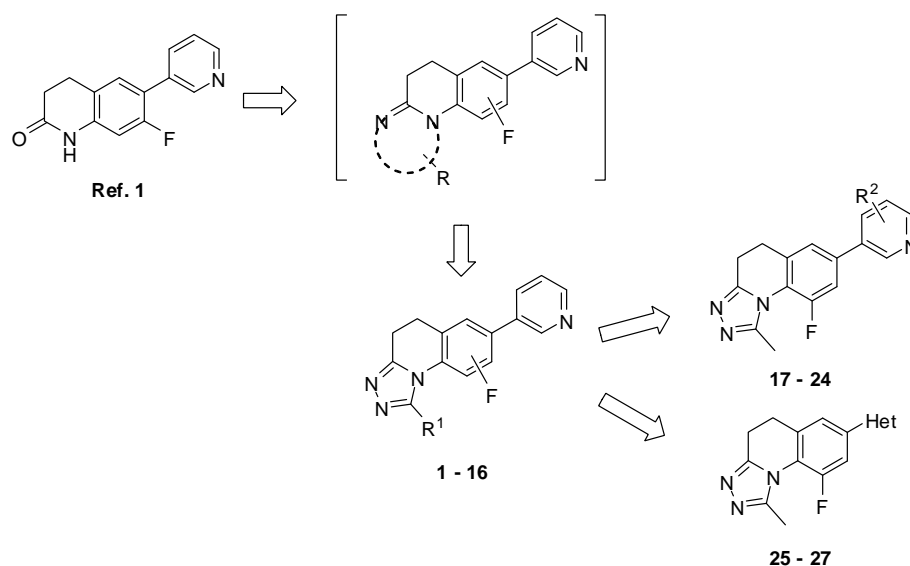
Our groups has designed and synthesized several series of CYP11B2 inhibitors.²⁰ Compared to FAD286, these compounds are not only potent, but also, importantly, much more selective over 11 β -hydroxylase (CYP11B1), which is responsible for the production of glucocorticoids. This selectivity is a challenging task to achieve because of more than 93% homology between these two enzymes. In aim to further optimize these inhibitors, a series of heterocycle substituted 4,5-dihydro-[1,2,4]triazolo[4,3-*a*]quinolines (**1–27**) were designed. In this study, the syntheses and biological evaluation of these compounds are described. The inhibition of CYP11B1 and CYP11B2 are presented with Fadrozole (Chart 1) as a reference, which is a potent CYP19 inhibitor showing unselective inhibition toward CYP11B1 and CYP11B2. Moreover, the selectivity of these compounds against aromatase (CYP19) and 17 α -hydroxylase-17,20-lyase (CYP17), which are the crucial enzymes in the biosynthesis of estrogens and androgens respectively, are also determined as a safety criteria.

Inhibitors design conception

All the reported CYP11B2 inhibitors competitively bind to the enzyme via the coordination of their sp^2 hybrid nitrogen to the heme iron, which is the common catalytic centre of all CYP enzymes. This reversible inhibition mechanism was first identified for CYP19 inhibitors,^{21a} and later on was also applied to other CYP19,^{21b-g} CYP17 and CYP11B1 inhibitors.²² Due to the similar structure and conformation among

steroidogenic enzymes and the same mode of action shown by their inhibitors, selectivity is always a tough aim to pursue. Fortunately, after careful design of the hydrophobic core and subsequent optimization, high selectivity is achieved for these steroidogenic enzymes, especially CYP11B2²⁰ and CYP17.^{22e} It is realized that sometimes the key to high selectivity lays in one or two small substituents,^{20h,22e} which also provided clues to design dual inhibitors.^{20h,22d} We have identified fluorinated pyridyl 3,4-dihydroquinolin-2(1*H*)-one analogue **Ref. 1**^{20h} (Chart 2) as a potent and selective CYP11B2 inhibitor (IC₅₀ = 11 nM, selectivity factor = 122). For this series of CYP11B2 inhibitors, the O from amide is believed to form H-bond with some amino acids nearby, which is important for the inhibitory potency.^{20a,b} Moreover, methylation of amide to remove the proton also contributes to the CYP11B2 inhibition.^{20a,h} Assisted by these SARs, we continue with the structural optimization to probe the surrounding of the amide moiety, to further improve activity and selectivity and to conceal the amide moiety, which is possibly vulnerable in vivo. The O was firstly replaced by its bio-isostere N. Next, an additional ring was fused onto the 3,4-dihydroquinolin-2(1*H*)-one core embodying the N and the methyl group. Considering the possibility of extra H-bond forming, another N was inserted into the ring additionally. Thereby, 4,5-dihydro-[1,2,4]triazolo[4,3-*a*]quinoline core was designed (Chart 2). Since fluorine substitution significantly increased the CYP11B2 inhibitory potency,^{20h} it was sustained as well; and the scrutiny on influence of F in different position was performed. Introduction of alkyl or aryl substituents in various bulk and electrostatic potential into the triazolo moiety lead to compound **1–16**. After ascertaining the most suitable substituents and F position, the optimization on heterocycle was carried out. Inserting of various substituents on pyridyl or displacing pyridyl by other N containing heterocycles yielded compounds **17–27**.

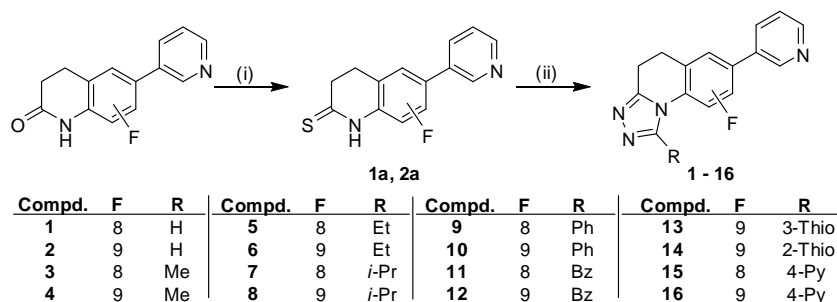
Chart 1. Inhibitor design conception.



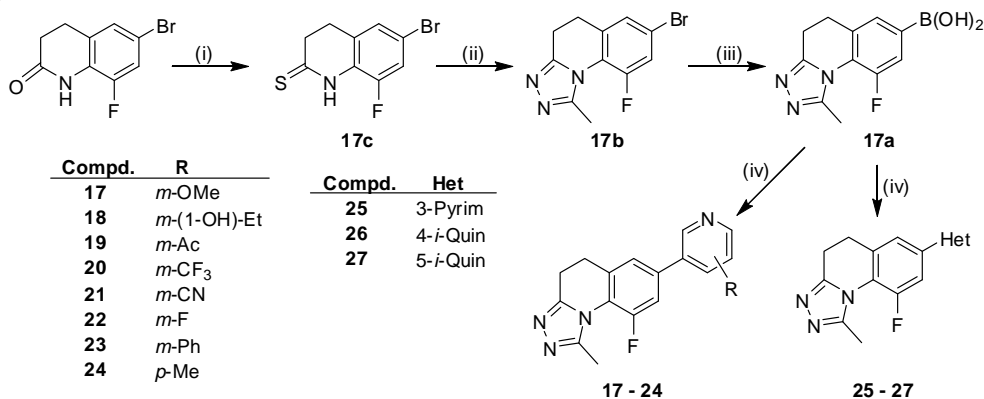
Results and Discussion

Chemistry. The synthesis of compounds **1–27** is shown in Schemes 1–2. All the compounds can be disassembled into three moieties: the 4,5-dihydro-[1,2,4]triazolo[4,3-*a*]quinolines core, substituents at the 1-position of the core and N-containing heterocycles. According to the moieties to be optimized, different strategies were employed to facilitate the syntheses. For compounds with various substituents at the 1-

position of the dihydrotriazoloquinolines core (**1–16**), it started with the corresponding fluorinated 6-(pyridin-3-yl)-3,4-dihydroquinolin-2(1*H*)-ones.^{20h} The starting materials were firstly sulphurated with Lawesson's reagent to give the dihydroquinolinethiones intermediates **1a** and **2a**, which were subsequently annulated with acylhydrazine in cyclohexanol to afford the corresponding products. However, as for the compounds with different heterocycles (**17–27**), 9-fluoro-1-methyl-4,5-dihydro-[1,2,4]triazolo[4,3-*a*]quinolin-7-yl boronic acid (**17a**) was exploited as a common building block, which was obtained from 6-bromo-8-fluoro-3,4-dihydroquinolin-2(1*H*)-one via sulphuration, cyclization and then borylation with triisopropyl borate and *n*-BuLi. This building block was subsequently coupled with corresponding heterocyclic bromines to yield the desired final compounds.

Scheme 1.^a

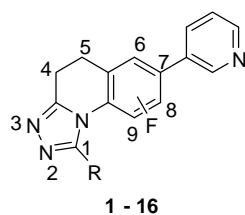
^a Reagents and conditions: (i) Method A: Lawesson's reagent, toluene, reflux, 2h; (ii) Method B: corresponding acylhydrazine, cyclohexanol, reflux, 6h.

Scheme 2.^a

^a Reagents and conditions: (i) Method A: Lawesson's reagent, toluene, reflux, 2h; (ii) Method B: corresponding acylhydrazine, cyclohexanol, reflux, 6h; (iii) *n*-BuLi, triisopropyl borate, toluene, THF, HCl, -40 °C, 3h; (iv) Method C: Pd(OAc)₂, corresponding boronic acid, Na₂CO₃, TBAB, toluene, H₂O, ethanol, reflux, 6h.

CYP11B2 and CYP11B1 inhibition. The inhibitory activities of the compounds were determined in V79 MZh cells expressing human CYP11B2 or CYP11B1^{23a-b} with [¹⁴C]-deoxycorticosterone as substrate. The products were measured using HPTLC with a phosphoimager. Inhibition percentage or IC₅₀ values are presented in comparison to Fadrozole in Tables 1–2, which is a CYP19 inhibitor capable of reducing corticoid formation.

It is apparent that the substituents on the dihydrotriazoloquinolines core showed significant influence on the inhibitory potency toward CYP11B2 (Table 1). The bulk of the substituent was found to be a crucial determinant. It can be observed that the analogues without substitution (**1** and **2**) exhibited potent inhibition around 200 nM; nevertheless, the introduction of methyl group (**3** and **4**) promoted the potency by 2 to 3 fold

Table 1. Inhibition of CYP11B1 and CYP11B2 by compounds **1** – **16**.

Compd.	Structure		CYP11B2		CYP11B1		SF ^d
	F	R	Inhibit.% ^{a,c}	IC ₅₀ (nM) ^{b,c}	Inhibit.% ^{a,c}	IC ₅₀ (nM) ^{b,c}	
1	8	H	69.5%	244.0	3.4%	7900	32
2	9	H	73.0%	172.2	4.8%	16100	94
3	8	Me	66.9%	131.4	0.8%	12620	96
4	9	Me	86.6%	62.5	1.3%	16990	272
5	8	Et	33.8%		0.0%		
6	9	Et	48.0%		1.8%		
7	8	<i>i</i> -Pr	9.8%		2.3%		
8	9	<i>i</i> -Pr	2.4%		2.2%		
9	8	Ph	2.5%		3.5%		
10	9	Ph	0.5%		1.0%		
11	8	Bz	10.3%		0.0%		
12	9	Bz	41.4%		1.4%		
13	9	3-Thio	51.0%		8.4%		
14	9	2-Thio	52.8%		7.3%		
15	8	4-Py	1.0%		0.8%		
16	9	4-Py	0.0%		2.8%		
FDZ^d				0.8		6.3	8.3

^a Inhibition percentage with compound concentration of 500 nM. Standard deviations were within $< \pm 5\%$; All the data are the mean values of at least 3 tests.

^b Concentration of inhibitors required to give 50 % inhibition. Standard deviations were within $< \pm 5\%$; All the data are the mean values of at least 3 tests.

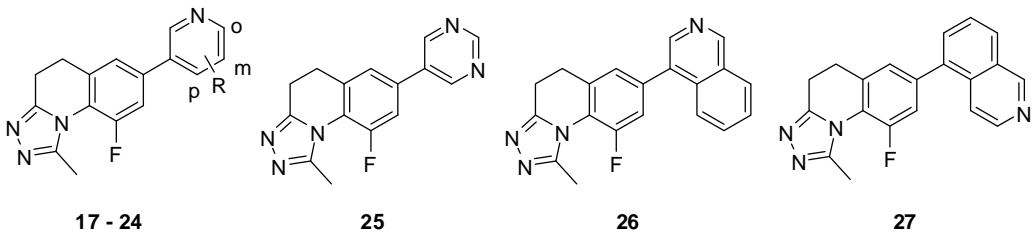
^c Hamster fibroblasts expressing human CYP11B1 or CYP11B2 are used with deoxycorticosterone as the substrate at a concentration of 100 nM.

^d **FDZ**: Fadrozole; SF: selective factor = $IC_{50\text{ CYP11B1}} / IC_{50\text{ CYP11B2}}$; n.d. not determined.

to 63 and 131 nM, respectively. However, ethyl analogues **5** and **6** showed largely reduced inhibition around 40% at 500 nM; and further augment of bulk to *i*-propyl resulting in compounds **7** and **8** dramatically decreased the inhibition to less than 10%. The demolition of inhibition was also observed for aryl substitution such as phenyl (**9** and **10**), benzyl (**11** and **12**) and 4-pyridyl (**15** and **16**). Interestingly, thiophenyl as a bio-isostere of phenyl rendered the compounds **13** and **14** to be modest inhibitors with about 50% inhibition at 500 nM. This is probably due to its smaller bulk compared to phenyl made it tolerable to the hydrophobic pocket of the enzyme. Furthermore, the position that fluorine furnished also profoundly influence the inhibition. 9-F analogue **4** ($IC_{50} = 63$ nM) is two fold more potent than the corresponding 8-F analogue **3** ($IC_{50} = 131$ nM). Same phenomenon can be observed for compounds pairs of **1** and **2** (244 nM vs

172 nM), **5** and **6** (34% vs 48%) and so on. As for the CYP11B1 inhibition, no response to the substituents alternation was found. Almost all compounds exhibited less than 5% inhibition at 500 nM, which rendered the potent CYP11B2 inhibitors also very selective, especially compound **4** with 9-F, 1-Me substitution exhibiting IC_{50} value of 63 nM and selectivity of 272. This substitution pattern was therefore sustained when investigation of heterocycles was further performed.

Because the inhibitors coordinate to the heme iron of the enzyme with the sp^2 hybrid N, the heterocycle presenting N is considered to be an important influence factor for the inhibitory potency. Hence, various substituents in different bulk and electro features are introduced to the *meta*- or *para*- position of pyridyl ring leading to compounds **17–24** (Table 2) and different N containing heterocycles were employed to replace pyridyl resulting in compounds **25–27** (Table 2). It can be seen that when electron donating groups like methoxyl (**17**) and 1-OH-ethyl (**18**) furnished at the *meta*-position of pyridyl, the analogues showed 3 fold more potent inhibition than their precursor compound **4** with IC_{50} values around 25 nM. These twocompounds also exhibited good selectivity over CYP11B1 with selective factors ($IC_{50\text{ CYP11B1}} / IC_{50\text{ CYP11B2}}$) of 89 and 138, respectively. However, introduction of electron withdrawing groups such as acetyl (**19**), trifluoromethyl (**20**) and fluoro (**22**) conferred these analogues similar to or slightly less potent than parent compound **4** with IC_{50} values ranged 57 to 90 nM. Interestingly, compound **21** with cyano substituted lost inhibitory ability showing only 30% inhibition at 500 nM. After the substitution of electron withdrawing groups, these compounds still exhibited good selectivity around 70, excepting fluoro analogue **22**, for which excellent selectivity of 329 was achieved. Moreover, after the bulky electron donating group phenyl was introduced to the *meta*-position of pyridyl leading to compound **23**, significant elevation of inhibitory potency toward both CYP11B2 and CYP11B1 was observed. Since similar phenomenon was also noticed for pyridyl substituted 3,4-dihydroquinolin-2(1*H*)-ones,^{20a} the class **Ref. 1** belongs to; this may indicates the same binding mode is adopted by these two series of CYP11B2 inhibitors. Despite compound **23** showed increased inhibition toward CYP11B1 ($IC_{50} = 428$ nM), good selectivity of 60 was achieved due to really strong inhibition exhibited toward CYP11B2 with an IC_{50} value of 7 nM. Subsequently, fusing the phenyl group to pyridyl to form 4-isoquinoliny, which is a kind of bio-isostere transformation of pyridyl substituted by phenyl, was further performed leading to compound **26**. This bio-isostere transformation led to significant increase of inhibition toward both enzymes rendering **26** as the most potent inhibitor for both enzymes in this study with IC_{50} values of 2.2 nM for CYP11B2 and 110 nM for CYP11B1. Three possible reasons were considered for the improvement of CYP11B2 inhibition. Firstly, electron donating feature of the fused phenyl group increased the electron density on the N atom, which facilitated the coordination of the inhibitor to the heme iron. Secondly, the fused phenyl as a hydrophobic moiety occupied the spar pocket nearby and formed extra interactions. Finally, the fused phenyl reduced the rotation freedom of the 4,5-dihydro-[1,2,4]triazolo[4,3-*a*]quinolines core resulting in a more favourable conformation. Meanwhile, the increased bulk by the fused phenyl occupying the spar pocket was thought also to be responsible for the elevation of CYP11B1 inhibition. Therefore, to improve selectivity the fused phenyl was removed; whereas a methyl group was sustained at the *para*-position as a residue to donate electron and to limit rotation. The yielded compound **24** showed potent inhibition toward CYP11B2 with an IC_{50} of 4.2 nM, while its inhibition of CYP11B1 was largely decreased ($IC_{50} = 1772$ nM). Since excellent selectivity of 422 was also achieved, this

Table 2. Inhibition of CYP11B1 and CYP11B2 by compounds **17** – **24**.


Compd.	R	CYP11B2		CYP11B1		SF ^d
		Inhibit.% ^{a,c}	IC ₅₀ (nM) ^{b,c}	Inhibit.% ^{a,c}	IC ₅₀ (nM) ^{b,c}	
17	<i>m</i> -OMe	95.8%	20.3	12.4%	1810	89
18	<i>m</i> -(1-OH)-Et	90.6%	28.3	3.1%	3910	138
19	<i>m</i> -Ac	86.1%	87.6	7.4%	6970	78
20	<i>m</i> -CF ₃	87.7%	57.2	16.1%	3570	63
21	<i>m</i> -CN	29.8%	n.d. ^d	0.0%	n.d. ^d	n.d. ^d
22	<i>m</i> -F	81.8%	89.7	6.5%	29540	329
23	<i>m</i> -Ph	100.0%	7.1	44.1%	428	60
24	<i>p</i> -Me	100.0%	4.2	19.8%	1770	422
25		18.5%	n.d. ^d	0.0%	n.d. ^d	n.d. ^d
26		100.0%	2.2	76.1%	110	49
27		5.3%	n.d. ^d	1.9%	n.d. ^d	n.d. ^d
FDZ^d			0.8		6.3	8.3

^a Inhibition percentage with compound concentration of 500 nM. Standard deviations were within $\pm 5\%$; All the data are the mean values of at least 3 tests.

^b Concentration of inhibitors required to give 50 % inhibition. Standard deviations were within $\pm 5\%$; All the data are the mean values of at least 3 tests.

^c Hamster fibroblasts expressing human CYP11B1 or CYP11B2 are used with deoxycorticosterone as the substrate at a concentration of 100 nM.

^d **FDZ**: Fadrozole; SF: selective factor = $IC_{50\text{ CYP11B1}} / IC_{50\text{ CYP11B2}}$; n.d. not determined.

compound was considered as the most promising inhibitor throughout this study. Furthermore, the replacement of pyridyl by other heterocycles such as pyrimidinyl or 5-isoquinoliny ended up loss of inhibitory potency probably due to low electron density of N and unsuitable distance between hydrophobic core and N, respectively.

Selectivity. The inhibition of other steroidogenic enzymes like CYP17 and CYP19 by synthesized compounds was also determined as criterions to evaluate safety. CYP17 and CYP19 are crucial enzymes in the biosynthesis of androgen and estrogen, respectively. Their inhibition would result in severe disorder of the sexual hormone dependent organs. Moreover, estrogen has been shown some protection effects on heart; the estrogen deficiency caused by CYP19 inhibition would increase the risk of cardiovascular diseases. It turned out all compounds exhibited IC₅₀ values more than 10000 nM for each enzyme (data not shown) indicating no interference with CYP17 and CYP19.

Conclusion

The benefits of CYP11B2 inhibition as a promising treatment for diseases related to high aldosterone level

has been demonstrated in rats with heart failure¹⁹ with FAD286. However, although this compound is very potent, it exhibits poor selectivity over CYP11B1, which indicates potential side effects associated with glucocorticoids dysfunction. Therefore, potent and selective CYP11B2 inhibitors are still in urgent need to be developed. Based on our previously identified CYP11B2 inhibitors, a series of novel heterocycle substituted 4,5-dihydro-[1,2,4]triazolo[4,3-*a*]quinolines were designed, synthesized and biologically evaluated.

It has been elucidated that the substituents on the 1-position of triazolo moiety have profound influence on the CYP11B2 inhibitory potency, where the bulk is the crucial determinant. Methyl, as the most suitable group, was found significantly improve the potency; whereas larger substituents led to lost of activity. Moreover, analogues with fluorine furnished at 9-position are more potent than the ones with 8-F substitution. Furthermore, substituents on the pyridyl are important for the affinity of compounds to the enzyme by altering the electron density on sp^2 hybrid N, where electron donating groups increase inhibition, whereas electron withdrawing groups slightly reduce it. Increase of inhibitory potency by occupancy of additional hydrophobic pocket near heme is also observed, despite of coinstantaneous selectivity impairment. Conformation rigidification is considered as an advantageous factor for the CYP11B2 inhibition as well, which is substantiated by the fusion of additional phenyl and *para*-methyl substituted on pyridyl. The current study results in many potent and highly selective CYP11B2 inhibitors, especially compound **24** ($IC_{50} = 4.2$ nM, selectivity factor = 422). This compound is considered as a promising drug candidate after further evaluation in vivo.

Experimental Section

Inhibition of CYP11B1 and CYP11B2

V79 MZh cells expressing human CYP11B2 or CYP11B1^{23a} were incubated with [¹⁴C]-deoxycorticosterone as substrate and inhibitors in various concentrations. After 6 hours, the reaction was stopped and the steroids were extracted with ethyl acetate, separated by HPTLC and quantified using a phosphoimager. Then the inhibitory potency was calculated from the reduced substrate conversion.^{23b}

Inhibition of CYP19

The inhibition of CYP19 was determined in vitro using human placental microsomes with [¹⁴C]-androstenedione as substrate.^{23c}

Inhibition of CYP17

Human CYP17 was expressed in *E. coli*^{23d} (coexpressing human CYP17 and NADPH-P450 reductase) and the assay was performed as previously described.^{23e}

Chemistry Section

General

Melting points were determined on a Mettler FP1 melting point apparatus and are uncorrected. IR spectra were recorded neat on a Bruker Vector 33FT-infrared spectrometer. ¹H-NMR spectra were measured on a Bruker DRX-500 (500 MHz). Chemical shifts are given in parts per million (ppm), and TMS was used as an internal standard for spectra obtained. All coupling constants (*J*) are given in Hz. ESI (electrospray ionization) mass spectra were determined on a TSQ quantum (Thermo Electron Corporation) instrument.

The purities of the final compounds were controlled by Surveyor[®]-LC-system. Purities were greater than 95%. Column chromatography was performed using silica-gel 60 (50-200 μm), and reaction progress was determined by TLC analysis on Alugram[®] SIL G/UV₂₅₄ (Macherey-Nagel).

Method A: Sulphuration with Lawesson's reagent

To the suspension of the corresponding dihydroquinolinone (1.0 eq.) in toluene (5 mL / mmol) was added Lawesson's reagent (1.5 eq.). After reflux for 2 hours, toluene was distilled off to give the crude product, which was then purified by flash chromatography on silica gel.

7-Fluoro-6-pyridin-3-yl-3,4-dihydro-1H-quinoline-2-thione (1a). Synthesized according to Method A using 7-fluoro-6-(pyridin-3-yl)-3,4-dihydroquinolin-2(1H)-one (0.35 g, 1.44 mmol); yield: 0.28 g (76%); light yellow solid: mp 245–246 °C; $R_f = 0.22$ (DCM/MeOH, 50:1); δ_{H} (DMSO, 500 MHz) 2.85 (t, $J = 7.8$ Hz, 2H, CH₂), 2.99 (t, $J = 7.8$ Hz, 2H, CH₂), 7.02 (d, $^3J_{\text{HF}} = 11.5$ Hz, 1H), 7.49 (ddd, $J = 0.7, 4.9, 8.0$ Hz, 1H), 7.50 (d, $^4J_{\text{HF}} = 8.2$ Hz, 1H), 7.95 (dt, $J = 2.0, 7.9$ Hz, 1H), 8.58 (dd, $J = 1.6, 4.8$ Hz, 1H), 8.74 (s, 1H), 12.33 (s, br, 1H, NH); MS (ESI): $m/z = 258$ [$\text{M}^+ + \text{H}$].

8-Fluoro-6-pyridin-3-yl-3,4-dihydro-1H-quinoline-2-thione (2a). Synthesized according to Method A using 8-fluoro-6-(pyridin-3-yl)-3,4-dihydroquinolin-2(1H)-one (0.35 g, 1.44 mmol); yield: 0.30 g (81%); light yellow solid: mp 229–230 °C; $R_f = 0.22$ (DCM/MeOH, 50:1); δ_{H} (DMSO, 500 MHz) 2.91 (t, $J = 7.8$ Hz, 2H, CH₂), 3.00 (t, $J = 7.8$ Hz, 2H, CH₂), 7.47 (ddd, $J = 0.7, 4.9, 8.0$ Hz, 1H), 7.52 (s, 1H), 7.59 (dd, $J = 1.9$ Hz, $^3J_{\text{HF}} = 11.7$ Hz, 1H), 8.10 (dt, $J = 1.7, 8.0$ Hz, 1H), 8.56 (dd, $J = 1.5, 4.7$ Hz, 1H), 8.92 (d, $J = 1.7$ Hz, 1H), 12.16 (s, br, 1H, NH); MS (ESI): $m/z = 258$ [$\text{M}^+ + \text{H}$].

Method B: Cyclization with acylhydrazine

The suspension of dihydroquinoline-2-thione (1.0 eq.) and corresponding acylhydrazine (1.2 eq.) in cyclohexanol (1 mL / mmol) was refluxed for 6 hours under inert atmosphere. After cooling down to ambient temperature, cyclohexanol was distilled off, and the residue was taken up with ethyl acetate (10 mL) and water (10 mL). Then the organic phase was separated, and the water phase was extracted with ethyl acetate (2 x 10 mL). The combined organic phases were washed with brine, dried over Na₂SO₄, and evaporated under reduced pressure to afford the crude products. The compounds were purified by flash chromatography on silica gel.

8-Fluoro-7-pyridin-3-yl-4,5-dihydro-[1,2,4]triazolo[4,3-*a*]quinoline (1). Synthesized according to Method B using **1a** (0.50 g, 1.94 mmol) and formohydrazide (0.14 g, 2.32 mmol); yield: 0.39 g (75%); white solid: mp 246–247 °C; $R_f = 0.21$ (DCM/MeOH, 20:1); δ_{H} (CDCl₃, 500 MHz) 3.11 (t, $J = 7.5$ Hz, 2H, CH₂), 3.27 (t, $J = 7.5$ Hz, 2H, CH₂), 7.27 (d, $^3J_{\text{HF}} = 10.0$ Hz, 1H), 7.41 (ddd, $J = 0.7, 4.8, 8.0$ Hz, 1H), 7.45 (d, $^4J_{\text{HF}} = 7.7$ Hz, 1H), 7.88 (dq, $J = 1.8, 7.9$ Hz, 1H), 8.61 (s, 1H), 8.66 (dd, $J = 1.6, 4.8$ Hz, 1H), 8.79 (s, 1H); MS (ESI): $m/z = 267$ [$\text{M}^+ + \text{H}$].

9-Fluoro-7-pyridin-3-yl-4,5-dihydro-[1,2,4]triazolo[4,3-*a*]quinoline (2). Synthesized according to Method B using **2a** (0.50 g, 1.94 mmol) and 4-aminophenyl boronic acid (0.14 g, 2.32 mmol); yield: 0.41 g (79%); white solid: mp 210–211 °C; $R_f = 0.19$ (DCM/MeOH, 20:1); δ_{H} (CDCl₃, 500 MHz) 3.19 (t, $J = 7.5$ Hz, 2H, CH₂), 3.30 (t, $J = 7.5$ Hz, 2H, CH₂), 7.39–7.43 (m, 3H), 7.87 (dt, $J = 2.1, 7.9$ Hz, 1H), 8.66 (dd, $J = 1.3, 4.8$ Hz, 1H), 8.83 (d, $J_{\text{HF}} = 3.5$ Hz, 1H), 8.84 (d, $J = 2.0$ Hz, 1H); MS (ESI): $m/z = 267$ [$\text{M}^+ + \text{H}$].

8-Fluoro-1-methyl-7-pyridin-3-yl-4,5-dihydro-[1,2,4]triazolo[4,3-*a*]quinoline (3). Synthesized

according to Method B using **1a** (0.50 g, 1.94 mmol) and acetohydrazide (0.17 g, 2.32 mmol); yield: 0.42 g (78%); white solid: mp 227–228 °C; $R_f = 0.19$ (DCM/MeOH, 20:1); δ_H (CDCl₃, 500 MHz) 2.78 (s, 3H, CH₃), 3.04 (t, $J = 7.5$ Hz, 2H, CH₂), 3.15 (t, $J = 7.5$ Hz, 2H, CH₂), 7.33 (d, $^3J_{HF} = 10.9$ Hz, 1H), 7.39 (ddd, $J = 0.7, 4.8, 8.0$ Hz, 1H), 7.44 (d, $^4J_{HF} = 8.0$ Hz, 1H), 7.86 (dq, $J = 1.8, 8.0$ Hz, 1H), 8.62 (dd, $J = 1.6, 4.8$ Hz, 1H), 8.77 (s, 1H); MS (ESI): $m/z = 281$ [M⁺+H].

9-Fluoro-1-methyl-7-pyridin-3-yl-4,5-dihydro-[1,2,4]triazolo[4,3-*a*]quinoline (4). Synthesized according to Method B using **2a** (0.50 g, 1.94 mmol) and acetohydrazide (0.17 g, 2.32 mmol); yield: 0.44 g (81%); white solid: mp 195–196 °C; $R_f = 0.20$ (DCM/MeOH, 20:1); δ_H (CDCl₃, 500 MHz) 2.51 (d, $J_{HF} = 8.2$ Hz, 3H, CH₃), 2.89 (t, $J = 7.5$ Hz, 2H, CH₂), 2.99 (t, $J = 7.5$ Hz, 2H, CH₂), 7.11 (s, 1H), 7.23–7.28 (m, 2H), 7.73 (dt, $J = 2.1, 8.0$ Hz, 1H), 8.51 (dd, $J = 1.3, 4.8$ Hz, 1H), 8.71 (d, $J = 2.0$ Hz, 1H); MS (ESI): $m/z = 281$ [M⁺+H].

Method C: Suzuki-Coupling

The corresponding brominated aromatic compound (1.0 eq.) was dissolved in toluene (7 mL / mmol), and an aqueous 2.0 M Na₂CO₃ solution (3.2 mL / mmol), an ethanolic solution (3.2 mL / mmol) of the corresponding boronic acid (1.5-2.0 eq.) and tetrabutylammonium bromide (1.0 eq) were added. The mixture was deoxygenated under reduced pressure and flushed with nitrogen. After having repeated this cycle several times Pd(OAc)₂ (5 mol%) was added and the resulting suspension was heated under reflux for 2-6 h. After cooling, ethyl acetate (10 mL) and water (10 mL) were added and the organic phase was separated. The water phase was extracted with ethyl acetate (2 x 10 mL). The combined organic phases were washed with brine, dried over Na₂SO₄, filtered over a short plug of celite® and evaporated under reduced pressure. The compounds were purified by flash chromatography on silica gel.

9-Fluoro-7-(5-methoxy-pyridin-3-yl)-1-methyl-4,5-dihydro-[1,2,4]triazolo[4,3-*a*] quinoline (17). Synthesized according to Method C using **17a** (0.35 g, 1.42 mmol) and 3-bromo-5-methoxypyridine (0.32 g, 1.70 mmol); yield: 0.39 g (89%); white solid: mp 196–197 °C; $R_f = 0.22$ (DCM/MeOH, 20:1); δ_H (CDCl₃, 500 MHz) 2.65 (d, $J_{HF} = 8.2$ Hz, 3H, CH₃), 3.04 (t, $J = 7.5$ Hz, 2H, CH₂), 3.12 (t, $J = 7.5$ Hz, 2H, CH₂), 3.95 (s, 3H, OCH₃), 7.34 (dd, $J = 1.9, 2.6$ Hz, 1H), 7.38 (dd, $J = 1.8$ Hz, $^3J_{HF} = 11.4$ Hz, 1H), 7.40 (d, $J = 1.7$ Hz, 1H), 8.35 (d, $J = 2.7$ Hz, 1H), 8.45 (d, $J = 1.8$ Hz, 1H); MS (ESI): $m/z = 311$ [M⁺+H].

1-[5-(9-Fluoro-1-methyl-4,5-dihydro-[1,2,4]triazolo[4,3-*a*]quinolin-7-yl)-pyridin-3-yl]-ethanol (18). Synthesized according to Method C using **17a** (0.35 g, 1.42 mmol) and 1-(5-bromopyridin-3-yl)ethanol (0.34 g, 1.70 mmol); yield: 0.33 g (72%); white solid: mp 228–229 °C; $R_f = 0.12$ (DCM/MeOH, 20:1); δ_H (CDCl₃, 500 MHz) 1.59 (d, $J = 6.5$ Hz, 3H, CH₃), 2.01 (s, br, 1H, OH), 2.65 (d, $J_{HF} = 8.2$ Hz, 3H, CH₃), 3.04 (t, $J = 7.5$ Hz, 2H, CH₂), 3.09 (t, $J = 7.5$ Hz, 2H, CH₂), 5.08 (q, $J = 6.5$ Hz, 1H, CH), 7.42 (dd, $J = 1.8$ Hz, $^3J_{HF} = 13.2$ Hz, 1H), 7.43 (d, $J = 1.7$ Hz, 1H), 7.99 (dd, $J = 1.9, 2.6$ Hz, 1H), 8.61 (d, $J = 2.7$ Hz, 1H), 8.71 (d, $J = 1.8$ Hz, 1H); MS (ESI): $m/z = 325$ [M⁺+H].

1-[5-(9-Fluoro-1-methyl-4,5-dihydro-[1,2,4]triazolo[4,3-*a*]quinolin-7-yl)-pyridin-3-yl]-ethanone (19). Synthesized according to Method C using **17a** (0.35 g, 1.42 mmol) and 1-(5-bromopyridin-3-yl)ethanone (0.34 g, 1.70 mmol); yield: 0.39 g (86%); white solid: mp 216–217 °C; $R_f = 0.19$ (DCM/MeOH, 20:1); δ_H (CDCl₃, 500 MHz) 2.66 (d, $J_{HF} = 8.3$ Hz, 3H, CH₃), 2.72 (s, 3H, CH₃), 3.07 (t, $J = 7.5$ Hz, 2H, CH₂), 3.14 (t, $J = 7.5$ Hz, 2H, CH₂), 7.45 (dd, $J = 1.8$ Hz, $^3J_{HF} = 13.3$ Hz, 1H), 7.46 (d, $J = 1.7$ Hz, 1H), 8.43 (dd, $J = 2.0,$

2.1 Hz, 1H), 9.02 (d, $J = 2.2$ Hz, 1H), 9.19 (d, $J = 1.9$ Hz, 1H); MS (ESI): $m/z = 323$ [$M^+ + H$].

9-Fluoro-1-methyl-7-(5-trifluoromethyl-pyridin-3-yl)-4,5-dihydro-[1,2,4]triazolo[4,3-*a*]quinoline (20). Synthesized according to Method C using **17a** (0.35 g, 1.42 mmol) and 3-bromo-5-(trifluoromethyl)pyridine (0.38 g, 1.70 mmol); yield: 0.43 g (88%); white solid: mp 243–244 °C; $R_f = 0.21$ (DCM/MeOH, 20:1); δ_H (CDCl₃, 500 MHz) 2.66 (d, $J_{HF} = 8.3$ Hz, 3H, CH₃), 3.07 (t, $J = 7.5$ Hz, 2H, CH₂), 3.14 (t, $J = 7.5$ Hz, 2H, CH₂), 7.43 (dd, $J = 1.8$ Hz, $^3J_{HF} = 10.2$ Hz, 1H), 7.45 (d, $J = 1.7$ Hz, 1H), 8.10 (dd, $J = 2.0, 2.1$ Hz, 1H), 8.94 (d, $J = 2.2$ Hz, 1H), 9.03 (d, $J = 2.0$ Hz, 1H); MS (ESI): $m/z = 349$ [$M^+ + H$].

5-(9-Fluoro-1-methyl-4,5-dihydro-[1,2,4]triazolo[4,3-*a*]quinolin-7-yl)-nicotinonitrile (21). Synthesized according to Method C using **17a** (0.35 g, 1.42 mmol) and 5-bromonicotinonitrile (0.31 g, 1.70 mmol); yield: 0.38 g (89%); white solid: mp 267–268 °C; $R_f = 0.20$ (DCM/MeOH, 20:1); δ_H (CDCl₃, 500 MHz) 2.66 (d, $J_{HF} = 8.3$ Hz, 3H, CH₃), 3.07 (t, $J = 7.5$ Hz, 2H, CH₂), 3.14 (t, $J = 7.5$ Hz, 2H, CH₂), 7.41 (dd, $J = 1.8$ Hz, $^3J_{HF} = 11.9$ Hz, 1H), 7.42 (d, $J = 1.7$ Hz, 1H), 8.15 (dd, $J = 2.0, 2.1$ Hz, 1H), 8.92 (d, $J = 1.9$ Hz, 1H), 9.03 (d, $J = 2.3$ Hz, 1H); MS (ESI): $m/z = 306$ [$M^+ + H$].

9-Fluoro-7-(5-fluoro-pyridin-3-yl)-1-methyl-4,5-dihydro-[1,2,4]triazolo[4,3-*a*]quinoline (22). Synthesized according to Method C using **17a** (0.35 g, 1.42 mmol) and 3-bromo-5-fluoropyridine (0.30 g, 1.70 mmol); yield: 0.39 g (92%); white solid: mp 215–216 °C; $R_f = 0.23$ (DCM/MeOH, 20:1); δ_H (CDCl₃, 500 MHz) 2.65 (d, $J_{HF} = 8.3$ Hz, 3H, CH₃), 3.04 (t, $J = 7.5$ Hz, 2H, CH₂), 3.13 (t, $J = 7.5$ Hz, 2H, CH₂), 7.39 (dd, $J = 1.9$ Hz, $^3J_{HF} = 14.6$ Hz, 1H), 7.41 (d, $J = 1.7$ Hz, 1H), 7.59 (ddd, $J = 2.0, 2.6$ Hz, $^3J_{HF} = 9.2$ Hz, 1H), 8.52 (d, $J = 2.7$ Hz, 1H), 8.67 (t, $J = 1.5$ Hz, 1H); MS (ESI): $m/z = 299$ [$M^+ + H$].

9-Fluoro-1-methyl-7-(5-phenyl-pyridin-3-yl)-4,5-dihydro-[1,2,4]triazolo[4,3-*a*]quinoline (23). Synthesized according to Method C using **17a** (0.35 g, 1.42 mmol) and 3-bromo-5-phenylpyridine (0.40 g, 1.70 mmol); yield: 0.43 g (85%); white solid: mp 209–210 °C; $R_f = 0.20$ (DCM/MeOH, 20:1); δ_H (CDCl₃, 500 MHz) 2.65 (d, $J_{HF} = 8.3$ Hz, 3H, CH₃), 3.05 (t, $J = 7.5$ Hz, 2H, CH₂), 3.14 (t, $J = 7.5$ Hz, 2H, CH₂), 7.44–7.47 (m, 3H), 7.51 (dd, $J = 7.6, 7.8$ Hz, 2H), 7.64 (d, $J = 7.7$ Hz, 1H), 8.03 (t, $J = 2.1$ Hz, 1H), 8.81 (d, $J = 1.8$ Hz, 1H), 8.88 (d, $J = 2.3$ Hz, 1H); MS (ESI): $m/z = 357$ [$M^+ + H$].

9-Fluoro-1-methyl-7-(4-methyl-pyridin-3-yl)-4,5-dihydro-[1,2,4]triazolo[4,3-*a*]quinoline (24). Synthesized according to Method C using **17a** (0.35 g, 1.42 mmol) and 3-bromo-4-methylpyridine (0.29 g, 1.70 mmol); yield: 0.38 g (91%); white solid: mp 157–158 °C; $R_f = 0.22$ (DCM/MeOH, 20:1); δ_H (CDCl₃, 500 MHz) 2.62 (d, $J_{HF} = 8.2$ Hz, 3H, CH₃), 2.99 (t, $J = 7.5$ Hz, 2H, CH₂), 3.09 (t, $J = 7.5$ Hz, 2H, CH₂), 7.12 (dd, $J = 1.8$ Hz, $^3J_{HF} = 11.7$ Hz, 1H), 7.13 (d, $J = 1.9$ Hz, 1H), 7.20 (d, $J = 5.0$ Hz, 1H), 8.39 (s, 1H), 8.45 (d, $J = 5.0$ Hz, 1H); MS (ESI): $m/z = 295$ [$M^+ + H$].

9-Fluoro-7-isoquinolin-4-yl-1-methyl-4,5-dihydro-[1,2,4]triazolo[4,3-*a*]quinoline (26). Synthesized according to Method C using **17a** (0.35 g, 1.42 mmol) and 4-bromoisoquinoline (0.35 g, 1.70 mmol); yield: 0.25 g (86%); white solid: mp 209–210 °C; $R_f = 0.19$ (DCM/MeOH, 20:1); δ_H (CDCl₃, 500 MHz) 2.69 (d, $J_{HF} = 8.3$ Hz, 3H, CH₃), 3.05 (t, $J = 7.5$ Hz, 2H, CH₂), 3.17 (t, $J = 7.5$ Hz, 2H, CH₂), 7.34–7.37 (m, 2H), 7.67–7.70 (m, 1H), 7.74–7.77 (m, 1H), 7.89 (d, $J = 8.5$ Hz, 1H), 8.09 (d, $J = 8.0$ Hz, 1H), 8.49 (s, 2H), 9.30 (s, 1H); MS (ESI): $m/z = 331$ [$M^+ + H$].

Acknowledgements

The authors appreciate Christina Zimmer, Jeannine Jung and Jannine Ludwig for the help in determination of bioactivity, and thank Professor J. Hermans (Cardiovascular Research Institute, University of Maastricht, The Netherlands) and Professor R. Bernhardt (Saarland University, Germany) for providing us with V79MZh11B cells expressing human CYP11B1 and CYP11B2, respectively.

Supporting Information Available: The synthetic procedures and characterization of compounds **5** – **16**, **25**, **27** and rest intermediates as well as HPLC purities, ¹³C-NMR and IR spectra of all compounds. This material is available free of charge via the internet at <http://pubs.acs.org>.

References

1. Simpson, S. A.; Tait, J. F.; Wettstein, A.; Neher, R.; Von Euw, J.; Reichstein, T. Isolation from the adrenals of a new crystalline hormone with especially high effectiveness on mineral metabolism. *Experientia* **1953**, *9*, 333–335.
2. Silvestre, J. S.; Robert, V.; Heymes, C.; Aupetit-Faisant, B.; Mouas, C.; Moalic, J. M.; Swynghedauw, B.; Delcayre, C. Myocardial production of aldosterone and corticosterone in the rat physiological regulation. *J. Biol. Chem.* **1998**, *273*, 4883–4891.
3. Rudolph, A. E.; Blasi, E. R.; Delyani, J. A. Tissue-specific corticosteroidogenesis in the rat. *Mol. Cell. Endocrinol.* **2000**, *165*, 221–224.
4. Gekle, M.; Grossmann, C. Actions of aldosterone in the cardiovascular system: the good, the bad, and the ugly? *Eur. J. Physiol.* **2009**, *458*, 231–246.
5. (a) Joffe, H. V.; Adler, G. K. Effect of aldosterone and mineralocorticoid receptor blockade on vascular inflammation. *Heart Fail. Rev.* **2005**, *10*, 31–37. (b) Brown, N. J. Aldosterone and vascular inflammation. *Hypertension* **2008**, *51*, 161–167.
6. Fiebeler, A.; Luft, F. C. The mineralocorticoid receptor and oxidative stress. *Heart Fail. Rev.* **2005**, *10*, 47–52.
7. Leibovitz, E.; Ebrahimian, T.; Paradis, P.; Schiffrin, E. L. Aldosterone induces arterial stiffness in absence of oxidative stress and endothelial dysfunction. *J. Hypertens.* **2009**, *27*, 2192–2200.
8. Rader, D. J.; Daugherty, A. Translating molecular discoveries into new therapies for atherosclerosis. *Nature* **2008**, *451*, 904–913.
9. Romagni, P.; Rossi, F.; Guerrini, L.; Quirini, C.; Santemma, V. Aldosterone induces contraction of the resistance arteries in man. *Atherosclerosis* **2003**, *166*, 345–349.
10. Fejes-Tóth, G.; Náráy-Fejes-Tóth, A. Early aldosterone-regulated genes in cardiomyocytes: clues to cardiac remodeling? *Endocrinology* **2007**, *148*, 1502–1510.
11. Lal, A.; Veinot, J. P.; Leenen, F. H. H. Critical role of CNS effects of aldosterone in cardiac remodeling post-myocardial infarction in rats. *Cardiovasc. Res.* **2004**, *64*, 437–447.
12. (a) Zannad, F.; Radauceanu, A. Effect of MR blockade on collagen formation and cardiovascular disease with a specific emphasis on heart failure. *Heart Fail. Rev.* **2005**, *10*, 71–78. (b) Weber, K. T.; Brilla, C. G.; Campbell, S. E.; Guarda, E.; Zhou, G.; Sriram, K. Myocardial fibrosis: role of angiotensin II and aldosterone. *Basic Res. Cardiol.* **1993**, *88*, 107–124.
13. (a) Felder, R. B. Mineralocorticoid receptors, inflammation and sympathetic drive in a rat model of systolic heart failure. *Exp. Physiol.* **2009**, *95*, 19–25. (b) Nicoletti, A.; Michel, J. B. Cardiac fibrosis and inflammation: interaction with hemodynamic and hormonal factors. *Cardiovasc. Res.* **1999**, *41*, 532–543.
14. Cortinovis, M.; Perico, N.; Cattaneo, D.; Remuzzi, G. Aldosterone and progression of kidney disease. *Ther. Adv. Cardiovasc. Dis.* **2009**, *3*, 133–143.
15. Sato, A.; Saruta, T. Aldosterone escape during angiotensin-converting enzyme inhibitor therapy in essential hypertensive patients with left ventricular hypertrophy. *J. Int. Med. Res.* **2001**, *29*, 13–21.
16. Rousseau, M. F.; Gurne, O.; Dupre, D.; Van Mieghem, W.; Robert, A.; Ahn, S.; Galanti, L.; Ketelslegers, J. M. Beneficial neurohormonal profile of spironolactone in severe congestive heart failure: results from the RALES neurohormonal substudy. *J. Am. Coll. Cardiol.* **2002**, *40*, 1596–1601.
17. Chai, W.; Garrelds, I. M.; de Vries, R.; Batenburg, W. W.; van Kats, J. P.; Danser, A. H. J. Nongenomic effects of aldosterone in the human heart: interaction with angiotensin II. *Hypertension* **2005**, *46*, 701–706.
18. Fiebeler, A.; Nussberger, J.; Shagdarsuren, E.; Rong, S.; Hilfenhaus, G.; Al-Saadi, N.; Dechend, R.; Wellner, M.; Meiners, S.; Master-Gluth, C.; Jeng, A. Y.; Webb, R. L.; Luft, F. C.; Müller, D. N. Aldosterone synthase inhibitor ameliorates angiotensin II-induced organ damage. *Circulation* **2005**, *111*, 3087–3094.
19. Aldosterone synthase inhibition improves cardiovascular function and structure in rats with heart failure—a comparison with spironolactone. *Eur. Heart J.* **2008**, *29*, 2171–2179.
20. (a) Lucas, S.; Heim, R.; Ries, C.; Schewe, K. E.; Birk, B.; Hartmann, R. W. In vivo active aldosterone synthase inhibitors with improved selectivity: lead optimization providing a series of pyridine substituted 3,4-dihydro-1H-quinolin-2-one derivatives. *J. Med. Chem.* **2008**, *51*, 8077–8087. (b) Lucas, S.; Heim, R.; Negri, M.; Antes, I.; Ries, C.; Schewe, K. E.; Bisi, A.; Gobbi, S.; Hartmann, R. W. Novel aldosterone synthase inhibitors with extended carbocyclic skeleton by a combined ligand-based and structure-based drug design approach. *J. Med. Chem.* **2008**, *51*, 6138–6149. (c) Heim, R.; Lucas, S.; Grombein, C. M.; Ries, C.; Schewe, K. E.; Negri, M.; Müller-Vieira, U.; Birk, B.; Hartmann, R. W. Overcoming undesirable CYP1A2 inhibition of pyridyl-naphthalene-type aldosterone synthase inhibitors: influence of heteroaryl derivatization on potency and selectivity. *J. Med. Chem.* **2008**, *51*, 5064–5074. (d) Voets, M.; Antes, I.; Scherer, C.; Müller-Vieira, U.; Biemel, K.; Marchais-Oberwinkler, S.; Hartmann, R. W. Synthesis and evaluation of heteroaryl-substituted dihydronaphthalenes and indenyls: potent and selective inhibitors of aldosterone synthase (CYP11B2) for the treatment of congestive heart failure and myocardial fibrosis. *J. Med. Chem.* **2006**, *49*, 2222–2231. (e) Voets, M.; Antes, I.; Scherer, C.; Müller-Vieira, U.; Biemel, K.; Barassin, C.; Marchais-Oberwinkler, S.; Hartmann, R. W. Heteroaryl-substituted naphthalenes and structurally modified derivatives: selective inhibitors of CYP11B2 for the treatment of congestive heart failure and myocardial fibrosis. *J. Med. Chem.* **2005**, *48*, 6632–6642. (f)

- Ulmschneider, S.; Müller-Vieira, U.; Klein, C. D.; Antes, I.; Lengauer, T.; Hartmann, R. W. Synthesis and evaluation of (pyridylmethylene) tetrahydronaphthalenes/-indanes and structurally modified derivatives: potent and selective inhibitors of aldosterone synthase. *J. Med. Chem.* **2005**, *48*, 1563–1575. (g) Ulmschneider, S.; Müller-Vieira, U.; Mitrenga, M.; Hartmann, R. W.; Oberwinkler-Marchais, S.; Klein, C. D.; Bureik, M.; Bernhardt, R.; Antes, I.; Lengauer, T. Synthesis and evaluation of imidazolymethylene tetrahydronaphthalenes and imidazolymethyleneindanes: potent inhibitors of aldosterone synthase. *J. Med. Chem.* **2005**, *48*, 1796–1805. (h) Hu, Q.; Yin, L.; Hartmann, R. W. Selective Dual Inhibitors of CYP19 / 11B2: Targeting Cardiovascular Diseases Hiding in the Shadow of Breast Cancer. *J. Med. Chem.* **2012**, In Press.
21. (a) Hartmann, R. W.; Bayer, H.; Grün, G. Aromatase inhibitors. Syntheses and structure-activity studies of novel pyridyl-substituted indanones, indans, and tetralins. *J. Med. Chem.* **1994**, *37*, 1275–81. (b) Gobbi, S.; Cavalli, A.; Rampa, A.; Belluti, F.; Piazza, L.; Paluszczak, A.; Hartmann, R. W.; Recanatini, M.; Bisi, A. Lead optimization providing a series of flavone derivatives as potent nonsteroidal inhibitors of the cytochrome P450 aromatase enzyme. *J. Med. Chem.* **2006**, *49*, 4777–4780. (c) Gobbi, S.; Zimmer, C.; Belluti, F.; Rampa, A.; Hartmann, R. W.; Recanatini, M.; Bisi, A. Novel highly potent and selective nonsteroidal aromatase inhibitors: synthesis, biological evaluation and structureactivity relationships investigation. *J. Med. Chem.* Im press. (d) Le Borgne, M.; Marchand, P.; Duflos, M.; Delevoeye-Seiller, B.; Piessard-Robert, S.; Le Baut, G.; Hartmann, R. W.; Palzer, M. Synthesis and in vitro evaluation of 3-(1-azolylmethyl)-1H-indoles and 3-(1-azoly-1-phenylmethyl)-1H-indoles as inhibitors of P450 arom. *Arch. Pharm. (Weinheim, Ger.)* **1997**, *330*, 141–145. (e) Woo, L. W. L.; Jackson, T.; Putey, A.; Cozier, G.; Leonard, P.; Acharya, K. R.; Chander, S. K.; Purohit, A.; Reed, M. J.; Potter, B. V. L. Highly Potent First Examples of Dual Aromatase-Steroid Sulfatase Inhibitors based on a Biphenyl Template. *J. Med. Chem.* **2010**, *53*, 2155–2170. (f) Leze, M. P.; Le Borgne, M.; Pinson, P.; Paluszczak, A.; Duflos, M.; Le Baut, G.; Hartmann, R. W. Synthesis and biological evaluation of 5-[(aryl)(1H-imidazol-1-yl)methyl]-1H-indoles: potent and selective aromatase inhibitors. *Bioorg. Med. Chem. Lett.* **2006**, *16*, 1134–1137. (g) Gobbi, S.; Cavalli, A.; Negri, M.; Schewe, K. E.; Belluti, F.; Piazza, L.; Hartmann, R. W.; Recanatini, M.; Bisi, A. Imidazolymethylbenzophenones as highly potent aromatase inhibitors. *J. Med. Chem.* **2007**, *50*, 3420–3422. (h) Leonetti, F.; Favia, A.; Rao, A.; Aliano, R.; Paluszczak, A.; Hartmann, R. W.; Carotti, A. Design, synthesis, and 3D QSAR of novel potent and selective aromatase inhibitors. *J. Med. Chem.* **2004**, *47*, 6792–6803.
22. (a) Hu, Q.; Negri, M.; Jahn-Hoffmann, K.; Zhuang, Y.; Olgen, S.; Bartels, M.; Müller-Vieira, U.; Lauterbach, T.; Hartmann, R. W. Synthesis, biological evaluation, and molecular modeling studies of methylene imidazole substituted biaryls as inhibitors of human 17 α -hydroxylase-17,20-lyase (CYP17)-Part II: Core rigidification and influence of substituents at the methylene bridge. *Bioorg. Med. Chem.* **2008**, *16*, 7715–7727. (b) Hille, U. E.; Hu, Q.; Vock, C.; Negri, M.; Bartels, M.; Müller-Vieira, U.; Lauterbach, T.; Hartmann, R. W. Novel CYP17 inhibitors: Synthesis, biological evaluation, structure-activity relationships and modeling of methoxy- and hydroxy-substituted methyleneimidazolyl biphenyls. *Eur. J. Med. Chem.* **2009**, *44*, 2765–2775. (c) Hu, Q.; Negri, M.; Olgen, S.; Hartmann, R. W. The role of fluorine substitution in biphenyl methylene imidazole type CYP17 inhibitors for the treatment of prostate carcinoma. *ChemMedChem.* **2010**, *5*, 899–910. (d) Hu, Q.; Jagusch, C.; Hille, U. E.; Hauptenthal, J.; Hartmann, R. W. Replacement of imidazolyl by pyridyl in biphenyl methylenes results in selective CYP17 and dual CYP17 / CYP11B1 inhibitors for the treatment of prostate cancer. *J. Med. Chem.* **2010**, In Press. (e) Hu, Q.; Yin, L.; Jagusch, C.; Hille, U. E.; Hartmann, R. W. Isopropylidene substitution increases activity and selectivity of biphenyl methylene 4-pyridine type CYP17 inhibitors. *J. Med. Chem.* **2010**, *53*, 5049–5053.
23. (a) Denner, K.; Doehmer, J.; Bernhardt, R. Cloning of CYP11B1 and CYP11B2 from normal human adrenal and their functional expression in COS-7 and V79 chinese hamster cells. *Endocr. Res.* **1995**, *21*, 443–448. (b) Ehmer, P. B.; Bureik, M.; Bernhardt, R.; Müller, U.; Hartmann, R. W. Development of a test system for inhibitors of human aldosterone synthase (CYP11B2): Screening in fission yeast and evaluation of selectivity in V79 cells. *J. Steroid Biochem. Mol. Biol.* **2002**, *81*, 173–179. (c) Hartmann, R. W.; Batzl, C. Aromatase inhibitors. Synthesis and evaluation of mammary tumor inhibiting activity of 3-alkylated 3-(4-aminophenyl)piperidine-2,6-diones. *J. Med. Chem.* **1986**, *29*, 1362–1369. (d) Hutschenreuter, T. U.; Ehmer, P. E.; Hartmann, R. W. Synthesis of hydroxy derivatives of highly potent non-steroidal CYP 17 Inhibitors as potential metabolites and evaluation of their activity by a non cellular assay using recombinant human enzyme. *J. Enzyme Inhib. Med. Chem.* **2004**, *19*, 17–32. (e) Ehmer, P. B.; Jose, J.; Hartmann, R. W. Development of a simple and rapid assay for the evaluation of inhibitors of human 17 α -hydroxylase-C(17,20)-lyase (P450c17) by coexpression of P450c17 with NADPH-cytochrome-P450-reductase in Escherichia coli. *J. Steroid Biochem. Mol. Biol.* **2000**, *75*, 57–63

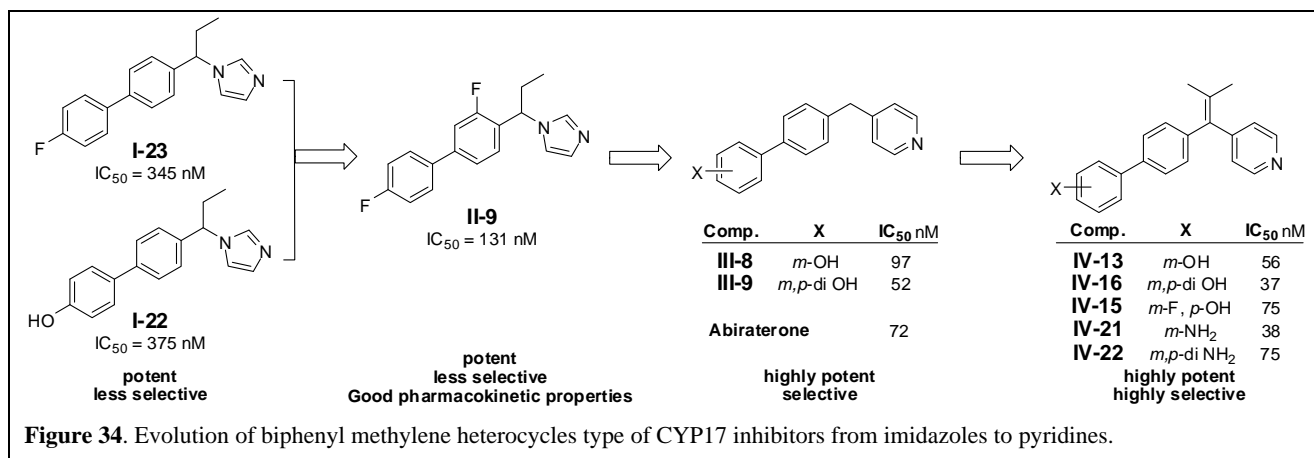
4 Summary and Conclusions

4.1 CYP17 Inhibitors

In mimicking the natural steroidal substrates, several series of biphenyl methylene heterocycles were designed, synthesized and tested as CYP17 inhibitors.

The studies started with imidazoles, among which potent inhibitors were identified with IC_{50} values ranging from 100 to 350 nM (compounds **I-22**, **I-23** and **II-9**, Figure 34). Several factors are found to exhibit a great deal of influences on the inhibitory potency. It has been revealed that alkyl groups at the methylene bridge, if in suitable length, can strongly improve the inhibitory potency. Screening of substituents in various bulk and electrostatic potential presented ethyl as the most suitable one. Moreover, analogues substituted with polar substituents at the A-ring, capable of H-bond formation, always led to potent inhibitors. Besides, the rigidification of the biphenyl core to form a carbazole or 9H-fluorene ring also significantly elevated the activity, probably due to planar conjugated scaffolds. However, this planar conformation impaired the selectivity as well. Further investigation on fluorine revealed that fluorine in the *meta*-position of the C-ring increased the activity compared with the non-substituted analogues, whereas *ortho*-substitution reduced the potency. On the contrary, multi-F substitution on the A-ring reduced the electron density of the A-ring, which thereby weakens the T-shaped interaction between the A-ring and Phe114, and consequently decreases the inhibitory potency.

Furthermore, compounds **I-23** and **II-9** showed potent activity *in vivo*, long plasma half-lives and high bioavailability. Intriguingly, only when fluorine is substituted in an appropriate position, such as in the *meta*-position of the C-ring, is the plasma half life prolonged. If found in an unsuitable position, however, the $t_{1/2}$ value was decreased probably due to the electron withdrawing effects by multi F substitutions, which significantly weaken the adjacent aromatic C-H bonds conferring them vulnerable to metabolic reactions.



Despite the fact that orally active CYP17 inhibitors were obtained in imidazoles, the inhibitory potency and selectivity need further improvement. The replacement of imidazolyl by 4-pyridyl significantly increase the inhibition toward CYP17 with the best compounds (**III-8**, **III-9**, **IV-13**, **IV-15**, **IV-16**, **IV-21** and **IV-22**) being comparable to or even more potent than the drug candidate Abiraterone (Figure 34). This improvement

might be due to the prolonged distance between the sp^2 hybrid N and the methylene C. The elongation of the molecule places the H-bond forming groups at the A-ring closer to the amino acid residues, thereby facilitating better H-bond formation. Similar as observed for the imidazoles, hydrogen bond forming groups, like OH and NH_2 , significantly elevated CYP17 inhibition. OH analogues were found to be more potent than the corresponding NH_2 analogues probably because the hydrogen bonds formed by O are stronger than the ones formed by N. Interestingly, *meta*-substituted analogues are more potent than the corresponding *para*-analogues. Nevertheless, a different SAR was observed concerning the substituents on the methylene bridge. For imidazoles, ethyl was identified as the most suitable group. However, for pyridines, flexible alkyl groups reduced activity, whereas conformation rigidifying isopropylidene groups significantly promoted the inhibitory activity. Most of the isopropylidene compounds also exhibited better selectivity profiles toward CYP11B1, CYP11B2, CYP19 and hepatic CYP3A4 than the parent compounds and Abiraterone, which is a good example that a single substituent can be the key for selectivity among several CYP enzymes.

Docking studies of the potent CYP17 inhibitor using our homology model revealed that both imidazoles and pyridines predominantly adopted a similar binding mode (Figure 35). It has been observed that the compounds coordinated to the heme iron with the N-containing heterocycle in a perpendicular way. The conjugated scaffold of biphenyl moiety orienting almost parallel to the I-helix was considered one of the key factors for high

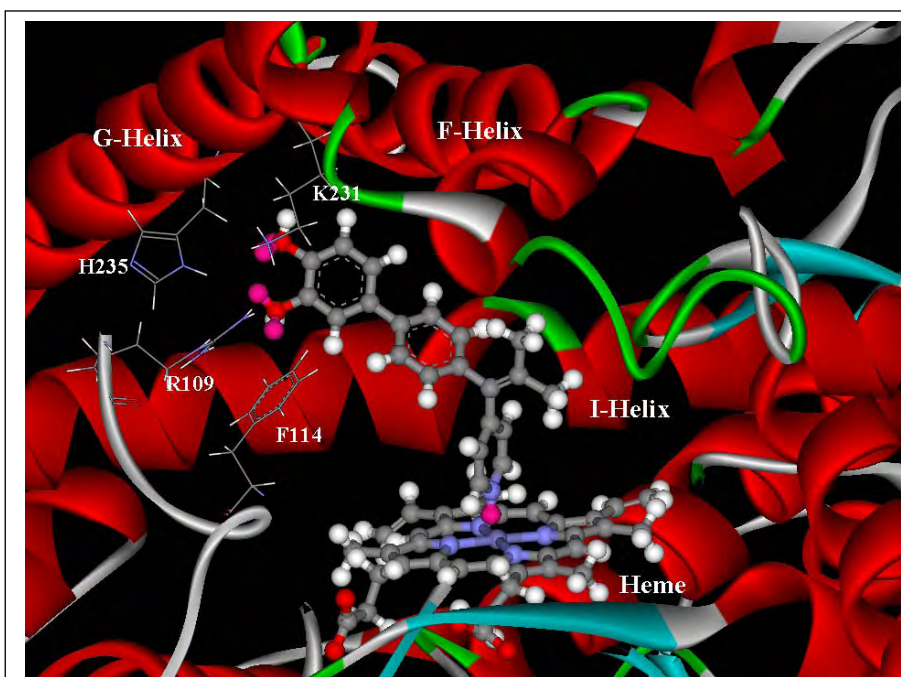


Figure 35. Typical binding mode of biphenyl methylene heterocycles in CYP17 (illustrated with IV-16).

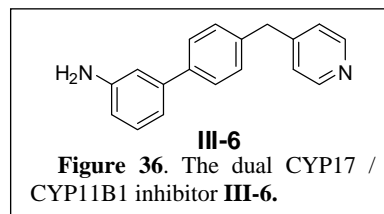
activity. This extended π -system obviously interacted not only with the π -system of the amino acid backbone in the I-helix (i.e. Gly301, Ala302, Gly303, Val304), but also with Phe114, which was oriented in a perpendicular fashion toward the A-ring (Figure 35) to form a quadrupole-quadrupole interaction. More importantly, H-bond forming groups, such as OH, NH_2 and F, on the A-ring interacted with Arg109, Lys231 and His235 (Figure 35). These interactions significantly increased the affinity between the inhibitors and the enzyme. Furthermore, the elevated activity of C-ring *meta*-F substituted compounds was attributed to the multi-polar interaction between F and the N-H group of Glu305 stabilizing the π - π interaction between the C-ring and the backbone π -system of Gly301-Ala302.

Via this evolution of biphenyl methylene heterocycles from imidazoles to pyridines, CYP17 inhibitors, which are more potent and more selective than the drug candidate Abiraterone, were identified. These compounds can be considered to be promising drug candidates after further evaluation *in vivo*. Moreover, the

finding of isopropylidene as a key to the excellent selectivity between CYP17 and other steroidogenic and hepatic CYP enzymes can be exploited in the further design of CYP17 inhibitors. It may also provide clues to solve the selectivity puzzles for inhibitors toward other CYP enzymes.

4.2 Dual Inhibitors of CYP17 / CYP11B1

The design strategy of segmentation and hybridization applied with the steroidal CYP17 inhibitor Abiraterone, the CYP11B1 inhibitor Metyrapone and our experience in non-steroidal biphenyl methylene based CYP17 inhibitors successfully led to dual inhibitors. Since maximization of CYP17 inhibition was pursued as the first priority



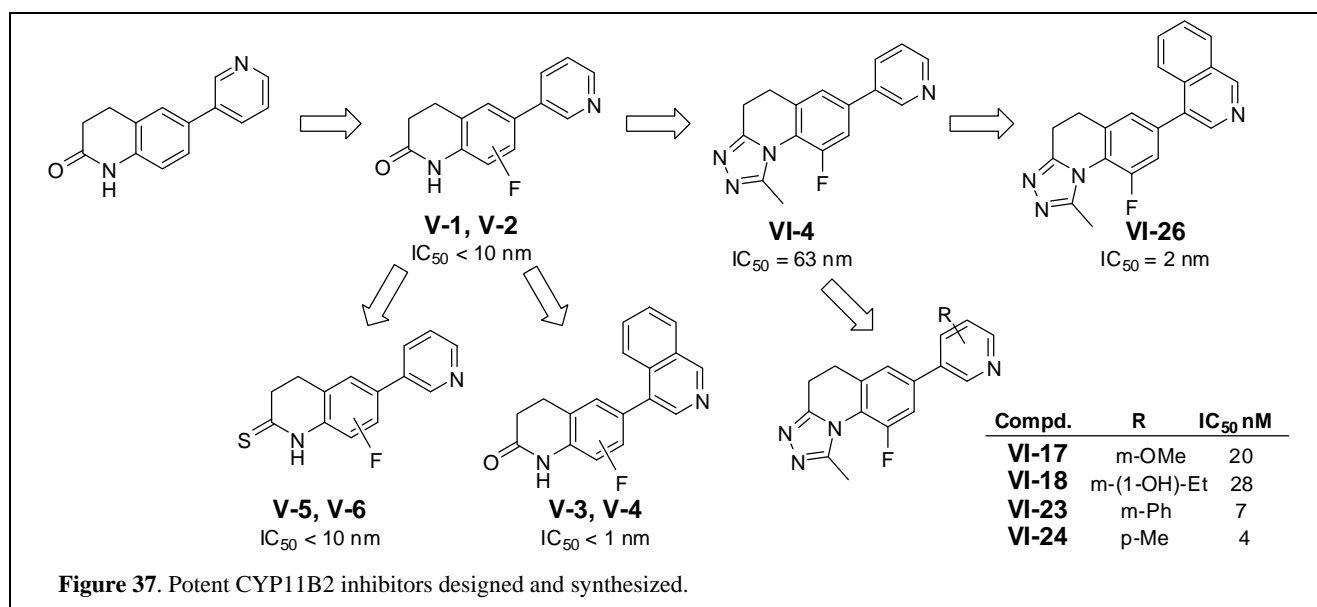
during the segment selection, high inhibitory potency toward this enzyme is guaranteed; whereas the inhibition toward CYP11B1 will largely depend on the substituents on the core. It was found that compounds with one single H-bond donor showed potent to modest inhibition toward CYP11B1 (IC_{50} values ranged 250 to 350 nM), whereas H-bond acceptors or two donors resulted in rather weak inhibition. Hence compound **III-6** (Figure 36) was obtained showing a good dual inhibition of CYP17 and CYP11B1 with IC_{50} values around 200 nM for both enzymes, a three fold selectivity for CYP11B1 over CYP11B2 and nearly no inhibition of CYP19 and CYP3A4. As selectivity for CYP11B2 should be further enhanced, compound **III-6** could be an ideal candidate for the optimization process.

Based on these interesting results a novel strategy for the treatment of prostate cancer was proposed: CYP17 inhibitors with different selectivity profiles according to the status of the patients should be applied. For normal patients, selective CYP17 inhibitors that do not interfere with other steroidogenic CYPs should be used to avoid side effects. However, for patients with mutated androgen receptors or ectopic adrenocorticotrophic hormone syndrome, dual inhibitors of CYP17 and CYP11B1 are the best choice in the view of a personalized medicine.

4.3 CYP11B2 Inhibitors

With 6-(pyridin-3-yl)-3,4-dihydroquinolin-2(1H)-one ($IC_{50} = 28$ nM, Figure 37) as the lead compound, a series of optimization was performed. It has been found that introduction of F onto the core increased the inhibitory potency to less than 10 nM (Figure 37, **V-1** and **V-2**). Bioisostere exchange of ketone O to S (**V-5** and **V-6**) or replacement of pyridyl by isoquinolinyl (**V-3** and **V-4**) further enhanced the CYP11B2 inhibition. Furthermore, an additional triazolo cycle was fused to the dihydroquinolinone core to form extra H-bonds and to conceal amide moiety, which is possibly vulnerable in vivo. A series of novel heterocycle substituted 4,5-dihydro-[1,2,4]triazolo[4,3-*a*]quinolines were thus designed, synthesized and biologically evaluated. It has been elucidated that the substituents on the 1-position of triazolo moiety have profound influence on the CYP11B2 inhibitory potency, where the bulk is the crucial determinant. Methyl, as the most suitable group, was found to significantly improve the potency (**VI-4**, Figure 37). Nevertheless, larger substituents led to the loss of activity. It is intriguing that analogues with fluorine furnished at 9-position are more potent than the

ones with 8-F substitution. Furthermore, substituents on the pyridyl are important for the affinity of compounds to the enzyme by altering the electron density on sp^2 hybrid N, whereby electron donating groups

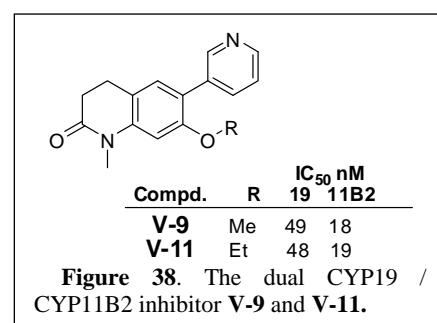


increase inhibition (**VI-17**, **VI-18**, **VI-23** and **VI-24**; Figure 37), whereas electron withdrawing groups slightly reduce it. The increase of inhibitory potency by occupancy of additional hydrophobic pocket near heme is also observed, despite of coinstantaneous selectivity impairment. Conformation rigidification is considered as an advantageous factor for the CYP11B2 inhibition as well, which is substantiated by the fusing of additional phenyl (**VI-23**) and *para*-methyl substituntson pyridyl (**VI-24**). The current study results in many potent ($IC_{50} < 10$ nM) and highly selective (selectivity factor > 100) CYP11B2 inhibitors, especially compound **VI-24** ($IC_{50} = 4.2$ nM, selectivity factor = 422). These compounds are considered to be promising drug candidates after further evaluation in vivo.

4.4 Dual Inhibitors of CYP19 / CYP11B2

The approach of combining important structural features of CYP19 and CYP11B2 inhibitors to design dual inhibitors led to the introduction of alkoxy onto the dihydroquinolinone core. It has been found that the bulky augment of alkoxy groups at the 7-position largely elevated CYP19 inhibition, yet, reduced CYP11B2 inhibition and selectivity over CYP11B1. On the contrary, methylation of amide increased inhibitory potency toward all of these three enzymes. After

balancing the different influence on SARs, selective dual inhibitors were successfully obtained as compounds **V-9** and **V-11** (Figure 38) with IC_{50} values around 50 and 20 nM toward CYP19 and CYP11B2, respectively. These compounds also showed good selectivity against CYP11B1 with selectivity factors around 50 and no interference with CYP17. After further evaluation in vivo, these dual inhibitors can be considered to be promising drug candidates as the treatment for BC patients with risks of CVD.



4 Summary and Conclusions

4.1 CYP17 Inhibitors

In mimicking the natural steroidal substrates, several series of biphenyl methylene heterocycles were designed, synthesized and tested as CYP17 inhibitors.

The studies started with imidazoles, among which potent inhibitors were identified with IC_{50} values ranging from 100 to 350 nM (compounds **I-22**, **I-23** and **II-9**, Figure 34). Several factors are found to exhibit a great deal of influences on the inhibitory potency. It has been revealed that alkyl groups at the methylene bridge, if in suitable length, can strongly improve the inhibitory potency. Screening of substituents in various bulk and electrostatic potential presented ethyl as the most suitable one. Moreover, analogues substituted with polar substituents at the A-ring, capable of H-bond formation, always led to potent inhibitors. Besides, the rigidification of the biphenyl core to form a carbazole or 9H-fluorene ring also significantly elevated the activity, probably due to planar conjugated scaffolds. However, this planar conformation impaired the selectivity as well. Further investigation on fluorine revealed that fluorine in the *meta*-position of the C-ring increased the activity compared with the non-substituted analogues, whereas *ortho*-substitution reduced the potency. On the contrary, multi-F substitution on the A-ring reduced the electron density of the A-ring, which thereby weakens the T-shaped interaction between the A-ring and Phe114, and consequently decreases the inhibitory potency.

Furthermore, compounds **I-23** and **II-9** showed potent activity *in vivo*, long plasma half-lives and high bioavailability. Intriguingly, only when fluorine is substituted in an appropriate position, such as in the *meta*-position of the C-ring, is the plasma half life prolonged. If found in an unsuitable position, however, the $t_{1/2}$ value was decreased probably due to the electron withdrawing effects by multi F substitutions, which significantly weaken the adjacent aromatic C-H bonds conferring them vulnerable to metabolic reactions.

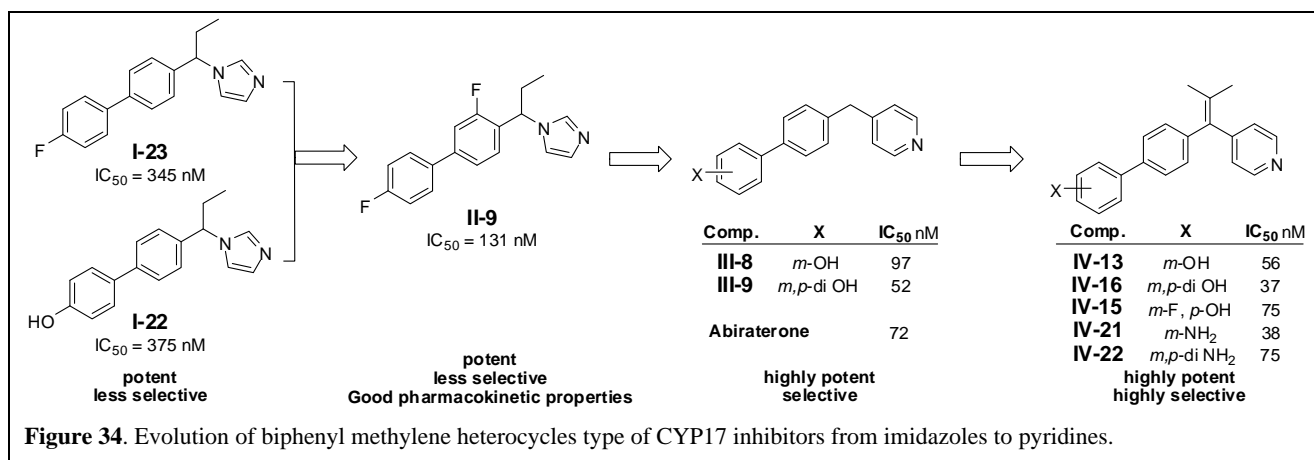


Figure 34. Evolution of biphenyl methylene heterocycles type of CYP17 inhibitors from imidazoles to pyridines.

Despite the fact that orally active CYP17 inhibitors were obtained in imidazoles, the inhibitory potency and selectivity need further improvement. The replacement of imidazolyl by 4-pyridyl significantly increase the inhibition toward CYP17 with the best compounds (**III-8**, **III-9**, **IV-13**, **IV-15**, **IV-16**, **IV-21** and **IV-22**) being comparable to or even more potent than the drug candidate Abiraterone (Figure 34). This improvement

might be due to the prolonged distance between the sp^2 hybrid N and the methylene C. The elongation of the molecule places the H-bond forming groups at the A-ring closer to the amino acid residues, thereby facilitating better H-bond formation. Similar as observed for the imidazoles, hydrogen bond forming groups, like OH and NH_2 , significantly elevated CYP17 inhibition. OH analogues were found to be more potent than the corresponding NH_2 analogues probably because the hydrogen bonds formed by O are stronger than the ones formed by N. Interestingly, *meta*-substituted analogues are more potent than the corresponding *para*-analogues. Nevertheless, a different SAR was observed concerning the substituents on the methylene bridge. For imidazoles, ethyl was identified as the most suitable group. However, for pyridines, flexible alkyl groups reduced activity, whereas conformation rigidifying isopropylidene groups significantly promoted the inhibitory activity. Most of the isopropylidene compounds also exhibited better selectivity profiles toward CYP11B1, CYP11B2, CYP19 and hepatic CYP3A4 than the parent compounds and Abiraterone, which is a good example that a single substituent can be the key for selectivity among several CYP enzymes.

Docking studies of the potent CYP17 inhibitor using our homology model revealed that both imidazoles and pyridines predominantly adopted a similar binding mode (Figure 35). It has been observed that the compounds coordinated to the heme iron with the N-containing heterocycle in a perpendicular way. The conjugated scaffold of biphenyl moiety orienting almost parallel to the I-helix was considered one of the key factors for high

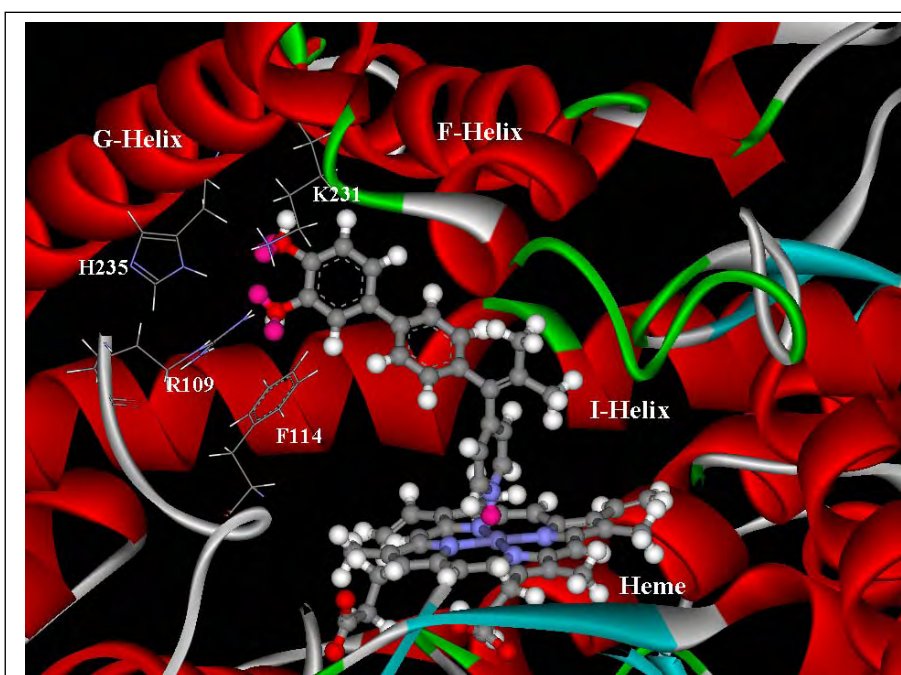


Figure 35. Typical binding mode of biphenyl methylene heterocycles in CYP17 (illustrated with IV-16).

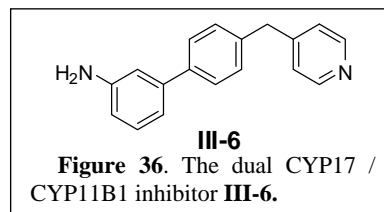
activity. This extended π -system obviously interacted not only with the π -system of the amino acid backbone in the I-helix (i.e. Gly301, Ala302, Gly303, Val304), but also with Phe114, which was oriented in a perpendicular fashion toward the A-ring (Figure 35) to form a quadrupole-quadrupole interaction. More importantly, H-bond forming groups, such as OH, NH_2 and F, on the A-ring interacted with Arg109, Lys231 and His235 (Figure 35). These interactions significantly increased the affinity between the inhibitors and the enzyme. Furthermore, the elevated activity of C-ring *meta*-F substituted compounds was attributed to the multi-polar interaction between F and the N-H group of Glu305 stabilizing the π - π interaction between the C-ring and the backbone π -system of Gly301-Ala302.

Via this evolution of biphenyl methylene heterocycles from imidazoles to pyridines, CYP17 inhibitors, which are more potent and more selective than the drug candidate Abiraterone, were identified. These compounds can be considered to be promising drug candidates after further evaluation in vivo. Moreover, the

finding of isopropylidene as a key to the excellent selectivity between CYP17 and other steroidogenic and hepatic CYP enzymes can be exploited in the further design of CYP17 inhibitors. It may also provide clues to solve the selectivity puzzles for inhibitors toward other CYP enzymes.

4.2 Dual Inhibitors of CYP17 / CYP11B1

The design strategy of segmentation and hybridization applied with the steroidal CYP17 inhibitor Abiraterone, the CYP11B1 inhibitor Metyrapone and our experience in non-steroidal biphenyl methylene based CYP17 inhibitors successfully led to dual inhibitors. Since maximization of CYP17 inhibition was pursued as the first priority



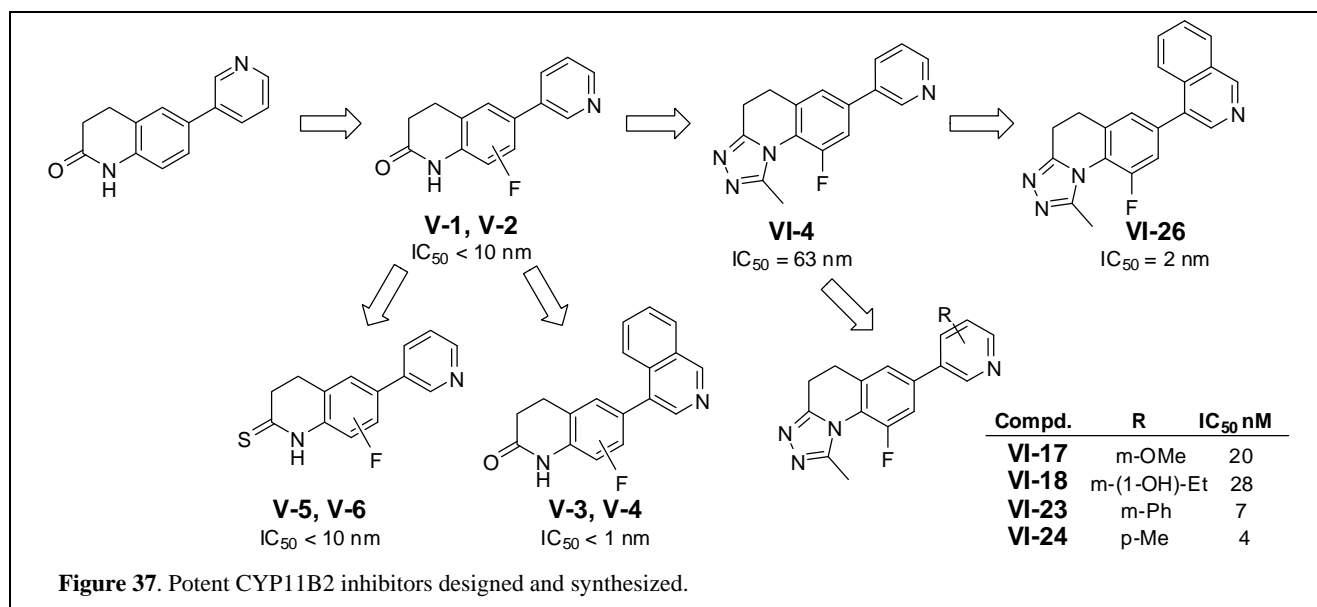
during the segment selection, high inhibitory potency toward this enzyme is guaranteed; whereas the inhibition toward CYP11B1 will largely depend on the substituents on the core. It was found that compounds with one single H-bond donor showed potent to modest inhibition toward CYP11B1 (IC_{50} values ranged 250 to 350 nM), whereas H-bond acceptors or two donors resulted in rather weak inhibition. Hence compound **III-6** (Figure 36) was obtained showing a good dual inhibition of CYP17 and CYP11B1 with IC_{50} values around 200 nM for both enzymes, a three fold selectivity for CYP11B1 over CYP11B2 and nearly no inhibition of CYP19 and CYP3A4. As selectivity for CYP11B2 should be further enhanced, compound **III-6** could be an ideal candidate for the optimization process.

Based on these interesting results a novel strategy for the treatment of prostate cancer was proposed: CYP17 inhibitors with different selectivity profiles according to the status of the patients should be applied. For normal patients, selective CYP17 inhibitors that do not interfere with other steroidogenic CYPs should be used to avoid side effects. However, for patients with mutated androgen receptors or ectopic adrenocorticotrophic hormone syndrome, dual inhibitors of CYP17 and CYP11B1 are the best choice in the view of a personalized medicine.

4.3 CYP11B2 Inhibitors

With 6-(pyridin-3-yl)-3,4-dihydroquinolin-2(1H)-one ($IC_{50} = 28$ nM, Figure 37) as the lead compound, a series of optimization was performed. It has been found that introduction of F onto the core increased the inhibitory potency to less than 10 nM (Figure 37, **V-1** and **V-2**). Bioisostere exchange of ketone O to S (**V-5** and **V-6**) or replacement of pyridyl by isoquinolinyl (**V-3** and **V-4**) further enhanced the CYP11B2 inhibition. Furthermore, an additional triazolo cycle was fused to the dihydroquinolinone core to form extra H-bonds and to conceal amide moiety, which is possibly vulnerable in vivo. A series of novel heterocycle substituted 4,5-dihydro-[1,2,4]triazolo[4,3-*a*]quinolines were thus designed, synthesized and biologically evaluated. It has been elucidated that the substituents on the 1-position of triazolo moiety have profound influence on the CYP11B2 inhibitory potency, where the bulk is the crucial determinant. Methyl, as the most suitable group, was found to significantly improve the potency (**VI-4**, Figure 37). Nevertheless, larger substituents led to the loss of activity. It is intriguing that analogues with fluorine furnished at 9-position are more potent than the

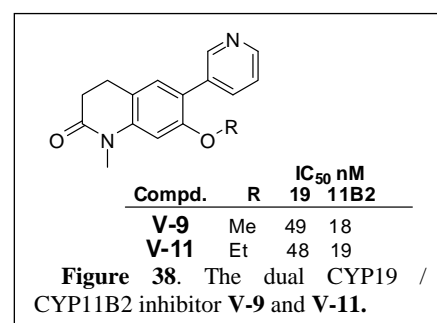
ones with 8-F substitution. Furthermore, substituents on the pyridyl are important for the affinity of compounds to the enzyme by altering the electron density on sp^2 hybrid N, whereby electron donating groups



increase inhibition (**VI-17**, **VI-18**, **VI-23** and **VI-24**; Figure 37), whereas electron withdrawing groups slightly reduce it. The increase of inhibitory potency by occupancy of additional hydrophobic pocket near heme is also observed, despite of coinstantaneous selectivity impairment. Conformation rigidification is considered as an advantageous factor for the CYP11B2 inhibition as well, which is substantiated by the fusing of additional phenyl (**VI-23**) and *para*-methyl substitutson pyridyl (**VI-24**). The current study results in many potent ($IC_{50} < 10$ nM) and highly selective (selectivity factor > 100) CYP11B2 inhibitors, especially compound **VI-24** ($IC_{50} = 4.2$ nM, selectivity factor = 422). These compounds are considered to be promising drug candidates after further evaluation in vivo.

4.4 Dual Inhibitors of CYP19 / CYP11B2

The approach of combining important structural features of CYP19 and CYP11B2 inhibitors to design dual inhibitors led to the introduction of alkoxy onto the dihydroquinolinone core. It has been found that the bulky augment of alkoxy groups at the 7-position largely elevated CYP19 inhibition, yet, reduced CYP11B2 inhibition and selectivity over CYP11B1. On the contrary, methylation of amide increased inhibitory potency toward all of these three enzymes. After



balancing the different influence on SARs, selective dual inhibitors were successfully obtained as compounds **V-9** and **V-11** (Figure 38) with IC_{50} values around 50 and 20 nM toward CYP19 and CYP11B2, respectively. These compounds also showed good selectivity against CYP11B1 with selectivity factors around 50 and no interference with CYP17. After further evaluation in vivo, these dual inhibitors can be considered to be promising drug candidates as the treatment for BC patients with risks of CVD.

5. Reference

1. Mojzsis, S. J.; Arrhenius, G.; McKeegan, K. D.; Harrison, T. M.; Nutman, A. P.; Friend, C. R. L. Evidence for life on Earth before 3,800 million years ago. *Nature* **1996**, *384*, 55–59.
2. Ghosh, D.; Griswold, J.; Erman, M.; Pangborn, W. Structural basis for androgen specificity and oestrogen synthesis in human aromatase. *Nature* **2009**, *457*, 219–223.
3. Guengerich, F. P. Common and uncommon cytochrome P450 reactions related to metabolism and chemical toxicity. *Chem. Res. Toxicol.* **2001**, *14*, 611–650.
4. Denisov, L. G.; Makris, T. M.; Sligar, S. G.; Schlichting, I. Structure and chemistry of cytochrome P450. *Chem. Rev.* **2005**, *105*, 2253–2277.
5. Evans, W. E.; Relling, M. V. Pharmacogenomics: translating functional genomics into rational therapeutics. *Science* **1999**, *286*, 487–491.
6. Emoto, C.; Murase, S.; Iwasaki, K. Approach to the prediction of the contribution of major cytochrome P450 enzymes to drug metabolism in the early drug discovery stage. *Xenobiotica* **2006**, *36*, 667–683.
7. Shimada, T.; Yamazaki, H.; Mimura, M.; Inui, Y.; Guengerich, F. P. Interindividual variations in human liver cytochrome P-450 enzymes involved in the oxidation of drugs, carcinogens and toxic chemicals: studies with liver microsomes of 30 Japanese and 30 Caucasians. *J. Pharmacol. Exp. Ther.* **1994**, *270*, 414–423.
8. <http://seer.cancer.gov/statfacts/html/prost.html>
9. LeBeau, A. M.; Singh, P.; Isaacs, J. T.; Denmeade, S. R. Prostate-specific antigen is a "chymotrypsin-like" serine protease with unique P1 substrate specificity. *Biochemistry* **2009**, *48*, 3490–3496.
10. Welch, H. G.; Albertsen, P. C. Prostate cancer diagnosis and treatment after the introduction of prostate-specific antigen screening: 1986–2005. *J. Natl. Cancer Inst.* **2009**, *101*, 1325–1329.
11. Schroder, F. H.; Hugosson, J.; Roobol, M. J.; Tammela, T. L. J.; Ciatto, S.; Nelen, V.; Kwiatkowski, M.; Lujan, M.; Lilja, H.; Zappa, M.; Denis, L. J.; Recker, F.; Berenguer, A.; Maattanen, L.; Bangma, C. H.; Aus, G.; Villers, A.; Rebillard, X.; van der Kwast, T.; Blijenberg, B. G.; Moss, S. M.; de Koning, H. J.; Auvinen, A. Screening and prostate-cancer mortality in a randomized European study. *New Engl. J. Med.* **2009**, *360*, 1320–1328.
12. van Leeuwen, P. J.; Connolly, D.; Gavin, A.; Roobol, M. J.; Black, A.; Bangma, C. H.; Schroder, F. H. Prostate cancer mortality in screen and clinically detected prostate cancer: estimating the screening benefit. *Eur. J. cancer* **2010**, *46*, 377–383.
13. Makarov, D. V.; Carter, H. B. The discovery of prostate specific antigen as a biomarker for the early detection of adenocarcinoma of the prostate. *J. Urol.* **2006**, *176*, 2383–2385.
14. Weinzimer, S. A.; Gibson, T. B.; Collett-Solberg, P. F.; Khare, A.; Liu, B.; Cohen, P. Transferrin is an insulin-like growth factor-binding protein-3 binding protein. *J. Clin. Endocrinol. Metab.* **2001**, *86*, 1806–1813.
15. Prostate Cancer. In *Wiley Handbook of Current and Emerging Drug Therapies*; Pidgeon, S., Eds.; Copyright 2007 by Decision Resources, Inc; John Wiley and Sons Inc, Hoboken, New Jersey, **2007**. pp 233.
16. Johansson, J. E., Andrén, O.; Andersson, S. O.; Dickman, P. W.; Holmberg, L.; Magnuson, A.; Adami, H. O. Natural history of early, localized prostate cancer. *J. Am. Med. Assoc.* **2004**, *291*, 2713–2719.
17. D'Amico, A. V.; Schultz, D.; Loffredo, M.; Dugal, R.; Hurwitz, M.; Kaplan, I.; Beard, C. J.; Renshaw, A. A.; Kantoff, P. W. Biochemical outcome following external beam radiation therapy with or without androgen suppression therapy for clinically localized prostate cancer. *J. Am. Med. Assoc.* **2000**, *284*, 1280–1283.
18. Tannock, I. F.; de Wit, R.; Berry, W. R.; Horti, J.; Pluzanska, A.; Chi, K. N.; Oudard, S.; Théodore, C.; James, N. D.; Turesson, I.; Rosenthal, M. A.; Eisenberger, M. A.; TAX 327 Investigators. Docetaxel plus prednisone or mitoxantrone plus prednisone for advanced prostate cancer. *New Engl. J. Med.* **2004**, *351*, 1502–1512.
19. Dulal Panda, D.; Miller, H. P.; Islam, K.; Wilson, L. Stabilization of microtubule dynamics by estramustine by binding to a novel site in tubulin: a possible mechanistic basis for its antitumor action. *Proc. Natl. Acad. Sci. U. S. A.* **1997**, *94*, 10560–10564.
20. Smith, P. H.; Suci, S.; Robinson, M. R.; Richards, B.; Bastable, J. R.; Glashan, R. W.; Bouffieux, C.; Lardennois, B.; Williams, R. E.; de Pauw, M. A comparison of the effect of diethylstilbestrol with low-dose estramustine phosphate in the treatment of advanced prostatic cancer: Pnal analysis of a Phase III trial of the European Organization for Research on Treatment of Cancer. *J. Urol.* **1986**, *136*, 619–623.
21. Petrylak, D. P. SWOG 99.16: randomized Phase III trial of docetaxel (D) / estramustine (E) versus mitoxantrone(M) / prednisone (p) in men with androgen-independent prostate cancer (AIPCA). *Proceedings of the American Society of Clinical Oncology Annual Meeting*. 2004. Abstract 3.
22. Tannock, I. F.; Osoba, D.; Stockler, M. R.; Ernst, D. S.; Neville, A. J.; Moore, M. J.; Armitage, G. R.; Wilson, J. J.; Venner, P. M.; Coppin, C. M.; Murphy, K. C. Chemotherapy with mitoxantrone plus prednisone or prednisone alone for symptomatic hormone-resistant prostate cancer: a Canadian randomized trial with palliative endpoints. *J. Clin. Oncol.* **1996**, *14*, 1756–1764.
23. Rini, B. I. A Phase II study of prostatic acid phosphatase-pulsed dendritic cells (APC-8015; Provenge) in combination with evacizumab in patients with serologic progression of prostate cancer after local therapy. *Proceedings of the American Society of Clinical Oncology Annual Meeting*. **2003**. Abstract 699.
24. Figg, W. D.; Dahut, W.; Duray, P.; Hamilton, M.; Tompkins, A.; Steinberg, S. M.; Jones, E.; Premkumar, A.; Linehan, W.

- M.; Floeter, M. K.; Chen, C. C.; Dixon, S.; Kohler, D. R.; Krüger, E.A.; Gubish, E.; Pluda, J. M.; Reed, E. A randomized Phase II trial of thalidomide, an angiogenesis inhibitor, in patients with androgen-independent prostate cancer. *Clin. Cancer Res.* **2001**, *7*, 1888–1893.
25. Dreicer, R. Phase I/II trial of bortezomib plus docetaxel in patients with advanced androgen-independent prostate cancer. *Proceedings of the American Association of Clinical Oncology Annual Meeting.* **2004**. Abstract 4654.
 26. Carducci, M. A. Effects of atrasentan on disease progression and biological markers in men with metastatic, hormone-refractory prostate cancer: Phase III study. *Proceedings of the American Society of Clinical Oncology.* **2004**. Abstract 4508.
 27. Kris, M. G. A Phase II trial of ZD1839 (Iressa) in advanced non-small-cell lung cancer (NSCLC) patients who had failed platinum- and docetaxel-based regimens (IDEAL 2). *Proceedings of the American Society of Clinical Oncology Annual Meeting.* **2002**. Abstract 1166.
 28. Chi, K. N. A Phase II study of oblimersen sodium (G3139) and docetaxel (D) in patients (pts) with metastatic, hormone-refractory prostate cancer (HRPC). *Proceedings of the American Society for Clinical Oncology.* **2003**. Abstract 1580.
 29. Small, E. J.; Fratesi, P.; Reese, D. M.; Strang, G.; Laus, R.; Peshwa, M. V.; Valone, F. H. Immunotherapy of hormone-refractory prostate cancer with antigen-loaded dendritic cells. *J. Clin. Oncol.* **2000**, *18*, 3894–3903.
 30. Simons, J. Phase II trials of a GM-CSF gene-transduced prostate cancer cell line vaccine (GVAX) in hormone-refractory prostate cancer. *Proceedings of the American Association of Clinical Oncology Annual Meeting.* **2002**. Abstract 729.
 31. Geller, J. Basis for hormonal management of advanced prostate cancer. *Cancer* **1993**, *71*, 1039–1045.
 32. Freedman, L. P. *Molecular biology of steroid and nuclear hormone receptors*; Birkhauser: Boston, MA, **1998**.
 33. Zhou, X. E.; Suino-Powell, K. M.; Li, J.; He, Y.; Mackeigan, J. P.; Melcher, K.; Yong, E. L.; Xu, H. E. Identification of SRC3/AIB1 as a preferred coactivator for hormone-activated androgen receptor. *J. Biol. Chem.* **2010**, *285*, 9161–9171.
 34. Gao, W.; Bohl, C. E.; Dalton, J. T. Chemistry and structural biology of androgen receptor. *Chem. Rev.* **2005**, *105*, 3352–3370.
 35. Pratt, W. B.; Toft, D. O. Steroid receptor interactions with heat shock protein and immunophilin chaperones. *Endocr. Rev.* **1997**, *18*, 306–360.
 36. Wang, L. G.; Liu, X. M.; Kreis, W.; Budman, D. R. Phosphorylation/dephosphorylation of androgen receptor as a determinant of androgen agonistic or antagonistic activity. *Biochem. Biophys. Res. Commun.* **1999**, *259*, 21–18.
 37. Heinlein, C. A.; Chang, C. Androgen receptor (AR) coregulators: an overview. *Endocr. Rev.* **2002**, *23*, 175–200.
 38. Shang, Y.; Myers, M.; Brown, M. Formation of the androgen receptor transcription complex. *Mol. Cell* **2002**, *9*, 601–610.
 39. Masiello, D.; Cheng, S.; Bubley, G. J.; Lu, M. L.; Balk, S. P. Bicalutamide functions as an androgen receptor antagonist by assembly of a transcriptionally inactive receptor. *J. Bio. Chem.* **2002**, *277*, 26321–26326.
 40. Zagar, Y.; Chaumaz, G.; Lieberherr, M. Signaling cross-talk from Gbeta4 subunit to Elk-1 in the rapid action of androgens. *J. Bio. Chem.* **2004**, *279*, 2403–2413.
 41. Kampa, M.; Papakonstanti, E. A.; Hatzoglou, A.; Stathopoulos, E. N.; Stournaras, C.; Castanas, E. The human prostate cancer cell line LNCaP bears functional membrane testosterone receptors, which increase PSA secretion and modify actin cytoskeleton. *FASEB J.* **2002**, *16*, 1429–1431.
 42. Migliaccio, A.; Castoria, G.; Di Domenico, M.; de Falco, A.; Bilancio, A.; Lombardi, M.; Barone, M. V.; Ametrano, D.; Zannini, M. S.; Abbondanza, C.; Auricchio, F. Steroid-induced androgen receptor-oestradiol receptor beta-*Src* complex triggers prostate cancer cell proliferation. *EMBO J.* **2000**, *19*, 5406–5417.
 43. Stanbrough, M.; Bubley, G. J.; Ross, K.; Golub, T. R.; Rubin, M. A.; Penning, T. M.; Febbo, P. G.; Balk, S. P. Increased expression of genes converting adrenal androgens to testosterone in androgen-independent prostate cancer. *Cancer Res.* **2006**, *66*, 2815–2825.
 44. Montgomery, R. B.; Mostaghel, E. A.; Vessella, R.; Hess, D. L.; Kalthorn, T. F.; Higano, C. S.; True, L. D.; Nelson, P. S. Maintenance of intratumoral androgens in metastatic prostate cancer: A mechanism for castration-resistant tumor growth. *Cancer Res.* **2008**, *68*, 4447–4454.
 45. Holzbeierlein, J.; Lal, P.; La Tulippe, E.; Smith, A.; Satagopan, J.; Zhang, L.; Ryan, C.; Smith, S.; Scher, H.; Scardino, P.; Reuter, V.; Gerald, W. L. Gene expression analysis of human prostate carcinoma during hormonal therapy identifies androgen-responsive genes and mechanisms of therapy resistance. *Am. J. Pathol.* **2004**, *164*, 217–227.
 46. Huggins, C.; Hodges, C. V. Studies in prostatic cancer. I. The effect of castration, estrogens and androgen injections on serum phosphatases in metastatic carcinoma of the prostate. *Cancer Res.* **1941**, *1*, 293–297.
 47. Huhtaniemi, I.; Nikula, H.; Parvinen, M.; Rannikko, S. Histological and functional changes of the testis tissue during GnRH agonist treatment of prostatic cancer. *Am. J. Clin. Oncol.* **1988**, *11*, S11–S15.
 48. Titus, M. A.; Schell, M. J.; Lih, F. B.; Tomer, K. B.; Mohler, J. L. Testosterone and dihydrotestosterone tissue levels in recurrent prostate cancer. *Clin. Cancer Res.* **2005**, *11*, 4653–4657.
 49. Stanbrough, M.; Bubley, G. J.; Ross, K.; Golub, T. R.; Rubin, M. A.; Penning, T. M.; Febbo, P. G.; Balk, S. P. Increased expression of genes converting adrenal androgens to testosterone in androgen-independent prostate cancer. *Cancer Res.* **2006**, *66*, 2815–2825.
 50. Crawford, E. D.; Eisenberger, M. A.; McLeod, D. G.; Spaulding, J. T.; Benson, R.; Dorr, F. A.; Blumenstein, B. A.; Davis, M. A.; Goodman, P. J. A controlled trial of leuprolide with and without flutamide in prostatic carcinoma. *New Engl. J. Med.* **1989**, *321*, 419–424.
 51. Efstathiou, J. A.; Bae, K.; Shipley, W. U.; Hanks, G. E.; Pilepich, M. V.; Sandler, H. M.; Smith, M. R. Cardiovascular mortality after androgen deprivation therapy for locally advanced prostate cancer: RTOG 85-31. *J. Clin. Oncol.* **2008**, *27*, 92–99.
 52. Suzuki, H.; Akakura, K.; Komiya, A.; Aida, S.; Akimoto, S.; Shimazaki, J. Codon 877 mutation in the androgen receptor

- gene in advanced prostate cancer: relation to antiandrogen withdrawal syndrome. *Prostate* **1996**, *29*, 153–158.
53. Hara, T.; Miyazaki, J.; Araki, H.; Yamaoka, M.; Kanzaki, N.; Kusaka, M.; Miyamoto, M. Novel mutations of androgen receptor: a possible mechanism of bicalutamide withdrawal syndrome. *Cancer Res.* **2003**, *63*, 149–153.
 54. Zhao, X. Y.; Malloy, P. J.; Krishnan, A. V.; Swami, S.; Navone, N. M.; Peehl, D. M.; Feldman, D. Glucocorticoids can promote androgen-independent growth of prostate cancer cells through a mutated androgen receptor. *Nat. Med. (N. Y., NY, U. S.)* **2000**, *6*, 703–706.
 55. Imai, T.; Globerman, H.; Gertner, J. M.; Kagawa, N.; Waterman, M. R. Expression and purification of functional human 17 alpha-hydroxylase/17,20-lyase (P450c17) in *Escherichia coli*. Use of this system for study of a novel form of combined 17 alpha-hydroxylase/17,20-lyase deficiency. *J. Biol. Chem.* **1993**, *268*, 19681–19689.
 56. Lin, D.; Zhang, L. H.; Chiao, E.; Miller, W. L. Modeling and mutagenesis of the active site of human P450c17. *Mol. Endocrinol.* **1994**, *8*, 392–402.
 57. Haider, S. M.; Patel, J. M.; Poojari, C. S.; Neidle, S. Molecular modeling on inhibitor complexes and active-site dynamics of cytochrome P450 C17, a target for prostate cancer therapy. *J. Mol. Biol.* **2010**, doi:10.1016/j.jmb.2010.05.069.
 58. Miller, W. L.; Auchus, R. J.; Geller, D. H. The regulation of 17,20 lyase activity. *Steroids* **1997**, *62*, 133–142.
 59. Yanagibashi, K.; Hall, P. F. Role of electron transport in the regulation of the lyase activity of C-21 side-chain cleavage P450 from porcine adrenal and testicular microsomes. *J. Biol. Chem.* **1986**, *261*, 8429–8433.
 60. Kominami, S.; Ogawa, N.; Morimune, R.; Huang, D.Y.; Takemori, S. The role of cytochrome b5 in adrenal microsomal steroidogenesis. *J. Steroid Biochem. Mol. Biol.* **1992**, *42*, 57–64.
 61. Zhang, L. H.; Rodriguez, H.; Ohno, S.; Miller, W. L. Serine phosphorylation of human P450c17 increases 17,20-lyase activity: implications for adrenarche and the polycystic ovary syndrome. *Proc. Natl. Acad. Sci. USA* **1995**, *92*, 10619–10623.
 62. Guengerich, F. P.; Willard, R. J.; Shea, J. P.; Richards, L. R.; Macdonald, T. L. Mechanism-based inactivation of cytochrome P-450 by heteroatom-substituted cyclopropanes and formation of ring-opened products. *J. Am. Chem. Soc.* **1984**, *106*, 6446–6447.
 63. Hanzlik, R. P.; Tullman, R. H. Suicidal inactivation of cytochrome P-450 by cyclopropylamines. Evidence for cation-radical intermediates. *J. Am. Chem. Soc.* **1982**, *104*, 2048–2050.
 64. Angelastro, M. R.; Laughlin, M. E.; Schatzman, G. L.; Bey, P.; Blohm, T. R. 17 β -(Cyclopropylamino)-androst-5-en-3 β -ol, a selective mechanism-based inhibitor of cytochrome P450 17 α (steroid 17 α -hydroxylase/C₁₇₋₂₀ lyase). *Biochem. Biophys. Res. Commun.* **1989**, *162*, 1571–1577.
 65. Angelastro, M. R.; Marquart, A. L.; Weintraub, P. M.; Gates, C. A.; Laughlin, M. E.; Blohm, T. R.; Peet, N. P. Time-dependent inactivation of steroid C₁₇₍₂₀₎ lyase by 17 β -cyclopropyl ether-substituted steroids. *Bioorg. Med. Chem. Lett.* **1996**, *6*, 97–100.
 66. Patents: EP0288053, US4966897, US4966898, WO9730069 and WO9428010.
 67. Hartmann, R. W.; Bayer, H.; Grün, G. Aromatase inhibitors. Syntheses and structure-activity studies of novel pyridyl-substituted indanones, indans, and tetralins. *J. Med. Chem.* **1994**, *37*, 1275–1281.
 68. WO9215604.
 69. Burkhart, J. P.; Gates, C. A.; Laughlin, M. E.; Resvick, R. J.; Peet, N. P. Inhibition of steroid C₁₇₍₂₀₎ lyase with C-17-heteroaryl steroids. *Bioorg. Med. Chem.* **1996**, *4*, 1411–1420.
 70. Moreira, V. M.; Salvador, J. A. R.; Vasaitis, T. S.; Njar, V. C. O. CYP17 inhibitors for prostate cancer treatment – an update. *Curr. Med. Chem.* **2008**, *15*, 868–899.
 71. Potter, G. A.; Barrie, S. E.; Jarman, M.; Rowlands, M. G. Novel steroidal inhibitors of human cytochrome P450 17, (17 α -hydroxylase- C_{17,20}-lyase): potential agents for the treatment of prostatic cancer. *J. Med. Chem.* **1995**, *38*, 2463–2471.
 72. Jarman, M.; Barrie, S. E.; Llera, J. M. The 16, 17-double bond is needed for irreversible inhibition of human cytochrome P450_{17 α} by Abiraterone (17-(3-pyridyl) androsta-5, 16-dien-3 α -ol) and related steroidal inhibitors. *J. Med. Chem.* **1998**, *41*, 5375–5381.
 73. Attard, G.; Reid, A. H. M.; Yap, T. A.; Raynaud, F.; Dowsett, M.; Settatree, S.; Barrett, M.; Parker, C.; Martins, V.; Folkerd, E.; Clark, J.; Cooper, C. S.; Kaye, S. B.; Dearnaley, D.; Lee, G.; de Bono, J. S. Phase I clinical trial of a selective inhibitor of CYP17, Abiraterone acetate, confirms that castration-resistant prostate cancer commonly remains hormone driven. *J. Clin. Oncol.* **2008**, *26*, 4563–4571.
 74. Attard, G.; Reid, A. H. M.; A'Hern, R.; Parker, C.; Oommen, N. B.; Folkerd, E.; Messiou, C.; Molife, L. R.; Maier, G.; Thompson, E.; Olmos, D.; Sinha, R.; Lee, G.; Dowsett, M.; Kaye, S. B.; Dearnaley, D.; Kheoh, T.; Molina, A.; de Bono, J. S. Selective inhibition of CYP17 with Abiraterone acetate is highly active in the treatment of castration-resistant prostate cancer. *J. Clin. Oncol.* **2009**, *27*, 3742–3748.
 75. Haidar, S.; Ehmer P. B.; Barassin S.; Batzl-Hartmann C.; Hartmann R. W. Effects of novel 17alpha-hydroxylase/C17, 20-lyase (P450 17, CYP 17) inhibitors on androgen biosynthesis in vitro and in vivo. *J. Steroid Biochem. Mol. Biol.* **2003**, *84*, 555–562.
 76. Handratta, V. D.; Vasaitis, T. S.; Njar, V. C. O.; Gediya, L. K.; Kataria, R.; Chopra, P.; Newman, D. Jr.; Farquhar, R.; Guo, Z.; Qiu, Y.; Brodie, A. M. H. Novel C-17-heteroaryl steroidal CYP17 inhibitors/antiandrogens: Synthesis, in vitro biological activity, pharmacokinetics, and antitumor activity in the LAPC4 human prostate cancer xenograft model. *J. Med. Chem.* **2005**, *48*, 2972–2984.
 77. Bruno, R. D.; Gover, T. D.; Burger, A. M.; Brodie, A. M.; Njar, V. C. O. 17-Hydroxylase/17,20 lyase inhibitor VN/124-1 inhibits growth of androgen-independent prostate cancer cells via induction of the endoplasmic reticulum stress response. *Mol. Cancer Ther.* **2008**, *7*, 2828–2836.
 78. Vasaitis, T.; Belosay, A.; Schayowitz, A.; Khandelwal, A.; Chopra, P.; Gediya, L. K.; Guo, Z.; Fang, H.; Njar, V. C. O.;

- Brodie, A. M. H. Androgen receptor inactivation contributes to antitumor efficacy of 17-hydroxylase/17,20-lyase inhibitor 3 β -hydroxy-17-(1H-benzimidazole-1-yl)androsta-5,16-diene in prostate cancer. *Mol. Cancer Ther.* **2008**, *7*, 2348–2357.
79. Eklund, J.; Kozloff, M.; Vlamakis, J.; Starr, A.; Mariott, M.; Gallot, L.; Jovanovic, B.; Schilder, L.; Robin, E.; Pins, M.; Bergan, R. C. Phase II study of mitoxantrone and ketoconazole for hormone-refractory prostate cancer. *Cancer* **2006**, *106*, 2459–2465.
80. Patents: EP1348706, WO03027085, WO03027094, WO03027095, WO03027096, WO03027100, WO03027101, WO03027107, WO2006064944, EP1283208 and EP1283209.
81. Ideyama, Y.; Kudoh, M.; Tanimoto, K.; Susaki, Y.; Nanya, T.; Nakahara, T.; Ishikawa, H.; Yoden, T.; Okada, M.; Fujikura, T.; Akaza, H.; Shikama, H. Novel nonsteroidal inhibitor of cytochrome P450(17 α) (17 α -hydroxylase/C17-20 lyase), YMI16, decreased prostatic weights by reducing serum concentrations of testosterone and adrenal androgens in rats. *Prostate* **1998**, *37*, 10–18.
82. Patents: US3956295, WO9427989, WO9509157 and WO9626927.
83. EP1028110.
84. Wachter, G. A.; Hartmann, R. W.; Sergejew, T.; Grun, G. L.; Ledergerber, D. Tetrahydronaphthalenes: influence of heterocyclic substituents on inhibition of steroid enzymes P450 arom and P450 17. *J. Med. Chem.* **1996**, *39*, 834–841.
85. GB2253851, JP2005200317, WO9323375, WO2005005390, WO2006041037.
86. Rowlands, M. G.; Barrie, S. E.; Chan, F.; Houghton, J.; Jarman, M.; McCague, R.; Potter, G. A. Esters of 3-pyridylacetic acid that combine potent inhibition of 17 α -hydroxylase/C17,20-lyase (cytochrome P45017 α) with resistance to esterase hydrolysis. *J. Med. Chem.* **1995**, *38*, 4191–4197.
87. Chan, F. C.; Potter, G. A.; Barrie, S. E.; Haynes, B. P.; Rowlands, M. G.; Houghton, J.; Jarman, M. 3- and 4-pyridylalkyl adamantancarboxylates: inhibitors of human cytochrome P450(17 α) (17 α -hydroxylase/C17,20-lyase). Potential nonsteroidal agents for the treatment of prostatic cancer. *J. Med. Chem.* **1996**, *39*, 3319–3323.
88. Patents: WO0240484, WO0240470, EP1227085, WO0130762, WO0130764 and WO9954309.
89. Matsunaga, N.; Kaku, T.; Itoh, F.; Tanaka, T.; Hara, T.; Miki, H.; Iwasaki, M.; Aono, T.; Yamaoka, M.; Kusaka, M.; Tasaka, A. C17,20-Lyase inhibitors I. Structure-based de novo design and SAR study of C17,20-lyase inhibitors. *Bioorg. Med. Chem.* **2004**, *12*, 2251–2273.
90. Matsunaga, N.; Kaku, T.; Ojida, A.; Tanaka, T.; Hara, T.; Yamaoka, M.; Kusaka, M.; Tasaka, A. C17,20-lyase inhibitors. Part 2: Design, synthesis and structure-activity relationships of (2-naphthylmethyl)-1H-imidazoles as novel C17,20-lyase inhibitors. *Bioorg. Med. Chem.* **2004**, *12*, 4313–4336.
91. WO9837070
92. Patel, C. H.; Dhanani, S.; Owen, C. P.; Ahmed, S. Synthesis, biochemical evaluation and rationalisation of the inhibitory activity of a range of 4-substituted phenyl alkyl imidazole-based inhibitors of the enzyme complex 17 α -hydroxylase/17,20-lyase (P450(17 α)). *Bioorg. Med. Chem. Lett.* **2006**, *16*, 4752–4756.
93. Wachall, B. G.; Hector, M.; Zhuang, Y.; Hartmann, R. W. Imidazole substituted biphenyls: a new class of highly potent and in vivo active inhibitors of P450 17 as potential therapeutics for treatment of prostate cancer. *Bioorg. Med. Chem.* **1999**, *7*, 1913–1924.
94. Zhuang, Y.; Wachall, B. G.; Hartmann, R. W. Novel imidazolyl and triazolyl substituted biphenyl compounds: synthesis and evaluation as nonsteroidal inhibitors of human 17 α -hydroxylase-C17, 20-lyase (P450 17). *Bioorg. Med. Chem.* **2000**, *8*, 1245–1252.
95. Leroux, F.; Hutschenreuter, T. U.; Charriere, C.; Scopelliti, R.; Hartmann, R. W. N-(4-biphenylmethyl)imidazoles as potential therapeutics for the treatment of prostate cancer: metabolic robustness due to fluorine substitution? *Helv. Chim. Acta* **2003**, *86*, 2671–2686.
96. JP 10195056.
97. Simpson, S. A.; Tait, J. F.; Wettstein, A.; Neher, R.; Von Euw, J.; Reichstein, T. Isolation from the adrenals of a new crystalline hormone with especially high effectiveness on mineral metabolism. *Experientia* **1953**, *9*, 333–335.
98. Gekle, M.; Grossmann, C. Actions of aldosterone in the cardiovascular system: the good, the bad, and the ugly? *Eur. J. Physiol.* **2009**, *458*, 231–246.
99. Joffe, H. V.; Adler, G. K. Effect of aldosterone and mineralocorticoid receptor blockade on vascular inflammation. *Heart Fail. Rev.* **2005**, *10*, 31–37.
100. Brown, N. J. Aldosterone and vascular inflammation. *Hypertension* **2008**, *51*, 161–167.
101. Fiebeler, A.; Luft, F. C. The mineralocorticoid receptor and oxidative stress. *Heart Fail. Rev.* **2005**, *10*, 47–52.
102. Leibovitz, E.; Ebrahimian, T.; Paradis, P.; Schiffrin, E. L. Aldosterone induces arterial stiffness in absence of oxidative stress and endothelial dysfunction. *J. Hypertens.* **2009**, *27*, 2192–2200.
103. Rader, D. J.; Daugherty, A. Translating molecular discoveries into new therapies for atherosclerosis. *Nature* **2008**, *451*, 904–913.
104. Romagni, P.; Rossi, F.; Guerrini, L.; Quirini, C.; Santemma, V. Aldosterone induces contraction of the resistance arteries in man. *Atherosclerosis* **2003**, *166*, 345–349.
105. Fejes-Tóth, G.; Náráy-Fejes-Tóth, A. Early aldosterone-regulated genes in cardiomyocytes: clues to cardiac remodeling? *Endocrinology* **2007**, *148*, 1502–1510.
106. Lal, A.; Veinot, J. P.; Leenen, F. H. H. Critical role of CNS effects of aldosterone in cardiac remodeling post-myocardial infarction in rats. *Cardiovasc. Res.* **2004**, *64*, 437–447.
107. Zannad, F.; Radauceanu, A. Effect of MR blockade on collagen formation and cardiovascular disease with a specific

- emphasis on heart failure. *Heart Fail. Rev.* **2005**, *10*, 71–78.
108. Weber, K. T.; Brilla, C. G.; Campbell, S. E.; Guarda, E.; Zhou, G.; Sriram, K. Myocardial fibrosis: role of angiotensin II and aldosterone. *Basic Res. Cardiol.* **1993**, *88*, 107–124.
 109. Felder, R. B. Mineralocorticoid receptors, inflammation and sympathetic drive in a rat model of systolic heart failure. *Exp. Physiol.* **2009**, *95*, 19–25.
 110. Nicoletti, A.; Michel, J. B. Cardiac fibrosis and inflammation: interaction with hemodynamic and hormonal factors. *Cardiovasc. Res.* **1999**, *41*, 532–543.
 111. Cortinovis, M.; Perico, N.; Cattaneo, D.; Remuzzi, G. Aldosterone and progression of kidney disease. *Ther. Adv. Cardiovasc. Dis.* **2009**, *3*, 133–143.
 112. Jalaguier, S.; Mornet, D.; Mesnier, D.; Leger, J. J.; Auzou, G. Human mineralocorticoid receptor interacts with actin under mineralocorticoid ligand modulation. *FEBS Lett.* **1996**, *384*, 112–116.
 113. Pascual-Le Tallec, L.; Lombes, M. The mineralocorticoid receptor: a journey exploring its diversity and specificity of action. *Mol. Endocrinol.* **2005**, *19*, 2211–2221.
 114. Freiman, R. N.; Tjian, R. Regulating the regulators: lysine modifications make their mark. *Cell* **2003**, *112*, 11–17.
 115. Rosenfeld, M. G.; Lunyak, V. V.; Glass, C. K. Sensors and signals: a coactivator/corepressor/epigenetic code for integrating signal-dependent programs of transcriptional response. *Genes Dev.* **2006**, *20*, 1405–1428.
 116. Viengchareun, S.; Le Menuet, D.; Martinerie, L.; Munier, M.; Tallec, L. P.; Lombès, M. The mineralocorticoid receptor: insights into its molecular and (patho)physiological biology. *Nuclear Receptor Signaling* **2007**, *5*, e012
 117. Funder, J. W. The nongenomic actions of aldosterone. *Endocr. Rev.* **2005**, *26*, 313–321.
 118. Losel, R.; Wehling, M. Nongenomic actions of steroid hormones. *Nat. Rev. Mol. Cell Biol.* **2003**, *4*, 46–56.
 119. Rude, M. K.; Duhaney, T. A.; Kuster, G. M.; Judge, S.; Heo, J.; Colucci, W. S.; Siwik, D. A.; Sam, F. Aldosterone stimulates matrix metalloproteinases and reactive oxygen species in adult rat ventricular cardiomyocytes. *Hypertension* **2005**, *46*, 555–561.
 120. Grossmann, C.; Benesic, A.; Krug, A. W.; Freudinger, R.; Mildenerger, S.; Gassner, B.; Gekle, M. Human mineralocorticoid receptor expression renders cells responsive for nongenotropic aldosterone actions. *Mol. Endocrinol.* **2005**, *19*, 1697–1710.
 121. Silvestre, J. S.; Robert, V.; Heymes, C.; Aupetit-Faisant, B.; Mouas, C.; Moalic, J. M.; Swynghedauw, B.; Delcayre, C. Myocardial production of aldosterone and corticosterone in the rat physiological regulation. *J. Biol. Chem.* **1998**, *273*, 4883–4891.
 122. Rudolph, A. E.; Blasi, E. R.; Delyani, J. A. Tissue-specific corticosteroidogenesis in the rat. *Mol. Cell. Endocrinol.* **2000**, *165*, 221–224.
 123. Dluhy, R. G.; Williams, G. H. Adrenal cortex. In: Kasper, D. L.; Braunwald, E.; Fauci, A. S. Eds. *Harrison's Principles of Internal Medicine 16 ed.* McGraw Hill, New York, **2005**, pp 321.
 124. Williams, G. H. Aldosterone biosynthesis, regulation, and classical mechanism of action. *Heart Fail. Rev.* **2005**, *10*, 7–13.
 125. Rousseau, M. F.; Gurne, O.; Dupre, D.; Van Mieghem, W.; Robert, A.; Ahn, S.; Galanti, L.; Ketelslegers, J. M. Beneficial neurohormonal profile of spironolactone in severe congestive heart failure: results from the RALES neurohormonal substudy. *J. Am. Coll. Cardiol.* **2002**, *40*, 1596–1601.
 126. Chai, W.; Garrelts, I. M.; de Vries, R.; Batenburg, W. W.; van Kats, J. P.; Danser, A. H. J. Nongenomic effects of aldosterone in the human heart: interaction with angiotensin II. *Hypertension* **2005**, *46*, 701–706.
 127. Goshke, R.; Cohen, N. C.; Wood, J. M.; Maibaum, J. Design and synthesis of novel 2,7-dialkyl substituted 5(S)-amino-4(S)-hydroxy-8-phenyl-octanecarboxamides as in vitro potent peptidomimetic inhibitors of human renin. *Bioorg. Med. Chem. Lett.* **1997**, *7*, 2735–2740.
 128. Goshke, R.; Stutz, S.; Rasetti, V.; Cohen, N. C.; Rahuel, J.; Rigollier, P.; Baum, H. P.; Forgiarini, P.; Schnell, C. R.; Wagner, T.; Gruetter, M. G.; Fuhrer, W.; Schilling, W.; Cumin, F.; Wood, J. M.; Maibaum, J. Novel 2,7-dialkyl substituted 5(S)-amino-4(S)-hydroxy-8-phenyl-octanecarboxamides transition state peptidomimetics are potent and orally active inhibitors of human renin. *J. Med. Chem.* **2007**, *50*, 4818–4831.
 129. Maibaum, J.; Stutz, S.; Goshke, R.; Rigollier, P.; Yamaguchi, Cumin, F.; Rahuel, J.; Baum, H. P.; Cohen, N. C.; Schnell, C. R.; Fuhrer, W.; Gruetter, M. G.; Schilling, W.; Wood, J. M. Structural modifications of the P2' Position of 2,7-dialkyl substituted 5(S)-amino-4(S)-hydroxy-8-phenyl-octanecarboxamides: The discovery of aliskiren, a potent nonpeptide human renin inhibitor active after once daily dosing in marmosets. *J. Med. Chem.* **2007**, *50*, 4832–4844.
 130. Vieira, E.; Binggeli, A.; Breu, V.; Bur, D.; Fischli, W.; Guller, R.; Hirth, G.; Marki, H. P.; Muller, M.; Oefner, C.; Scalone, M.; Stadler, H.; Wilhelm, M.; Wostl, W. Substituted piperidines- highly potent renin inhibitors due to induced fit adaptation of the active site. *Bioorg. Med. Chem. Lett.* **1999**, *9*, 1397–1402.
 131. Guller, R.; Binggeli, A.; Breu, V.; Bur, D.; Fischli, W.; Hirth, G.; Jenny, C.; Kansy, M.; Montavon, F.; Muller, M.; Oefner, C.; Stadler, H.; Vieira, E.; Wilhelm, M.; Wostl, W.; Marki, H. P. Piperidine-Renin Inhibitors: compounds with improved physicochemical properties. *Bioorg. Med. Chem. Lett.* **1999**, *9*, 1403–1408.
 132. Marki, H. P.; Binggeli, A.; Bittner, B.; Bohner-Lang, V.; Breu, V.; Bur, D.; Coassolo, P.; Clozel, J. P.; D'Arcy, A.; Doebeli, H.; Fischli, W.; Funk, C.; Foricher, J.; Giller, T.; Gruninger, F.; Guenzi, A.; Guller, R.; Hartung, T.; Hirth, G.; Jenny, C.; Kansy, M.; Klinkhammer, U.; Lave, T.; Lohri, B.; Luft, F. C.; Mervala, E. M.; Muller, D. N.; Muller, M.; Montavon, F.; Oefner, C.; Qiu, C.; Reichel, A.; Sandwald-Ducray, P.; Scalone, M.; Schleimer, M.; Schmid, R.; Stadler, H.; Treiber, A.; Valdenaire, O.; Vieira, E.; Waldmeier, P.; Wiegand-Chou, R.; Wilhelm, M.; Wostl, W.; Zell, M.; Zell, R. Piperidine renin inhibitors: from leads to drug candidates. *Il Farmaco* **2001**, *56*, 21–27.
 133. Holsworth, D. D.; Powell, N. A.; Downing, D. M.; Cai, C.; Cody, W. L.; Ryan, M.; Ostroski, R.; Jalaie, M.; Bryant, J. W.;

- Edmunds, J. J. Discovery of novel non-peptidic ketopiperazine-based renin inhibitors. *Bioorg. Med. Chem.* **2005**, *13*, 2657–2664.
134. Holsworth, D. D.; Cai, C.; Cheng, X. M.; Cody, W. L.; Downing, D. M.; Erasga, N.; Lee, C.; Powell, N. A.; Edmunds, J. J.; Stier, M.; Jalaie, M.; Zhang, E.; McConnell, P.; Ryan, M. J.; Bryant, J.; Li, T.; Kasani, A.; Hall, E.; Subedi, R.; Rahim, M.; Maiti, S. Ketopiperazine-based renin inhibitors: Optimization of the “C” ring. *Bioorg. Med. Chem. Lett.* **2006**, *16*, 2500–2504.
135. Bezencon, O.; Bur, D.; Weller, T.; Bildstein, S. R.; Remen, L.; Stifferlen, T.; Corminboeuf, O.; Grisostomi, C.; Boss, C.; Prade, L.; Delahaye, S.; Treiber, A.; Strickner, P.; Binkert, C.; Hess, P.; Steiner, B.; Fischli, W. Design and preparation of potent, nonpeptidic, bioavailable renin inhibitors. *J. Med. Chem.* **2009**, *52*, 3689–3702.
136. Tice, C. M.; Xu, Z.; Yuan, J.; Simpson, R. D.; Cacatian, S. T.; Flaherty, P. T.; Zhao, W.; Guo, J.; Ishchenko, A.; Singh, S. B.; Wu, Z.; Scott, B. B.; Bukhtiyarov, Y.; Berbaum, J.; Mason, J.; Panemangalore, R.; Cappiello, M. G.; Muller, D.; Harrison, R. K.; McGeehan, G. M.; Dillard, L. W.; Baldwin, J. J.; Claremon, D. A. Design and optimization of renin inhibitors: Orally bioavailable alkyl amines. *Bioorg. Med. Chem. Lett.* **2009**, *19*, 3541–3545.
137. Hoogwerf, B. J.; Young, J. B. The HOPE study. Ramipril lowered cardiovascular risk, but vitamin E did not. *Cleve Clin J Med.* **2000**, *67*, 287–293.
138. Sato, A.; Saruta, T. Aldosterone escape during angiotensin-converting enzyme inhibitor therapy in essential hypertensive patients with left ventricular hypertrophy. *J. Int. Med. Res.* **2001**, *29*, 13–21.
139. Fiebler, A.; Nussberger, J.; Shagdarsuren, E.; Rong, S.; Hilfenhaus, G.; Al-Saadi, N.; Dechend, R.; Wellner, M.; Meiners, S.; Master-Gluth, C.; Jeng, A. Y.; Webb, R. L.; Luft, F. C.; Muller, D. N. Aldosterone synthase inhibitor ameliorates angiotensin II-induced organ damage. *Circulation* **2005**, *111*, 3087–3094.
140. Aldosterone synthase inhibition improves cardiovascular function and structure in rats with heart failure—a comparison with spironolactone. *Eur. Heart J.* **2008**, *29*, 2171–2179.
141. Roumen, L.; Peeters, J. W.; Emmen, J. M. A.; Beugels, I. P. E.; Custers, E. M. G.; de Gooyer, M.; Plate, R.; Pieterse, K.; Hilbers, P. A. J.; Smits, J. F. M.; Vekemans, J. A. J.; Leysen, D.; Ottenheijm, H. C. J.; Janssen, H. M.; Hermans, J. J. R. Synthesis, biological evaluation, and molecular modeling of 1-benzyl-1H-imidazoles as selective inhibitors of aldosterone synthase (CYP11B2). *J. Med. Chem.* **2010**, *53*, 1712–1725.
142. Patents: WO2004046145, WO2004014914, WO2007139992, WO2008027284, WO2007024945, WO2005118557, WO2005118541, WO2005118581, WO2006005726, WO2007065942, WO2007116097, WO2007116099, WO2006128853, WO2006128851, WO2006128852, WO2007116098, WO2008119744
143. Ulmschneider, S.; Müller-Vieira, U.; Klein, C. D.; Antes, I.; Lengauer, T.; Hartmann, R. W. Synthesis and evaluation of (pyridylmethylene)tetrahydronaphthalenes/-indanes and structurally modified derivatives: potent and selective inhibitors of aldosterone synthase. *J. Med. Chem.* **2005**, *48*, 1563–1575.
144. Ulmschneider, S.; Müller-Vieira, U.; Mitrenga, M.; Hartmann, R. W.; Oberwinkler-Marchais, S.; Klein, C. D.; Bureik, M.; Bernhardt, R.; Antes, I.; Lengauer, T. Synthesis and evaluation of imidazolylmethylenetetrahydronaphthalenes and imidazolylmethyleindanes: potent inhibitors of aldosterone Synthase. *J. Med. Chem.* **2005**, *48*, 1796–1805.
145. Voets, M.; Antes, I.; Scherer, C.; Müller-Vieira, U.; Biemel, K.; Marchais-Oberwinkler, S.; Hartmann, R. W. Synthesis and evaluation of heteroaryl-substituted dihydronaphthalenes and indenes: potent and selective inhibitors of aldosterone synthase (CYP11B2) for the treatment of congestive heart failure and myocardial fibrosis. *J. Med. Chem.* **2006**, *49*, 2222–2231.
146. Voets, M.; Antes, I.; Scherer, C.; Müller-Vieira, U.; Biemel, K.; Barassin, C.; Marchais-Oberwinkler, S.; Hartmann, R. W. Heteroaryl-substituted naphthalenes and structurally modified derivatives: selective inhibitors of CYP11B2 for the treatment of congestive heart failure and myocardial fibrosis. *J. Med. Chem.* **2005**, *48*, 6632–6642.
147. Heim, R.; Lucas, S.; Grombein, C. M.; Ries, C.; Schewe, K. E.; Negri, M.; Müller-Vieira, U.; Birk, B.; Hartmann, R. W. Overcoming undesirable CYP1A2 inhibition of pyridyl-naphthalene-type aldosterone synthase inhibitors: influence of heteroaryl derivatization on potency and selectivity. *J. Med. Chem.* **2008**, *51*, 5064–5074.
148. WO2009256462.
149. Lucas, S.; Heim, R.; Ries, C.; Schewe, K. E.; Birk, B.; Hartmann, R. W. In vivo active aldosterone synthase inhibitors with improved selectivity: lead optimization providing a series of pyridine substituted 3,4-dihydro-1H-quinolin-2-one derivatives. *J. Med. Chem.* **2008**, *51*, 8077–8087.
150. Lucas, S.; Heim, R.; Negri, M.; Antes, I.; Ries, C.; Schewe, K. E.; Bisi, A.; Gobbi, S.; Hartmann, R. W. Novel aldosterone synthase inhibitors with extended carbocyclic skeleton by a combined ligand-based and structure-based drug design approach. *J. Med. Chem.* **2008**, *51*, 6138–6149.
151. Richard, M.; Zoran, R. Designed multiple ligands. An emerging drug discovery paradigm. *J. Med. Chem.* **2005**, *48*, 6523–6543.
152. Andrea, C.; Laura, B. M.; Anna, M.; Michela, R.; Vincenzo, T.; Maurizio, R.; Carlo, M. Multi-target-directed ligands to combat neurodegenerative diseases. *J. Med. Chem.* **2008**, *51*, 347–372.
153. Marco, R.; Chiara, U. Polysulfated/sulfonated compounds for the development of drugs at the crossroad of viral infection and oncogenesis. *Curr. Pharm. Des.* **2009**, *15*, 2946–2957.
154. Richard, M. Selectively nonselective kinase inhibition: striking the right balance. *J. Med. Chem.* **2010**, *53*, 1413–1437.
155. Palmgren, J. S.; Karavadia, S. S.; Wakefield, M. R. Unusual and Underappreciated: Small Cell Carcinoma of the Prostate. *Semin. Oncol.* **2007**, *34*, 22–29.
156. Rajec, J.; Mego, M.; Sycova-mila, Z.; Obertova, J.; Brozmanova, K.; Mardiak, J. Paraneoplastic Cushing's syndrome as the first sign of progression of prostate cancer. *Bratisl lek Listy.* **2008**, *109*, 362–363.
157. Kataoka, K.; Akasaka, Y.; Nakajima, K.; Nagao, K.; Hara, H.; Miura, K.; Ishii, N. Cushing syndrome associated with prostatic tumor adrenocorticotrophic hormone (ACTH) expression after maximal androgen blockade therapy. *Int. J. Urol.* **2007**, *14*, 436–439.

158. Hussein, W. I.; Kowalyk, S.; Hoogwerf, B. J. Ectopic adrenocorticotrophic hormone syndrome caused by metastatic carcinoma of the prostate: therapeutic response to Ketoconazole. *Endocr. Pract.* **2002**, *8*, 381–384.
159. Puliti, D.; Miccinesi, G.; Collina, N.; De Lisi, V.; Federico, M.; Ferretti, S.; Finarelli, A. C.; Foca, F.; Mangone, L.; Naldoni, C.; Petrella, M.; Ponti, A.; Segnan, N.; Sigonal, A.; Zarcone, M.; Zorzi, M.; Zappa, M.; Paci, E.; the IMPACT Working Group. Effectiveness of service screening: a case-control study to assess breast cancer mortality reduction. *Brit. J. Cancer* **2008**, *99*, 423–427.
160. Miller, W. R. Endocrine treatment for breast cancers: biological rationale and current progress. *J. Steroid Biochem. Mol. Biol.* **1990**, *37*, 467–480.
161. Wang, T.; You, Q.; Huang, F. S.; Xiang, H. Recent advances in selective estrogen receptor modulators for breast cancer. *Mini Rev. Med. Chem.* **2009**, *9*, 1191–1201.
162. Perez, E. A. Safety profiles of tamoxifen and the aromatase inhibitors in adjuvant therapy of hormone-responsive early breast cancer. *Ann. Oncol.* **2007**, *18*, viii26–viii35.
163. Jurgen, G.; Ben, H.; Gun, A.; Mitch, D.; Per Eystein, L. Influence of letrozole and anastrozole on total body aromatization and plasma estrogen levels in postmenopausal breast cancer patients evaluated in a randomized, cross-over study. *J. Clin. Oncol.* **2002**, *20*, 751–757.
164. Jurgen, G.; Nick, K.; Gun, A.; Giorgio, O.; Enrico, D. S.; Per Eystein, L.; Mitch, D. In vivo inhibition of aromatization by exemestane, a novel irreversible aromatase inhibitor, in postmenopausal breast cancer patients. *Clin. Cancer Res.* **1998**, *4*, 2089–2093.
165. Coombes, R. C.; Kilburn, L. S.; Snowdon, C. F.; Paridaens, R.; Coleman, R. E.; Jones, S. E.; Jassem, J.; Van de Velde, C. J.; Delozier, T.; Alvarez, I.; Del Mastro, L.; Ortmann, O.; Diedrich, K.; Coates, A. S.; Bajetta, E.; Holmberg, S. B.; Dodwell, D.; Mickiewicz, E.; Andersen, J.; Lonning, P. E.; Cocconi, G.; Forbes, J.; Castiglione, M.; Stuart, N.; Stewart, A.; Fallowfield, L. J.; Bertelli, G.; Hall, E.; Bogle, R. G.; Carpentieri, M.; Colajori, E.; Subar, M.; Ireland, E.; Bliss, J. M. Survival and safety of exemestane versus tamoxifen after 2-3 years' tamoxifen treatment (Intergroup Exemestane Study): a randomised controlled trial. *Lancet* **2007**, *369*, 559–570.
166. Coates, A. S.; Keshaviah, A.; Thurlimann, B.; Mouridsen, H.; Mauriac, L.; Forbes, J. F.; Paridaens, R.; Castiglione-Gertsch, M.; Gelber, R. D.; Colleoni, M.; Lang, I.; Del Mastro, L.; Smith, I.; Chirgwin, J.; Nogaret, J. M.; Pienkowski, T.; Wardley, A.; Jakobsen, E. H.; Price, K. N.; Goldhirsch, A. Five years of letrozole compared with tamoxifen as initial adjuvant therapy for postmenopausal women with endocrine-responsive early breast cancer: update of study BIG 1-98. *J. Clin. Oncol.* **2007**, *25*, 486–492.
167. Goss, P. E.; Ingle, J. N.; Martino, S.; Robert, N. J.; Muss, H. B.; Piccart, M. J.; Castiglione, M.; Tu, D.; Shepherd, L. E.; Pritchard, K. I.; Livingston, R. B.; Davidson, N. E.; Norton, L.; Perez, E. A.; Abrams, J. S.; Therasse, P.; Palmer, M. J.; Pater, J. L. A randomized trial of letrozole in postmenopausal women after five years of tamoxifen therapy for early-stage breast cancer. *N. Engl. J. Med.* **2003**, *349*, 1793–1802.
168. Goss, P. E.; Ingle, J. N.; Martino, S.; Robert, N. J.; Muss, H. B.; Piccart, M. J.; Castiglione, M.; Tu, D.; Shepherd, L. E.; Pritchard, K. I.; Livingston, R. B.; Davidson, N. E.; Norton, L.; Perez, E. A.; Abrams, J. S.; Cameron, D. A.; Palmer, M. J.; Pater, J. L. Efficacy of Letrozole extended adjuvant therapy according to estrogen receptor and progesterone receptor status of the primary tumor: national cancer institute of canada clinical trials group MA.17. *J. Clin. Oncol.* **2007**, *25*, 2006–2011.
169. Chapman, J. W.; Meng, D.; Shepherd, L.; Parulekar, W.; Ingle, J. N.; Muss, H. B.; Palmer, M.; Yu, C.; Goss, P. E. Competing causes of death from a randomized trial of extended adjuvant endocrine therapy for breast cancer. *J. Natl. Cancer Inst.* **2008**, *100*, 252–260.
170. Wang, Y.; Wang, Q.; Zhao, Y.; Gong, D.; Wang, D.; Li, C.; Zhao, H. Protective effects of estrogen against reperfusion arrhythmias following severe myocardial ischemia in rats. *Circ. J.* **2010**, *74*, 634–643.
171. Merchanthaler, I.; Dellovade, T. L.; Shughrue, P. J. Neuroprotection by estrogen in animal models of global and focal ischemia. *Ann. N. Y. Acad. Sci.* **2003**, *1007*, 89–100.
172. Booth, E. A.; Marchesi, M.; Kilbourne, E. J.; Lucchesi, B. R. 17 β -Estradiol as a receptor-mediated cardioprotective agent. *J. Pharmacol. Exp. Ther.* **2003**, *307*, 395–401.
173. Jazbutyte, V.; Arias-Loza, P. A.; Hu, K.; Widder, J.; Govindaraj, V.; von Poser-Klein, C.; Bauersachs, J.; Fritzemeier, K. H.; Hegele-Hartung, C.; Neyses, L.; Ertl, G.; Pelzer, T. Ligand-dependent activation of ER β lowers blood pressure and attenuates cardiac hypertrophy in ovariectomized spontaneously hypertensive rats. *Cardiovasc. Res.* **2008**, *77*, 774–781.
174. Beer, S.; Reincke, M.; Kral, M.; Callies, F.; Ströer, H.; Dienesch, C.; Steinhauer, S.; Ertl, G.; Allolio, B.; Neubauer, S. High-dose 17 β -estradiol treatment prevents development of heart failure post-myocardial infarction in the rat. *Basic Res. Cardiol.* **2007**, *102*, 9–18.
175. Gardner, J. D.; Murray, D. B.; Voloshenyuk, T. G.; Brower, G. L.; Bradley, J. M.; Janicki, J. S. Estrogen attenuates chronic volume overload induced structural and functional remodeling in male rat hearts. *Am. J. Physiol. Heart Circ. Physiol.* **2010**, *298*, H497–H504.
176. Donaldson, C.; Eder, S.; Baker, C.; Aronovitz, M. J.; Weiss, A. D.; Hall-Porter, M.; Wang, F.; Ackerman, A.; Karas, R. H.; Molkentin, J. D.; Patten, R. D. Estrogen attenuates left ventricular and cardiomyocyte hypertrophy by an estrogen receptor-dependent pathway that increases calcineurin degradation. *Circ. Res.* **2009**, *104*, 265–275.
177. Arias-Loza, P. A.; Muehlfelder, M.; Elmore, S. A.; Maronpot, R.; Hu, K.; Blode, H.; Hegele-Hartung, C.; Fritzemeier, K. H.; Ertl, G.; Pelzer, T. Differential effects of 17 β -estradiol and of synthetic progestins on aldosterone-salt-induced kidney disease. *Toxicol. Pathol.* **2009**, *37*, 969–982.
178. American Heart Association. Heart disease and stroke statistics: 2004 update. Dallas, TX: American Heart Association; **2003**.
179. Witteman, J. C.; Grobbee, D. E.; Kok, F. J.; Hofman, A.; Valkenburg, H. A. Increased risk of atherosclerosis in women after the menopause. *Br. Med. J.* **1989**, *298*, 642–644.

180. Nabholz, J. M.; Gligorov, J. Cardiovascular safety profiles of aromatase inhibitors: a comparative review. *Drug Saf.* **2006**, *29*, 785–801.
181. Pritchard, K. I.; Abramson, B. L. Cardiovascular health and aromatase inhibitors. *Drugs* **2006**, *66*, 1727–1740.
182. Cuppone, F.; Bria, E.; Verma, S.; Pritchard, K. I.; Gandhi, S.; Carlini, P.; Milella, M.; Nistico, C.; Terzoli, E.; Cognetti, F.; Giannarelli, D. Do adjuvant aromatase inhibitors increase the cardiovascular risk in postmenopausal women with early breast cancer? *Cancer* **2008**, *112*, 260–267.
183. Bundred, N. J. The effects of aromatase inhibitors on lipids and thrombosis. *Br. J. Cancer* **2005**, *93*, S23–S27.
184. Ewer, M. S.; Glück, S. A woman's heart. The impact of adjuvant endocrine therapy on cardiovascular health. *Cancer* **2009**, *115*, 1813–1826.
185. Healey Bird, B. R. J.; Swain, S. M. Cardiac toxicity in breast cancer survivors: review of potential cardiac problems. *Clin. Cancer Res.* **2008**, *14*, 14–24.
186. Macova, M.; Armando, I.; Zhou, J.; Baiardi, G.; Tyurmin, D.; Larrayoz-Roldan, I. M.; Saavedra, J. M. Estrogen reduces aldosterone, upregulates adrenal angiotensin II AT2 receptors and normalizes adrenomedullary Fra-2 in ovariectomized rats. *Neuroendocrinology* **2008**, *88*, 276–286.
187. Hoshi-Fukushima, R.; Nakamoto, H.; Imai, H.; Kanno, Y.; Ishida, Y.; Yamanouchi, Y.; Suzuki, H. Estrogen and angiotensin II interactions determine cardio-renal damage in Dahl salt-sensitive rats with heart failure. *Am. J. Nephrol.* **2008**, *28*, 413–423.
188. Castelli, W. P. Cardiovascular disease in women. *Am. J. Obstet. Gynecol.* **1988**, *158*, 1553–1560.
189. Fischer, M.; Baessler, A.; Schunkert, H. Renin angiotensin system and gender differences in the cardiovascular system. *Cardiovasc. Res.* **2002**, *53*, 672–677.
190. Roesch, D. M.; Tian, Y.; Zheng, W.; Shi, M.; Verbalis, J. G.; Sandberg, K. Estradiol attenuates angiotensin-induced aldosterone secretion in ovariectomized rats. *Endocrinology* **2000**, *141*, 4629–4636.
191. Chappell, M. C.; Gallagher, P. E.; Averill, D. B.; Ferrario, C. M.; Brosnihan, K. B. Estrogen or the AT1 antagonist olmesartan reverses the development of profound hypertension in the congenic mRen2.Lewis rat. *Hypertension* **2003**, *42*, 781–786.
192. Harrison-Bernard, L. M.; Schulman, I. H.; Raji, L. Post-ovariectomy hypertension is linked to increased renal AT1 receptor and salt sensitivity. *Hypertension* **2003**, *42*, 1157–1163.
193. Krishnamurthi, K.; Verbalis, J. G.; Zheng, W.; Wu, Z.; Clerch, L. B.; Sandberg, K. Estrogen regulates angiotensin AT1 receptor expression via cytosolic proteins that bind to the 5' leader sequence of the receptor mRNA. *Endocrinology* **1999**, *140*, 5435–5438.
194. Zheng, W.; Shi, M.; Yoo, S. E.; Ji, H.; Roesch, D. M. Estrogens contribute to a sex difference in plasma potassium concentration: a mechanism for regulation of adrenal angiotensin receptors. *Gender Med.* **2006**, *3*, 43–53.
195. Ji, H.; Zheng, W.; Falconetti, C.; Roesch, D. M.; Mulrone, S. E.; Sandberg, K. 17 β -Estradiol deficiency reduces potassium excretion in an angiotensin type 1 receptor-dependent manner. *Am. J. Physiol. Heart Circ. Physiol.* **2007**, *293*, H17–H22.